Experimental and numerical investigation of flushing in combined sewer networks : case study of a Parisian trunk sewer

Gashin Shahsavari

Thèse de doctorat

de l'Université Sorbonne Paris Cité

Préparée à l'Université Paris Diderot

Ecole doctorale Sciences Humaines et Sociales (ED382)

Laboratoire PRODIG

Expérimentations et Modélisations de la Chasse Hydraulique dans les Réseaux d'Assainissement Unitaires – Cas d'étude d'un Collecteur Parisien

Experimental and Numerical investigation of Flushing in Combined sewer Networks – Case study of a Parisian Trunk Sewer

Par

Mme Gashin Shahsavari

Pour obtenir le grade de

« Docteur de l'université Sorbonne Paris Cité à l'Université de Paris Diderot en dynamique des milieux et risques »

Présentée et soutenue publiquement le 10/12/2018 devant le Jury :

Présidente du jury : PONS, Marie-Noëlle : Directrice de recherche de l'Université de Lorraine
Rapporteur : CREACO, Enrico : Associate Professor de l'Université de Pavie (Italie)
Rapporteure: GAUTIER, Emmanuèle : Professeure de l'Université de Panthéon-Sorbonne
Examinateur : MÉTIVIER, François : Professor de l'Institut de Physique du Globe de Paris
Directeur de thèse : ARNAUD-FASSETTA, Gilles : Professeur de l'Université de Paris Diderot
Co-directeur de thèse : BERTILOTTI, Roberto : Directeur de PROLOG Ingénierie
Co-encadrant : CAMPISANO, Alberto : Associate Professor de l'Université de Catane (Italie)

Abstract in English

Sediment accumulation on the invert of sewer channels has been recognized as one of the important sources of problems for the management of sewer networks.
In the two most recent decades, flushing has been put forward as one of the most common methods of sewer cleaning, to limit sediment accumulation especially in large trunk sewers.
Sewer sediment transport processes are not fully understood yet, due to numerous unknown variables and difficult measuring conditions. The current research aimed firstly to setup a field experimental campaign to obtain high-quality data. This data allowed understanding of the processes associated with flushing operation in sewers. In addition, this study aimed to model the flushing processes properly in order to set-up an adequate and practical numerical tool able to predict sediment removal of flushing in the sewer network of Paris. To this purpose, two models were used: *(i)* a simple model for uniform sediment transport, which is the most common used approach; and *(ii)* a more complex model for non-uniform sediment transport of mixtures. A comparative analysis was carried out to highlight advantages and drawbacks of either. Overall, the results pointed out that the numerical modelling is able to reproduce faithfully hydrodynamics and sediment transport during flushing operations. In fact, both models enabled evaluation of flush behaviour and associated sediment transport. However, despite its higher complexity and computational burden, the latter model provides better insight into the prediction of the removal effectiveness of flushes.

Key Words: Flushing, Combined sewer network, Numerical modeling, Transport of non-uniform sediment mixtures.

Résumé en Français

L'accumulation de sédiments sur le fond des égouts à faible pente est une contrainte au bon fonctionnement hydraulique et à la gestion des réseaux d'assainissement unitaire. Le recours à la chasse hydraulique est alors une pratique envisagée par les gestionnaires de réseau pour le nettoyage des canaux souterrains.

Les processus de transport sédimentaire dans les réseaux d'assainissement unitaire est rendu complexe en raison du jeu de nombreux phénomènes tels que la variabilité de l'étendue granulométrique des sédiments et la cohésion.

La thèse présente les résultats expérimentaux et numériques obtenus avant et après une chasse hydraulique réalisée dans le réseau unitaire parisien.

Une campagne de mesures a permis d'acquérir des données hydro-sédimentaires à haute résolution, permettant de caractériser et quantifier les processus d'érosion, de transport et de sédimentation agissant sous l'effet de la chasse hydraulique, du reste performante dans le nettoyage du réseau étudié.

Deux modèles de transport sédimentaire comportant un modèle simple en condition de transport uniforme, et un modèle plus complexe impliquant le transport non-uniforme ont été développés afin de mettre en place un outil prédictif des mouvements des particules solides pendant le phénomène de chasse. Les deux modèles ont été capables d'évaluer à différents niveaux de précision l'efficacité de la chasse hydraulique en termes de transport sédimentaire. La comparaison des résultats issus des deux modèles permet de déterminer les avantages et les contraintes de chacun, révélant ainsi l'importance de prendre en compte l'hétérogénéité texturale des dépôts dans l'analyse de l'érosion, du transport et de la sédimentation des particules solides sous l'effet des chasses hydrauliques. De plus, une analyse de sensibilité de la gamme d'application de certains paramètres d'entrée du modèle de transport non-uniforme des sédiments a été réalisée. Les résultats ont confirmé le bon fonctionnement du modèle.

Mots clés : Chasse hydraulique, réseau unitaire d'assainissement, modélisation numérique, transport des sédiments non-uniformes.

Acknowledgments

There are people in everyone's life who make success both possible and rewarding:

I firstly think of my husband. At this moment that I'm writing the last lines of this dissertation, I would like to thank my love Hoshyar, for his amazing encouragements and helps during these years. I'm so grateful to him for his understanding, patience and supports (both financial and moral). I also do apologize to him as well as to my lovely son Adrien "*dilakay Maman*" (my sweet heart in Kurdish), for all those times that I spent without them to accomplish this work.

I would like to sincerely thank my advisors; Professor Gilles Arnaud-Fassetta, Professor Alberto Campisano as well as Roberto Bertilotti. A special thank goes to Gilles for his human being, kindness, patience and presence whenever I needed his help (*Un grand merci* Gilles!). It was a real pleasure working with him. Particular thanks go to Alberto for his precious and unforgettable helps. It was impossible to bring this research to the end without his supports (*Grazie mille* Alberto!). I have been above all blessed to have him as supervisor who always treated my questions promptly and carefully who cared about the quality of this work so meticulously. I will never forget his supports, patience, encouragements and for all that I learned from him.

I am sincerely grateful to my jury members: Emmanuèle Gautier (rapporteur), Enrico Creaco (rapporteur), Marie-Noëlle Pons (examinatrice) and François Métavier (examinateur), for their time and expertise during the course of this dissertation.

Likewise, I must express my great gratitude to Professor Carlo Modica, such the precious person for his valuable advices, energy and kindness. He sincerely sacrificed hours and hours of his precious time, for obtaining a "*pullito"* sediment transport model.

I am grateful to all of those people with whom I had the pleasure to work during these years. Special thanks goes to "*la Section de l'Assainissement de Paris* (SAP) "of Paris Municipality for the financial support of the experimental measurement campaign. Special thanks to Mr. Jean-François Ferrandez from SAP for his sincere collaboration.

Special appreciation is extended to Max Lamanière from the "Geo-physics laboratory" of Paris Diderot University for his kindness and frank help during and after laboratory analyses.

I wish to express my specific and special appreciation to Hydroconseil Engineering. In particular I'm thankful of Bruno VALFREY and Christine Lagarde, who kindly accepted me as co-worker in their office where I finalized my redaction in concentrated and calm conditions.

I also send my special thanks to the colleagues from Paris Diderot University who always helped and encouraged me: Malika Madelin, Émilie Lavie, Jean-Claude Bergès, Vincent Viel, Candid Lissak, François Bétard, Monique Fort, and other friends: Lucile, Romain, Luc, Rémi, Laurent. In particular, I'm grateful to my Italian colleagues and friends, from the Catania University who were always ready to help me: Stefania, Massimiliano, Antonio, David, Laura, and also Marco and Daniele with whom I was honored to follow-up with their master thesis.

I'm thankful to my lovely friends from ENGREF who encouraged me during these years: Katia, Lionel, Victor, Roman, Tristan, Fannie, Charles, Nicolas. I must specially thank Anneli, who helped, advised and comforted me like a real sister when I needed it. I'm also grateful to Steve for his advices in preparation of my defense. I'm so lucky to have such the good friends.

I would like to thank those with whom I had the possibility to publish: Professor Sebastiano Battiato, Oliver Guidice, Isa Ebtehaj, and Hossein Bonakdari.

Similarly, I'm very grateful to the Kurdish Institute of Paris as well as the Campus France for funding three years of this research.

At the end, I would like to thank my mother, *Shahin*, my precious pearl in life, my sisters *Soma*, *Nina* and *Shadi* who always refreshed me, who beard with me, who understood me. You are my eternal love!! Finally, I extend my gratitude to my family-in-law, especially, *Giti*, my lovely mother-in-law for her delicious meals like *âwgôchte* when I was finalizing last lines.

Table of Content

List of Figures

List of Tables

List of Symboles

A: Cross-section area (in m²)
A_s: Sediment cross-section area (in m²)
a: Surface of the bed layer
C: Average volumetric sediment concentration in the water column (in mg/l)
$C_{\min}$: Lower limit sediment concentrations in Velikanov (in g/l)
$C_{\max}$ Upper limit sediment concentrations in Velikanov (in g/l)
c: flow wave celerity (in m/s)
cc: Local concentration in the cross section (in mg/l)
c_D: Drag coefficient of particle (-)
D_* : Non-dimensional grain size (-)
d: Particle diameter (in m)
d_{50}: Median diameter of bed sediment (50% of the particles in the sediment sample are finer than the d_{50} grain size; in m)
$d_{50\,ave}$: Median diameter for each section (in m)
F_h: Hydrostatic force over the cross-section (in N)
F_D: Drag force acting on sediment particle (in N)
F_L: Lift force acting on sediment particle (in N)
F_G: Gravity force acting on sediment particle (in N)
F_L: Buoyancy force acting on sediment particle (in N)
g: Acceleration due to gravity (in m/s²)
h: Water level (in m)
h_0: Initial water level
h_s: Sediment height (in m)
i and j: integer subscripts representing space and time, respectively.
J: Energy friction slope (in m/m)
k_{eq}: Composite roughness coefficient
k_b: Roughness coefficient of the channel bed
k_w: Roughness coefficient of the channel wall
M_s: Mass of the sediment (in kg)
P: Wetted perimeter (in m)
P: porosity (-)
Q: Flow discharge (in m^3/s)
Q_s: Volumetric sediment discharge (in m^3/s)
qs: Lateral sediment discharge (in m²/s)
q_{sb}: Bed-load sediment transport (in $m^3/s \times m$)
q_{ss}: Suspended-load sediment transport (in $m^3/s \times m$)
q_{st}: Total load sediment transport (in $m^3/s \times m$)
R_h: Hydraulic radius (in m)
R: Rouse number (-)
s: Specific gravity of particle (-)
S_f : Friction slope (in m)

S_b: Slope of the mobile bed (in m/m)
t: Temporal variable or time (in s)
u*: Shear velocity (in m/s)
U: Dependent variable vector in hyperbolic system of DSV
F(U): Flux vector in hyperbolic system of DSV
D(U): Source term vector in hyperbolic system of DSV
R_e: Shear Reynolds number (-)
V: Flow velocity (in m/s)
V_s: Volume of the sediment (in m^3)
Vol_{por}: Pore volume of the sediment sample (in m^3)
Vol_{tot}: Total volume of the sediment sample (in m^3)
W_i: Iinitial weight of sample to determine OM (in kg)
W_d: Re-dried sample weight after destructing the OM (in kg)
W: Volume of particle (in m^3)
w_s: Fall velocity of a sediment particle (in cm/s)
$w_{s_{50}}$: Median settling velocity (in cm/s)
x, *y*, *z*: spatial independent coordinates (in m)
Δt: Time step
η : Porosity of a sediment sample (-)
$\eta_{\min}$: Minimum efficiency coefficients in Velikanov module (-)
$\eta_{\max}$: Maximum efficiency coefficients in Velikanov (-)
κ : Von Karman coefficient (-)
δ_p : Thickness of the pavement layer (in m)
δ_s : Thickness of the sub-pavement layer (in m)
τ : Bottom shear stress (in N/m^2)
τ_0 : Average shear stress (in N/m^2)
τ_c : Critical bed shear stress (in N/m^2)
θ : Non-dimensional effective bed shear stresses
θ_c : Critical shear stresses.
ρ : Flow density (in kg/m^3)
ρ_s : Specific weight of sediment (in kg/m^3)
ρ_m : Density of water-sediments mixture (in kg/m^3)
γ : Flow specific weight (in N/m^3)
γ_s : Specific weight of sediment in flow (in N/m^3)
ν : Kinematic viscosity of water (in $N\times s/m^2$)
$\Delta = (\rho - \rho_s)/\rho$: Relative submerged density of sediment (-)

Abbreviations

DSV: De Saint Venant
WWTP: Waste Water Treatment Plant
BF: Before the flush
AF: After the flush
SSC: Suspended Sediment Concentration

Résumé étendu en français

0.1 État de l'art

Les réseaux d'assainissement unitaires drainent non seulement les eaux usées mais aussi les solides qui entrent dans le système par différentes voies. Ces solides ont des caractéristiques (type, nature) très variées. Les solides dans les égouts unitaires à faible pente, où les conditions hydrauliques n'assurent pas le transport des sédiments, s'accumulent et se consolident au fil du temps. Ces dépôts sont problématiques dans la gestion des réseaux d'assainissement pour plusieurs raisons *e.g.,* baisse de la capacité hydraulique résultant à réduire la capacité d'évacuer les eaux usées, rejet des pollutions dans la nature en cas de surcharge dans les stations d'épuration lors des orages. L'une des préoccupations des gestionnaires du réseau de drainage urbain, dans les pays européens tels que la France, est l'accumulation des solides dans les canaux d'assainissement. Ce problème concerne notamment les grands collecteurs des réseaux unitaires. C'est ainsi que la maintenance des canaux (*e.g.,* curage) est important (Ashley *et al.* 2004).

Des méthodes de curage des égouts existent, permettant de limiter la sédimentation sur le fond des canaux. L'application de ces méthodes peut être dans le cadre de curages préventifs ou de nettoyages de base (curage proactive). Il existe un nettoyage des réseaux de manière 'automatique' grâce à des appareils (vannes) à fonctionnement autonome et à effacement rapide. Ce système d'auto-curage a pour l'objectif d'éliminer ou de diminuer l'intervention humaine lors du nettoyage régulier des réseaux. En effet, le curage des égouts à l'aide des techniques manuelles cause des problèmes de santé pour les égoutiers qui sont directement exposés à des gaz toxiques. Parmi les techniques de nettoyage existantes, la chasse hydraulique est la plus prometteuse, considérée comme une méthode à la fois pratique et économique, écologique et environnementale (Chebbo *et al.* 1996 ; EPA 1999 ; Fan 2004). C'est pourquoi les gestionnaires des réseaux sont de plus en plus intéressées par cette technique.

Depuis les dernières décennies, la chasse hydraulique a été étudiée par de nombreux chercheurs de différents pays (Pisano *et al.* 1979 ; Ristenpart 1998 ; Pisano *et al.* 1998 ; Campisano et Modica 2003 ; Bertrand-Krajewski *et al.* 2005). Globalement, les objectifs principaux de ces études sont de :

- Comprendre le fonctionnement hydraulique des vannes à chasse et leur capacité à produire des ondes d'écoulement tout au long des canaux (Bertran-Krajewski *et al*. 2003 ; Guo *et al*. 2004 ; Campisano *et al.* 2007 ; Bong *et al*. 2013) ;
- Comprendre les processus du transport solide sous l'effet de la chasse hydraulique ainsi que l'efficacité des chasses sur le transport et l'élimination des sédiments accumulés dans les égouts (Lorenzen *et*

al. 1996 ; De Sutter *et al*. 1999 ; Creaco and Bertrand-Krajewski 2007) ;

- Obtenir des indications pratiques liées 1) au *design* des réseaux d'assainissement ainsi que des vannes à effacement rapide (Goormans *et al*. 2009 ; Ruiloba *et al.* 2018) et 2) à une meilleure gestion des réseaux en termes de planning (Dettmar 2007 ; Staufer *et al.* 2007).

Les résultats découlent principalement des investigations expérimentales de la chasse hydrauliques ainsi que celles numériques. Ces dernières ont été validées par les données expérimentales conduites dans les laboratoires (Guo *et al.* 2004 ; Campisano *et al.* 2006 ; Todeschini *et al.* 2010) et/ou sur les sites réels (Lrenzen *et al*. 1995 ; Bertrand-Krajewski *et al*. 2004 ; Dettmar and Staufer 2005 ; Bertrand-Krajewski *et al*. 2006). D'une part, les résultats des expérimentations hydrauliques et du transport sédimentaire réalisées dans les laboratoires ont été obtenus dans les conditions simplifiées telles que les canaux expérimentaux (texture en plexiglass, forme transversale, pente uniforme, longueur courte, etc.) avec des sédiments uniformes et synthétiques (Campisano *et al.* 2008 ; Shirazi *et al.* 2014). Ces résultats ne représentent pas pleinement les conditions réelles des réseaux d'assainissement. C'est la raison pour laquelle les modèles validés à partir des données expérimentales provenant des laboratoires ne peuvent pas être fiables dans la gestion et la maintenance des réseaux. D'autre part, les conditions hostiles et complexes dans les égouts rendent erronées les mesures hydrodynamiques, notamment celles du transport sédimentaire. De plus, à ce jour, les appareils de mesures ne sont pas tout à fait compatibles avec les conditions des égouts (*e.g.,* forte turbidité) et ils demandent une maintenance régulière. Ce sont les raisons pour lesquelles les modèles "sophistiqués et multidimensionnels" ne pourront pas tout-à-fait être validés par les données expérimentales obtenues à partir des cas réels.

Les études expérimentales (laboratoire ou site réel) effectuées ont évalué la performance des chasses et la capacité érosive des ondes sur les dépôts uniquement à l'aide des mesures d'épaisseur des dépôts durant la chasse ou après la chasse (Lorenzen *et al.* 1996 ; Ristenpart, 1998 ; Campisano et al. 2004 ; Bertrand-Krajewski *et al.* 2005, 2006 ; Creaco et Bertrand-Krajewski 2009). On trouve rarement des études qui se sont intéressées à des mesures plus détaillées, concernant notamment la composition des sédiments et son évolution suite à ce phénomène (Campisano *et al.* 2008 ; Todeschini *et al.* 2010). Les études expérimentales au laboratoire se sont notamment intéressées à la mesure du pourcentage en sédiments fins (cohésion) et à son évolution après la chasse. La littérature souligne ce manque de compréhension des processus sédimentaires (l'érosion, le transport et la sédimentation) pendant la chasse hydraulique, dû à l'absence de mesures *in situ* des sédiments (*e.g.,* texture, structure).

En revanche, les études numériques de chasse hydraulique ont étudié le phénomène complexe de transport sédimentaire par des approches simplifiées.

Les simplifications reposent sur les caractéristiques des sédiments, la texture (rugosité) réelle des égouts et le fonctionnement réel des vannes à chasse. De plus, la majorité des modèles ont été validés en laboratoire en raison des limites associées aux mesures sur le terrain. Il est clair que les modèles sont incapables de décrire et d'expliquer la variabilité spatiale de la taille des grains, en particulier dans des conditions instables. En outre, il n'est pas certain que l'inclusion de distributions de tailles de sédiments non uniformes affecte la hauteur du lit et d'autres paramètres obtenus à l'aide de simulations. Ainsi, l'application de modèles de sédiments non uniformes pourrait fournir des informations précieuses sur l'effet nettoyant du rinçage sur les sédiments déposés le long du canal en aval des dispositifs de rinçage. Ces informations sont pourtant essentielles pour une meilleure gestion des sédiments d'égout. Cela nécessite de disposer non seulement des modèles qui prennent en compte des granulométries variables (la composition des dépôts) et des données expérimentales fiables afin de valider ces modèles.

À cet égard, dans l'étude de la chasse hydraulique et du transport sédimentaire associé, les informations sur les propriétés physiques (et parfois chimiques) des sédiments dans les égouts sont essentielles. D'après la littérature, très peu d'études existent, qui évaluent l'évolution granulométrique fractionnée des sédiments sous l'effet de la chasse hydraulique. En effet, ce paramètre est essentiel pour comprendre l'efficacité des chasses sur les dépôts sédimentaires. Des études ont déjà montré l'importance de l'approche prenant en compte la non-uniformité des sédiments dans la quantification des processus liés à la dynamique des sédiments dans le fond des égouts (Campisano *et al.* 2008 ; Todeschini *et al.* 2010).

Le réseau d'assainissement unitaire souterrain de Paris fait partie des monuments historiques nationaux qui ont été construits depuis 1857 grâce à Georges Eugène Haussmann et Eugène Belgrand. L'écoulement dans le réseau est gravitaire avec des pentes variées selon la géométrie naturelle de la surface. Certains tronçons du réseau à faible pente n'assurent pas un bon fonctionnement hydraulique, causant une accumulation des sédiments transportés dans le système. L'accumulation des solides sur le fond du radier entraîne des conséquences néfastes dans la gestion du réseau. Ces problèmes appellent à des stratégies de nettoyage afin de limiter l'accumulation des sédiments. Parmi les méthodes de nettoyage, le curage du réseau à l'aide de la chasse hydraulique est considéré en comme l'un des moyens les plus pratiques d'un point de vue environnemental et économique (Chebbo *et al.* 1996).

0.2 Objectifs de l'étude

La présente recherche a pour objectif principal d'étudier la chasse hydraulique dans un collecteur appartenant au réseau unitaire parisien. Elle s'inscrit dans l'accomplissement de trois objectifs secondaires :

1) Mettre en place une campagne de mesures dans l'idée d'obtenir des données fiables et de haute qualité. Ces données permettront de mieux comprendre les processus de transport sédimentaire associé à la procédure d'opération de la chasse hydraulique.

2) Simuler les processus hydrodynamique et sédimentaire de la chasse en employant deux modèles physiques comme outils pratiques et appropriés à la prédiction des processus hydrosédimentaires.

3) Comparer l'applicabilité ainsi que les résultats des deux modèles avec deux approches différentes : sédiments uniformes *vs*. sédiments non-uniformes. Cette comparaison permettra de déterminer les avantages et les inconvénients de chacun des modèles.

Le premier modèle 1D (transport des sédiments uniformes) est une approche classique du transport solide dans tous les domaines et dans les procédés du curage en particulier. L'aspect novateur de la présente étude est l'élaboration du deuxième modèle 1D (transport des sédiments non-uniformes). Ce modèle prend en compte la composition et la large distribution granulométrique des dépôts : il permet donc de reproduire l'évolution de ces deux paramètres après l'opération de curage. Les deux modèles ont été développés au Département de Génie civil et d'Architecture de l'université de Catane (Italie). Les deux modèles ont été validés à partir de mesures expérimentales *in situ* d'une opération de chasse hydraulique.

0.3 Étude expérimentale de la chasse hydraulique

0.3.1 Expérimentations d'une chasse hydraulique dans un collecteur parisien

Un tronçon de 1,1 km du collecteur Des Coteaux, faisant partie du réseau d'assainissement unitaire situé dans le 11ème arrondissement de la ville de Paris, a été choisi pour réaliser ces expérimentations. La situation géographique est présentée dans les Figure 0.1 et Figure 0.2. Le profil longitudinal du collecteur étudié représente une faible pente (0,09 %). La forme transversale du collecteur est de type cunette avec des banquettes à circulation latérale. Les détails de la coupe du collecteur sont illustrés dans les Figure 0.3 et Figure 0.4. Ce tronçon d'étude présente des singularités sur sa pente longitudinale tout au long du canal. Étant par sa géométrie favorable à une sédimentation considérable, ce tronçon fait objet d'un curage annuel de façon manuelle par les égoutiers. En plus de la sédimentation, sur ce canal d'étude une vanne est déjà installée à 50 m en aval du tronçon étudié, ce qui permet potentiellement de générer des effets importants de chasse hydraulique. La position de la vanne est indiquée sur la Figure 0.3. Figure 0.4 montre la forme du collecteur (cunette avec des banquettes latérales de circulation).

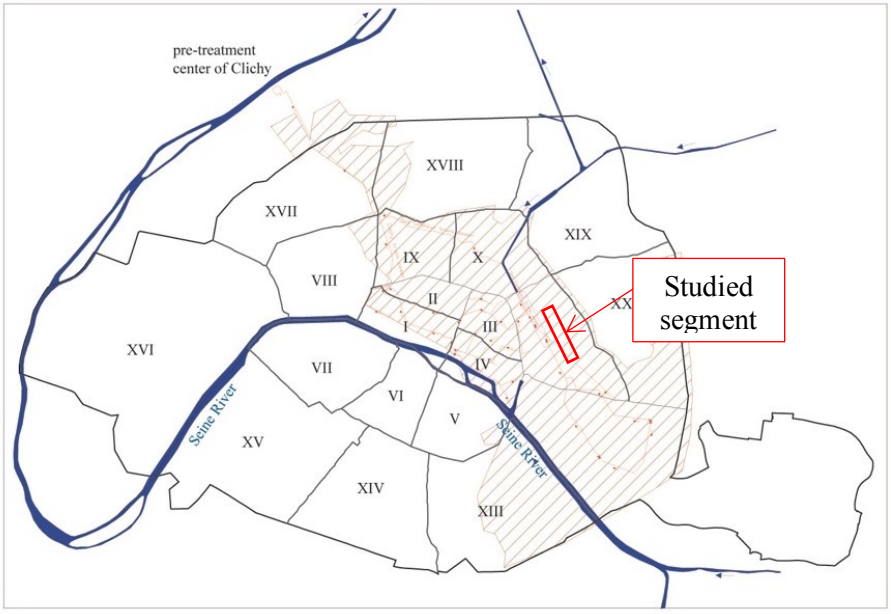

Figure 0.1 Situation géographique du site d'étude dans la ville de Paris.

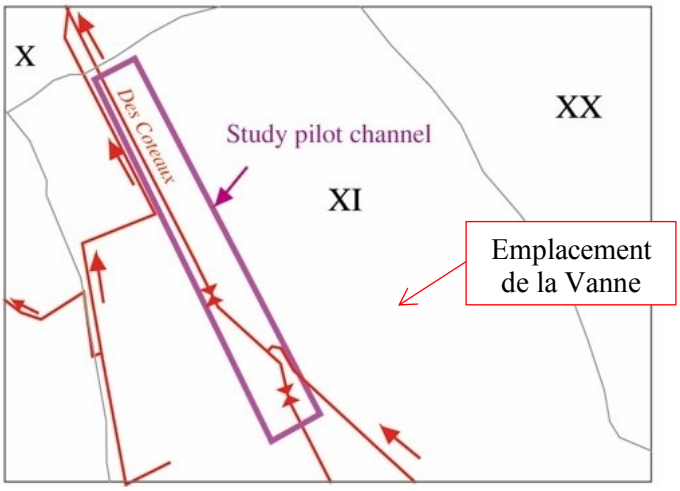

Figure 0.2 Tronçon d'étude et l'emplacement de la vanne.

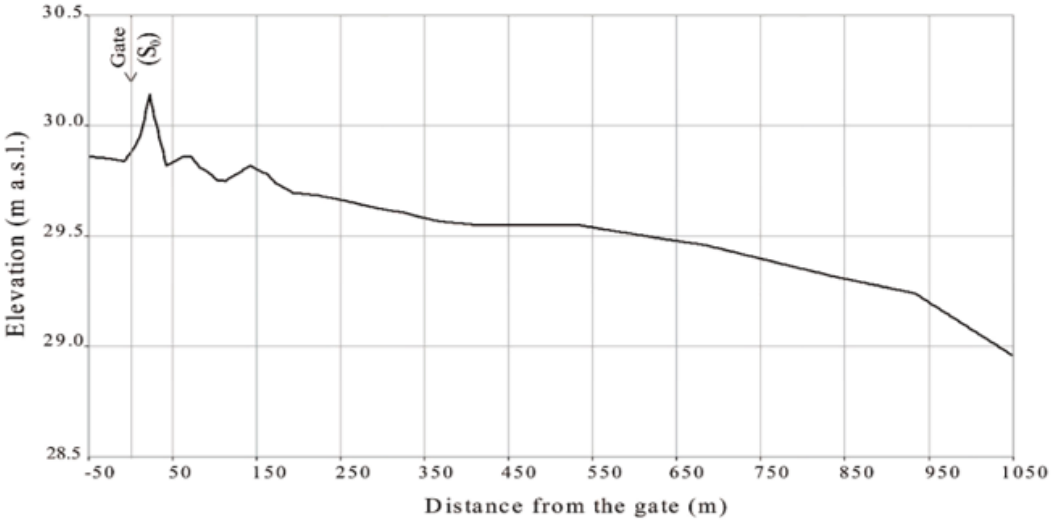

Figure 0.3 Profil longitudinal du collecteur d'étude (la position de la vanne est indiquée).

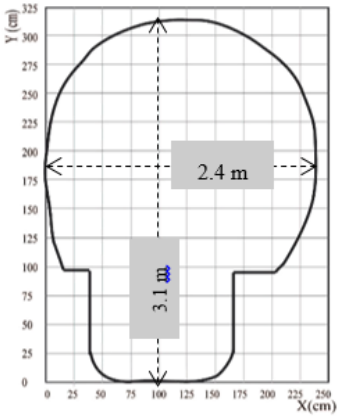

Figure 0.4 Coupe transversal du collecteur d'étude avec les dimensions.

Afin d'étudier l'effet de la chasse générée par la vanne sur les dépôts sédimentaires, une campagne de mesures hydrauliques et sédimentaires a été mise en place. Un protocole de mesures a été défini, permettant de collecter les données précieuses en trois épisodes : avant la chasse, durant la chasse et après la chasse sur cinq jours consécutifs (Tableau 0.1).

Tableau 0.1 Détails du déroulement de la campagne de mesures.

Date [j/m/a]	Activités expérimentales
07-08/08/2014	Collecte des données avant la réalisation de la chasse : • Échantillonnage des sédiments • Mesure Radar/sonar measurement
09/08/2014	Mise en place des équipements de mesures
10/08/2014	• Déroulement de la chasse hydraulique (stockage d'eau, lâché d'eau) • Mesures des variables pendant la chasse
11/08/2014	Collecte des données après la réalisation de la chasse : • Échantillonnage des sédiments • Mesure Radar/sonar measurement

Cinque sections de mesures ont été déterminées afin que les paramètres hydrauliques (*i.e.,* les variables d'écoulement) et sédimentaires (*i.e.,* la turbidité) soient relevés. Les paramètres mesurés avec le nom des appareils des mesures sur cinq sections sont présentés dans la Figure 0.5 et leur installation dans chaque section est illustrée dans la Figure 0.6.

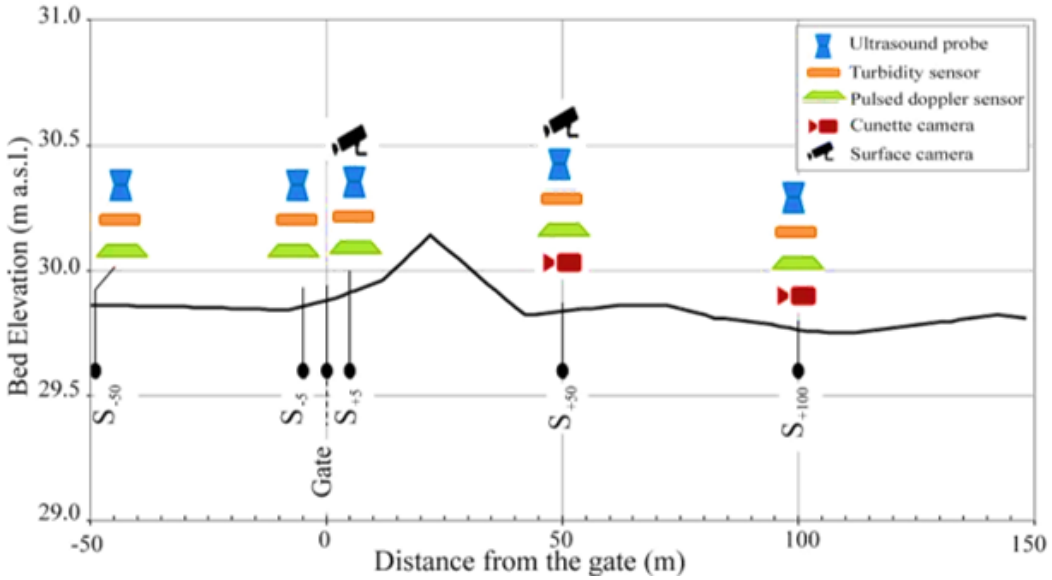

Figure 0.5 Emplacement des sections de mesures avec les appareils de mesures installés.

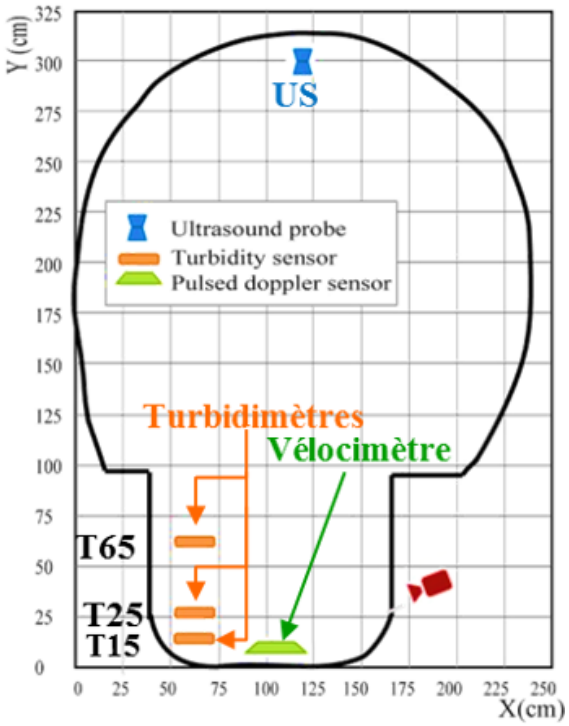

Figure 0.6 Installation des appareils de mesures hydro-sédimentaires sur la coupe transversale.

Les dépôts sédimentaires avant et après la chasse ont été évalués par deux procédures de mesure : 1) mesure en continue de l'épaisseur/volume des sédiments sur l'axe longitudinal ; 2) échantillonnage multiple des sédiments tout au long du collecteur. Ce dernier a été réalisé par extraction des sédiments puis analyse au laboratoire (granulométrie, teneur en matière organique). Ces mesures nous permettent d'obtenir l'évolution des dépôts sous l'effet de la chasse en comparant les sédiments en termes de volumétrie et de composition.

0.3.2 Résultats des analyses expérimentales

Les données ont été collectées durant les trois épisodes de mesures. Durant l'opération les variables ont été enregistrées pendant environ 1,5 h. La chasse elle-même a duré plus de 5 h. Les mesures de l'analyse des échantillons ainsi que les mesures volumétriques du dépôt initial et celui après le passage de la chasse ont été obtenues. Tout d'abord, les résultats des mesures volumétriques présentées dans la Figure 0.7, qui montre bien l'efficacité de la chasse sur les dépôts existants en termes d'érosion ou la déposition. La chasse a plus d'effet érosif sur toute la longueur du collecteur d'étude. Un volume de 5,61 m^3 a été éliminé de tout le canal (entre S_{-50} et S_{+1050}) dont 0,21 m^3 dans la section avant la vanne. Les résultats montent que la chasse a éliminé seulement 21 % des sédiments par rapport au dépôt avant la chasse.

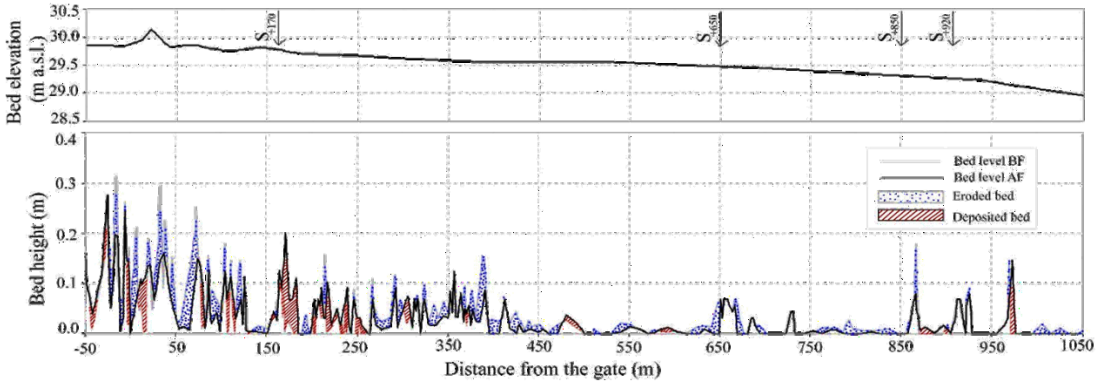

Figure 0.7 Résultats des mesures volumétriques des dépôts avant et après la chasse.

En s'intéressant à la composition des sédiments qui ont été emportés par la chasse, le volume (avant et après la chasse) de chaque section est décomposé en 4 fractions de taille de sédiments ($d<0.9$, $0.9<d<2$, $2<d<4$ et $d>4$ mm). On observe que les sédiments les plus fins notamment <4 mm ont été considérablement éliminés quasiment tout au long du canal d'étude. Au contraire, les sédiments grossiers ont été augmentés en quantité après la chasse car celle-ci a éliminé les sédiments les plus fins (particulières moins de 2 mm). Par ailleurs, l'arrivée des nouveaux sédiments grossiers de la partie plus en amont du site d'étude pourrait également être une autre raison de l'accroissement de la taille d'une partie des sédiments.

Afin de montrer la tendance de la composition des dépôts suite au passage de la chasse, toutes les courbes granulométriques avant et après la chasse ont été moyennées (Figure 0.9). On montre clairement une augmentation de la taille moyenne des sédiments sous l'effet de la chasse avec une moyenne de 2,67 et 4,06 mm avant et après la chasse, respectivement.

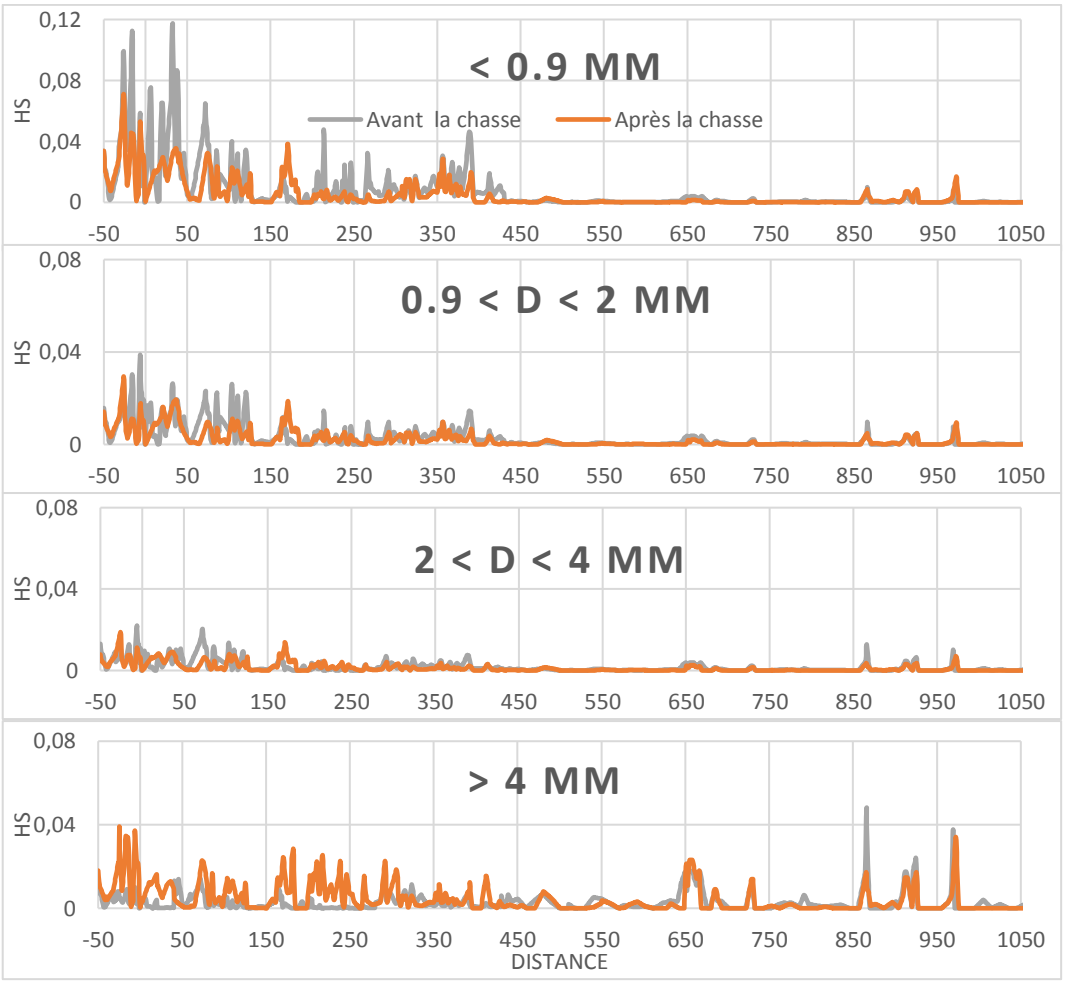

Figure 0.8 Evolution volumétrique des sédiments après la chasse décomposés en quatre fractions de sédiments.

En approfondissant cet effet de croissance de taille, les diamètres caractéristiques des sédiments (d_5, d_{10}, d_{16}, d_{50}, d_{84}, d_{90}, d_{95}) ont été évalués (Figure 0.10). Les diamètres choisis sont représentatifs des courbes granulométriques. La Figure 0.10 montre la comparaison des diamètres avant et après la chasse. Elle présente l'effet croissance dominant sur tous diamètres tout au long du collecteur.

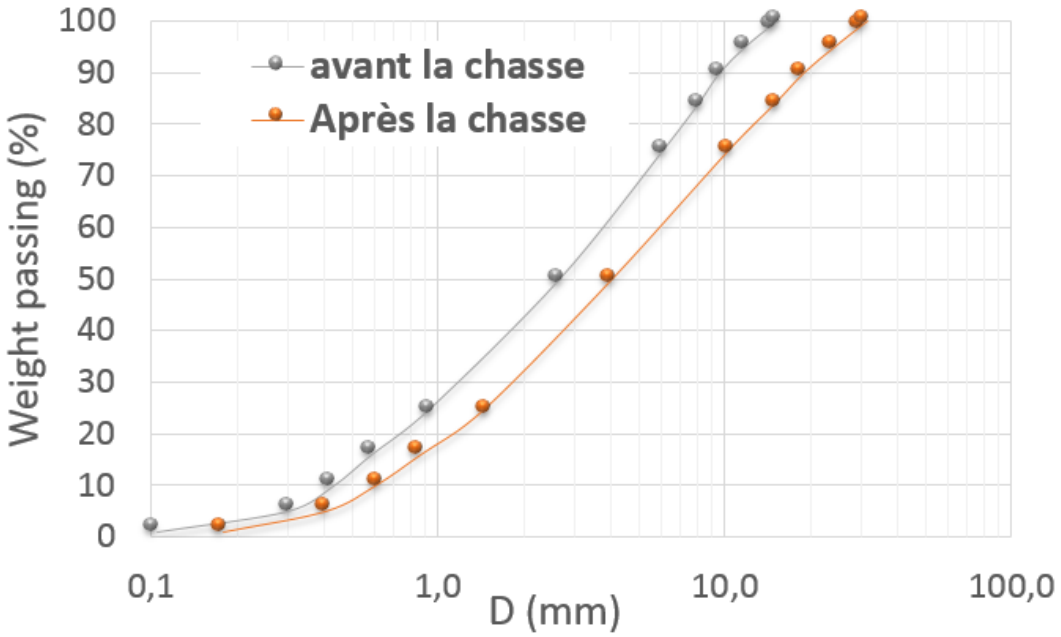

Figure 0.9 Moyenne granulométrique de toutes les courbes avant et après la chasse.

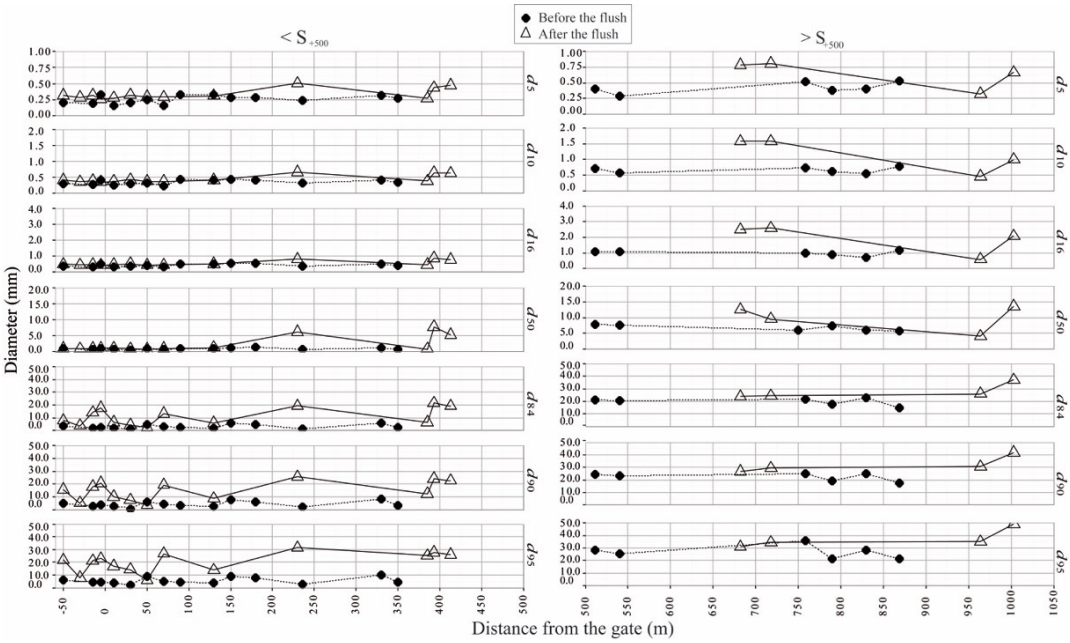

Figure 0.10 Effet de la chasse sur les diamètres caractéristiques des sédiments.

0.4 Étude numérique de la chasse hydraulique

0.3.1 Présentation des modèles

Un modèle de transport sédimentaire unidimensionnel a été développé sur la base des équations de Barré Saint Venant-Exner. Grâce à un schéma de résolution prédicteur-correcteur de MacCormack couplé avec TVD, le modèle est capable de simuler les écoulements non-stationnaires. Avec ce modèle deux approches ont été mises en avant pour simuler le phénomène de la chasse et le transport sédimentaire associé :

(i) Modèle avec une approche classique qui prend en compte les sédiments uniformes,

(ii) Modèle avec une approche qui prend en compte la non-uniformité des sédiments (composition). Dans cette modèle une approche de deux couches de lit sédimentaire a été mise en avant : couche active (couche d'échange des masses), couche rigide (lit de réserve des sédiments).

Le deuxième modèle calcule l'évolution de transport sédimentaire de chaque classe de sédiment. La dynamique sédimentaire est donc basée sur les caractéristiques appropriées de chaque classe des diamètres.

0.3.2 Comparaison des résultats de deux modèles

Les deux modèles décrivent non seulement les caractéristiques hydrauliques mais aussi ceux liés de transport des sédiments pendant la chasse hydraulique. Le niveau de précision de données est différent selon l'approche utilisée. Les sections suivantes présentent les résultats de chaque modèle. Afin de mieux présenter les résultats de façon synthétique, seulement deux sections de mesures situées avant et après la vanne ont été présentés.

Résultats hydrodynamiques des modèles

Les courbes présentées dans la Figure 0.11 et Figure 0.12 montrent que les deux modèles sont bien capables de décrire les caractéristiques hydrauliques du phénomène de la chasse. On remarque bien que le dégré de précision de deux modèles sont dans le même ordre avec une légère amélioration avec le modèle non-uniforme. Cela pourrait être expliqué par le fait que le modèle non-uniforme prend en compte les différentes tailles de sédiments permettant de mieux reproduire la rugosité du lit qui affecte les caractéristiques hydrauliques.

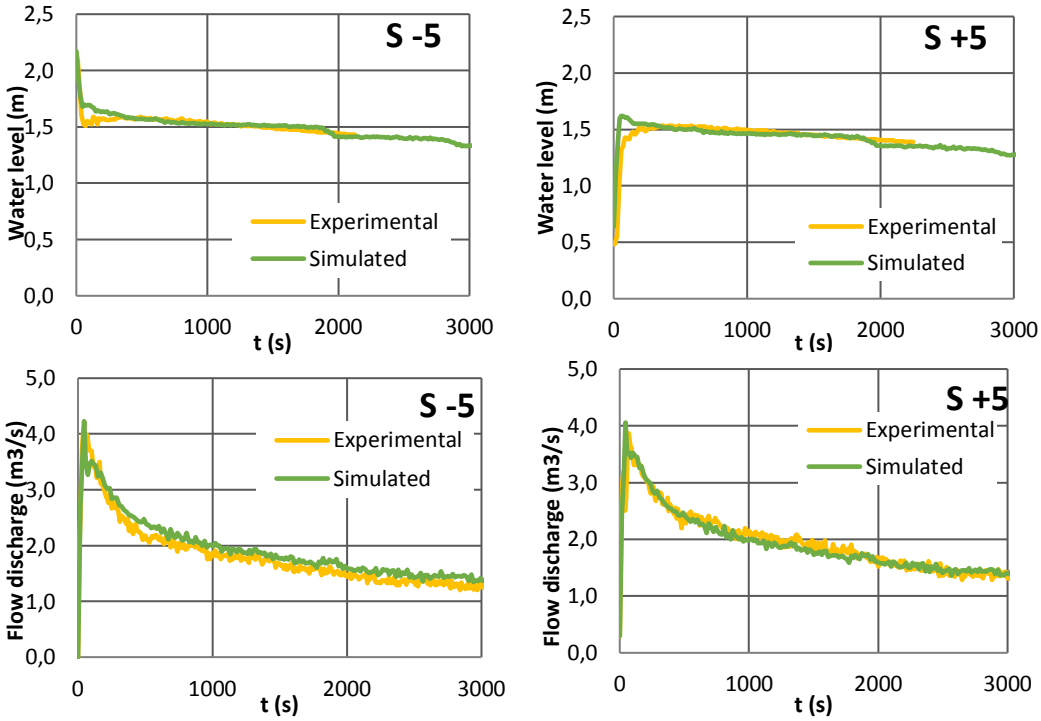

Figure 0.11 Résultats hydrodynamiques du modèle avec une approche de transport sédimentaire uniforme.

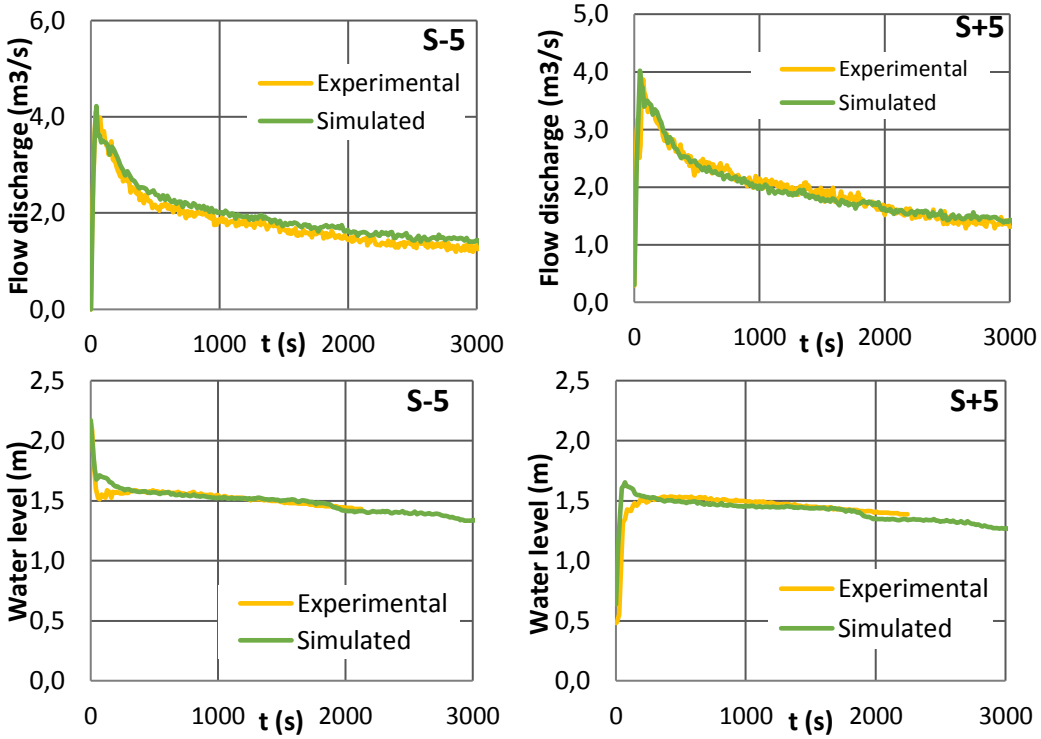

Figure 0.12 Résultats hydrodynamiques du modèle avec une approche de transport sédimentaire non-uniforme.

Résultat de transport sédimentaires décrit par les deux modèles

Les résultats des deux modèles sont présentés dans les figures suivantes. En termes de l'épaisseur des sédiments (Figure 0.13 et Figure 0.14), les résultats montrent que le modèle uniforme n'est pas capable de reproduire toutes les épaisseurs de dépôt tout au long du collecteur. Le modèle uniforme n'est pas capable de reproduire les mêmes dépôts accumulés après la chasse notamment sur le partie aval du collecteur (indiqués en cercle rouge sur la Figure 0.13). Ce manque de précision est principalement dû au fait que le modèle uniforme ne prend en compte qu'un seul diamètre qui ne représente pas toute la gamme de diamètres existant dans les dépôts. C'est la raison pour laquelle la dynamique des sédiments n'évolue pas en fonction de leur taille. Par ailleurs, une meilleure amélioration de la prédiction de transport sédimentaire est obtenue à l'aide du modèle non-uniforme. On observe que ce modèle a bien calculé le mouvement des sédiments sous l'effet de la chasse car les tailles réelles de sédiments (par classe granulométrique) ont été prises en compte. Cette amélioration peut être montrée par la diminution de l'erreur de prédiction RMSE (Square Root of MSE) de 0,045 à 0,028.

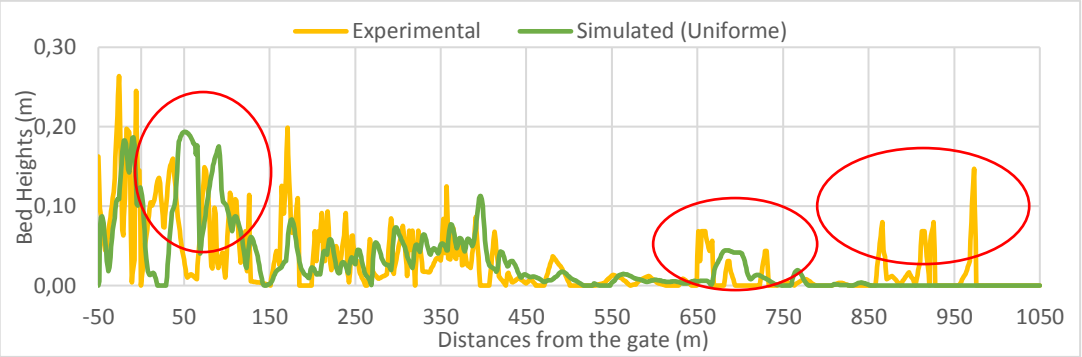

Figure 0.13 Résultats du transport sédimentaire obtenus par le modèle uniforme.

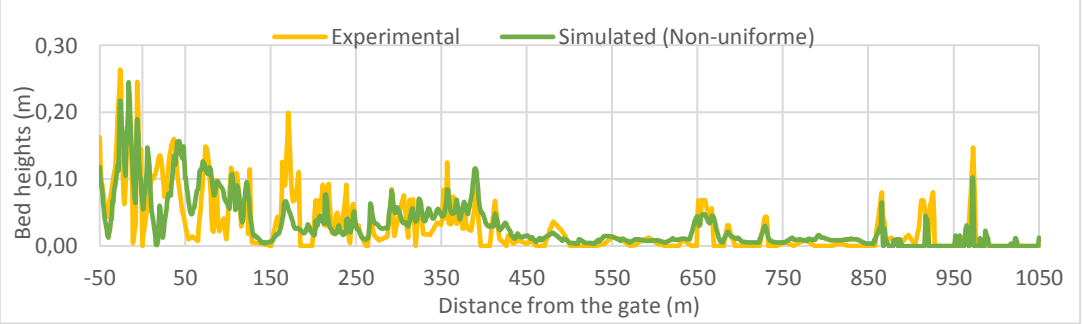

Figure 0.14 Résultats du transport sédimentaire obtenus par le modèle non-uniforme.

Le résultat des modèles en termes de volume des sédiments (Figure 0.15) représente des meilleurs volumes plus cohérents avec les données expérimentales (90 % volume obtenu par le modèle non-uniforme contre 68 % obtenu par le modèle uniforme).

Figure 0.15 Résultat des modèles en termes de volume de sédiments en comparaison avec les données expérimentales.

Éléments de comparaison	Modèle approche uniforme (Sim26)	Modèle approche non-uniforme (Sim16)	Données expérimentales
Volume amont de la vanne	0,84	0,60	0,21
Volume aval de la vanne	3,67	4,46	5,39
Volume restant	23,53	22,74	21,82

Hormis les améliorations observées, le modèle non-uniforme fournit des résultats complémentaires et consistants sur la composition des sédiments. Ces résultats sont importants dans l'étude de la chasse en s'intéressant à l'évolution de la composition des sédiments. Ces informations aident à comprendre l'effet de la chasse et sa performance sur les sédiments de différents diamètres.

Les résultats du modèle non-uniforme concernant trois différentes classes de sédiments sont présentés dans la Figure 0.16. Le coefficient de corrélation calculé (R^2) entre les données d'expérimentales et modélisées est de l'ordre 0,50, 0,32 et 0,19 pour les diamètres d_{16}, d_{50}, et d_{90}, respectivement. Ces valeurs confirment qu'une meilleure description a été obtenue pour les sédiments fins (diamètres < d_{50}). Par ailleurs, le résultat du modèle a été moins précis pour les sédiments grossiers (d_{90}) quasiment tout au long du collecteur.

De plus, afin de vérifier le bon fonctionnement du modèle non-uniforme, une analyse de sensibilité a été conduite. Vue le temps de simulation nécessaire, cette analyse a été limitée aux paramètres de l'entrée dont les valeurs basées sur la littérature. Ces paramètres sont le coefficient d'érosion de Velikanov (η_{min}) et l'épaisseur de la couche active ou pavement (δ_p). Un nouveau paramètre a aussi été activé afin de vérifier l'effet de la fonction *hiding* sur le transport sédimentaire durant la chasse. Les résultats de cette analyse de sensibilité sont présentés dans le Tableau 0.1. Ces résultats montrent que :

1) les valeurs maximale et minimale (recommandées dans la littérature) de coefficient d'érosion de Velikanov (η_{min}) n'ont pas des effets considérables sur le volume simulé remobilisé par la chasse. La valeur maximale ou minimale augmente et diminue légèrement le volume des sédiments éliminés par la chasse.
2) l'épaisseur de la couche active ou pavement (δ_p) a un effet considérable sur le volume de sédiments mobilisé par la chasse. La diminution de l'épaisseur de la chasse (de $3\times d_{90}$ à $1\times d_{90}$) diminue le volume éliminé par la chasse de l'ordre 30 %. Ceci pourrait être expliqué par un manque de sédiment (moins de stock des sédiments).
3) l'effet de l'activation de la fonction de *hiding* a montré une forte érosion des sédiments fins (partie amont) contrairement aux sédiments (partie aval) avec moins d'érosion.

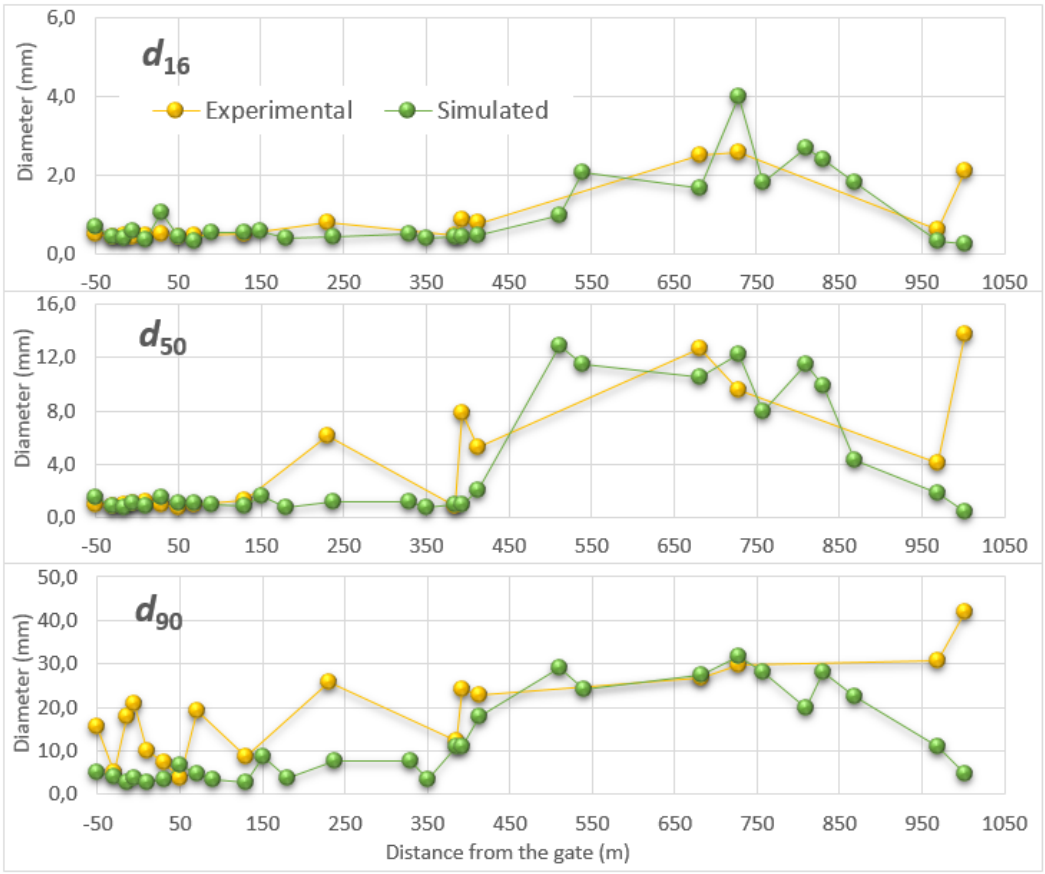

Figure 0.16 Résultats du transport sédimentaire obtenus par le modèle non-uniforme.

Tableau 0.1 Résultats de l'analyse de la sensibilité du modèle non-uniforme et comparaison avec les données expérimentales.

Distance		**Modèle approche non-uniforme (modèle de base)**	**η_{min}= 0.0005**	**η_{min} = 0.002**	**Sim16 + pavement avec 1*d_{90}**	**Sim16 + effet hiding**	**Données expérimentales**
Nom de simulation		**Sim16**	**Sim24**	**Sim32**	**Sim31**	**Sim29**	
all channel	(-50 to 1050)	5,06	4,81	5,09	3,67	5,22	5,61
Upstream gate	(-50 to 0)	0,60	0,60	0,60	0,24	1,10	0,21
Downstream gate	(0 to 1050)	4,46	4,22	4,49	3,42	4,11	5,39
Remained	(0 to 1050)	22,74	22,98	22,71	23,78	23,09	21,82
Bed heights	Max	24,47	24,62	24,65	28,04	20,21	26
	Mean	3,0	3,1	3,1	3,2	3,0	2,9
	RMSE	0,028	0,029	0,029	0,028	0,041	-

.

Tableau 0.2 présente une synthèse des avantages et des inconvenients de deux modèles de transport solide avec deux approches : uniforme et non-uniforme. Le deuxième modèle apporte plus d'avantages. Cependant, le premier pourrait être avantageux quand on s'intéresse seulement à une reproduction globale des épaisseurs/volumes déposés après la chasse.

Tableau 0.2 Synthèse avantages et inconvenants de deux modèles de transport solide uniforme et non-uniforme.

Prédiction de l'état des sédiments après la chasse	Uniforme	Non-uniforme
Temps de calcul	+ (5h)	- (24h)
Hydrodynamique	+	+
Taux de cisaillement sur le lit	+	++
Épaisseur des sédiments (profil)	+	++
Volume éliminé/restant de sédiments	+	++
Composition/texture	-	++

0.5 Conclusions générales

La présente thèse a eu pour l'objectif de :

1- Produire une base de données à travers des mesures *in-situ* et à haute résolution permettant d'expliquer de façon exhaustive la dynamique sédimentaire pendant la chasse;

2- Élaborer deux modèles (outils potentiels de gestion) permettant de décrire les phénomènes observés avec différentes approches du transport sédimentaire : uniforme (classique) et non-uniforme (nouvelle) ;

3- Analyser et comparer les résultats des deux modèles permettant de mettre en lumière leurs avantages et inconvénients.

Les travaux de cette thèse se résument en deux parties : expérimentale et numérique. Les résultats de ces deux parties nous ont permis d'arriver aux conclusions suivantes :

- L'importance des données expérimentales *in-situ* dans l'étude de la chasse, qui permet d'analyser les processus spécifiques à chaque site d'étude.
- Il est important de prendre en compte l'hétérogénéité des sédiments dans l'étude des processus de transport sédimentaire notamment par la modélisation numérique.
- Les deux modèles ont montré que les résultats hydrauliques sont assez fiables avec une légère amélioration pour le modèle non-uniforme.
- Le modèle uniforme est valable quand on s'intéresse seulement à l'hydraulique ou au volume global des dépôts.
- Le modèle non-uniforme apporte une meilleure définition convenablement fiable sur non seulement le comportement hydraulique mais aussi la dynamique des sédiments avec différents caractères physique (*i.e.,* diamètre de particule). Ceci explique que le modèle non-uniforme décrit correctement l'érosion et la déposition des particules de différentes tailles pendant la chasse. Ce qui résulte à l'évolution de la composition des sédiments. De plus, ce modèle est capable de reproduire les dépôts tout au long du collecteur en termes d'épaisseurs et de volume.
- A l'issu du point ci-dessus pourrait être encore utile lorsque nous nous intéressons à l'étude des chasses consécutives et leur impact

sur les dépôts.

- Les résultats montrent que les deux modèles pourront potentiellement se servir en tant que des outils de gestion selon les ressources, demande et objectifs (précision) lors des études de la chasse.

CHAPTER 1
INTRODUCTION

1.1 General background

Adopted European Water Framework Directive imposes the limitation of the pollution to be entered into the environment. Urban drainage systems as one of the main sources of pollution should be controlled. Like many concerned European countries, one of the preoccupations of Parisian sewer managers is the sediment accumulation on the bed inverts of the sewer channels and pollution problems that may derive. A considerable number of large sized sewers in Europe are suffering from deposition, accumulation and consolidation of sediments along the channels. The sediment accumulation can occur in both stormwater and combined sewer networks. This problem is mainly due to the low hydraulic conveyance of the flat channels where the hydraulic and geometric conditions lead to determine sedimentation (Ashley *et al.* 2004). Maintaining combined sewers free of deposits requires a good level of management with or without human intervention. However, the risk of human intervention is known to be dangerous for health due to the emission of toxic gases during cleaning operations. This is one of the reasons that new cleaning policies of municipalities tends to reduce the human intervention by enabling automatic strategies for sewer cleaning.

Among the existing strategies, flushing of deposits over the sewer channels is considered as one of the most practicable, operative, enviro-economic and efficient techniques to overcome problems associated to the deposited sediments.

In this perspective, during the last decades a number of researches from all around the world have spent efforts to study the conditions for optimal flushing in sewer systems. The required conditions to produce effective flushes on the sediments deposited on the channel have been studies both experimentally and numerically. Overall, the experimental and numerical studies of flushes involve mainly evaluating the shear stresses provided by the flush waves throughout the channels (Campisano *et al.* 2004; Bertrand-Krajewski *et al.* 2004, 2005; Creaco and Bertrand-Krajewski 2009). Then, hydrodynamic and sediment-transport processes associated to the flushes have been investigated at both the laboratory and/or the field scales. The available laboratory flushing experiments led to obtain important indications concluding the theoretical results on the erosive behaviour of flushes generated by various devices. However, very of the laboratory experiments have conducted within simplified conditions including sediment conditions (*e.g.,* use of synthetic sediments), simplified geometry of channels (*e.g.,* rectangular flumes) that may be far from the real sewer conditions (Campisano *et al.* 2006; Todeschini *et al.* 2008). In fact, real filed studies about flushing have shown increased complexities due to the heterogeneity of the sediments, local conditions and other unknown processes.

In addition to the experimental studies, numerical modelling investigations have so far been conducted by various researchers. These investigations were developed for various purposes such as: *i*) to improve flushing device design for their use in sewers with sedimentation problems; *ii*) to evaluate the deposit removal efficiency of flushing devices. As limitation, it can be mentioned that an appropriate numerical description of the flushing process requires a trustable quality of experimental data for model validation with an acceptable level of accuracy. However, reliable data arises from the use of suitable measurement devices specifically designed for sewer application. Many authors agree that the use of one-dimensional models could be enough detailed for predicting shear stresses and associated sediment transport during flushing. Nevertheless, the application of multidimensional models to describe the propagation of flushes in sewer channels could be an interesting option in particular in presence of singularities (*e.g.,* shape of cross-section).

Focusing on the wide range of sediments in sewers (in terms of physical and chemical properties), according to the literature, the analysis of flushing as method to remove in-sewer deposits is far from being understood. Sediment dynamics during flushing operations requires farther observation as well as improved simulation of a number of physical processes. More performant models are mandatory to study the erosion, transport and sedimentation processes of sediment mixtures in sewers. The importance of non-uniform sediment beds in the simulation of solid transport processes has been amply demonstrated. Indeed, most of the knowledge on the processes related to the bed-load sediment dynamics in sewers is based on simplified models, in which uniform sediment is assumed. In addition, majority of these models has been validated in laboratories due to the limitations associated to field measurements. Clearly, these models are unable to describe and explain spatial grain-size variations in particular under unsteady conditions. Besides, it is uncertain whether the inclusion of non-uniform sediment size distributions affects the bed heights and other parameters obtained from simulations. Thus, the application of non-uniform sediment models could provide valuable information about the cleaning effect of flushing on the sediment deposited along the channel downstream of flushing devices. Such information would be essential for a better management of sewer sediments *e.g.,* knowledge about flushing and corresponding transport capacity for different grain sizes of the deposits.

Parisian sewer network system, one of the most important French national patrimonies works hydraulically by gravitation. Thus, over the flat channel sections of the network problematic sediment accumulation occurs and within time, it becomes quasi permanent deposits. This, oblige the Paris Municipality to deal with the deposits by strategically removing them from the network. To this end, various sewer reaches are cleaned hydraulically but by the mean of sewer operators who are exposed to the toxic gases during the

cleaning operations. Therefore, the sewer network service of Paris Municipality has been engaged in finding out the most practicable, economic and performant solutions to overcome this problem and limit as maximum as possible the sediment accumulation over the channel inverts. They aimed to evaluate the feasibility and efficiency of possible and adapted gates for cleaning objectives to the sewers (*e.g.* collectors) and depending on sewer sector and channel conditions. Among the handled projects, an already existing gate (radial tipping gate with weir function) was considered to be a potential flushing device. In particular, the gate was initially designed to derivate water in case of high flows due to the storm events. The sewer channel downstream of the gate was prone to significant sedimentation that was cleaned yearly by the Municipality. The idea of flushing the sewer by using this gate was proposed after having made a sewer inspection and hydraulic studies of the gate performance. A single flushing operation was planned to monitor the flush by recording more variables possible related to the hydro and sediment dynamics during the event. Therefore, a protocol of a measuring campaign in co-operation with *Ville de Paris*, PROLOG *Ingénieurs* and Paris Diderot University was adopted in order to obtain high enough quality data using various apparatus that are compatible with the sewer conditions.

1.2 Aims and objectives

The current research was carried out in order to study the potential of flushing to clean the sewer channels and remove sediments. To this end, following objectives were defined:

1) to set-up a field experimental campaign to obtain high-quality data. This data allowed to understand the processes associated to the flushing operation in sewers.
2) to model the flushing hydrodynamics and associated sediment transport processes properly in order to set-up an adequate and practical numerical tool able to predict both flushing flow and associated sediment removal efficiency of in Paris sewer Network.
3) to compare model for uniform sediment transport with model for non-uniform sediment-transport mixtures and then determine the advantages and limitations of both approaches.

The study, in collaboration with the University of Catania, tries to obtain high quality and comprehensive data to develop a non-uniform sediment-transport model. Comparing to the common uniform sediment transport models, this novel approach, by taking into account a definite number of size of classes, is to be expected to reproduce the multi-grain-size distribution of the sediment after the flush operation. To this end, a non-uniform sediment-transport model developed in the University of Catania (Department of Civil and Architecture) was adapted for the analysis and validated using the experimental data. The capacity of the non-uniform sediment-transport model will be evaluated in particular, in describing the hydraulic and sediment-transport processes during the flush by reproducing the variations in the bed composition during the flush.

The experimental part of the present thesis was partially supported by PROLOG Engineering Consulting. Also, the project was supported by the Paris's sewer network (SAP) of the Paris Municipality (*Ville de Paris*) in 2014.

1.3 Synopsis and feature of current thesis

The outline of this dissertation is as follow:

Chapter 1 gives an introduction to the flushing operation in flat sewers, where deposits contain highly variable sediments that generate operational problems in sewers. In this chapter an overview of the problems of this research was presented. It was also described how this research can fill the gap in understanding the sediment transport during this flushing operation in sewers.

In Chapter 2, a general overview of the scientific and literature on sediment properties and sediment-transport mechanisms in open channel flows will be presented. The chapter firstly provides a basic review of papers dealing with in-sewer deposits characteristics, internal sediment processes, as well as sediment-transport mechanisms in combined sewers during dry- and wet-weather. Also, the techniques suitable to clean sewers are presented including flushing. Finally, a synthesis of experimental and numerical investigations on sewer flushing from the literature was developed.

The experiments carried out in the Parisian combined sewer network are presented in Chapter 3. Site characteristics, measuring protocols, execution of flush operation, flushing observation, data collection, etc. are examples of information that can be found in this chapter.

Chapter 4, summarizes the experimental results of the monitoring of the flush experiment in terms of hydrodynamic- and sediment transport-related parameters. Pre-processing and preparation of data for the analysis is firstly described. Furthermore, a comprehensive analysis of the collected experimental data is presented. An estimation of the performed flush experiment in terms of sediment removal efficiency in carried out.

In Chapter 5, a detailed description of numerical models used in this research to describe the flush process is given. Basic equations, solving methods, boundary conditions and numerical aspects can be found in this chapter.

Chapter 6 presents the application of the used models to the experimental case of flush in the Parisian large-sized sewer. The preparation of data as input to the models is firstly described. Furthermore, the initial and boundary conditions are defined for each model. Then, the results of the numerical simulations using the adapted models were presented for appropriate comparison. A sensitivity analysis of basic input parameters of the models is also presented in this chapter to evaluate the influence of the sediment transport-related outputs.

Finally, in Chapter 7, outcome of the present study is summarized and then concluding remarks are drawn. At the end, an outlook to the future work is presented.

Chapter 2
Literature Review on Sediment Transport under the Sewer Flushing

2.1 Sediment-transport mechanisms in open channels

Sediment-transport mechanisms in natural courses are not yet completely understood due to the complexities related to the sediment dynamics. This complexity in studying the processes being as specific phenomena is increasing for mechanisms in sewer network because various reasons for example the heterogeneity of sediments in-sewer sediment in terms of density and types, the major presence of non-mineral elements in sewers *e.g.,* microbial pollutants, micro-organisms, heavy metals, pharmaceutics.

In this chapter, a state of art on sewer flushing and on the associated sediment transport is presented. The chapter also discusses the results of literature review on cleaning techniques with emphasises on numerical and experimental studies dealing with sewer flushing operation. Preliminarily, an overview of sediment-transport processes including sewer sediment remobilisation, erosion, transport and sedimentation mechanisms is presented.

2.1.1 Generalities on hydrodynamics and sediment transport

After Vanoni (2006) all processes involving the erosion, entrainment, transport and deposition of sediment particles usually constitute the research branch of "sediment engineering". These are complex processes that typically occur in the flow streams as free surface flows such as in rivers. Movements of particles depend on many parameters relating to the particle and to the flow properties as well as their interaction due to the turbulence and the velocity of the flow. In this section, basic concepts of hydrodynamics in open channel flows, which is needed to explain sediment-transport mechanisms in sewers, are briefly presented.

Flow characteristics in open channels

Open channel flow is a flow in a channel (conduit) as schematized in Fig. 2.1 that is not completely filled and a free surface is formed between the flowing fluid (water) and the air. The gravity force is the main force that drives such flows (Chanson 2004). Main flow characteristics in open channels are:

1) The water discharge $Q = V \cdot A$ in (m^3/s) where V (m/s) is the flow velocity and A is flow cross-sectional area in (m^2),
2) R_h the hydraulic radius $R_h = A/P$ in (m) where P is the wetted perimeter,
3) The friction slope S_f in (m).

4) The shear velocity of the flow $u^* = \sqrt{\tau_0 / \rho}$ where τ_0 and ρ are the flow density in (kg/m^3) and the averaged bed shear stress (in N/m²). The shear velocity is a measure of the flow ability to remobilize the sediments.
5) The specific weight γ in (N/m^3) equals to $\gamma = \rho \cdot g$ where g is the gravity acceleration (m/s²).
6) The Reynolds number R_e used as the parameter to determine the flow types.

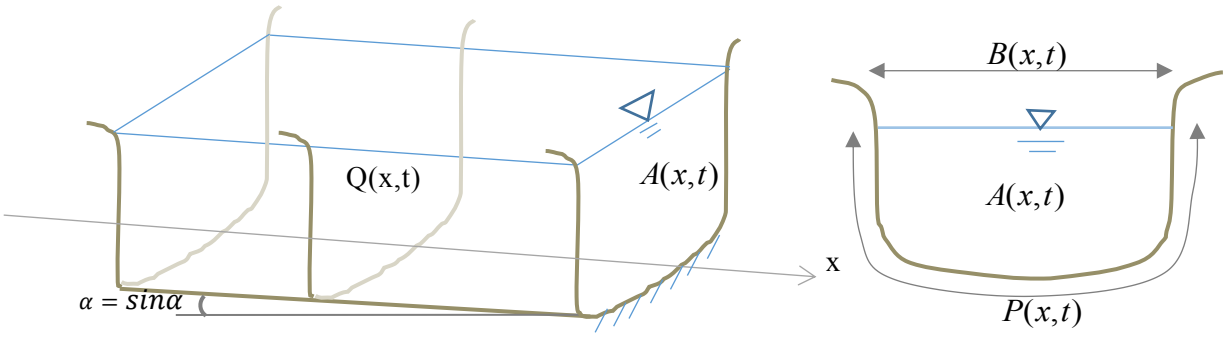

Fig. 2.1 Scheme of open channel flows.

Sediment characteristics

The bed sediment resistance to the flow in open channels is affected by several factors such as the bed characteristics and the sediment features. Main physical sediment characteristics for sediments in open channel flows are as follows:

1) The grain size: as natural particles have irregular shape, the grain size refers to the corresponding spherical diameter (by universal common definitions). Therefore, the sieve diameter equals to the fine mesh size through which the particle can pass. Sediment size is measured in mm as presented in Table 2.1.

Table 2.1 Sediment size classification.

Size range	**Aggregate class**	**Size range**	**Aggregate class**
64–256 mm	Cobbles	0.5–1 mm	Coarse sand
32–64 mm	Very coarse gravel	0.25–0.5 mm	Medium sand
16–32 mm	Coarse gravel	125–250 µm	Fine sand
8–16 mm	Medium gravel	62.5–125 µm	Very fine sand
4–8 mm	Fine gravel	3.9–62.5 µm	Silt
2–4 mm	Very fine gravel	< 3.9 µm	Clay
1–2 mm	Very coarse sand	< 1 µm	Colloid

2) The density ρ_s in (kg/m^3) and the specific weight of sediments γ_s in (kg/m^3) being the mass and weight of sediment per unit volume, respectively.
3) The porosity (-): that quantifies the fraction of a given volume of sediment that is composed of pore or void spaces between the solid particles. Sorting is in relation with porosity ratio of samples. Sandy sediments present often porosity around 0.4.

Other important parameters are:

1) The grain-size distribution: that represents the range of sediment diameters and their weight percentages in a given mixture. Cumulative or frequency grain-size distribution curves are derived from this data. Characteristic diameters (*e.g.,* mean diameter: d_{50}) are typically issued from such curves.

2) The volumetric sediment concentration of suspension: is a sediment mixture property by volume or weight (unitless) or sometimes by dried weight or mass of sediments per unit volume of water-sediment mixture (in N/m^3 or kg/m^3). The volumetric sediment concentration can modify the fall velocity of particles in a given flow due to the particle interactions in the water column.

3) The fall or settling velocity (w_s) being the terminal fall velocity of a particle in still water. In open channels the fall velocity of particles in suspension is affected by the turbulence characteristics as well as by

the volumetric sediment concentration (Graf 1971; Nielson 1993; Van Rijn 1993). According to the Stock's law this parameter could be expressed as follows.

$$w_s = \left(\frac{4}{3} \frac{(s-1)gd}{c_D} \right)^{1/2} \quad \text{Eq. 2.1}$$

where c_D is the drag coefficient, s is the specific gravity of the sediment ($s = \rho_s / \rho$), d is particle diameter (in m).

2.1.2 General aspects of sediment transport in open channels

Incipient motion

Threshold conditions to initiate sediment transport are usually described by observing motion of sediment grains. Flow acts on the grains and, in turn, resistant forces (including gravity and internal cohesion forces) to entrainment can develop depending on the grain size as well as the distribution of the whole grain sizes in the bed sediments. The sediment motion will initiate when the downslope component of the gravity and sediment mass exceeds the total resistant forces to the movement. In order to understand the initiation of motion of a particle, it is necessary to take account all forces that impact a particle at equilibrium. In an open channel flow with loose bed sediments, the forces acting on each sediment particle are shown in Fig. 2.2. Such forces comprise:

The drag force (F_D) is friction of the flow on the exposed surface of the grain. This force is a function of the grain surface exposed to the flow as well as of the flow velocity.

The lift force (F_L) is due to vertical flows. This come into play when turbulent eddies aim to carry the particles.

The gravity force (F_G) is related to the weight of the particle and is calculated from the universal Einstein equation $F_G = \rho \cdot g \cdot W$ where W is the volume of the particle (in m^3) (Einstein 1950).

The buoyancy force (F_L) is the pressure-difference force on a single grain size that makes submerging the specific weight of the particle in water.

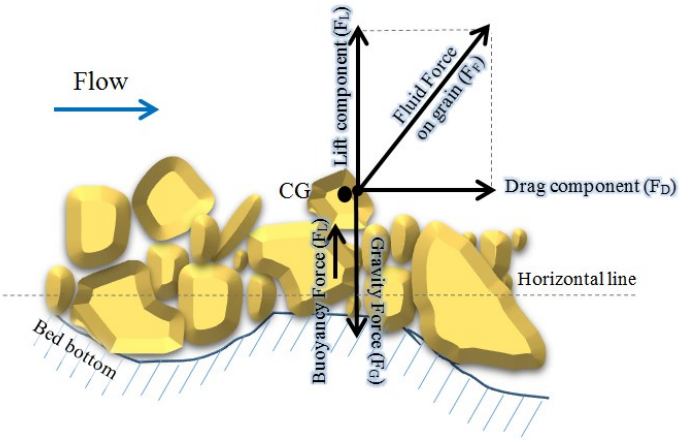

Fig. 2.2 Definition sketch of forces acting on a non-cohesive grain by the flow.

Fluctuating forces are caused by the turbulence, including the occurrence of coherent structures, as well as the interactions among the whole hydrodynamic system. In high Reynold number flows, due to the turbulence fluctuations and diffusion, particles on the bed may be exposed to instantaneous forces through different directions. However, the gravity force is always acting on the gravity centre of the particle. So, turbulent flow involves the instants in which resultant force on the grain is varying rapidly instantaneously. Moreover, at the same instance, as the particle geometry as well as the exposed position to the flow varies from one to another, the exerted forces are varying too due to the turbulence velocity in the field. Unfortunately, predicting the evolution of the sediment flux suspended within a turbulent carrier fluid is complicated. The complexity is due to a multitude of difficulties that stem from how the particles are organized within the flow structure, and how the dynamics of the particle feedback alters the turbulence characteristics of the carrier flow. Regarding to this point, highly stochastic particle movements lead to the difficulty to define bed initiation of motion and then to establish a unique sediment-transport capacity in time and space. In this regard, various sediment-related factors (*e.g.,* bed specific weight, angle of repose) play the role in determining the threshold motion of bed-load.

Drag and lift forces acting on particles are related to flow conditions. So, the threshold condition of movement for uniform sediment can be approximated by the Shields (1936) diagram which can be applied for non-cohesive particles ranged from silt to gravel sizes (Fig. 2.3). The diagram shows the roughness (shear) Reynolds number (equal to $u*\cdot d/\nu$, where d and ν is the particle diameter (in m) and kinematic viscosity of water (in N×s/m²), respectively) against dimensionless critical shear stress (θ) by the flow on the grain size represented on abscissa and ordinate, respectively. The dimensionless form of the bed shear stress (known also as *Shields stress* or *Shields parameter*) can be estimated from the following relationship:

$$\theta = \frac{\tau_0}{(\gamma_s - \gamma)d} = \frac{u^{*2}}{g(s-1)d} \qquad \text{Eq. 2.2}$$

in which s is the specific gravity of particle ($s = \rho_s / \rho$).

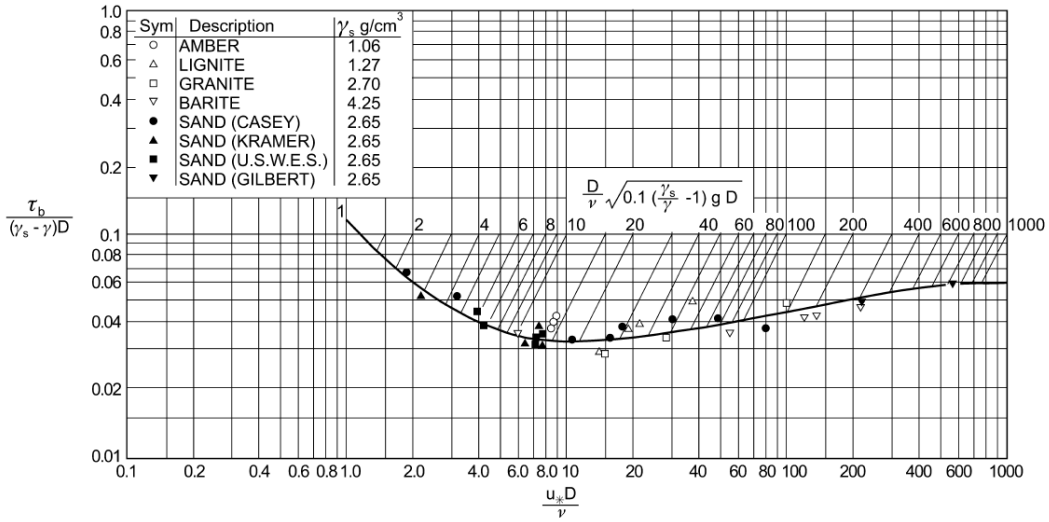

Fig. 2.3 Shield's diagram of incipient of motion (Adapted from Vanoni 1964).

From this relationship, the critical Shields number can be also derived which allows determining the threshold condition of sediment motion within given flow.

The critical Shields shear stress relationship commonly applied to describe the conditions under which bed sediment particles does not still move but are at the verge of entrainment. The Shields value obtained from the diagram for the critical condition is 0.06 for highly turbulent flow. However, further laboratory experiments suggest smaller values for the dimensionless critical shear stress for mixed size gravels such as 0.03 (Neill 1968) and 0.046 (Gessler 1971).

The value of Shields parameter is linked to the bed state. In reality, the work of Shields to assess initiation of motion of the grains is originally limited to non-cohesive sediments for uniform flows.

It should be noticed that the incipient motion of non-uniform sediment particles has been investigated by various authors who proposed empirical relationships or modified previous formulas such as Qin (1980); Parker *et al*. (1982). These formulas try to account for existing interactions among the various size classes within the sediment mixture (Wu 2008). Nevertheless, the Shields diagram is widely used to approximate measure of grain size that is in the threshold conditions of movement for all flow conditions.

As the threshold motion condition is achieved, when instantaneous vertical component of flow exceeds the settling velocity of particles, transport of grains occurs. Since the grain size goes into the motion, it is transported by the flow within two possible transport modes upon the flow conditions. The bed-load refers to the materials that are transported in the bed region whereas transporting at higher position in water column is known as suspended load (see next sections). These two modes can be roughly inferred from the ratio of settling velocity to shear velocity (w_s / u_*). Typically, values of this ratio smaller than 0.5 and larger than 1.0 denote dominant particles travelling in suspension and as bed-load, respectively.

Rouse (1937) proposed the number from the following relationship to evaluate the threshold of sediments transport modes (Armanini 2018):

$$R = \frac{w_s}{\kappa \cdot u*} \qquad \text{Eq. 2.3}$$

where κ is the Von Karman coefficient equal to 0.4.

Table 2.2 provides the range of values of *R* corresponding to the various modes of transport of the sediments. According to the table, Rouse number should remain larger than 2.5 to account for the bed-load transport, while values smaller than 1.2 ensure the presence of suspended load.

Table 2.2 Rouse method for classifying the transport regimes of particles.

Transport mode	**Rouse number** ($w_s / \kappa u_*$)
Bed-load	R>2.5
Incipient suspended load (50% suspended load)	1.2<R<2.5
100% suspended load	0.8<R<1.2
Wash load	R<0.8

Calculation of *R* for each grain size (size class) requires estimating the settling velocity (w_s) of the various grain sizes. Among the authors (Hallemeier 1981; Ahrens 2000, Stockes 1851) that have proposed empirical formulas to assess the fall velocity and then, to categorize particle transport regime, She *et al*. (2005) have established a relationship to estimate this parameter (Armanini 2018).

The fall velocity of each particle is calculated from the equation presented below (Eq. 2.4). In this equation, the left term denotes the dimensionless particle Reynold's number.

$$\frac{w_s \cdot d}{v} = 1.05 D_*^{1.5} \left[1 - \exp(-0.315 D_*^{0.765})\right] \quad \text{Eq. 2.4}$$

where D_* is a non-dimensional parameter value that is calculated from the following empirical formula (Bonnefille 1963):

$$D_* = d_n \left(\frac{(s-1)g}{v^2} \right)^{1/3} \quad \text{Eq. 2.5}$$

Type of transport for each particle is different upon various main particle physical characteristics and, in particular the size of grain. A particle in motion can be kept in suspension or move as bed-load regarding to the flow properties. These modes of displacement are explained hereafter.

Bed-load transport

A large literature exists on sediment transport in open channel flows. This section discusses fundamentals of sediment transport with reference to different authors such as Graf (1971); Vanoni (2006); Chanson (2004); Garcìa (2008) and Armanini (2018).

Commonly, total sediment-transport discharge comprises all the particles in motion in the whole water column that are transported within two main modes of displacement: bed-load transport and suspended-load transport (Fig. 2.4). Other classifications introduce a third mode of transport in which very fine particles are transported without interact with the existing bed of sediments (Einstein and Chien 1953). This mode of transport, called *wash load*, and is often included by much of the authors as suspended load.

Sediment goes into movement in different stages when the boundary shear stress just exceeds its critical value. At the beginning, sediment is transported by sliding and rolling over the upper layer of the bed. Saltation may occur when flow increases. In other words, as illustrated in Fig. 2.4, bed-load occurs when the flow velocity is high enough leading particles to roll, slide, and finally saltate. In the later mode of bed transport (rolling and sliding), particle makes short jumps into the water for a short time while in the two other modes, the particle remains always in contact to the bed (Vanoni 2006). Thus, bed-load transport is tangential to the bed. However, because distinguishing saltation mode from other is not easy, all these three modes are therefore considered as bed-load transport. In any case bed-load

transport is considered as tangential to the bed and to occur within the bed-load layer. According to Garcia (2008), such a layer, serves as an exchange zone between bed and suspension zone for the sediments going in to the flow.

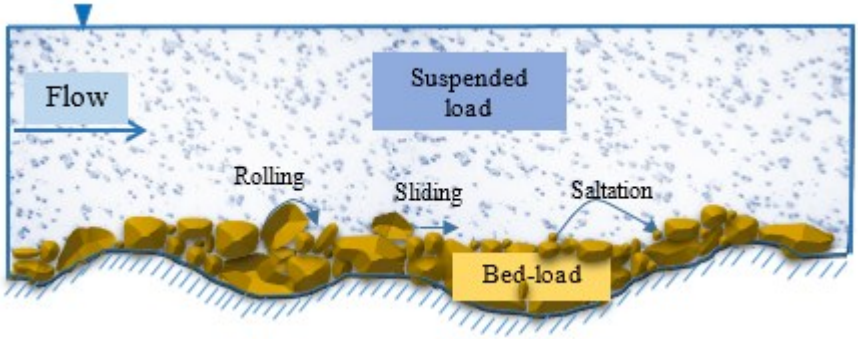

Fig. 2.4 Simple scheme of bed and suspended load in open channel flows.

In the nature, bed-load sediment transport presents many phenomena such as sediment armouring, hiding/exposure and downstream fining that result in grain-size sorting or segregation. Such phenomena may explain transport selectivity of the flow. In particular, selective transport of bed particles is enabled when the shear stress is smaller than the critical shear stress corresponding to d_{50}. In contrast, when shear stress exceeds the critical value, then, selectivity has no more significations because the particle interactions become much more dominant and influence the transport mechanism (Armanini and Di Salvio 1991).

Bed-load transport of sediments can be quantified by the bed-load flux (q_{sb} in $m^3/m \times s$, being as bed-load transport rate of non-suspended sediments by volume per unit time and width). The maximum value of q_{sb} that a flow of prefixed characteristics can transport is called bed-load transport capacity and can be determined using empirical relationships. Examples of these relationships are presented in Table 2.3. The most used formulas are a function of excess shear stress (*i.e.,* the difference between the flow shear stress and the critical shear stress) which causes the bed sediment to be transported. In these formulas shear stress of the flow is usually related to the critical shear stress taking into account a grain size representative of the bed sediment.

Table 2.3 More commonly used sediment-transport formulas for bed-load sediment transport.

References	Sediment-transport discharge equation	Range of validity	Parameter definition
Ackers-White (1980)	$q_{st} = \frac{u*}{\sqrt{gd(s-1)}}\left(\frac{V}{\sqrt{32}\log_{10}(10h/d)}\right)^{1-n}$	d>2.4 mm	n: constant value depending on d h: water depth
Van Rijn (1984)	$\frac{q_{sb}}{d\sqrt{g\Delta d}} = 0.053(\frac{\tau-\tau_c}{\tau_c})^{2.1} D_*^{-0.3}$	d>0.2 mm	$\Delta = \frac{(\rho-\rho_s)}{\rho}$
Meyer-Peter and Müller (1948)	$q_{sb} = 8(\tau-\tau_c)^{3/2}$	0.4<d<30 mm Bed slope <0.02	τ_c : critical Shields number
Engelund-Hansen (1967)	$q_{sb} = 0.05\gamma_s V^2\sqrt{\frac{d_{50}(\gamma-1)}{g\gamma_s}}\left(\frac{\tau_0}{(\gamma_s-\gamma)d_{50}}\right)^{3/2}$	d>0.15 mm	-
Wilson (1967)	$q_{sb} = 12(\tau-\tau_c)^{3/2}$	Sand sizes	-

Suspended load

When the ratio of $(w_s/\kappa u_*)$ is smaller than 1.0, then sediment particles start to move as suspension. This means that the fluctuating lift force (upward turbulent component of velocity) overcomes the gravity force (fall velocity) in the balance of the acting forces on a particle. Transport as suspension concern particles in motion far from the bed due to the vertical component of the turbulence eddied carrying particles into the flow water column. Practically, comparing to the bed-load transport, particles in suspension do not show a precise transport mechanism due to the chaotic turbulent fluctuations. Indeed, differences between bed-load and suspended load are related to the ratio of tangential and normal shear stresses excreting on the grain by the flow. Suspended sediment concentration profile (gradient) occurs when downward settling velocity and upward turbulent velocity tend to occur independently. So, the concentration of particles C (in mg/L) in the water column (wetted area) is the volume of sediment per total volume of the control volume (comprises fluid + solids). It is necessary to undertake an adequate law to describe the variation of the suspended sediment transport (concentration) through the vertical flow direction. For example, distribution of the sediment concentration can be numerically approximated by using the method of Rouse based on the parabolic distribution of the turbulent (velocity) in the depth direction. The Rouse solution proposes distribution of the particles based on the turbulent diffusion of eddies (*i.e.,* shear stress

distribution) taking account the friction velocity through the water column.

Vertical concentration profile of the particles within the water column *C(y)* can be described from the following general relationship (Davis and Dalrymple, 2010):

$$q_{ss} = \int_{a}^{h} V(z) \cdot c(z) \cdot dz \qquad \text{Eq. 2.6}$$

where *a* and *h* are bed surface and water surface levels, respectively and *z* is the vertical coordinate representing water depth.

Total sediment-transport rate

In order to estimate the total sediment-transport rate (discharge), various empirical relationships based on laboratory experiments have been proposed by several authors in the past. Most of the formulations covers the steady uniform (flow and sediment) conditions. However, other authors have experimentally used approaches to evaluate the sediment transport under unsteady flow conditions and the reliability of these relationships (*e.g.,* Graf and Song 1995). In practice, total load of sediment consists of the sum of bed-load and suspended-load discharges ($q_{st} = q_{sb} + q_{ss}$). Some of the existing sediment-transport formulas used to predict bed-load transport are also calibrated for the evaluation of total load transport. Many formulas such as Einstein (1950) and Van Rijn (1984 a and b) cover the ranges from suspension to bed-load transport.

It should be noticed that the selection and the application of the formulas is varying from case to case. No global assumption exists that can be taken into account to derive adequate sediment-transport formulas for all the conditions.

2.2 In-sewer solids

2.2.1 Generalities

Sewers being as underground galleries, drain not only different origins of wastewaters (*e.g.,* domestic, industrial), but also all types of runoff waters from the urban catchment area (Fig. 2.5). Therefore, sewer systems allow entering a high variety of solids together with these flows from different origins and activities. Further, solids entering the combined sewer systems originate not only from these wastewaters, but also from the atmosphere, erosion of urban surface during storm flow events and deterioration of sewer structure (Dessoy 1987; Artière 1987, adapted from Laplace 1990; Butler and Davies 2011).

Fig. 2.5 Practice of street cleaning in Paris leading to sediment entering into the combined sewers (photo by G. Shahsavari).

Different reasons could cause and accelerate solids entering into the sewers within the runoff flows (*e.g*., broken street gratings or the mesh sizes of gutters that make discharge of 'unusual' solids into the sewers and change the bed characteristics). It is recognised that the impact and behaviour of the solid entering on the sewer system could be various according to the local and punctual circumstances and sewer channel-types (Ashley *et al*. 1992). The presence of unwanted solids and associated pollutants in sewers creates problems for all components of the sewer network. In particular, during heavy rain events, these sediments could be remobilized and be discharged directly without treatment into receiving waters.

According to the European Water Framework Directive that is set up in the water and wastewater sector to protect the environment, it is mandatory to control and manage the solids and associated pollutants in sewer networks. Therefore, to have control on sedimentation for making strategic and operational decisions in the point view of sewer management, it is essential to acknowledge the sediment origin, nature and their movements within the sewers. Around years 90s, a large number of studies was conducted through different research programs aiming to characterize the sewer sediments and to categorize the potential ranges of the sediments. Table 2.4 highlights several examples of field-based researches and the motivations of the research programs (Ashley *et al*. 2005). Later, other studies were undertaken to understand how sediments settle, accumulate, consolidate and erode with time (processes during dry and wet weather) (Nalluri and Alvarez 1990; Ristenpart and Uhl 1993; Tait *et al*. 1998). However, the mechanism and processes related to the sewer sediments are far from being completely understood, despite the existing large literature.

Table 2.4 Example of research programs aimed to study the in-sewer deposits.

Reference	Country	Research project motivation(s)
Crabtree 1989, 1988	UK	Understanding the function of sewer system in management point of view to permit flow quality simulation
Ashley and Crabtree (1992)	UK	. Model development . Knowledge improvement on cohesive behaviour of sediments . Sediment management in sewers
Michelbach (1995)	Germany	Design of sewers in order to protect the receiving water bodies from the pollution.
Aiguier *et al*. (1996); Lacour (2009); Hannouche (2012)	France	Qualify the potential pollutants discharging
Pisano and Queiroz (1977); Pisano (1979)	USA	Assess flushing effect by high precipitations on deposits in combined sewer channels to manage solids
Verbanck (1990); Verbanck *et al*. (1994)	Belgium	Quantifying the impact of the combined sewer overflows (CSO) on natural receiving streams. Understanding sewer sediment processes via their nature and origin which is varying in each site
Ahyerre *et al*. (2000); Ahyerre and Chebbo, (2002)	France	Identifying the sources of pollution contributing in the storm events
Vollertsen and Hvitved-Jacobsen, (2000)	Denmark	Understanding the deposition and accumulation processes in sewers
Ristenpart and Uhl (1993); Ristenpart (1995)	Germany	Quantifying the pollutants discharging into receiving water systems
Kukla *et al*. (2012)	Myanmar	Solid management in WWTP operations
Regueiro-Picallo *et al*. (2018)	Spain	Solid management in urban system

In the scope of this chapter, a literature review will be presented on the sewer sediment characteristics and their behaviour in sewers. Then, the state of art on sewer cleaning methods and principally on the flushing techniques will be presented.

2.2.2 Negative effects of sediments in sewer networks

Authors such as Thornton and Saul (1986) and Clegg *et al*. (1992) have pointed out main problems resulting from sediment accumulation in sewers networks. Negative effects in combined sewer networks are exacerbated due to the presence of bioorganic elements causing the occurrence of biochemical processes.

Multiple potential impacts of sediments in sewers exits that can be harmful for the environment, for the sewer infrastructures, as well as for the health of sewer workers. A summary of impacts of sediment deposits in sewers is reported in Table 2.5. For example, it has been shown that, during high flows, bed sediments, depending on the local conditions, can be entirely eroded and contribute to the pollutant discharge (Ristenpart 1995; Butler and Davies 2011). The erosion and resuspension of sediments and attached pollutants during storm flows may affect severely the fauna and flora in the receiving water bodies because of non-treated overflowing wastewaters. Moreover, high flows could overload the WWTPs if their dimension does not permit to treat high-polluted discharges such as bacteria, heavy metals and hydrocarbons (Chebbo 1992). Consequently, pollution can enter directly the nature habitats thus creating a number of severe long-lasting environmental and ecological impacts depending on the concentration, load and frequency of the pollution. Authors have observed a high contribution (up to 80%) of the remobilised deposits due to the high storms (Krejci *et al*. 1987; Crabtree 1989; Gromaire 1998; Ahyerre 1999: Banasiak *et al*. 2005). Indeed, the major part of pollutions is originating from the accumulated and developed bed sediments over the sewer channels that can potentially re-entrained during the storm flows. A very recent work has been conducted to investigate experimentally the effect of cohesion of the bed-load on the erosion and accumulation processes in sewers (Regueiro-Picallo *et al*. 2018). According to their observations, 25-50% of the pollutants within the bed deposits can be realised into the sewer during high flows. In addition, researches have highlighted the acute and chronic impact of high-pollution load of the overflows during the storms in the combined sewers that are provenance of the accumulated sediments on the sewer inverts (Verbanck 1990; Butler and Davies 2011).

Another considerable impact of sewer sediment deposits (from the operational point of view) is threatening the performance of the sewer

network as well as reduction of hydraulic conveyance (Crabtree 1989). This has been a real problem for Parisian sewers over sections with flat slope. Also, sewer deposits by emitting gases and corrosive acids can cause detachment of the wall cladding and degrade the infrastructures.

Table 2.5 Outline of the potential negative impacts resulting from the deposits.

Impact and problematics	**Secondary effects**	**References**
Hydraulic conveyance reduction	° WWTP surcharging during storms ° Remobilisation of pollutants when wet weather ° Pollution discharge due to re-suspension and receiving water-body quality ° Cost and operational constraints (human and material resources to clean)	Pisano *et al*. (1979); Chebbo *et al*. (1995); Ackers *et al*. (1996); Gromaire *et al*. (2001); Ahyerre *et al*. (2000); Fan *et al*. (2001), (2003) Bertrand-Krajewski (2003); Schellart *et al*. (2007)
Channel blockages	° Flow conveyance disfunctioning	Ashley *et al*. (2000); Ashley *et al*. (2004); Perrusquia *et al*. (1995); Butler *et al*. (1996); Novak and Nalluri (1984)
Progressive decay of sewers	° Deposition and blockages	
Gas emissions, noises, odours	° Health risk of operating personnel ° Structural degradations and chemical corrosion	Dettmar *et al*. (2002); Alzabadi (2010); Hvitved-Jacobsen (2002)
Gross solids	° Aesthetic environmental pollution	Gujer and Krejci (1987)

2.2.3 Content of deposited load in sewers

Early experimental researches about sewer solids and pollutants are referenced by Ashley *et al*. (2004) and show the existence of problems due to solids in sewers since many centuries. Several studies have shown the interest to observe in-sewer sediment related processes mainly in the context of the qualification and quantification of pollutants associated to solids (Laursen 1956; American Public Works Association 1969; Bertrand-Krajewski 2003). Nonetheless, an increase of the awareness of the need to study sediment characteristics and related processes has started by the end of the 80s. This was due to the progresses of informatics that permitted to model hydraulic performance of sewer flows thus allowing exploring such complex systems. An extensive literature review related to sewer solid

characterization is presented by Ashley *et al*. (2004) that explores various types of in-sewer sediments, origins and their sources.

Combined sewers may drain and transport particles including elements such as food wastes, faeces, hygienic articles, paper, mineral particles (sand, gravel, etc.). A large number of factors exists that vary the source, composition and properties of the sewer sediments. These elements are variable place to place and depend also on local circumstances such as the population, domestic and cultural habits, public education, and sewer characteristics (Ashley and Crabtree 1992; Spence *et al*. 2016). Also, sediment entry into the sewers depends on dry or wet-weather conditions, as well as on the geographic area drained by the sewers that affects the composition of the bed in a different way (Ashley and Crabtree (1992 (CIRIA 1986; Michelbach 1995).

A large body of knowledge has been built-up for solids in sewers showing a wide heterogeneity of the sediments in terms of physical, chemical and biological characteristics (Queiroz 1977; Ashley *et al*. 1990; Brombach *et al*. 1992; Clegg *et al*. 1992; Chebbo *et al*. 1995). The main objective of several studies was to understand and quantify the contribution of the pollutants associated to bed deposits into the flow during dry and wet weather conditions. Other researches have shown that the composition of deposits varies on time and in space due to the occurrence of non-stationary sewer flows. Ristenpart (1993, 1995) experimentally evaluated in details the temporal evolution of physical and chemical characteristics of the bed deposits of the Hildesheim sewer in Germany. By monitoring several characteristics of sediments during nine months, he showed even rapid temporal variations of the sediment sizes, densities and therefore chemical parameters during dry-weathers (Ristenpart *et al*. 1995). In addition, it has been showed that the characteristics of deposits may vary also vertically (in time and space) through the bed depth (Schmitt 1992, cited by Ristenpart 1995; Lacour 2009; Hannouche 2012).

The most common physical property of sediments is the grain-size distribution of bed deposits since sewer sediments contain a wide range of sizes from very small microorganisms to particles of tens of centimetres (Levine *et al*. 1985). These particles on composed of organic and inorganic (in particular mineral) matters that are why many authors use sediment mixtures of organic and mineral solids for laboratory experiments (Ashley et Verbanck 1996; Rushforrt *et al*. 2003; Banasiak *et al*. 2005). A summary of studies that aimed to investigate the range of in-sewer sediments are presented in Table 2.6. The table shows also the motivation of these studies to characterize the sediment highlighting the importance of knowledge about the nature of sediments. Globally, research programs have concluded that in-sewer sediment origins are highly variable. For example, Crabtree (1989), Laplace (1993), Oms (2003) and Ahyerre (1999) experimentally observed large ranges of sediments in sewers.

Size distribution of the solids accumulated in sewers during dry-weathers has been measured in a number of studies. Table 2.6 shows also the ranges of the bed sediments found by authors which are found to be variable. Ashley *et al.* (2004) have discussed variability of ranges from very fine to large gravel-size particles. For example, up to 18% of the bed sediment composition was found to be more than 20 mm in French trunk sewers). Marseille data (La Place 1993) has showed a d_{50} of more than 8 mm for the bed deposits.

Table 2.6. Example of fieldworks which measured size ranges of the bed deposits in sewers.

Reference	**Sampling motivation**	**Observed sewer information**	**Average size (d_{50}) (from A, C or A/C for bed-load in general)**
Crabtree (1989)	study bed deposits and pollution sources	Combined sewers in UK	(A): 100µm – 10mm (C): < 170µm
Laplace (1993)	Bed deposits dynamics et evolution during dry and wet weather	Man-entry Collector N°13 in Marseille (France)	A/C: 0.35-8.5mm
Ashley *et al.* (1994)	Investigate linking bed deposits to the foul flush pollutant load	3 combined sewers with different sizes in Dundee (UK) and in Marseille (France)	(A): 0.15- >20 mm
Michelbach (1995)	First foul flush pollution	Combined sewer of "Schellenhauschen" in Germany	A/C: 0.6-2 mm
Verbanck (1990)	Pollution quantification	Combined sewer in Brussels (Belgium)	(A/C): 350 µm
Bertrand-Krajewski *et al.* (2006)	Operational solid management to understand sediment accumulation	Combined sewer in Lyon (France)	(A/C): 270 µm

Furthermore, authors have classified sewer deposits differently. Verbanck *et al.* (1994) have mainly categorized in-sewer sediments into three classes of sewer grits, sanitary solids and materials coming toward surface run-off. According to the observations of Crabtree (1989), five categories of sediments were recognized within the sewers. Each class of sediment was identified regarding to its physical and chemical properties as well as the behaviour of the particles. The work of Crabtree has led to characterize the in-sewer deposits. He examined deposits from real field in a combined sewer in the UK (Crabtree 1988, 1989). Various locations of sediment accumulation were identified that led to separately sample the observed deposits. Fig. 2.6 schematizes the results of the classification of sewer deposits based on their characteristics identified from the samples (Crabtree and Forster 1989).

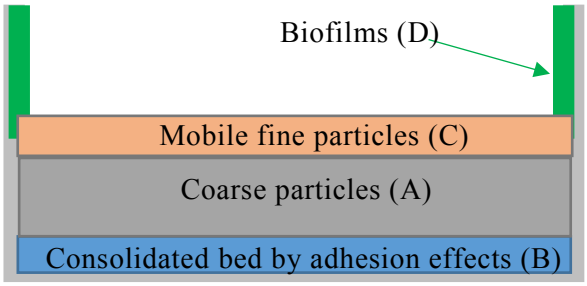

Fig. 2.6 In-sewer deposit classification based on Crabtree's study.

Crabtree's observation showed the evidence of a stratified bed layers constituted from two classes of sediments indicated by A and C. The lower layer of the bed (A), with tens of centimetres, constitutes the larger sizes of materials (mainly from mineral particles). This layer is eroded only during extreme storms because of the high yield stress that they need to be remobilized. Conversely, he found that, above this layer, a finer layer exists that contains mainly organic matter (layer C) which is eroded during minor storms and partly during dry-weather flows (Crabtree 1989; Verbanck *et al*. 1994). Layer C shows a smaller thickness, contains finer sediments (with d<1.5 mm. Later, this stratification of the bed was confirmed by other studies such as those by Verbanck *et al*. 1994 and Berlamont and Torfs (1996). In particular, the investigations done by Ahyerre *et al*. (2000) and Oms (2003) using a monitoring equipment to film the bed/sediment interface and its temporal evolution, showed clearly this stratification and the dynamics of deposits specific to each layer.

As discussed, combined sewer sediments consist of organic and in-organic types (called also mineral or non-cohesive material; Artières 1987). Researches have concluded that the organic substances modify the bed characteristics as well as the sedimentation processes in particular the erosion condition of the sediments on the bottom of the sewer (Wotherspoon and Ashley 1992; Williams and Crabtree 1989). In fact, the presence of organic matters (in any forms such as dissolve form or as particulates with different sizes) within deposits can cause the development of cohesive effects in the sewer deposits (Beyer 1989; Williams *et al*. 1989; Verbanck 1990). Fine organic matters among minerals create the biochemical binding between bed particles. Berlamont *et al*. (1993); Wotherspoon and Ashley (1992) and Ristenpart *et al*. (1995) pointed out the variable distribution of organic matters within time and space affecting the yield stress (shear resistance) of the bed. Crabtree (1989) by measuring the rheological parameter of the sewer solids assessed the cohesion between the sampled bed sediments. He concluded that the cohesion effect of sewer deposits is not universal in all the areas. Based on his results, the presence of organic matter was much related

to the bed with higher bulk density of sediment because of the biological and chemical oxygen demand (BOD and COD, respectively; Ristenpart 1995). Further studies were led aiming at identifying the sources and behaviour of the organic mass and the possibility of 'artificial' erosion to limit their accumulation (*e.g.,* substantial organic, nutrient and heavy metal; Pisano *et al*. 1979: Ahyerre *et al*. 2000; Laplace *et al*. 2003; Rocher *et al*. 2004; Berndtsson 2013).

Looking at the bed structure of deposits in sewers, the upper layer of the bed (layer C) contains high-polluted organic sediments. In fact, it was shown that the organic content has been the responsible of the bed stratification (Banasiak *et al*. 2005). This layer is called "mobile organic layer", "near-bed layer", "mobile fluid sediment" or "interface layer between deposited bed and sewage" in to various field studies and observations (Ristenpart *et al*. 1995; Verbanck 1995; Ahyerre 1999; Chebbo *et al*. 2002; Oms 2003). One of the main properties of this layer is the cohesive-like characteristics denoting the cohesive binding among the mineral (granular) particles. Many authors who investigated the cohesive-like property used this property to describe the erosive behaviour of bed sediments (Tait *et al*. 1998; Skipworth *et al*. 1999; Rushforth *et al*. 2003; Banasiak *et al*. 2005).

2.2.4 Consolidation of deposits in combined sewers

Combined sewer deposits show complex processes such as bed consolidation that distinguish them from "classical" sediment beds. Consolidation (or self-weight consolidation) of sewer deposits occurs to an accumulated bed over time principally during dry-weather. This complex time-dependent process depends mainly on the presence of the (fine) organic matters and microorganisms that create the bio-chemical binding between particles (Berlamont *et al*. 1993; Ashley and Verbanck 1996). Torfs (1995) has estimated 10-20% of fine (<63µm) organic within cohesive-like bed. Indeed, the cohesiveness of sediments is one of the key-components of consolidation conditions. Results from experimental investigations conducted by Ristenpart and Uhl (1993), show that consolidation modifies the erosive shear stress of the bed during dry-weather flows by increasing the threshold of motion. Recent researches have outlined that not only the organic matters but also the oxygen content for bacterial activity can have significant influence in the consolidation processes (Vollertsen and Hvitved-Jacobsen 2000; Tait 2008; Seco *et al*. 2014).

Moreover, the age of deposits accumulated during dry-weather plays an important role in the degree of the bed consolidation that increases the threshold value to remobilize the bed (Lau and Droppo 2000; Regueiro-Picallo *et al*. 2018). However, dry-weather duration depends on the climate

(and seasons) and environmental conditions (Gupta and Saul 1996; Tait *et al*. 2003a). Ristenpart (1995) experimentally observed the relation of the bed history and sediment properties such as cohesion and thus consolidation. Further, exhaustive laboratory studies investigated this process more in details and showed that the level of consolidation depends on the time length (dry-weather duration) of the consolidation as well as the biological activity within the deposits (Skipworth *et al*. 1996; Tait *et al*. 2003; Banasiak *et al*. 2005).

2.3 Movement of solids in sewers

Sewer sediments are transported by gravity flow conditions along the sewer channels through different modes of transport. In addition, many processes exist that influence the movement of sediments due to the presence of the organic content.

Understanding sediment-transport mechanisms in sewers requires knowledge of complex processes and interactions between sediments and water during both dry- and wet- weather flows. Chemical, physical and (micro) biological processes in sewers are different from typical river sediment-transport processes (Berlamont and Torfs 1996; De Sutter *et al*. 2003). Moreover, these processes affect significantly the sediment transport in addition to the flow conditions (Ristenpart and Uhl 1993; Arthur *et al*. 1998). Based on Ashley and Verbanck (1996), compared to the natural streams, sediment transport in sewers shows the following elements that influence the sediment transport: the cross-sectional shape of the sewers, the availability of sediment source as well as the spatio-temporal variations of the hydraulic and sediment characteristics. In this regard, sediment transport in sewers needs more experimental and numerical efforts to progress the comprehension of the processes. Following, the in-sewer modes of transport including deposition, accumulation, erosion and transport are discussed in detail.

2.3.1 Deposition (settling) and accumulation of sediments in sewers

Particle settlement

Intermittence of sewer flows cannot appropriately transport the (mineral) sediments due to decreased flow energy. Therefore, particles in suspension in the water column start to settle down over the bed invert. The settling velocity, being as a property of particles in suspension, is one of the parameters that govern transport processes (Berlamont *et al*. 1993). This is usually represented by $w_{s_{50}}$ (median settling velocity) by various authors. Physically, deposition processes within the flow can occur since the buoyant weight force component is greater than the lift forces. Conversely, a higher lifting force than buoyant weight tends to retain the particle in suspension. Various values of settling velocities are reported in the literature that may be due to the variability of local conditions and measurement techniques (Bertrand-Krajewski 2006). Aiguier *et al*. (1996) evaluated settling velocity of the solids in sewer by comparing three selected methods. Observing the differences between the results from the used methods, they highlighted various factors that can change the settling velocity. It has been shown that

the rate of settling depends on the hydraulic conditions, particle characteristics as well as on flow concentration. It should be noticed that the quantity and quality of the settable mass are connected to the available source of material entering the sewers. Basically, availability of materials depends not only on solid entrance rate but also on the weak shear resistance locally existing in the sewer channels (Ashley *et al*. 2004).

The settling characteristics of solids during dry and wet-weather are variable (Piro *et al*. 2011). According to the results obtained from field investigations by Krishnappan *et al*. (2012) who used four methods to measure the settling velocity, higher settling velocities were measured during wet-weather. This could be explained by the presence of finer particles that cause the aggregation/degradation of flocs, as well as the remobilized inorganic materials with faster settling velocity (Ashley *et al*. 2004).

Sediment accumulation

Depending on the flow conditions and the settling velocity of the particles, sediments can form permanent deposits at specific points (in particular at the entry) of the sewer channels (Pisano *et al*. 1979; Fan *et al*. 2001; 2003).

Sedimentation and deposit build-up in sewers take place mainly during dry-weather as well as during the recession of the storms (Chebbo *et al*. 1995). It was outlined that deposition takes place during dry-weather period when equilibrium state is obtained with the formation of deposits stable sediment height (Ristenpart and Uhl 1993). However, the build-up rates and the composition of accumulated sediments are different depending on a large number of factors, mainly related to the hydraulic parameters (Ashley and Crabtree 1992; Ashley *et al*. 1992).

Several authors have observed sediment deposition and accumulation processes in sewer channels by long-term monitoring to understand the reasons and potential locations of deposits (Ashley *et al*. 1989; Lin 1993; Bertrand-Krajewski *et al*. 2006). As result of the extensive fieldwork investigation by Laplace (1991) in a French man-entry sewer trunk, he observed various locations prone to sediment accumulation along the sewer channel bed such as junctions, confluences, bed-invert bumps and hollows were identified. According to observations, bed deposits tend to be finer in sediment sizes. This behaviour called downstream fining (observed also by Sanchez 1987) reveals the selective (sorting) mechanism of the flow along the channel that makes varying spatially sediment characteristics. Globally, various locations can potentially trap sediments (during dry- and wet-weathers) that are affected by the obstacles, slopes and discontinuities (Chebbo *et al*. 1995). Lorenzen *et al*. (1996), by monitoring sewer deposits along the sewer channel, found that sewer diameters widening cause considerable sedimentation. Ashley *et al*. (1992) observed coarser particles

with a granular texture at the sewer head confirming the downstream fining phenomenon.

Many reasons can be the origin of particle accumulation and build-up. Discontinuities such as abrupt changes in the invert slope and irregularities, junctions and flow inlet/outlets through the sewer channels are able to modify the flow conditions (*i.e.,* reduced velocity) resulting in the local sediment accumulation (Laplace 1991; Chebbo *et al*. 1995). In fact, the flow capacity together with sewer physical conditions (*e.g.,* shape, roughness and size) is one main responsible of sediments accumulation within the sewers (Perrusquía *et al*. 1987).

Globally, although the accumulation of solids in sewers is an important issue for pollution in urban areas, more research efforts are still needed to make a clear conclusion about the potential areas and mechanisms of sedimentation in sewers (Bertrand-Krajewski *et al*. 2006).

2.3.2 Erosion of sewer deposits

The self-cleaning condition of sewers depends principally on the boundary shear distribution needed to remobilize the bed deposits (Butler *et al*. 2003). Deposits can be (partly) remobilized and carried by diurnal or storm flows as the exerted shear stresses begin to increase more than a certain threshold value. The critical shear stress separates the deposited from transported particles in sewers. Once the bed shear stress exceeds the threshold value to initiate the motion, due the increase of the flow velocity and turbulences, particles can be remobilized. However, the shear stress is a main but not the only parameter determining the erosion in sewers (Ristenpart and Uhl 1993; Verbanck *et al*. 1994). Indeed, the erosion is also affected by other factors such as sediment properties as well as geometry of sewers. For example, the role of geometry on local bed and mean shear stresses was highlighted by Oms *et al*. (2008), who led a series of experiments in real combined sewers. They highlighted the role of slope in the estimation of the average shear stress.

Using different approaches, authors from different countries have tried to define critical bed shear stresses needed to initiate the particle motion in sewer systems. Table 2.7 summarizes values obtained at both field or laboratory scales (Nalluri and Alvrez 1992; Ristenpart 1995). Novak and Nalluri (1984) carried out investigations in a laboratory flume with a rectangular cross-section and proposed a formulation to obtain the incipient motion of the bed deposit for sewer channels. Later, Hrissanthou and Hartmann (1998) measured the critical shear stress using the automatic image processing using the videos taken to observe the bed particle motions in the laboratory. Taking into account the real conditions, they estimated the critical shear stress in terms of its corresponding critical discharge with good results

compared to the data from the literature. Very recently, Bong *et al*. (2013) by investigating incipient motion in a laboratory flume have proposed a developed version of the relationship proposed by Novak and Nalluri (1984). They confirmed that this equation provides an estimation of the threshold condition of sediment incipient motion by taking into account the depth of bed deposits.

Table 2.7 Example of studies who obtained the minimum (critical bed) shear stress corresponding to the beginning of erosion of a given particle

Author(s)	**Obtained shear stress for sedimentation (in N/m²)**	**Case study location**
Ashley *et al*. (1992)	Mean shear stress Type C: >1.8	Real field – Dundee, UK
Wotherspoon and Ashley (1992)	>10	Laboratory measurements of real cohesive sediments, UK
Nalluri and Alvrez (1992)	Mean shear stress Type C: >2.5 Type A: >6-7	Laboratory measurements-UK
Ristenpart and Uhl (1993)	> 0.7 Long dry-weather: >3.3	
Ristenpart (1995)	>0.44 – 1.02	Real field – Hildesheim, Germany
Skipworth *et al*. (1996)	>0.5	Laboratory synthetic cohesive particles
Ahyerre (1999)	>0.1	Real field - Paris, France
Laplace *et al*. (2003)	>0.1	Real field - Marseille, France
Johanson (2015)	Type C: >2.5 Type A: >6-7	Laboratory measurements-UK

During high flows in sewers when the erosion condition is obtained, particles can be remobilized from the bed deposits since the shear velocity is higher than the threshold value. Therefore, the in-situ estimation of the parameters such as the critical shear stress over the bed is of permanent importance to estimate the bed-load sediment-transport discharge in sewers. Due to the complex conditions of the sewers, obtaining this value from the real field is a difficult task. Therefore, the Shields diagram remains the most practical mean to estimate the critical shear stress. Ever if shear stresses in the real sewers are much higher than the values obtained from laboratory cases (Ashley and Verbanck 1996; Ashley *et al*. 2004).

The critical bed shear stress in real sewers can also vary on time due to the internal processes among the bed particles, the sewer geometry, the sewage and sediment properties. As previously mentioned the presence of organic matters (in any percentages) can vary the sediments behaviour (Vollertsen and Hvitved-Jacobsen 2000). Hence, the erosion of deposited bed is affected by the cohesion originating from these substances. Nevertheless, once the particles go into the flow, they are transported as the inorganic sediments (Nalluri and Alvarez 1992). The relation between the organic content and the erosional resistance was investigated by Seco *et al*. (2014) undertaking a complete series of laboratory experiments using in-sewer high organic matter sediments. By evaluating erosion rate, they outlined that the magnitude of critical shear stress is not only affected by the presence of organic matter but also by the nature of sediments as well as the bacterial reactions. For instance, Ahyerre *et al*. (2001) by in-situ measurements in various flow conditions in a combined sewer observed that the (organic) erosion occurs even at low shear stresses conditions (*i.e.,* 0.5 N/m^2).

Another interesting aspect concerns the erosion of fine-grained sediments deposited at the top layer of the bed (NBS), being this potentially the main source of the pollution, during wet weather flows. This phenomenon, called as “First Foul flush”, indicates the important erosional effect of the initial part of the storm flow hydrograph. Different authors tried to characterize this phenomenon by linking it to the pollution transport, thus aiming to quantify the downstream impacts (Ashley *et al*. 1994; Barco *et al*. 2008; Sakrabani *et al*. 2009). Arthur and Ashley (1998) observed the flow and sediment characteristics during first flush of three real sites in Dundee. It was demonstrated that the top layer of the bed containing heterogeneous solids mainly (almost 90% of organic matters), can be easily eroded and transported in suspension during sewer flow and the eroded amount depends on the time length of antecedent dry-weather. Many authors, such as Chebbo *et al*. (1996), Verbank (1990), by characterizing physical and chemical properties of these solids in suspension during wet weather, reported the considerable portion of fine solids (25% of the mass) in the flow.

2.3.3 Transport of sediments

Once sediments entrain from the bed deposits, they can be separated and transported by the flow forces as bed-load and suspended load. The particle remobilisation can be obtained when particles are exposed to the critical flow conditions allowing the beginning of transport. Critical shear stresses can be determined for a non-cohesive bed particle based on Shields (1936) method. This method is also applicable for sewer systems to study the transport conditions of particles.

Being composed of a variety of properties and characteristics, sewer particles are transported differently in response to a given hydraulic and sewer condition. In addition, sediment-transport processes are different during dry- and wet-weather conditions. A number of studies have been carried out in an attempt to comprehend solid transport processes in sewers (combined and storm sewers) during dry- and wet-weathers (Nalluri *et al*. 1994; Chebbo *et al*. 1995; Coghlan *et al*. 1996; Ab Ghani and Azamathulla 2010). Various phenomena inside sewers might modify the 'classical' mechanism of sediment transport (previously discussed). Sometimes the biochemical reactions (agglomeration, degradation, etc.) cause changing in characteristics and therefore affect the movement of sediments (Ashley and Verbanck 1996). Other factors that can influence the transport of solids are related to the sewer conditions (Walski *et al*. 2011; Ab Ghani *et al*. 2018). For example, the sewer cross-sectional shape and longitudinal slope can influence the sediment-transport processes by increasing the shear and flow resistance (Verbanck 1996; Ashley *et al*. 2004). Other significant factor is the existing sediment bed that modifies the transport of particle in movement (Novak and Nalluri 1984). Indeed, the presence of fixed or mobile bed changes the roughness and consequently the boundary conditions that influence the flow velocity and the energy of the solid in motion.

Generally, particles in sewers are continuously interchanging the transport modes as bed, near-bed and suspended load. Basically, two modes of sewer sediment transport can be distinguished especially when talking about low-organic content sewers (non-cohesive deposits with <5% organic which is particularly the case for large sewers; Kleijwegt 1992): suspended load and "non-suspended load". The latter type consists of bed-load and near-bed-load in which particles are considered to be in contact with the bed. These two modes of transport are hereafter explained in more details.

Bed-load transport

This transport mode consists of particles in movement being as sliding, saltation and rolling which is the most observed by studies on combined and storm sewers (Ashley and Verbanck 1996; Ab Ghabi *et al*. 1999). The modes of sediment transport within the flow are depending on a variety of factors. Theoretically, several methods exist to classify particles in modes of transport. Since solids in sewers have very large differences in their movements, many authors have used different criteria categorizing the transport mode of particles according to their characteristics (Ota *et al*. 1999). Many authors such as Raudkivi (1990) have classified the transport modes using the Rouse criterion related to the settling velocity of a characteristic particle and the shear velocity of the flow (Ashley *et al*. 1994). This criterion, has been used by many researchers using various ranges to define the transport modes used for sewer cases.

Sewer deposits are continuously in evolution even under small shear stress that may be able to remobilize the very fine sediments (OMS 2003). Higher shear stresses (*i.e.,* wet-weather) cause the erosion and the transport of wider range of particle sizes containing mainly coarser particles (Laplace 1992). The bed erosion of both A and C layers usually occur during storms. However, followed by the storms, during the recession limb of the hydrograph, the (re-)deposition and therefore deposit build-up may take place again at the same locations. This mechanism can hide the occurrence of the erosion if the whole process is not appropriately monitored.

The build-up processes of the bed deposits were experimentally observed in various studies by monitoring the bed heights and its evolution within time in various contexts. These experimental works were conducted both at the field (Laplace 1992; Lin and Le Guennec 1996; Bertrand-Krajewski *et al*. 2005) and the laboratory scales (Banasiak *et al*. 2005; Campisano *et al*. 2008). It was shown that the mechanisms of the bed-load transport are highly affected by the flow, sediment and geometrical sewer conditions.

Suspended-load transport

Suspension occurs from the moment that particles are transported without any contact with the bed. In fact, particles in suspension (predominantly organic matters with about 40µm in size) within the flow column are maintained by the turbulence eddies. The suspended sediment-transport capacity of the flow can be related not only to the flow conditions (turbulent velocity) but also to the solids characteristics such as the settling velocity. Settling velocity information generally represented by $w_{s_{50}}$ is considered as an important factor to describe the suspension in sewers (Chebbo 1992).

Several authors have estimated various values of shear stresses for erosion during dry-weather. For example, Laplace *et al*. (2003) reported an average flow velocity of 0.35-0.4 m/s corresponding to 1N/m² for a trunk sewer in Marseille. These values are sometimes small to remobilise even fresh deposits in flat sewers. Moreover, during dry-weathers, the concentration of the suspended particles in the flow is linked to the presence of organic substances within deposits. Indeed, during dry-weather higher amount of organic matters of deposits can reduce the suspended load because the organic binding to the mineral particles does not allow the bed-load going into suspension (Skipworth *et al*. 1996; Du Sutter *et al*. 2000). It was outlined that by increasing the flow velocity, resuspension of particles (including organic and inorganic) may occur, leading to potentially contribute to the transport of pollution (Krejci *et al*. 1987; Chabbo *et al*. 1990; Field *et al*. 2000). Nevertheless, once the bed particles start moving into the flow, all particles transported by the flow behave as inorganic solids

and the cohesion can be ignored (Ristenpart *et al*. 1995; Gupta and Saul 1996).

2.3.4 Available studies concerning modelling sewer sediment transport

In the recent decades the progresses of sewer sediment-transport models have been significant due to the increase of demand for reliable approaches for the management of sewer networks (Bertrand-Krajewski *et al*. 1992). Although, modelling in-sewer sediment processes such as consolidation, chemical and biological interactions in addition to their temporal and spatial changes is a complex task (Ashley *et al*. 1999). Therefore, a variety of models has been applied to simulate sewer sediment transport but they had to encounter such complexities related to the real sewer conditions. Table 2.8 presents a summary of investigations dealing with of sediment-transport modelling in sewers. The table shows that authors have tried to predict the in-sewer processes by generally focusing on a couple or few aspects of sediment transport. In fact, description of these processes, require an appropriate model that is a challenge for researchers. In this context, good quality of data becomes essential for reliable model simulations (Gaume *et al*. 1998). Apart from experimental data features, the quality of models plays a crucial role in decision-making strategies in urban networks. This is why the numerical errors and uncertainty of modelling results are important issues when talking about sewer sediment models. Freni *et al*. (2008) relate the uncertainties to the number of parameters to measure or to describe that can increase model complexity and therefore the uncertainty of models.

Therefore, correct prediction of in-sewer sediment transport maybe strictly affected by the choice of formulas that are used. Since many years, researchers are trying to obtain or develop appropriate relationships for sediment-transport prediction for sewer cases. Several experimental and numerical researches were undertaken at the laboratory scale using uniform synthetic or real deposits from sewers to evaluate the application of various formulas (De Sutter *et al*. 2001; Laplace *et al*. 2003; Rushforth *et al*. 2003). On one hand, the aim of these studies was to validate sediment-transport formulas for uniform sediments deriving from the parental area of river engineering using, for example, correction factors. Nalluri *et al*. (1994) investigated bed-load transport of non-cohesive particles in laboratory using two channel shapes for the purpose of achieving design indications. Formulas were validated for various sewer shapes with a relatively good level of performance. Lin and LeGuennec (1996) derived a relationship able to predict the bed evolution that takes into account the erosion and

sedimentation based on the Meyer-Peter and Müller formula for bed-load sediment-transport discharge.

Table 2.8 Numerical simulations of sewer of sewer sediment movements

Reference	Motivation	Used model	Modelling method for transport
Ashley *et al*. (1992)	Erosion and behaviour of the particles and associated pollutants during foul flush events	MOSQUITO	Ackers-White equation to predict the sediment transport
Lin (1992)	Modelling sewer sediment processes (*i.e.,* evolution of bed profiles and composition)	MEDCA	Meyer-Peter and Müller equation
Coghlan *et al*. (1996)	Suspended sediment transport during dry- and wet-weather	SWMM + MOSQUITO	Regression equation
Faram and Harwood (2002)	Assessment of particle removal and retention efficiency at sewer inlets	Fluent CFD	Lagrangeian particle tracking
Schütze *et al*. (2000); Schütze *et al*. (2014)	Controlling discharge of aesthetic pollution (gross solids)	Simba# simulator	Regression after Mont-Carlo
Digman *et al*. (2002)	The movement of gross solids in combined systems	Gross Solid Simulator (GSS)	Mathematical model
Bertrand-Krajewski *et al*. (2006)	Simulation of sediment accumulation	Empiric model, Model Velikanov	
Celestini *et al*. (2007)	Modelling sediment transport to identify deposition locations, characterize and quantify bed deposits	SWMM	
Thinglas and Kaushal (2007)	Simulating invert trap to assess the effect of model precision	FLUENT	CFD + Renormalization Group (RNG) k–ε model along with discrete phase model (DPM)
Wu and He (2010)	Settling mechanism of sewage solids	Developed model	Interactions between the particles
Verbanck (2001)	Sewage quality modelling of near-bed solids	Innovative model	Two-layer suspended-load
Mouri and Oki (2010)	In-sewers sediment-transport processes in the context of flooding	Developed model	Taking account the specific in-sewer transport phenomena
Park *et al*. (2010)	Control sewer pollution during first flush	XP-SWMM	Probability density function
Campisano *et al*. (2013)	Bed evolution (deposition/transport) associated with aggradation process	1D DSV-Exner model	Semi-coupled modelling approach for uniform sediments
Wan Mohtar *et al*. (2018)	Predicting the incipient sediment motion	feed forward neural network (FFNN) and radial basis function (RBF)	Neural network algorithms

On the other hand, other researchers have been interested in the study of non-uniform sediment transport. For example, Einstein (1950) proposed the fractional sediment-transport theory for non-uniform sediment bed mixtures in estimating bed-load discharge for each grain-size class in

sediment mixtures. Since sediment-transport processes in the nature are strictly associated to the grain-size distribution of the sediments (Verbanck 2001), it is also important to take into account the variety of sediment grain sizes using an accurate theory to include mixture properties to predict the rate of transport. This is particularly important for low-organic content sewers with granular texture. However, up to now, few studies attempted to simulate transport mechanisms of sediment mixtures for sewer flows (Ota 1999; Ota *et al*. 1999). Different authors (Ashley *et al*. 1999; Rushforth (2001, adapted from Ashley *et al*. 2004) have remarked the importance of modelling sediment-transport processes using non-uniform particle sizes. For example, De Sutter *et al*. (2000) based on laboratory investigations on the erosion and transport of sediment, concluded that modelling sediment transport is useless without taking into account the heterogeneity of sediments. In fact, it has been clearly highlighted that modelling sediment-transport processes using single-sized sediment cannot represent the entire real sediment compositions (Ashley *et al*. 2004). The simplification of the heterogeneity in size and in density of sewer sediments for easy modelling, affects, in particular, the realistic estimation of bed-load transport discharge. Therefore, in order to appropriately describe sediment-transport processes in sewers, it is of parameter importance to include information about the variety of sizes of particles as model input information about deposit properties (Mark *et al*. 1995; Rushforth *et al*. 2003a; Rushforth *et al*. 2003b; Bertrand-Krajewski 2006). Indeed, the non-uniformity of sizes in the composition of the bed requires the modelling of various phenomena such as sorting, armoring, differential erosion and hiding/exposure that affect the transport of solids (Rahuel and Simon 1985; Holly and Karim 1986; Armanini and Di Salivio 1988; Rahuel *et al*. 1989; Parker 2008).

Models that account for the information related not only to flow conditions but also particle properties based on the real-field data can be more successful in describing the behaviour of in-sewer transport (Tränckner *et al*. 2008; Mouri and Oki 2010). However, collecting the real field data to observe and monitor the sediment-transport processes presents various constraints due to the hostile conditions of the sewer. That is why many researchers attempted to experimentally and numerically investigate the in-sewer sediments transport in laboratory using real sediments (De Sutter 2000; De Sutter *et al*. 2001; De Sutter *et al*. 2003).

Transport of sediment during dry-weather was subjected to a large number of studies (Mark *et al*. 1995; Coghlan *et al*. 1996; Schlütter 1999; Seco *et al*. 2014). Attempts were made to describe the movements of near-bed particles transported during dry-weather by proposing novel equations or models (Arthur and Ashley 1997; Verbanck 2001). In parallel, attention has been also paid to high flow conditions in sewers and consequently associated sediment transport in particular during wet-weather (storms; Coghlan *et al*. 1996; Tait *et al*. 2003; Celestini *et al*. 2007; Bong *et al*. 2016). These

numerical studies of suspended sediment transport in the context of sewer pollution management allowed setting up acceptable pattern for the first foul flush (Ashley *et al*. 1992; Skipworth *et al*. 1999; Rushforth *et al*. 2003; Saul *et al*. 2003; Lacour 2009).

In the past decades, with the increase of computational power, many authors have tried to use fully CFD models to simulate the sediment-transport problems in sewers (Faram and Harwood 2000, 2003; Yan 2013). They were able to predict on detailed infrastructures mainly for design aims in order to obtain indications about the sediment deposition to identify for example sediment trap or chambers (Fraser *et al*. 2001 adapted from Faram and Harwood 2003).

2.4 Sewer cleaning methods

Due to the structural effects as well as the management plans, deposits could be formed over time on the bed invert of sewer channels. Since hydraulic and geometrical conditions of old and flat sewers do not ensure self-cleaning conditions, appropriate actions for deposited on the sewer network are mandatory.

Literature shows that sewer cleaning is an exercise that has been practiced from centuries as a method to overcome the sedimentation problems in sewer channels (Bertrand-Krajewski 2008; De Feo *et al*. 2014). Nowadays, cleaning strategies become part of the normal operation of sewers to reserve the existing infrastructure (Schellart *et al*. 2007). The necessity of appropriate techniques for removing deposits from the bed invert in combined sewers is essential for keeping sewers clean (Sanchez 1987; Chebbo *et al*. 1995, 1996). Appropriate choice of the cleaning techniques depends, above all on the channel characteristics (*e.g*., cross-sectional shape and size, longitudinal slope); bed deposit features (*e.g*., sediment age, grain-size distribution and bed depth) and flow characteristics (*e.g*., flow velocity, shear stress, etc.) (Ashley *et al*. 2004). However, from the managerial point of view, proactive cleaning should take into account the economical, ecological and operational aspects. May *et al*. (1998) investigated low-cost options of cleaning, including those that are the most practicable and able to minimize the deposition on time. Various sewer cleaning techniques exist that help to manage the formation of deposits in sewer (EPA 1999). Cleaning techniques include traditional (*e.g.,* surface runoff), mechanical (*e.g.,* bucket machines) and hydraulic methods (*e.g.,* water jets; Bertrand-Krajewski 2002; Pisano *et al*. 2003; Fan 2004). The two latter techniques are implemented by the mean of devices to remove deposits. Among all cleaning practices, those that artificially make transporting the sediments in suspension (hydraulic techniques) are considered to be the most promising solutions (Gupta and Saul 1996; Chebbo *et al*. 1996). However, it should be noticed that cleaning solutions could be applied not only as reactive systems but also as preventive solutions to minimize the sedimentation in sewers (Ashley *et al*. 2004). Detailed description of all cleaning methods and their application can be found in EPA (1999), Fan (2004); Schaffner (2008) and Shirazi *et al*. (2013). During the last decades a large number of case studies and numerical investigations from all around the world have been conducted to evaluate and understand the removal efficiency of cleaning techniques in sewers (for example Laplace *et al*. 1992; Lorenzen *et al*. 1996; Campisano *et al*. 2004; Bertrand-Krajewski *et al*. 2009; Dettmar and Staufer 2005; Sequeiros *et al*. 2014).

According to the literature, examples of practical hydraulic cleaning (high-pressure) methods are mentioned as follows:

Ballig

Being as hydraulic cleaning method, the pressure of a water head generates high velocity flow around an inflated rubber ball. A scrubbing action of the water along the pipe happens by rotating the ball through the sewer channel due to the existence of an outside spiral thread and swivel connection. Therefore, the ball is able to remobilize and remove the settled grit and built- up grease inside the sewer line. This technique is limited to the sewer sizes smaller than 600 mm in diameter (Pisano *et al.* 2003; Fan 2004).

Water jetting

This method is also a hydraulic cleaning way which is implemented by directing high water velocities (and water pressure) against the sewer internal walls at various angles. The basic jetting machine is typically setup on a truck or trailer which is equipped with a water supply tank (with a capacity of at least 3.8 m^3), a high-pressure water pump, an auxiliary engine, a powered drum reel that holds a hose of at least 150-m long with a minimum diameter of 25 mm on a reel (with speed and direction controls), and a variety of nozzles. Jetting is practical for routine cleaning of small diameter low-flow sewers, and can efficiently remove grease build-up and debris from sewer reaches (Pisano *et al.* 2003; Fan 2004). The disadvantage of this method is high demand of fresh water and energy, creation of large noise levels, and occasionally unacceptable working conditions (Schaffner *et al.* 2004).

Flushing

Flushing consists of accumulating water behind a flushing device and then suddenly releasing it through downstream of the device. This method of cleaning of sewer pipes requires the application of hydraulic flushing devices that are variable in terms of characteristics such as form and functionality for different sewers. This technique is proposed by designers and researchers because of the cost-effectiveness of the application (Ashley *et al.* 2004). Other reasons exist such as economic, environmental and ecological that lead sewer managers to use this technique mainly in large-size sewers. The advantage of implementing these devices could be in situations when it is not feasible to regularly cleanse the sewers by means of other hydraulic devices, *e.g.* high-pressure jetting (Bertrand-Krajewski, 2002). Since manual application of this technique for cost, time and health reasons is no more recommended, researchers and designers are particularly focusing on the application of automated cleaning devices. However, in many countries (in particular in Europe), the cleaning of the sewers is led by human intervention. For example, in Germany 95% of sewer channels are cleaned manually (Schaffner 2008). A number of studies have been carried out to investigate and identify the optimal devices principally in terms of potential efficiency to remove the bed deposits in a regular and continuous

way. Studies such as those of Lorenzen *et al*. (1996); Campisano and Modica 2003; Laplace *et al*. 2003; Dettmar *et al*. 2002; Guo *et al*. 2004; Bertrand-Krajewski *et al*. 2005; Bong *et al*. 2015), shows that sedimentation in sewers concerns a very large number of countries.

This cleaning method is the main focus of the current research that will be detailed in the following sections.

2.4.1 Sewer flushing

One of the most common and efficient technique for cleaning large sewers is flushing. The basic concept of this technique is to release a large volume of stored water in the channel to increase abruptly the flow velocity and the shear stress), thus creating flushing waves able to remove sediment deposits accumulated on the invert of the sewer (Pisano *et al*. 1979). The use of flushing is dated back to more than a century. As an example, Fig. 2.7 shows a scheme of an historical flushing method to store the sewer flow and release it towards downstream channel. The flush device provides the same effect as the "dam-break" phenomenon. This technique can be considered both a reactive and preventive method to limit the accumulation of sediments thus maintaining the proper functioning of the network.

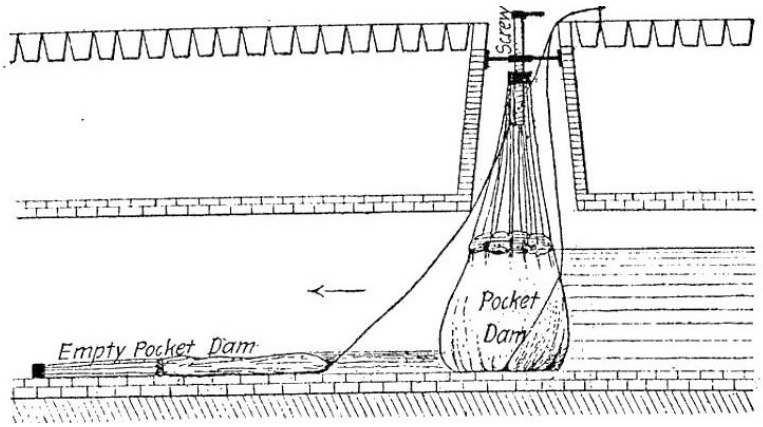

Fig. 2.7 Bag for flushing large sewers used in 1897 (source: www.sewerhistory.org).

Various devices with different level of 'cleaning' capacity can generate flush waves in sewers. Fig. 2.8 shows scheme of types of the gates could be used in sewers. They are different based on different operative conditions: automatic or manual, hydraulic electrical control, etc. (Pisano *et al*. 1998). Under controlled conditions, an automatic flushing device can be operated in two manners depending on the local circumstances and the sewer management: hydraulically or pneumatically with variable gate opening speeds. Further, it is possible to use fixed or mobile flushing gates. Some

devices are installed in a fixed sewer location and work "automatically" when the level of water achieves a certain threshold value. Water for flushing is typically stored using in-line pipe storage or specific reservoirs. Generally, reservoirs can be filled by off-line intake (using a tank and inject water) or in-line reservoir sewer.

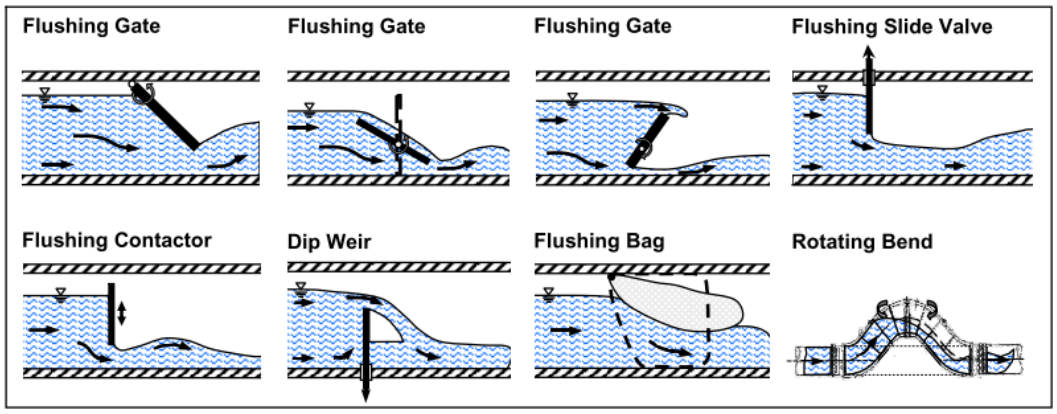

Fig. 2.8 Example of Storage-Volume-Activated-Devices (SVAD) used in sewers (Dettmar and Staufer 2005).

Globally, the application, implementation, result and management of each flushing device could vary from case to case. Depending on sewer circumstances, both manual and automated flushing could have potential ability to be performant. The performance and efficiency of flushes are strictly linked to the characteristics of the deposited sediments. Other parameters also play important roles in the performance of flushes such as the geometrical and hydraulic sewer conditions, the device mechanical characteristics (Fan 2004). Of course, the role of flushing gate setting (*e.g.,* stored water head, flushing volume) as well as the sewer conditions (*e.g.,* slope, cross-sectional shape) effect significantly the flushing performance. Staufer and Pinnekamp (2008) have pointed out that information about the bottom boundary helps to optimize the installation of flushing device. As the cleaning performance is concerned, it can be expected that flushing waves can provide removal effects up to several hundred meters downstream of the flushing device. Not only downstream but also upstream, flushing can affect the channel deposits due to the development of upstream surges that affect sediment build-up upstream the device (Staufer *et al*. 2008; Schaffner and Steinhardt 2009; 2011; Reichstetter and Chanso 2013).

Flushing can be obtained by the mean of various devices with different level of performance (Dettmar *et al*. 2002). Gate devices are very common because of their automated operation, which does not need power supply. The Hydrass® gate (Sikora 1989) and various types of tipping gates belong to this type of devices. The application of other flushing devices has been also investigated in sewers. For example, Hydroguard®, HydroFlush® and Hydroself® being developed by Steinhardt Company© (Pisano *et al*.

1998; Morin *et al*. 2008).

Introduced by Sikora (1989) and also called in French "Vanne cyclique autocurante à décantation", this type of gate has been largely used in France with a relatively good performance in particularly for ovoidal sewer channels. Fig. 2.9 shows a simple scheme of the function of Hydrass gate in different phases of water storage and releasing. The gate has the capacity of discharging a volume of stored water during a short period of time. This is the reason why this gate has been subject to several studies to characterize the hydraulic performance and associated sediment-transport capacity in sewers of various sizes (Chebbo *et al*. 1995; 1996; Lorenzen *et al*. 1996; Pisano *et al*. 1998, 2003; Fan *et al*. 2004; Bertrand-Krajewski *et al*. 2006). Bertrand-Krajewski *et al*. (2003) described the hydraulic behaviour of this gate in a real sewer channels (channel height of 1.8 m). Investigations were carried out to obtain a discharge relationship by taking into account the upstream water head, and to evaluate the flushing performance. This gate was also investigated at laboratory small scale by authors such as Bertrand-Krajewski *et al*. (2004), Bertrand-Krajewski *et al*. (2005), Campisano *et al*. (2006). The optimal setup and operation of gate can be obtained by controlling parameters such as flush frequency, stored water head, etc. Several authors have assessed the gate performance in sewer system under various sediment conditions (Chebbo *et al*. 1996; Bertrand-Krajewski *et al*. 2006). Other investigations by Gendreau *et al*. (1993), Gatke and Borcherding 1996, Ristenpart 1998 and Linehan (2001) have confirmed that the Hydrass gate allows performing repetitive flushes in order to scour deposits downstream.

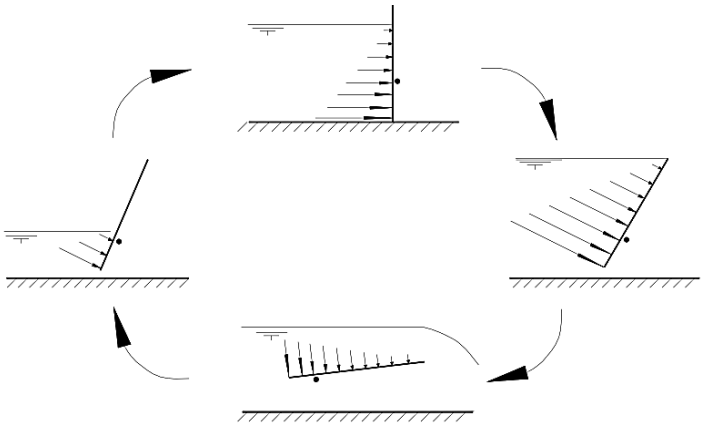

Fig. 2.9 Hydrass gate function in four steps (Chebbo *et al*. 1996).

Other types of tipping gate were mainly explored by Ab Ghani *et al*. (2016) and Bong *et al*. (2016) that aimed to assess the efficiency of such gate in a real open storm network in Malaysia. In their study, a storm channel that drains a small catchment of 0.11 km² was used to undertake flushing

experiments. They monitored a channel trunk of almost 40 m downstream the gate by measuring the sediment heights at every 2 m. They concluded that compared to the flushes generated by Hydrass gates, the tipping gate shows a better efficiency in terms of the time length of the flush. The hydraulic behaviour of the tipping gate for the application in sewer storm network was studied and a discharge relationship and discharge coefficient were determined. Besides, the flushing efficiency of the tipping gate was experimentally (at laboratory) and numerically evaluated using non-cohesive uniform sediments (Bong *et al*. 2013).

Moreover, the erosional and depositional behaviour of a downstream-type (sluice) gate was investigated by (Williams *et al*. 2009) in laboratory scale by using granular deposits. They demonstrated that such upstream control gate is able to provide effective successive flushes rather than a single one to erode granular deposits.

2.4.2 General evaluation of flush performance

Looking into the literature, different ways have been used to determine the performance of flushing in sewers. Indeed, flush efficiency prevalently evaluated based on the removal effects on the downstream deposits.

Flush efficiency is a function of the volume of the released hydrograph as well as of the sewer characteristics (Ashley *et al*. 2004). Geometrical singularities of the channel bed invert (counter slopes, junctions, bed degradations, etc.) are the causes of sediment accumulations on the bed. Such discontinuities result in the loss of the flow energy that influences the downstream flushing performance on its way (Bertrand-Krajewski *et al*. 2003; Ashley *et al*. 2004). Thus, propagation distance (length) of flushing waves as well as the magnitude of sediment deposits significantly affects the flushing performance in sewers.

One of the key parameters for flush performance evaluation is the shear stress (and flow velocity) values. In particular, shear stresses estimate the flush strength and its capacity to remove sediments (Schaffner and Steinhardt 2011). However, shear stress evaluation needs a reliable measurement of the flow variables during the flush (Campisano and Modica 2003). Several authors who evaluated flushing performance used information such as duration and distance over which the bottom shear stress exceeds the critical shear stress. Different critical bed shear stress for flushing condition is reported in the literature to ensure the bed erosion (cleaning performance). Dettmar and Staufer (2005a and b) suggest a value of 5 N/m² to optimize the flushing system while Ristenpart (1994) found values between 2.2-5.6 N/m².

According to Schaffner (2008) who investigated the flushing boundary conditions, a value of between 3-5 N/m² would be necessary to remove sediments. Studies confirm the erosional behaviour of even small flushes as compared with dry-weather conditions.

Furthermore, numerical investigations of shear stress values conducted by Campisano and Modica (2003) for a simplified unsteady flow using a non-dimensional approach. Regressive relationships were provided by the authors to estimate the channel length with erosive effects. An exhaustive series of numerical investigation of flushing and shear stress distribution was undertaken by Dettmar and Staufer (2005a) who aimed to obtain key parameters influencing the flush performance using a tipping gate. By varying the values of flushing- and geometrical-related parameters (sewer and slope diameter, storage length, flushing volume and water head) they performed simulations to analyse the propagation of shear stresses and consequently cleaning distance due to the flush. Unsurprisingly, they pointed out optimal flushes can be obtained with high slopes, high water heads and high volume of flushes. It was shown that the flushing volume on the longer distances. However, this efficiency can be satisfying when the water head is high enough to provide significant flush energy.

Globally, flushing can be evaluated by maximum shear stress values along the sewer channel downstream of the flushing device. This can explain the distance of the sewer channel where sediments were remobilized. Indeed, a critical value to shear stress larger than 5 N/m² can remobilize bed deposits during the flushing in sewers. For example, Staufer and Pinnekamp (2008) have observed a maximum shear stress value of 29 N/m² at 54 m downstream of the gate in t=5s. A maximum shear stress of 14 N/m² was observed by Dettmar and Staufer (2005a) which was able to transport bed deposits with d_{50}=2.2mm. Further, flushing performance over three flat combined sewer sections with various sizes (D: 1, 1.2 and 2 m) and shapes were analysed to investigate three different flushing devices (Dettmar *et al*. 2002). They observed a potential efficiency of more than 400m depending on the characteristics of the flushing gate. A later study of single flushing by Dettmar and Staufer (2005b) over 400 m (300 m downstream of the flushing gate) in a German combined sewer with variable diameters (2.5-3.4 m) and slopes (3.6-4.2 ‰) has shown promising results. The flushing operation with 1.6 m (mean maximum velocity of 3.6 m/s) of water head and 290 m^3 of volume over a deposited bed with d_{50} ranging between 1-18 mm (mean d_{50}=1cm) has generated a long-lasting shear stress that exceeded the critical value of 5 N/m².

Flush frequency is another element that allows increasing the removal efficiency on the bed deposits, which is confirmed by a number of authors: Balayn (1996), Lorenzen *et al*. (1996), Ristenpart (1998), Bertand-Krajewski *et al*. (2005). Various laboratory Campisano *et al*. (2004) and field Chebbo *et al*. 1996; Bertrand-Krajewski and Creaco 2007) experiments have

been conducted showing the advantages of the successive flushes. Other authors such as Dettmar *et al*. (2002) and Reichstetter *et al*. (2013) have demonstrated the effect of the successive flushes through upstream of the flushing device. However, various parameters such as sediment age, longitudinal bed slope, can play the role to limit number of flushes as the more efficient to remove the sediments (Lorenzen *et al*. 1996; Ristenpart 1998).

In addition, the use of automatic or continuous cleaning of the sewers has become the goal of sewer managers of different sewer networks. It is necessary to calculate the potential number of flushing during dry-weather is necessary when talking about the automatic flushing. For example, Bertrand-Krajewski *et al*. (2003) have observed 25-30 flushing per day in combined sewer channel with H=1.8 m. The number of flushing depends on the diurnal flow discharge and gate characteristics. The gate blockage plays the role in the number of flushes.

2.5 Experimental and Numerical investigations on flushing

2.5.1 Experimental analysis of flushing in sewers

In the last decades, several authors have described the hydrodynamics of the flush and how the flushing wave affects sediment transport in sewers. Studies from various authors around the world have concerned both sanitary sewers (Brombach 1982; Lorenzen 1996; Ristenpart 1998) and storm sewers (Ab Ghani *et al*. 2013; Bong *et al*. 2015). Nevertheless, a very limited number of flushing experiments in real sewer systems has been conducted to evaluate the feasibility and the performance of flushing devices as cleaning systems for sewer channels. Table 2.9 reports types of flushing devices used during field experiments. For most of the reported studies the flush impact on the downstream bed deposits of the flushing device has been evaluated in terms of:

- bed height modification (topography);
- bed structure modification (vertical layers);
- bed composition modification (grain-size distribution).

The bed height is probably the most common way in the literature to measure the evolution of the bed due to flushes (Balayn 1996; Lorenzen *et al*. 1996; Ristenpart 1998; Creaco and Bertrand-Krajewski 2009). The structural evolution of the bed was studied by few authors (*e.g.,* Laplace *et al*. 2003). The interest of such observation is principally associated to follow the organic layer in highly cohesive combined sewers. The modification of the bed composition can be rarely found in the literature which may be explained by the complexity of monitoring as well as the cost and the time of experimentation, which requires appropriate sediment sampling in sewer. Furthermore, models that take into account the variation of the sediment composition during the flush are very complex to setup and validate.

Table 2.9 Summary of example of experimental flushes in field cases.

References	Used gate type	Site characteristics (units in m)	Sediment diameter (in mm)	Sewer type
Laplace *et al*. (2003)	Hydrass gate	L(150), Ovoid (1.7) Slope: 0.02%	Upstream: d_{50}(8) Downstream: d_{50}(0.6)	Sewer network
Ab Ghani *et al*. (2013)	Tipping gate	L(40), D(1.2×0.6)	d_{50}(1.11)	Storm network
Ristenpart (1998)	Sewer gate valve	L(170), D(1.5), Slope: -0.6 and 0.7‰	No info	Combined sewer (Interceptor)
Lorenzen *et al*. (1996)	Hydrass gate H(1.9m)	L(2400), D(1.8-4) Slope: 0-1.2‰	d_{50}(0.6 mm)	Combined sewer (circular and rectangular)
Fan *et al*. (2004)	Tipping gate	Sanitary sewer: L: L(555), D(0.46-0.6), Strom sewer: L(1620), D(0.0975-1.83) Slope: 0.3-0.5‰	No info	Sewer and storm networks
Balayn (1996)	Hydrass gate	L(155), ovoid(1.7×1.0), Slope: 0.2-2.6%	d_{50}(2 mm)	Combined sewer (Collector)
Dettmar and Staufer (2005b)	SVAD-type gate	L(400), circular(2.5-3.4), Slope: 3.6-4.6‰	Mean d_{50}(1-18 mm, mean=10mm)	Combined sewer (Collector)
Bertrand-Krajewski *et al*. (2005)	Hydrass gate	L(300), ovoid(1.8-1.1), Slope: 4.54‰	No info	Sewer reach
Bertrand-Krajewski *et al*. (2006); Creaco and Bertrand-Krajewski (2007, 2009)	Hydrass gate	Ovoid(1.8-1.1), Slope: 4.54‰	d_{50}(270 µm) , 90% sediment mixture < 2 mm	Combined sewer (Trunk)
D: Sewer diameter, L: flushing distance, H: water head				

Lorenzen *et al*. (1996) have presented the results of a measurement campaign including both a single and a set of successive flushing tests in a German combined sewer with fine sand sediments. It was aimed at evaluating the effectiveness of a flushing gate within a channel trunk of about 2400 m and with different diameter (1.8-2.4 m), hydraulic capacity (average mean velocity equals to 0.5 m/s), slope (average slope equals to 0.66‰. Mean particle size was reported to be 0.6 mm with deposits having maximum bed height of about 20 cm. According to the adopted flushing protocol, bed thickness was measured every 5 m along the longitudinal sewer channel

before and after each flush. A long flush duration was observed downstream the gate. The comparison between the initial bed heights and those impacted by the flushes revealed a trunk length of that more than 600 m downstream of the gate was subject to considerable erosion. The authors pointed out the important impact of the flushing initial water head. Moreover, a coarsening of the bed composition was observed since the finer sediments were mainly flushed out of the channel.

The experimental work by Ristenpart (1998) in other German combined sewers has provided interesting results regarding the mechanism of sediment transport during the flushing. The geometrical conditions of the considered sewer (with two parallel channels of 1.5 m allowed to carry out different flushing operations with different water heads (0.8 and 1.5 m) and different flushing volumes. The continuous measuring of the bed level and of the suspended solid concentration (SSC) allowed associating the peak of suspended solid to the eroded bed deposits during the flush. Apart the erosional aspects of the flush, a considerable re-depositional impact along the downstream channel was also observed including mainly coarse mineral sediments that were transported as bed-load. Based on the volume of sediments washed out by each flush, the following parameters were considered to play important roles in the flushing performance: the deposit age, the sewer geometry and the flushing characteristics. Most efficient flushes were obtained using higher initial head.

Other in-sewer flushing experiments have been done by various authors who monitored the sediment evolution under the flush experiment by monitoring the bed height (Bertrand-Krajewski *et al*. 2005; Abderrezak and Paquier 2007). In the context of a research program (Bertrand-Krajewski *et al*. 2006), bed heights were recorded after each flushing operation of a large set of flushes generated using a Hydrass gate in an ovoidal combined sewer channel in Lyon. The mean grain size of particles was reported as fine sand. Before and after each flush was the thickness of the bed was measured (Creaco and Bertrand-Krajewski 2007, 2009). These studies were conducted, in particular, aiming to numerically describe the flushing that is presented in "numerical investigations". According to the results also bed irregularities play a role in reducing the flushing performance in removing the sediments.

One of the limitations of in-situ monitoring processes during flushing is the need of reliable measuring devices. Uncertain flow measurements can influence significantly the evaluation of the flush and hide the sudden increase of the shear stress (Staufer and Pinnekamp 2008). The measurement resolution (interval) of the flow data is then very important in particular at the early stage of the flush close to the peak of the generated flow (Staufer and Pinnekamp 2007). Another example found in the literature is the water level measurement of automatic flushes. In such case the data can be missed when recording sudden increase of water level that lead to erratic estimation of the shear stress (Dettmar *et al*. 2002).

2.5.2 Laboratory studies

Due to the field complexity, experimentations under laboratory controlled conditions have been carried out to study the detailed mechanisms of the flushing (Satufer and Pinnekamp 2008). On the one hand, at laboratory scale, studies on the flushing in flumes by using synthetic particles allowed to evaluate flush performance and to develop improved design indications. On the other hands, the simplifications needed at laboratory scale are evident limitations for the transformability of the obtained results. Within laboratory conditions, many processes (*e.g.,* sediment heterogeneity) cannot be fully reproduced as in real sewers. However, many restrictions are relevant in field cases, *e.g.,* sampling conditions, lack of appropriate high-quality devices for sewer systems and monitoring cost. In this respect, a number of researchers have focused on flushing and associated sediment transport in small laboratory flumes (Bertrand-Krajewski *et al*. 2004; Campisano *et al*. 2004, 2008; Todeschini *et al*. 2010; Shirazi *et al*. 2014).

Laboratory experiments on flushing have been developed by the research group of the Catania University. Laboratory (Laboratory of hydraulics of the *Dipartimento di Ingegneria Civile e Ambientale* (DICAR) at the University of Catania) investigations of the erosional performance of successive flushes were undertaken by Campisano *et al*. (2004). Two sets of experiments with 30 cm of uniform volcanic sands and without sediment in a 4 m flume were developed using a sluice gate as flushing gate device. Different flushes were generated by varying the water head and the flushing volume. Flow-related (water heads) and sediment-related (bed thickness and flushed-out sediments) were evaluated for each flush. Based on the results of flushing performance, variable flush efficiency was observed with reference to the thickness of the bed deposits. Based on the observations, successive flushes were more performant to remove the sediments. Relationships to correlate the needed number of flushes to scour sediments were developed for each flush type. Later, Bertrand-Krajewski *et al*. (2005) have investigated the behaviour of a Hydrass flushing device. Reliable series of data were obtained that allowed to investigate field and numerical experimental analysis of the flushing performance.

Further investigations of the effect of single flushes over the cohesive deposits were conducted in laboratory by Todeschini *et al*. (2010) who realized two sets of experiments without (to evaluate the flushing waves and propagations) and with sediments (to consider the removal capacity of the flush) with different slopes and water depths. Campisano *et al*. (2008) performed laboratory analysis on successive flushes over both non-cohesive (consisting of quartz sands) and cohesive sediments (consists of both quartz sands and silt-clay particles). Different cohesive bed mixtures were moreover adopted in the experiments. Two sets of experiments with different slopes and water levels were carried out. The authors have evaluated the flush

performance upon bed thickness evolution along the flume and accumulated sediment mass flushed out by consecutive flushes. According to the observations, it was found that sediment bed behaves as non-uniform granular mixtures that cause variable flushing efficiency in terms of consecutive flushes. Moreover, the effect of cohesion of the deposited bed was highlighted with an increase of the erosive effect of the flushes as the cohesive matrix of the sediment is broken.

Other laboratory investigations on the performance of successive flushes (with two water heads) over 30 cm uniform bed sediments (d_{50}=1.8 mm) in an 18 m long flume were carried out by Shirazi *et al*. (2014). Flushed sediment and characteristics of the scoured deposits at the end of each flush was compared with estimated values using four sediment-transport formulas. The comparative results by the formulas highlighted the importance of the chosen sediment-transport formulas implemented in models to describe the bed erosion.

2.5.3 Numerical studies of flushing in sewers

Sewer flushing has been commonly described using one-dimensional models because of the 1D nature of sewer systems. The hydrodynamic and sediment-transport characteristics of the flushing phenomenon have similarities with the dam-beak process. Predicting dam break flows and their consequential impacts over the movable river bed has been numerically investigated by many researchers (*e.g.,* Zhang *et al*. 2011). The literature shows that the propagation of the flushing flow throughout sewer channels has been so far the subject of various numerical investigations during the recent decades. Numerical studies have been undertaken for the following main motivations:

- understanding the hydraulic boundary shear conditions and cleaning performance of flushes in terms of scoured distance;
- determining sediment removal efficiency of flushing operations;
- evaluating the hydraulic behaviour of flushing to select the appropriate device for sewer systems under study;
- testing various sediment-transport formulas to develop or find a better relationship estimating the sediment-transport discharge under flushing operation (Creaco and Bertrand-Krajewski 2009; Shirazi *et al*. 2014);
- obtaining design and management indications for flush operatiob scheduling plans (Campisano and Modica 2003; Campisano *et al.* 2007; Tdeschini *et al*. 2010).

Some interesting investigation concerning flushing modelling are reported in the Table 2.10.

Table 2.10 Example of numerical research (field and laboratory-based) studies on flushing operation.

References	Site characteristics	Flushing characteristics	Used model	Investigation aim (s)
Balayn *et al*. (2003)	RS, O, L=160, D=(1.7×1), mean d_{50}=2 mm	Q_{max}=0.5	1D model Rubarbe	Relation between Q and H_w during sediment transport
Bertrand-Krajewski *et al*. (2003)	RS, Co, L=300, D=(1.8×1)	Mean Q= 51.1 L/s, Mean Vol= 44.4	Model-based outflow relationship	Hydraulic behaviour of Hydrass gate
Bertrand-Krajewski *et al*. (2004)	LS, R, L=3.9, S= variable	(Bertrand-Krajewski *et al*. 2003)	Model-based outflow relationship, discharge coefficient	
Bertrand-Krajewski *et al*. (2005)	1)LS, R, L=3.9, S= variable; 2)RS, Co, L=300, D=(1.8×1.1)	1) Q=0.34-5.71L/s, H=variable 2) S=4.2‰ (Bertrand-Krajewski *et al*. 2003)		
Staufer *et al*. (2007)	RS, Co, L=513, D=3, H=2.5	Vol=217, H_w=1.8, Sl=50m, Q_{max}=2	Fluvius 1Di and SSIIM (3D)	1D and 3D comparison of flushing τ_b
Staufer and Pinnekamp (2008)	RS, C, D=2.5, S=4.2‰,	Sl=101, SF, H_w=1.02	Fluvius 1Di	Effect of flushing waves on the τ_b
El Kadi Abderrezzak and Paquier (2007)	See Balayn *et al*. 2003	H_w=0.72, Sl=31m, Q_{max}=2	1D numerical model	Removal effect of flushing waves
Creaco and Bertrand-Krajewski (2009)	RS, Co, L=400, ovoid (1.8×1.1), d_{50}=270µm Mean slope≈0	H_w=0.8	Model-based outflow relationship	Evaluating the flushing efficiency by 4 formulas of sediment transport
Todeschini *et al*. (2010)	LS, R, L=5.5, S= 0.5, 2%, d_{50}=0.25, 0.48, 0.9 mm, H_s=0.5-1 cm)	H_w=0.15-0.25	1D DSV-Exner TVD- McCormack	Scouring effect of flushing waves
Schaffner and Steinhardt (2011)	Similar real scenarios: Circular (D=0.5-1)	Vol=15, H_s=0.6,	1D SWMM model	Evaluate flushing performance (shear stresses) in siphons
Shirazi *et al.* (2014)	LS, R(0.4×0.65), L=18, S= 1.5, 3%, d_{50}=1.8 mm	Vol=0.144, 0.48, H_s=0.12, 0.4 cm, Sl=50m, Q_{max}=2	1D DSV-Exner TVD- McCormack	Performance of successive flushes and validate transport formulas
Schaffner (2016)	Similar real scenarios: C, D=800, 1600, S=0.1, 0.15%, L(650, 1500)	For 1D: Vol=42.3, 145.8, H_s=0.4-1.6 For 3D: Vol=112.5, H_s=1-3	1D: EDWA model 3D: SSIIM model	Influence of flushing vol. and H_s on modelling

Units are in m; τ_b : Bottom shear stress

RS: Real case; LS: Laboratory scale;
C: Circular, R: Rectangular, O: Ovoid, Co: Compound, L: downstream studied sewer length; S:slope, D: sewer Diameter, H=sewer height, Q=discharge (m^3/s)
H_w: Flushing water head, Sl: Storage length, Vol: Flushing volume (m^3), H_s: sediment thickness, SF: Single flush; MF: Multiple flushes;

Various authors aimed to obtain a proper relationship to estimate sewer sediment-transport discharge during the flush operations. The removal efficiency of flushing was assessed experimentally by Creaco and Bertrand-Krajewski (2007) by leading a number of flushes during 5 months over a 36-months age deposits. Data from this experimental case was used to calibrate and validate a model, based on 1D DSV-Exner equations, in order to describe the sediment-transport processes during the flushing propagation. The Meyer-Peter and Müller (1948) formula was also used to evaluate the sediment-transport discharge. The authors highlighted the role of deposits age and accumulation history in the critical shear stress and therefore in the erosional effect of the flush. The same authors (Creaco and Bertrand-Krajewski 2009) have tested four formulas that gave a good agreement to predict the bed evolution due to successive flushes. It was pointed out that numerical simulations of flushing and associated sediment transport require taking into account the bed irregularities, detailed sediment data (*e.g.,* heterogeneity) to obtain more coherent description of the phenomenon. More recently, Shirazi *et al*. 2014 using a 1D effort compared four sediment-transport formulas showing that the use of such formulas is case-dependent and that to setup a general methodology to estimate the transport capacity of flushes is complicated.

Campisano and Modica (2003) investigated the flushing performance as a function of sewer pipe characteristics. Realistic simulations of flushing by using a 1D dimensionless approach were performed showing the relationship between the bed shear stresses and flush parameters (*e.g.,* flushing distance). They finally obtained useful and practical indications on the length of the trunk where the critical shear stress is achieved. The erosive behaviour of the flushing waves over deposited bed including cohesive particles (clay) was evaluated by Todeschini *et al*. (2010) who investigated various flush types using a 1D model. They confirmed the increase of the critical shear stress of the bed sediment mixture in presence of cohesion.

In general, the precision level of numerical analysis of sediment transport depends mainly on the aim of the study to assess the dynamic of the sediments. From the hydrodynamic point of view, flush procedure is considered as an unsteady rapidly varying flow which can be analysed by different dimensional flows (1D, 2D or 3D). The choice of the dimensions is limited to many conditions such as the scale size of the case study the computing time and power, as well as the amount of field data to be analysed. A comparative numerical study using a 1D and 3D models was led by Staufer *et al*. (2007), who aimed to describe the bed shear stresses of large-sized sewers in two different levels of accuracy. They highlighted the complexity of 1D-models in particular in terms of geometry. By simulating the flush head, an underestimation an overestimation of the estimated shear stresses were remarked for 3D and 1D, respectively.

As a flow caused by dam break, flushing produces the positive and

negative celerity surges resulting from sudden release of water instore. Schaffner (2008) has considered the flow turbulent effects in both directions and the erosive actions of the flushing waves on the deposits using 3D commercial software. Furthermore, mechanism of flushing behaviour and turbulence waves were numerically described by Staufer and Pinnekamp (2008). Relatively good agreement between experimental and numerical results was demonstrated for the peak value of the shear stresses. They explained the differences (16%) by the overestimation of the numerical approach that simplifies the flow conditions comparing to the reality.

Interestingly, the literature review has shown that the analysis of the sediment transport associated to flushing events (both in laboratory and field scales) has neglected the heterogeneity of the sewer sediment, thus considering the presence of uniform sediments simplify the problem (Lin and Wu 2013). This limitation comes also from the existing formulas to estimate sediment-transport discharge during the flush. Evidently, a research gap exists on this topic and efforts are needed to include processes associated to the non-uniformity of the bed sediments in the modelling of sewer flushing. In sewer cases, various authors have already highlighted the need of taking into account the granular mixtures of the bed to describe the sediment-transport processes (Ashley *et al*. 1999; Rushforth *et al*. 2003; Banasiak *et al*. 2005) under flushing circumstances (Balayn *et al*. 2003; Campisano *et al*. 2008; Todeschini *et al*. 2008, 2010).

Chapter 3
Experimental methodology and measurement campaign

3.1 Generality

The already mentioned gap of knowledge to understand the transport of sediments in sewers during the flush has motivated this study to investigate real sewer deposits. It was expected that these experiments lead to better understand the processes of bed mixture of grain sizes during the flushing event. Such examinations of the flushing effect (including the variation of the bed composition) previously have never been introduced in the literature. Then the available data from the experimental campaign will allow establishing models able to reproduce sediment-transport processes. Building-up such models could be a tool to predict the same processes in other cases.

In this regard, the present chapter is dedicated to detail the effectuated experimental protocol to observe the flushing event and consequently bed material modifications due to the flush. To this purpose, the pilot field is firstly presented which is following by the experimentation setup and facilities. It should be informed that the experimental setup is already explained in the published *Water Research* paper (*Shahsavari et al. 2017*).

3.2 The experimental pilot sewer channel

3.2.1 Aim of the flushing test and choice of the pilot channel

Based on information provided by the SAP's (*Section de l'Assainissement de Paris*) information, the Parisian combined sewer network comprises a number of man-entry trunk sewers with a total length in the order of several tens of kilometres. Several of these sewers are affected by problems of sediment accumulation discussed in Chapter 2 of the thesis. Therefore, the Paris municipality decided to explore through experiments the potential of various flushing devices to perform the "automatic" cleaning of sewer channel and reduce human intervention in the high-risk cleansing procedures. Based on the available information (personal communication, June 6, 2016), almost 250 sewer workers attended yet in manual cleaning of about 130 km trunk sewer channels of the Parisian network. Thus, acknowledging the local particularities of each sewer channel, the SAP intended to consider the most performant and applicable flushing device to help the sewer management strategy. Different sites of Paris sewer network were initially proposed for the study. The proposed sites had specials common particularities: *(i)* they were subject to significant sedimentation due to the channel geometry; *(ii)* an online gate was already installed on these channels to reduce cost of installation. Moreover, a preliminary hydraulic study of the gates and their capacity to generate flush waves through downstream channel was carried out for each site. The results of the study led to choose the experimental site called *Chemin Vert* (Fig. 3.1).

In this regard, the municipality was interested in exploring the possibility to reconvert the existing mobile gate (used to derivate flow during storm flow events) as a flushing gate device to evaluate its removal efficiency on the existing deposits. The channel trunk downstream of the gate was selected as pilot system as it is prone to large sedimentation. To this end, the experimental campaign was designed and planned to obtain high-fidelity data able to characterize he flushing performance and to allow validating a reliable model with a novel approach.

3.2.2 Characteristics of the pilot system

Characteristics of the study site

The *Chemin Vert* pilot trunk channel is a part of the *Des Coteaux* collector with a man-entry size (Fig. 3.1) which is belong to the Parisian combined sewer network. This name is given from the place where the gate is already installed gate that is situated under the *Chemin vert* street. The chosen combined trunk sewer (collector) is situated at the 11th arrondissement of Paris city. Based on the data provided by Paris municipality, this trunk is designed to drain partly the wastewater from 12th and 20th arrondissements. At the studied site location, the trunk sewer site collects wastewater of about 180.000 inhabitant equivalents over a surface area of about 640 ha. The collector also intercepts runoff from the catchment surface. The hebdomad/daily merchants, commercial and industrial activities are also presenting in this catchment. It should be noted that 1.700 street gutters exist on the catchment, which intake the water from surface runoff. APUR (2016) has highlighted the commercial surface of about 27.8 ha over the 11th arrondissement of Paris. The overall slope of *Des Coteaux* trunk channel is about 0.6 mm/m and the studied sewer channel being as 0.8 mm/m.

Geometry of the channel

The flushing test concerned a 1.1 km long trunk of the collector. The average longitudinal slope of the trunk (over 1.1 km) is almost 0.08‰. This weak slope is the reason why the channel is subject to deposition and accumulation of sediments on the pipe invert. Bed invert elevations on every 1 m along the longitudinal direction of the channel were collected by Paris Municipality by using a simple measuring stick (Fig. 3.2). The figure shows the longitudinal profile of the pilot sewer channel. The bottom of the channel shows both negative and positive slopes with the irregularities through the upstream part of the trunk that are other causes of sedimentation. Sewer channel walls are made of cement. From the picture of Fig. 3.3 it can be seen that inside the channel three main pipes collecting firefighter and cooling water as well as electrical tube are installed on the top of the channel.

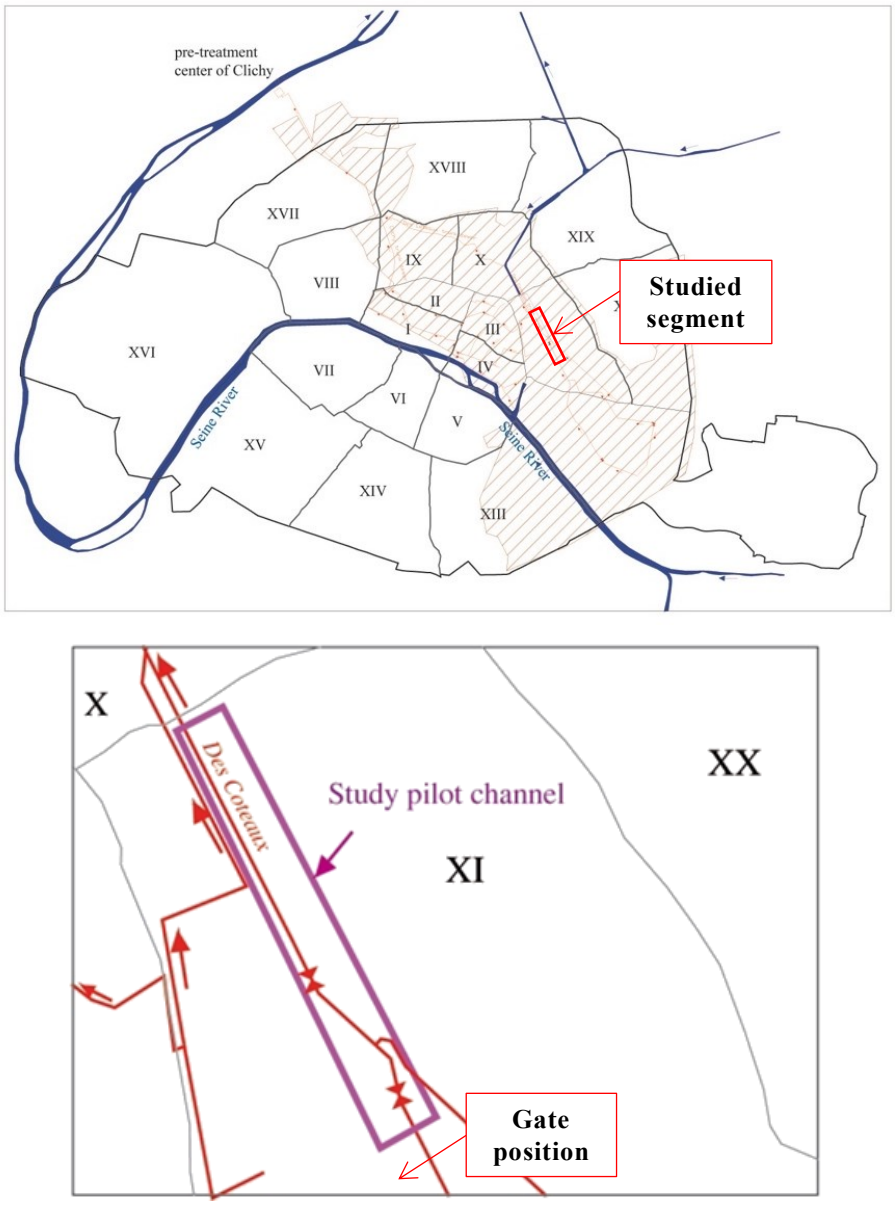

Fig. 3.1 Administrative arrondissement of Paris city; hatched area is the entire catchment zone drained by the whole collector of *Des Coteaux*. The figure below shows the position of the pilot channel in the city.

At the downstream of the sewer channel, a storage chamber was designed to trap sediments during high flows. The downstream segment of the channel has a higher slope with almost no considerable irregularities comparing to the upstream segment.

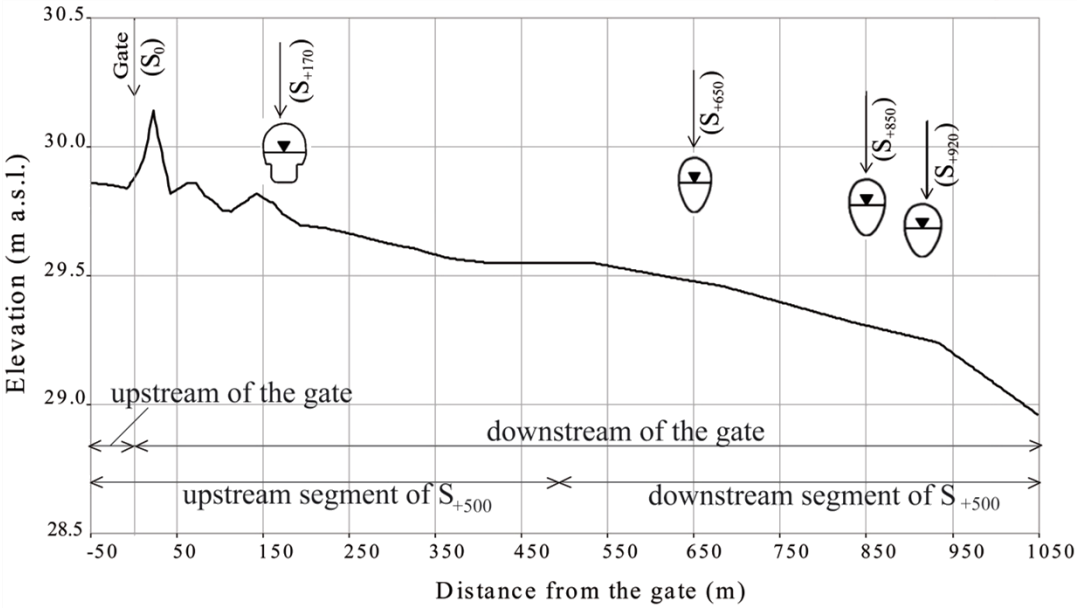

Fig. 3.2 Bottom elevation of the experimental pilot sewer channel. Flow inlet/outlet locations of the studied channel are illustrated.

Fig. 3.3 Studied sewer channel with pipelines installed on the top of the channel.

The gate is placed at 50 m from the upstream entrance of the channel (section S_0 as indicated in Fig. 3.2). It should be noted that the channel sections are referred to S_0 (*e.g.*, section 250 m downstream the gate is called S_{+250}). For simplicity, the channel was divided into two portions: upstream

and downstream of the gate. The figure reports also the names of the sewer sections significant for the experiment and for the numerical analysis.

The trunk sewer conveys an average daily flow rate of around 0.35 m^3/s during dry-weather. Also, the average maximum flow velocity during dry-weather time is almost 0.5 m/s. Moreover, the channel has various flow inlets in the downstream trunk. The largest inflow discharge is at S_{+170} (Voltaire Boulevard) with an average value of 200 l/s recorded during dry-weather flow.

Fig. 3.4 shows the channel cross-section: ovoidal shape with *cunette* for conveyance of the dry-weather flow. Two lateral walk-ways are used for various aims: channel inspection, manually operated cleaning procedure using the wagon *vanne* (Ashley *et al.* 2004).

Due to the geometrical characteristics of the channel, the sewer trunk is prone to deposition of sediments on the channel invert. Preliminary sampling carried out by sewer operators, has revealed sediment deposits in the order of 0-30 cm/year in depth.

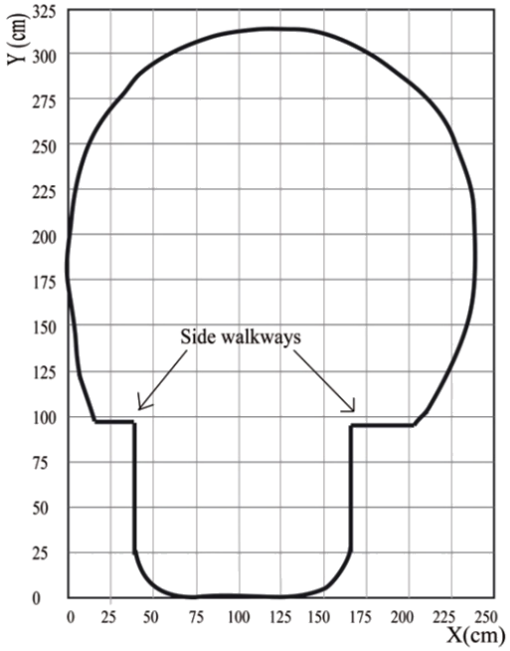

Fig. 3.4 Channel cross-section profile.

Characteristics of the flushing gate

A tipping gate is installed in-line within the experimental channel trunk at section S_0. It was implemented in 1995 and is used to derivate overflows toward the Seine River in the Paris city in the case of storm and high flows. Fig. 3.5 shows a picture taken from upstream of the gate illustrating the implementation of the gate in the sewer. The gate is

electrically-driven and opens by means of two hydraulic jacks installed on the side walls. Overflows are discharged over the crest.

The gate is schematized in Fig. 3.6. In the closed position, the gate prevents wastewaters flowing downstream by storing it in the upstream trunk behind the gate. Based on the gate design, the maximum stored water level can achieve almost 2.2 m just upstream the gate location. Conversely, in the open position, the gate find room within a compartment in the sewer invert to minimize the disturbance of the flow. It is important to note that the gate opening takes place in a short period of time within almost 1 min (56 s). This characteristic allows the gate to act as a flushing gate.

Successive detailed surveys of the sewer channel have been carried out at the beginning of the research in order to observe directly the sewer conditions as well as the depositional patterns. The survey allowed taking decisions about types of device to use and their installation inside the sewer.

In geometrical point of view, along the studied channel, the size of the sewer structure was slightly varying going toward downstream. In this study this slight variation is negligible.

Fig. 3.5 Implemented gate being as a radial tipping gate with weir function.

a)

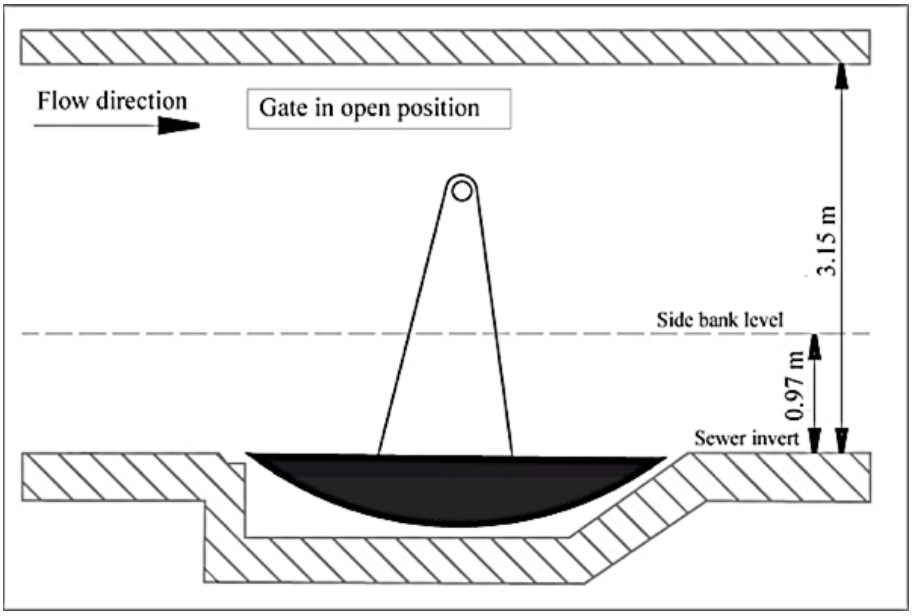

b)

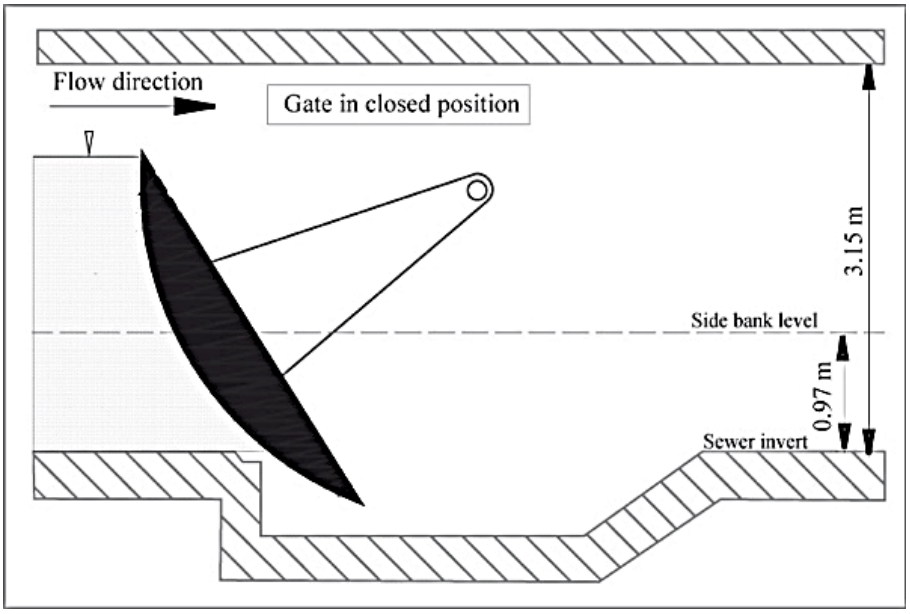

Fig. 3.6 Scheme of the gate profile, function and scheme of position in the channel: a) when closed and b) when open.

During in-sewer survey, bed sediments were roughly examined using a simple stick and a shovel. Fig. 3.7 shows two photos taken during the inspection from sediments upstream segment (at left) and downstream segment (at right).

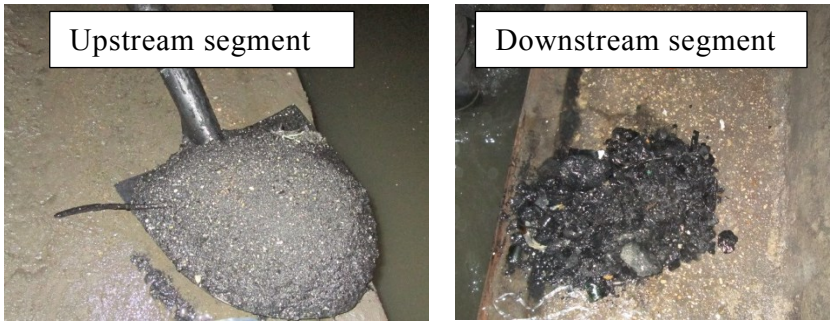

Fig. 3.7 Sediment types during preliminary visual observations of the sediments. Photo at left: taken from sediments of upstream segment of the channel ($<S_{+500}$); and photo at right: taken from sediments of downstream segment ($>S_{+500}$).

Remarkably, it was observed that:

(i) the sediment deposited in the segment downstream of S_{+500} was coarser than upstream of S_{+500}, containing fine to large sands up to gravel.

(ii) sediments tended to accumulate more in correspondence of singular points such as inlets or bumps;

(iii) finer sediments seemed to show a granular-type texture typical of loose sediment with low cohesion;

(iv) in the lower part of the channel (almost at the end), the bed sediment was observed to be compact as “armoured”;

(v) other solids of different nature and origins were found among the bed particles in the downstream of the channel (pieces of metal from the pipeline reparation inside the collector, asphalt and other construction pieces coming from the catchment surface;

(vi) in many sections of the channel, a significant amount of resin-type sediments and rags were found to partly form the sewer deposits (Fig. 3.8).

Fig. 3.8 Image of floating sewer deposits of rags/resin-type sediments through the studied channel.

3.3 Protocol of the flush experimentation

Due to the complexities of the sewers coming from a wide range of factors (*e.g.,* difficulties of direct measurement, lack of appropriate devices, non-adapted method), the choice of measuring apparatus and techniques becomes a challenge in particular regarding to the experiment costs (Ashley *et al*. 1999; De Sutter *et al*. 2001). Indeed, measuring equipment is one of the important sources for operators and municipalities to improve sewer sediment management (Bertrand-Krajewski *et al*. 2006). That is why device factories aim to more and more develop/design/adapt measuring devices to better monitor sediments and study processes within sewers and consequently the sediment-transport models. The hostile conditions of the sewers mainly due to the aggressive gas and flow as well as high turbidity of the water do not allow applying measuring devices used for clear waters. Besides, the use of non-suitable classical devices in sewers can lead to errors in experimental data (flow and bed deposits). Therefore, in this study, efforts were made to reduce as much as possible, the errors coming from equipment and installations.

3.3.1 Phases of the flush test

A protocol was proposed to monitor the flushing experiment and to measure the effects of the flush in the pilot channel. The whole measurement campaign was carried out during five consecutive days since 07/07/2014 to 11/07/2014. The overall schedule is summarized in Table 3.1. In-sewer access time restriction was imposed by the Paris Municipality provided that the experimental procedure was developed over five days. During the first two days, the bed deposits before the flush was examined which was followed by device setup into the sewer channel during the third day. During the fourth day (10^{th} July), the flushing procedure was carried out including the storage and releasing phase. Finally the bed deposited after the flush was examined during the last day by applying the same procedure done as before the flush. So, the measurement campaign of the sediments was carried out in two phases before the flush (called hereafter BF) and after the flush (called hereafter AF).

The day the flushing test was carried out, the sewer network flows were, modified to limit inlets into the trunk sewer. Furthermore, before the flushing test all devices that were in contact with the sewer flow, were cleaned to minimize the impacts on the quality of data. The gate closing procedure was launched to store inflows upstream the gate. The storage phase took almost 2 h. Then the gate was opened at 12:04:05 of the same day to release the flush in the downstream channel trunk. A sensor was installed on the gate to measure the crest position of the gate during the operation.

Table 3.1 Detail of the activities developed for the field measurement campaign.

Date [d/m/y]	Experimental activities
07-08/July/2014	Data collection: • Bed samples before the flush • Radar/sonar measurement before the flush
09/July/2014	Setup of experimental equipment
10/July/2014	Execution of the flush test and data acquisition during the flush
11/July/2014	Data collection: • Bed samples after the flush • Radar/sonar measurement after the flush

3.3.2 Measuring flow- and sediment-related parameters

A set of measurement devices was installed within the channel to monitor the flush experiment. Based on the results of the preliminary survey, the general idea was to measure as much as possible parameters related to the flow (*e.g.,* shear stress) and to the sediment transport. Researchers have outlined that obtaining high-quality flow-related parameters allows estimating more accurate values shear stress that lead to better study the sediment-transport processes (Hughes *et al*. 1996; Staufer and Pinnekamp 2008; Lepot *et al*. 2013; Momplot *et al*. 2013; Lepot *et al*. 2016).

Therefore, the measuring devices were selected based on their capability to 'catch' the evolution of rapidly varying flows due to the flush (in particular at the beginning of the flush). The choice of the devices was also influenced by the need of using probes able to resist to the sewer harsh environment. The other important limitation that was taken into account for the selection of devices was the level of turbidity of the sewer flow in particular during the flush. It should be noted that resistance to corrosion in the sewer was not considered as a problem because of the short period of use of the measurement equipment for the experiment. During the experiments the devices were set to record with the maximum data acquisition frequency.

Five cross-sections of the pilot trunk sewer were identified to install measuring devices for monitoring the flush performance. Devices were place in the exact positions for each cross-section. Indeed, the importance of device position to limit experimental errors has been emphasized by Bonakdari and Zinatizadeh (2011) who concluded that measuring methods are unique and specific to each experimental site. Fig. 3.9 shows the position of the installation of the sensors in each sewer section. The figure illustrates also the locations of the five cross-sections along the sewer channel (located at S_{-50}, S_{-5}, S_{+5}, S_{+50} and S_{+100}). The location of the measuring sections was

determined to be almost close to the gate in both upstream and downstream of the flushing device to obtain more information about the flush waves. Moreover, Table 3.2 summarizes the information on the used measuring devices for the experimental test. Main flow parameters were measured by using a pulsed doppler velocimeter and an ultrasound (US) device. The first device manufactured by SonTek Company is able to measure the flow velocity [m/s]. The measure of the flow discharge [m^3/s] is obtained based on the observed flow velocity and the associated wetted area at the given section. The device diffuses 5 signals towards different directions at a given an instance into the water column. According to the mode of operation the device provides both flow velocities and water levels separately and calculates time-averaged velocity over a lap of time.

The US device was manufactured by IJINUS© Company which calculates the depth of water based on the measure of distance between the device and the water free surface. The flow turbidity was measured at three elevations at each cross-section (15, 25 and 65 cm above the channel invert). Used devices are manufactured by PONSEL Company that measures the turbidity of water using optical technique in Nephelometric system. It should be emphasized that, as indicated in technical description of the device, measurement range of turbidimeters are between 0 and 4500 *NTU*. This is the range that sensor's error remains below 5% of the real value which is indicated by the company. All the described devices were set to synchronize reading times and frequencies. An already existing measuring station belonging to the Paris Municipality that permanently records water levels at section S_{+1050} was also checked for use during the test. This section can give valuable information on the flow during the flush operation. The station equipped with an ultrasonic flow meter by transit time. The probes record the water level with variable time steps with an average interval of 150 s.

Devices were firstly tested in laboratory before using then in the field. The calibration of turbidity devices was carried out using certified reference Formazin solution of 2000 Nephelometric Turbidity Unit (NTU).

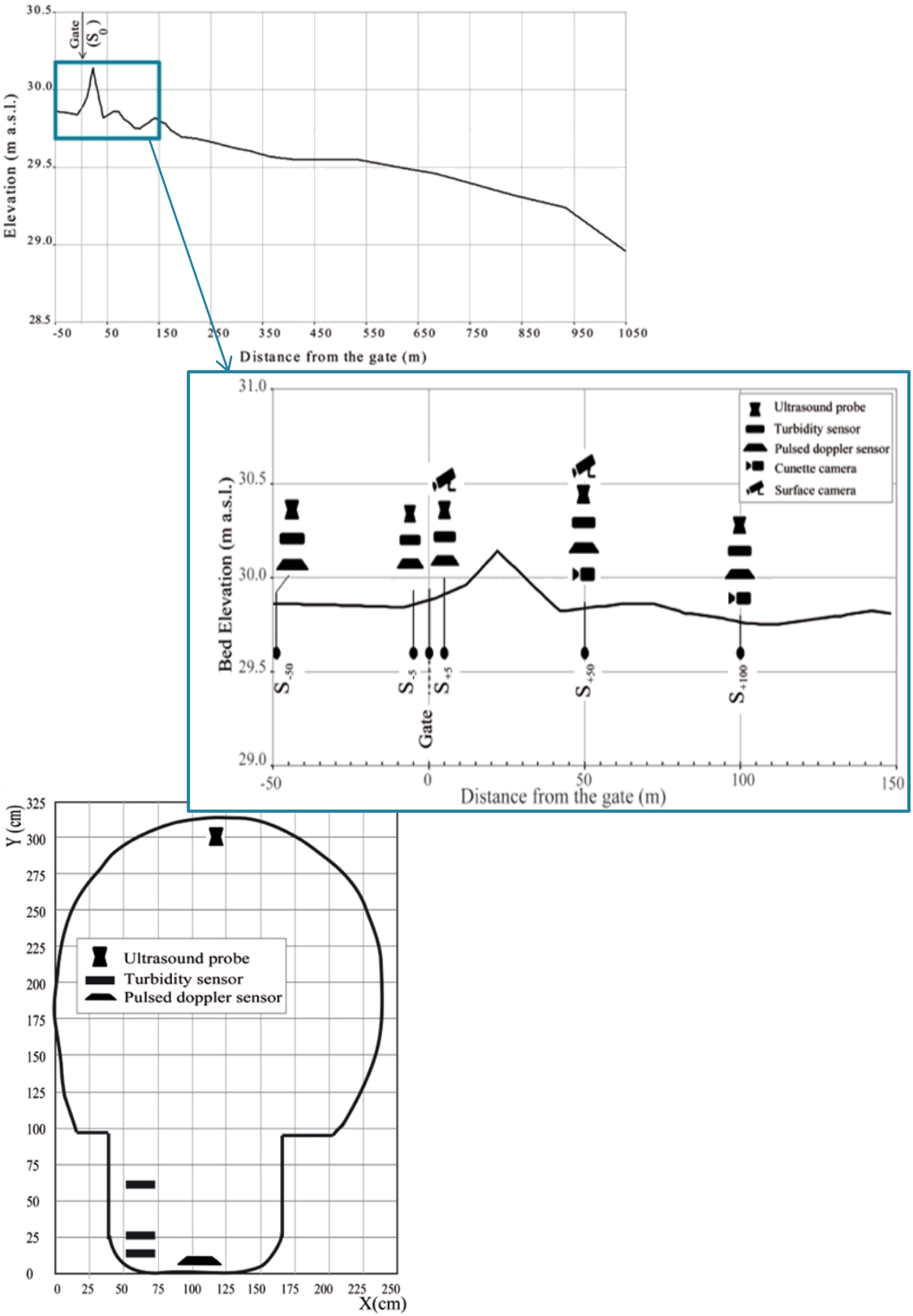

Fig. 3.9 Measuring cross-sections and device positions in the experimental sewer channel.

Table 3.2 General information on the used measuring devices based on factory notifications.

Devices	**Device name**	**Method of measurement**	**measured parameters (unit)**	**Overall accuracy**	**Time interval (in s)**	**Field installation (in cm from bottom)**
Doppler velocimeter	Pulsed Doppler Sontek IQ Plus™	Acoustics beams pulses	V, h (m^3/s)	±1%	10	+13
Ultrasound	IJINUS™	Acoustics measurement	h (m)	4mm/3m	15	+2.59
Turbidity sensors	Ponsel	Optical-Nephelometric 90°	concentration (NTU)	5% of recorded value	10	+15, +25, +65 *

* Three turbidimeters called hereafter T15, T25 and T65 designing the vertical positions.

Measurements before and after the flush experiment

Recent researches aimed to quantify sewer deposits by using new techniques to draw the bed topography in sewer channels (Bertrand-Krajewski and Gibello 2008). The recent techniques based 3D morphological draw of the sediments (Lepot *et al*. 2014) or image-based methods (Oms 2003; Nguyen *et al*. 2009; Regueiro-Picallo *et al*. 2018) try to fill the knowledge gaps on the sediment processes. In the context of the current study, protocols to measure the sediments forming the deposits in the channel BF and AF were also defined. The bed topography was measured using radar scanner techniques. Also, measurement included sampling of the deposits in various cross-sections of the sewer channel upstream and downstream of the gate. The details of procedure to realize these two investigations are presented in the next sections.

Bed scanning using radar/sonar technique

A bed-scan system was adapted to the sewer channel cross-section by GEOSCAN Company to scan the deposited bed topography. This technique is a combination of two measurement methods: radar and sonar monitoring which together allow obtaining the transversal cross-section of the bed (Fig. 3.10). The radar measures the longitudinal bed profiles in the axis of the channel while the sonar provides the transversal cross-section occupied by the sediments on the bed invert. The combination of these two data provided a 3D vision of the deposits throughout the whole channel. The more the spatial steps for sonar acquisition are short, the more the precision in the volume of deposits increases. Measurements BF and AF were carried out enabling comparison to establish erosional impact by the flush.

Fig. 3.10 The bed scan apparatus developed to measure the sewer bed topography before and after the flush.

This technique is a novel method to scan the reliefs of deposits by capturing two types of data:

1. Radar records: deposit height through longitudinal axis of the channel as it can be seen in Fig. 3.11.

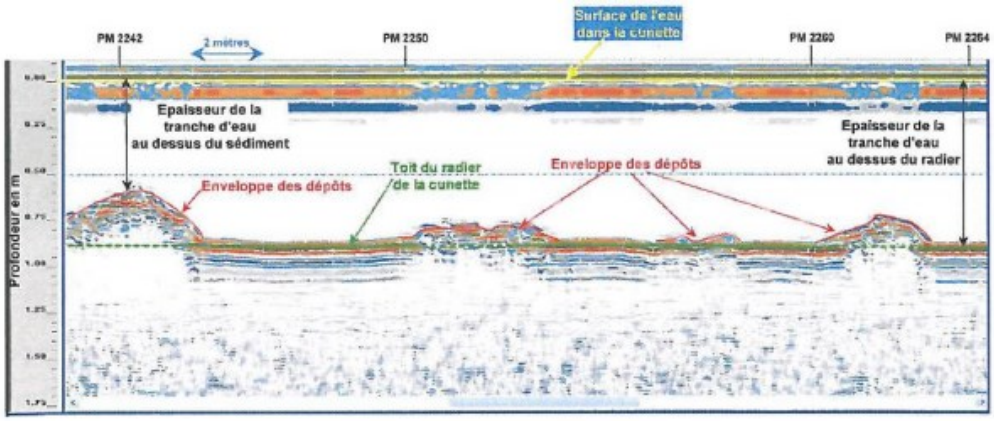

Fig. 3.11 Example of recorded data from radar technique.

2. Sonar measures: transversal information of deposits in each section as can be seen in Fig. 3.12.

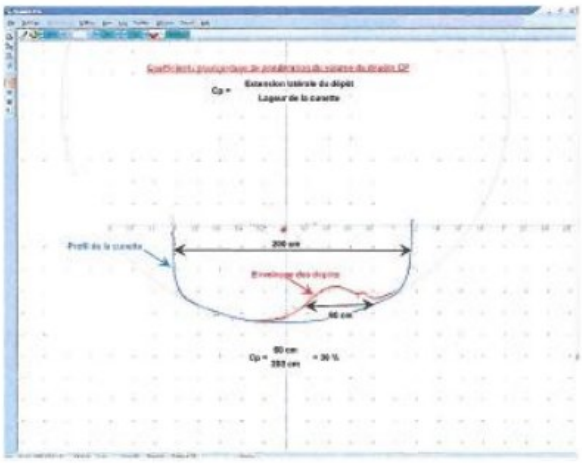

Fig. 3.12 Example of recorded data from sonar technique.

So the combination of both types of data gives the volume of sediments in height of sediments between two specific sections with a determined distance.

Sediment sampling procedures

Several studies were undertaken to examine also methods to extract sewer sediments samples. Many indications were obtained regarding various factors such as sewer sizes, sediment availabilities, and the complications to handle (Laplace *et al*. 1988; Ristenpart *et al*. 1992; Jefferies and Ashley 1994). More indications concerning measuring protocol and devices such as settling velocity (Aiguier *et al*. 1996), organic matter (Ahyerre *et al*. 2000), rheological property (Wotherspoon and Ashley 1992; Berlamont *et al*. 1993), flow and turbidity measurement (Bertrand-Krajewski *et al*. 2003; Bertrand-Krajewski 2004) can be found in the literature.

In the context of the present research, a sampling plan was defined to collect and analyse samples representative of the bed deposits: on the initial bed BF and on the bed AF. Comparison of the bed samples at same sections BF and AF allowed successive analysis of modifications induced by the flush on the distribution of grain sizes within the sediment deposits in the sewer. Protocols for bed sampling were finalized to multiple purposes that are summarized in the diagram of the Fig. 3.13. The diagram shows the number of samples and the analyses proceeded over the samples.

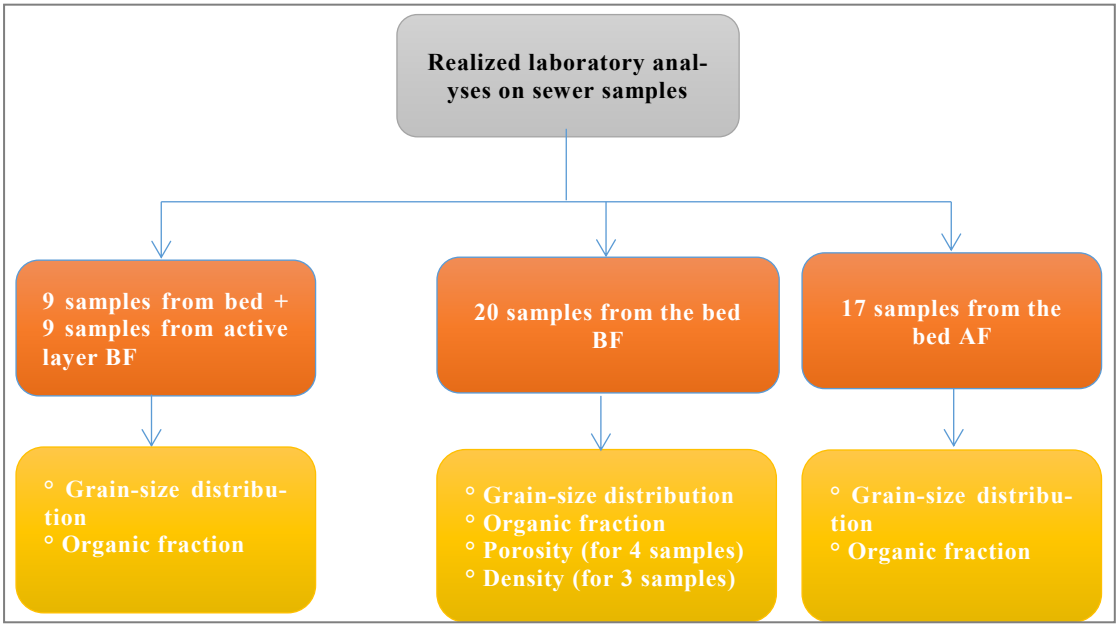

Fig. 3.13 Recapitulatif of the aboratory analyses undertaken for the extracted samples from the experimental sewer channel BF and AF.

Firstly, to investigate vertical bed distribution of the existing deposits BF. To this purpose each section was sampled at two elevations from the bottom: bottom layer (with in average depth of almost 4 cm) and surface layer of the bed (with in average depth of almost 2 cm; Fig. 3.14). The surface layer was expected to be highly organic while the mineral sediments were expected to be deposited at the bottom layer of the bed. This sampling protocol was applied over a distance of almost 450 m from the channel entrance (S_{-50} to S_{+400}) where the sediment particles were found to be finer. Globally, 18 (9 sections × 2 surface and bottom layers) samples were collected from the initial bed deposits (BF). The number of samples was defined during the field experiments. The use of the sampler, as a function of its internal diameter of the tube, did allow to extract sediments with a maximum range of diameters.

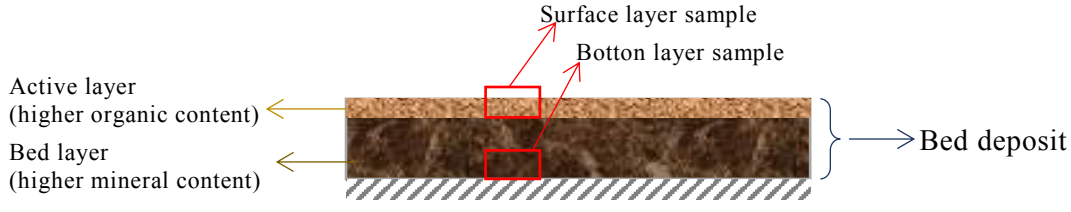

Fig. 3.14 Scheme of vertical bed sampling of the bed.

Secondly, other samples were collected to analyse the sediment composition of the bed. In this case the sampling procedure aimed to obtain a good description of the characteristics of the sediment along the whole channel. It was planned to collect the samples as following: on every 20 m on average for the first segment of the channel (where the major deposits take place), and on every 50 m on average for the downstream segment of the channel ($>S_{+500}$).

As mentioned previously, during the prelaminar observation of the bed sediments of the studied sewer channel, sediments were found to be different in terms of the composition and texture. Therefore, two sampling techniques were used regarding to encountered sediment types in different sections. Finer sediments in the upstream of the channel were sampled using a cylindrical device was used to extract cores (carrots) from deposits. The main usefulness of this device was that it extracts the samples without disturbing the rest of the deposits. This device was the same used to separate the lower from the upper layer of the deposited bed. Conversely, for larger sediments in the downstream segment of the channel the use of a shovel was the more appropriate way to collect sediments from the invert. Ristenpart *et al*. (1992) have introduced shovel as a simple way to extract the sediments but under a good handling condition.

As illustrated in Fig. 3.15, 20 samples in total were extracted from the bed before the flush experiment while the 17 samples were collected AF. Not all of the sampling sections after the flush corresponded to those locations selected for sampling BF because of modifications induced by the flush on the deposits.

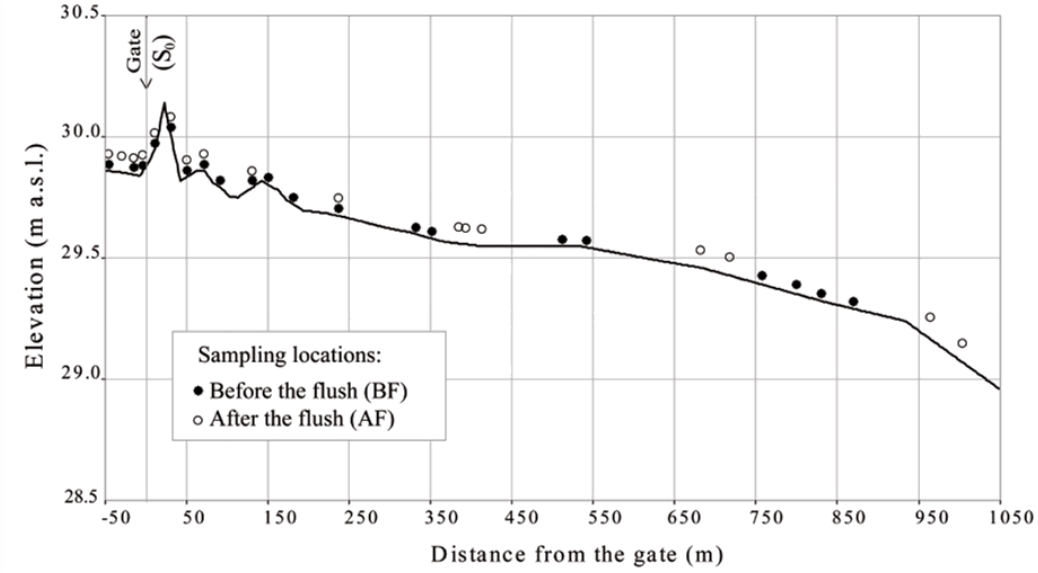

Fig. 3.15 Sediment sampling locations taken from deposits BF and AF.

Sediment samples were transported to the laboratory of Physical Geography at Paris Diderot University in special kits in three packing layers specifically designed for high-polluted samples (Fig. 3.16). Then, the procedure of analysing on the samples was begun. Laboratory analyses (summarized in the flowchart of Fig. 3.13) that will be detailed in the next paragraphs.

Fig. 3.16 Image of security transporting kit containing samples.

Grain-size distribution of the samples. Deposited sediments were characterized by determining the grain-size distribution of dried mass of all the sample cores using sieve analysis or gradation tests (Fig. 3.17). In particular, samples were dried at 105°C in the oven for 24h. After being dried, fine coagulated grain sediments as pulverized by using mortar and pestle. A sieve shaker was used for grading particles larger than 1 mm. Sieve contents were weighted separately using an analytical balance with 0.01 g accuracy. The fraction with diameters under 1 mm were initially weighted and treated by laser diffraction technique using the *Coulter LS300* device, to obtain their distribution within the samples.

Results from the sieve and the diffraction analyses were combined to determine the grain-size distribution (of passing by weight) and related cumulated frequency curves. Furthermore, statistical analyses were carried out from these results to evaluate the composition and texture class of each sample.

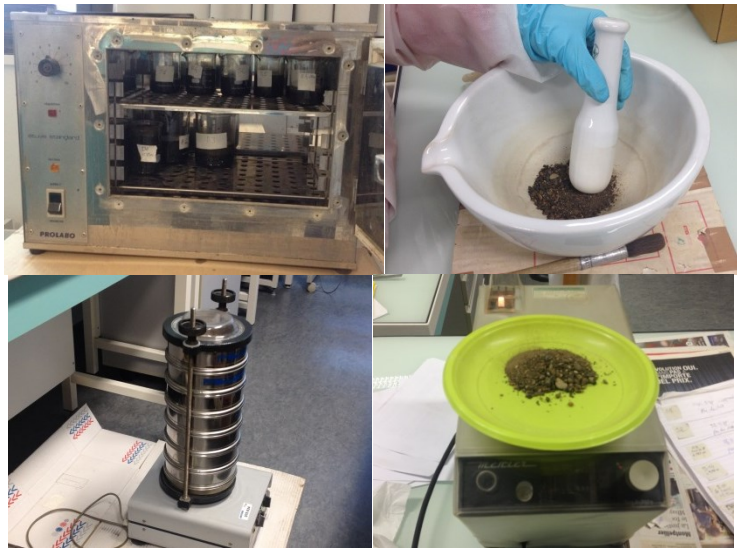

Fig. 3.17 Laboratory procedures for determination of the deposits grain-size distribution including drying (top-left), grinding (top-right), vibrating (bottom-left) and weighting (bottom-right).

Organic matter content. Sediment cores from the samples extracted by the segments were further subject to evaluation of organic matter fraction. The used method is based on the removal of organic matter by Hydrogen peroxide based on the French ORSTOM protocol. This method was introduced by Robinson (1922), which is widely used for abatement of organic matter in the soil texture. The following specific procedure was undertaken:

1. Separation of 20 g of dry sediment from the samples containing particles smaller than 2 mm and their placement in a beaker;
2. Addition of 100 g Hydrogen peroxide (H_2O_2) for reaction at room temperature (Stirring with a glass rod to better expose the organic matter to H_2O_2);
3. Re-drying of sediments after the complete reaction;
4. Determination of the loss mass portion of organic matter lost by re-weighting the amount of remained sediments.

The later step was obtained by using the following relationship:

$$OM\% = \frac{W_i - W_d}{W_i} \times 100 \qquad \text{Eq. 3.1}$$

where W_i is the initial is weight of the sample (*e.g.*, 20 g) and W_d is the re-dried sample after destructing the organic fraction.

Volumetric mass density. Density of three samples from S_{-50}, S_{+150}, S_{+790} was determined by the method of pycnometer which is considered to be a precise technique. The volume of measured solid object V_S is the difference between the volume of water that fills the empty pycnometer V and volume V_{H2O}. Density of the solid mass was calculated from the general relation indicated below:

$$\rho_s = \frac{m_s}{V_s} \quad [\text{kg/m}^3] \qquad \text{Eq. 3.2}$$

where m_s and V_s are the mass and volume of the sediment, respectively.

Porosity. The porosity of four samples was determined from the difference between sediment pore volume and sediment volume. Dried sample was put in a graduated cylinder and after softly shake it, the volume was read. A known volume of water was added to fill the pores up to sample saturation. The porosity is then obtained from $\eta = \frac{Vol_{por}}{Vol_{tot}}$, where Vol_{por} and Vol_{tot} are the volume of pores (*i.e.,* the volume of the added water) and the total volume, respectively.

3.3.3 Video recording during the flush

In addition to the previous devices flow and sediment transport were also monitored through installation of video cameras at different monitoring sections. In total, four cameras were installed into the sewer to record videos during the flush (Fig. 3.9). Two cameras were placed in the *cunette* wall of the channel in order to capture the sediment-transport processes at the bed level. To this end, a hermetic Plexiglas box was designed to install the camera inside (cf. Fig. 3.18). A side of the channel was modified to make place for the boxes. The cameras were installed in two different locations at S_{+50} and at S_{+100} (Fig. 3.9). Description of the used cameras and generated output videos is summarized in Table 3.3. The cameras were able to film the flushing procedure for almost 1.5 h with a relatively good quality of images.

Fig. 3.18 Camera placed in a hermetic Plexiglas box to be placed inside the channel wall.

Table 3.3 Description of the implemented cameras inside the cunette wall if the channel.

Camera type	GoPro Hero 3^+ silver edition
Frame rate	24 fps
Image resolution (pixel)	1920 × 1090
Recorded video duration (hr)	Almost 1.5

Two other cameras were further placed on the top of the channel to simply provide images of the correct gate tipping, of flush flowing and to confirm the successful execution of the test.

Chapter 4
Results of the field experiments

4.1 Recorded data during the experiment

4.1.1 Collected data and missing information

Raw flow- and sediment-related data obtained during the flush experiment were analysed mainly in order to understand the sediment-transport processes due to the flush. Table 4.1 summarizes the state of measured variables acquired from all 5 sections during the flush test. The black cells in the table show data missing or invalid records. Yellow and green cells indicate the partly missing and validated data, respectively.

Doppler flowmeters simultaneously measured the flow variables of velocity, discharge, water level and wetted area, etc. at each time step (10s) for a given section. Unfortunately, flow variables did not recorded at section S_{+100} because of a malfunction of the doppler velocimeters. However, the water level measurement was obtained by the US device at this section. The ultrasound meters did register time series of the water levels every 15s during the flush in all the monitoring sections. The reliability of water level measurements obtained by US meters was double-checked with the same measurements as obtained by the doppler device. Missing values can be seen in the recorded turbidity values, in particular at 15 cm (T15) over the bed invert.

Table 4.1 Evaluation of the recorded data. Colours indicate the status of collected data as green: complete data; yellow: data with missing values; black: no recorded data. Value inside each cell signifies the time interval of sampling.

Device / Section	Doppler (time step)	Ultrasound (time step)	Turbidimeter (time step)		
			T15	T25	T65
S_{-50}	(10)	(15)	(10)	(10)	(10)
S_{-5}	(10)	(15)	(10)	(10)	(10)
S_{+5}	(10)	(15)		(10)	(10)
S_{+50}	(10)	(15)	(10)		(10)
S_{+100}		(15)	(10)	(10)	(10)

4.1.2 Data preparation

The collected data (*i.e.,* flow parameters, bed scan output, turbidity records and sediment samples) were re-processed to make easier the analysing of the flush impact.

The output results of the bed scan procedure for deposits before and after the flush consisted of sediment volume deposited in the different sections of the channel. The values of volume were then converted easily to sediment heights at each section. Since data on deposited volumes were available at variable spatial steps, interpolation was required to obtain deposits heights with a fixed spatial step along the longitudinal sewer channel (every 1 m).

Concerning the turbidity measurements, time series provided by the used optical sensors contained a high number of spikes and "noise" with various magnitudes. Sometimes, recorded values were out of the measurement range indicated by the device manufacturer. The noise was caused by (for example) ephemeral fouling or sensor blinding due to objects trapped by the sensor. It was therefore necessary to filter raw data and eliminate outlier values from the turbidity time series of all measuring section. Then, the generated missing values due to these ephemeral fouling were examined and interpolated. In addition, the invalid records were filtered using a threshold value indicated by the company as a maximum reliable limit of the ranges. Finally, all of the turbidity time series were averaged over every 1 min to show better the trends and fluctuations. This interval of time (considered as an average of 6 values) was chosen based on the literature and previous references in sewer conditions. However, the conditions, context of the studies found in the literature are not the same (Joannis and Aumond 2005; Lacour 2009). Considering these studies with different intervals, objectives and aims, the most appropriate and representative value was determined for the flushing phenomenon. It is worth mentioning that unfortunately turbidity time series (in NTU) could not be converted into concentration units such as in mg/l. The reason refers to the fact that sewer conditions during the flushing experiment did not allow taking flow samples corresponding to the turbidity records. Consequently, the sediment concentration in the flow was not estimated from turbidity time series. However, turbidity trends provided valuable information of the flushing evolution.

Pre-processing of data from sediment sampling was performed as follows. Firstly, a few sediments that were considered as outliers (such as gross solids) were eliminated from the samples. In fact, such solid particles were not representative of the sediment that generate deposits on the sewer channel but artificial elements as pieces of electrical cables, large-diameter stones from construction sites or broken asphalts. Fig. 4.1 shows an example of such elements which were eliminated.

Fig. 4.1 Example of samples containing atypical particles that were finally eliminated from the samples (marked particles).

4.2 Results of the experimental test

4.2.1 Gate operation during the test

According to the database and duration of time series, the flush lasted at least more than 1.5 h (devices were set to measure only 1.5 h). The storing phase of the flush took almost 2 h before releasing phase. The gate was opened at 12:04 at 10/07/2014 after the storage phase. The storing phase was started about 2 h before the gate opening. Based on the calculations, taking into account the dry-weather flow, a volume of more than 8000 m^3 of wastewater was accumulated behind the gate. The high volume of stored water during the storage phase was accumulated without specific sewer dysfunction. The gate sensor recorded opening heights of the gate in time so, a speed of 4.85 cm/s from the maximum elevation of 2.12 to 0.8 m height from the bed invert. For the flush test the opening procedure of the gate took 56 s with an opening speed with almost 5 cm/s set by the hydraulic jacks.

4.2.2 Videos recorded from surface and cunette cameras

The video cameras captured the flush process. In total about 1.5 h (5 videos × 17.5 min duration) video was recorded. Fig. 4.2 shows a screen shot of the video taken by one of the cunette cameras placed at S_{+50} that gave clear images of the bed load and, partly, the sediments in suspension. The second cunette camera placed further downstream at S_{+100} was also filmed the transport of the sediments during the flushing test. However, the images were less clear and did not allow to fully observe the behaviour of the sediments during the entire flush test. The analysis of the videos from both cameras showed the sediment wash-off process due to the transit of the flush at sections S_{+50} and S_{+100}. High turbulence and secondary flows visibly affected the behaviour of the sediments within the flow column, mainly at the beginning of the flush. A few minutes after the flow peak, well defined sediment-transport modalities were observed, with distinguished bed-load and suspended-load transport patterns at S_{+50}. Conversely, suspension was identified as the prevalent mode of transport at S_{+100}. Sanitary solids such as papers and fine miscellaneous sewage litter were also observed to be transported in the water column during the experiment. During the flow receding phase, the flush erosional effects visibly tended to decrease. As expected, during this phase, the transport involved mainly the fine and medium sediment sizes, while the flow was not able to scour large grain-sizes anymore, thus leading to the partial re-establishment of bed deposits.

Surface cameras on the top of the sewer channel at S_{+5} and S_{+50} showed that the flush test was operated in appropriate way (the gate opening procedure was operated correctly. The camera slow showed that, as already observed in oth-

er experiments (Campisano *et al*. 2004), an up-going negative wave associated with the emptying/release process developed upstream of the gate.

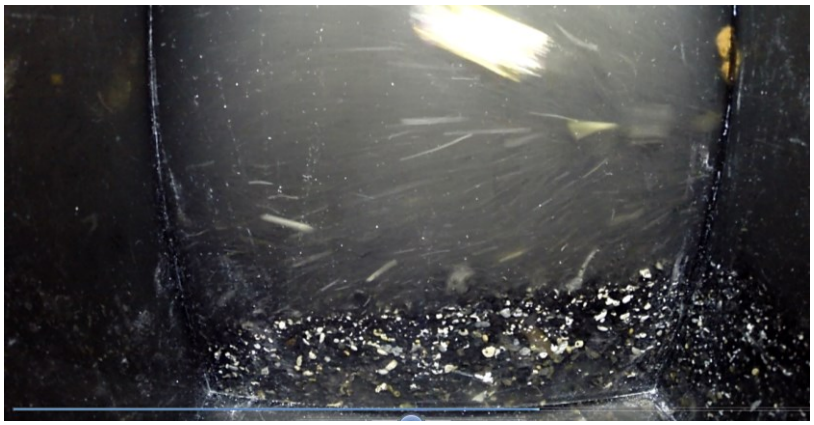

Fig. 4.2 A screenshot of the video recorded by the bed-load camera located at S_{+50}.

It should be noted that a further preliminary investigation of the video images recorded from the camera installed at S_{+50} was carried out to evaluate the bed-load sediment transport over the bed. A summary of this investigation was presented at ICUD2017 conference in Prague (The Czech Republic) - 10-15 September 2017 (Grasso *et al.* 2017 in Appendix B).

4.2.3 Analysis of the hydrodynamics of the flush operation

Flow-related variables were recorded during the flush at various sections as presented in Fig. 4.3. These graphs are drawn based on 1-min averaged data allowing smoothing the curves and better illustrating the flow parameters. The figure shows the sudden increase in flow discharge at the different sections after the flush release. According to the figure, a maximum flow discharge of 3.9 m^3/s can be observed at sections close to the gate. Almost after 1 h since the beginning of the flush, the discharge yet remains high close to 1.4 m^3/s. Unfortunately, due to a malfunctioning of the flow measurement device, flow discharge data was not recorded at S_{+100}. A similar concern regarded also section S_{+50} where the flow was not recorded for a relatively long period including the peak time. In addition, the figure shows also the sudden drop-off of the water level in sections before the gate (around 0.65 m drop just behind the gate); while downstream of the gate shows an increase of almost 1 *m* within few minutes. It should be mentioned that the water level downstream of the gate before the gate opening and flush releasing was almost 0.5 m. This could be due to the bed slope downstream of the gate. Another reason that can explain this water level is the water flowing through the closed gate that was not completely hermetic to retain the stored water. This was observed thank to the surface cameras. However, based on the recorded data by the Doppler, the velocity before the gate opening is small and negligible.

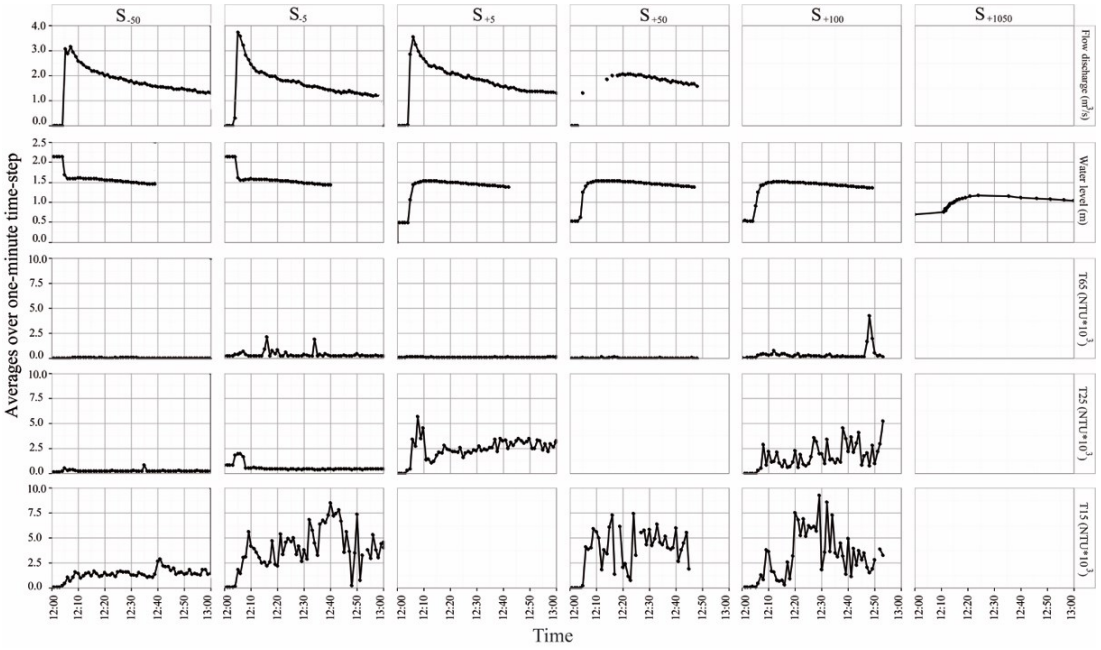

Fig. 4.3 Flow and sediment-related variables recorded during the flush experiment in various measuring sections along the sewer channel.

Concerning the turbidity records, globally the figure illustrates the high variations for all the sensors occurring during the flushing event. Results show that, the rising limb of the flow discharge (up to the flow peak value) was accompanied, at least for sensors T15 and T25, by a sudden increase in turbidity for almost all the sections downstream the gate. Fluctuations can be observed for the curves registered by sensors placed close to the bed (T15). Conversely, the sensors at higher levels have provided minor dispersion of the sensors. As expected the turbidity values decrease vertically from the bed to the water surface. Moreover, for the majority of sensors installed near the bed, an increasing trend of the turbidity can be perceived during the flush. The standard deviation of the turbidity values for each sensor is presented in Table 4.2. Overall, as fluctuation of turbidity is concerned, evaluation of the standard deviation provided average values of 1168.2, 463.6, and 180.3 NTU for sensors T15, T25 and T65, respectively. The values confirm major variability for the sensors near the bed. In addition, from upstream to downstream of the channel, but no clear trend can be observed. Conversely, lower values of turbidity were recorded by sensors T25 and T65. Unexpectedly, a peak value for sensor T65 was achieved at S_{+100} (about 4500 NTU) after almost 45 min since the start of the experiment. Later, the analysis of the video clip captured by the camera at S_{+100} helped explaining this turbidity peak with the temporary blockage of sanitary paper in front of the turbidity sensor.

Table 4.2 standard deviation of turbidity records obtained from all the measuring sections.

Turbidimeter	**S_{-50}**	**S_{-5}**	**S_{+5}**	**S_{+50}**	**S_{+100}**
T15	480.0	1870.7	-	2141.6	1153.8
T25	90.2	313.4	1063.6	-	837.2
T65	25.6	241.8	9.4	31.0	593.5

A further analysis of the turbidity data was done in the context of a conference preceding paper (Appendix B). The paper entitled "Preliminary analysis of turbidity measurements during a flushing operation in combined sewer channel" was presented in the 8th International Conference on Sewer Processes and Networks held in Rotterdam, The Netherlands on August 31st September 2016.

4.2.4 Deposit evolution due to the flush

Results from radar/sonar scanner output in terms of bed heights are illustrated in Fig. 4.4. The figure shows that before the flush the major part of the initial sediments deposits were accumulated upstream of S_{+500}. This sewer segment shows flat slope but also various bed irregularities such as hollows and bumps and counter slopes. Based on the results of the scanner, average and maximum thickness of the deposit in this segment were about 5.6 and 31.5 cm, respectively. In contrast, less sediment accumulation was observed over the segment downstream of S_{+500}. This segment exhibited an initial average height of the deposits of about 1.2 cm with a maximum of 17.9 cm.

The accumulation of sediments is influenced by many factors related to the geometrical conditions (*e.g.* bed slope, inflow/outflows) of the sewer. Therefore, the different spatial distributions of the existing deposits before the flush reveals the influence of the local channel longitudinal slope (average 0.07% and 0.1% for the segments upstream and downstream of S_{+500}, respectively) on the sediment erosional/depositional attitude of the different channel sections. Also, the figure shows that the irregularities of channel invert locally impact the sediment transport, causing sediment accumulation due to the reduced sewer self-cleansing capacity. Moreover, as it can be seen from the figure, accumulation in the channel also occurs close to the lateral inlets due to sediments supplied by such inlets.

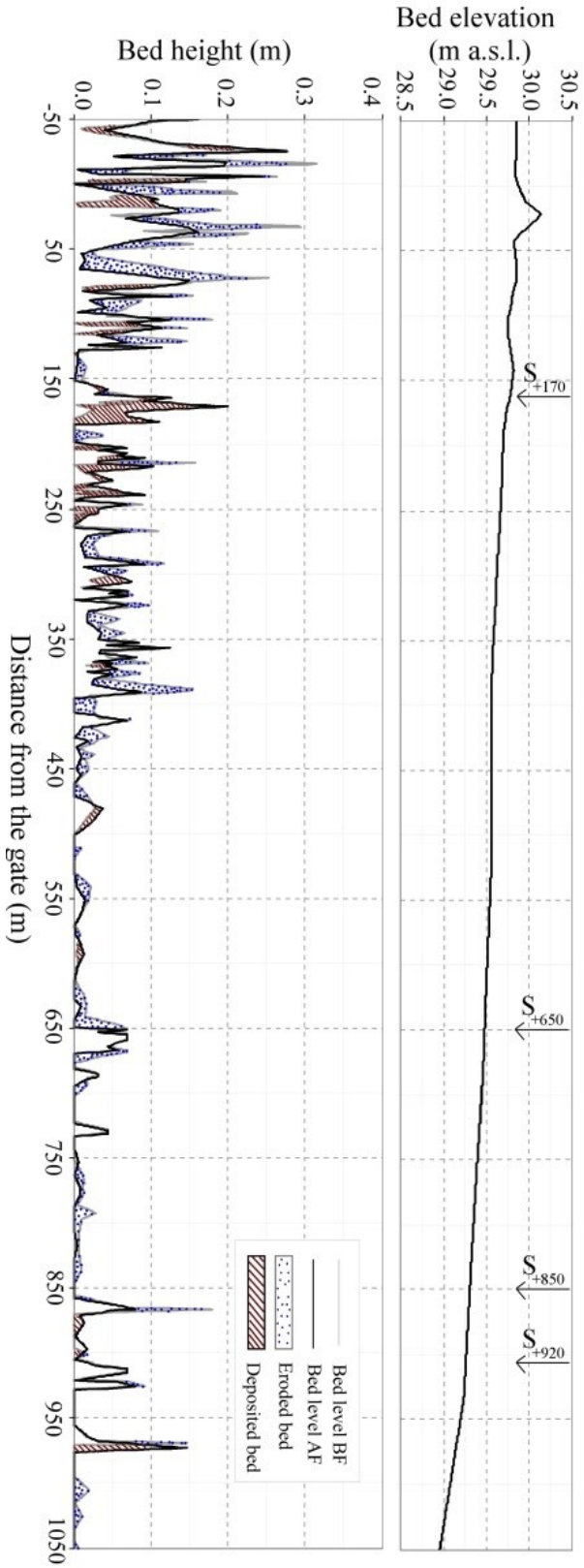

Fig. 4.4 Bed profiles along the sewer channel obtained from bed scan technique.

Globally, the comparison of bed profiles BF and AF highlights the significant erosive effect of the flush over bed deposits up to S_{+850}, which shows an appreciable cleaning efficiency of the gate on the most of the channel length. However, depositional effects over few sections of this trunk can be observed. As the figure shows, erosion was prevalently concentrated between S_0 and S_{+120}, whereas limited deposition occurred between S_{+10} and S_{+20} due to the local negative slope of the channel. Erosion was also observed (even if to a minor extent) downstream of section S_{+250}. Conversely, deposition occurred in the channel portion between S_{+120} and S_{+250}.

The volumetric analysis of the deposits BF and AF provided an estimation of the cleaning performance of the flush. The comparison of radar/sonar output data confirmed a significant reduction of the deposits in the channel. Overall, the total sediment volume accumulated in the whole channel trunk downstream of the gate (from S_0 to S_{+1050}) decreased (up to 5.4 m^3) from 27.2 m^3 to 21.8 m^3. Fig. 4.4 shows that the sediment removed from S_0 to S_{+850} summed up to about 5.3 m^3, thus providing a flush cleaning performance of 21.4% sediment reduction (the initial sediment in this segment was about 25 m^3).

4.2.5 Modification of the deposit grain-size distribution

Grain-size distributions for the sediment samples extracted from BF and AF were determined. Since the characteristics of sediments upstream and downstream segments were a bit different (see Chapter 3), bed composition of the initial bed (BF) was studied with reference to segments (upstream S_{+500} and downstream S_{+500}), respectively. Before the section S_{+500}, the bed mixture prevalently contained fine particles (mainly sand-type particles) while downstream of this section the deposits was constituted principally by large size particles (gravel-type particles). According to the data and textural analysis of the deposits BF revealed dominant mode diameters of 0.8, 1.6, 2.5, 4.2 and 8.0 mm, thus indicating potential for sediment-transport selectivity by the flush (Vanoni 2006; Garcia 2008).

After having analysed the samples, characteristic sizes including d_5, d_{10}, d_{16}, d_{50}, d_{84}, d_{90}, d_{95} were calculated and averaged over both segments, and separately for the upstream and downstream segments of the channel. Results are illustrated in the graph of Fig. 4.5. Firstly, the figure shows clearly the diffence of global diameter sizes for two channel segments for both BF and AF. Looking more in detail the graph, the effects of the flush on the various sediment fractions composing the deposits can be observed. The figure reports the "average" grain-size distributions relative to all the samples extracted from the channel segments upstream and downstream of S_{+500}, respectively. The distributions representing the initial bed composition (BF) show that - excluding very fine particles (smaller than d_1) - grain sizes ranged between 0.08– 8.5 mm (d_{50}=0.90 mm, d_{90}=4.15 mm) upstream of S_{+500} (see BF<S_{+500}) and between 0.17– 34.9 mm (d_{50}=6.78 mm, d_{90}=22.51 mm) downstream of S_{+500} (see BF>S_{+500}). The plotted distributions analytically confirm qualitative information acquired during the preliminary sewer survey. Therefore, according to the quantitative evaluation of the initial deposits, about 73% of the sediment bed upstream of S_{+500} was composed of sand-sized particles (63 μm - 2 mm) while the gravel-sized particle fraction (2-64 mm) was nearby 26%. Conversely, the initial bed downstream of S_{+500} was in large part made of gravel-sized particles (close to 74%) with a minor fraction of sand (25%). The fine fraction (sediments smaller than 63 μm) was less than 1% all over the channel trunk.

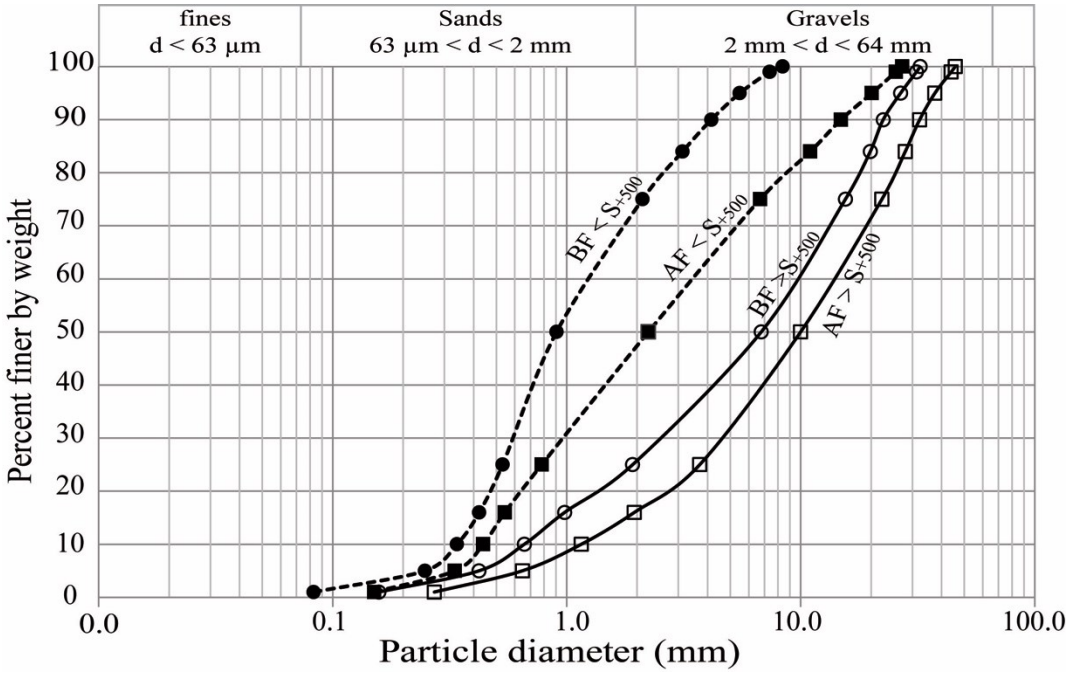

Fig. 4.5 Grain-size distribution of samples averaged over two segments before and after S_{+500}.

Due to the flushing operation, deposits have been subject to considerable changes in terms of compositions. Bed compositions were altered and different impacts on the different segments have been observed. Globally, Fig. 4.5 shows an evident right-shift of the distribution AF<S_{+500} as compared to the analogous curve BF<S_{+500}, thus revealing sediment bed coarsening for all the characteristic grain sizes in the upstream part of the trunk. Similar sediment coarsening effects were observed also downstream of S_{+500}. Accordingly, the evolution of average median size of the bed samples is as follows: for the upper segment (< S_{+500}) an increased from 0.90 to 2.23 mm and for the lower segment (> S_{+500}) an increase from 6.78 to 9.99 mm. From the graph it can be seen also that the range of sediments was reduced under the effect of the flush. So, the averaged d_{90} has increased from 4.15 to 14.87 and from 22.51 to 32.24 for < S_{+500} and > S_{+500}, respectively. In addition, results show also that, due to the flush experiment, the percentages of sand-sized particles in the bed deposits decreased from 73% to 47% and from 25% to 16% upstream and downstream of S_{+500}, respectively; correspondingly, gravel-sized fractions increased from 26% to 52% and from 74% to 83% upstream and downstream of S_{+500}, respectively.

The coarsening effects of the flushing operation on the bed deposit were quantified by using a statistical index describing the average skewness *Sk* for all the grain-size distributions. This factor can be calculated from the equation introduced by Inman, 1952. This equation is one of the most used formulas for the sediments which is well supported by the literature and gives idea of how samples are. This equation is written as following:

$$Sk = \frac{\log(\frac{d_g}{d_{50}})}{\log \sigma_g} \qquad \text{(Eq. 4.1)}$$

where $d_g = \sqrt{d_{16} \cdot d_{84}}$ is the geometric mean size and $\sigma_g = \sqrt{d_{84}/d_{16}}$ is the geometric standard deviation of each sample. A summary of the results is presented in Table 4.3. The table shows the skewness to increase from 0.20 (BF) to 0.27 (AF) and from -0.29 (BF) to -0.23 (AF) for the segments upstream and downstream of S_{+500}, respectively, thus confirming a shift of the asymmetry of the distributions toward the large particle sizes.

Table 4.3 Statistical sediment grain-size characteristics BF and AF for the upstream and downstream segments of the channel

index	**BF < S_{+500}**	**BF > S_{+500}**	**AF < S_{+500}**	**AF > S_{+500}**
d_{50}	0.90	6.78	2.23	9.99
d_{90}	4.15	22.51	14.86	32.24
S_k	0.20	-0.29	0.27	-0.23

Due to the flush, sediments were subjected not only to qualitative but also quantitative modification of the composition in terms of fractional volumes. The accumulated fractional volumes of deposits AF are compared to the same values BF as shown in Fig. 4.6. The graphs in the figure highlight the different impacts of the event on the non-uniform sediment mixtures forming the mobile bed in the channel. As it can be seen, the plotted results are referred to four selected fractions ($d<d_{50}$; $d_{50}<d<d_{sand}$; $d_{sand}<d<d_{90}$; and $d>d_{90}$ with d_{sand}= 2 mm being the limit of sand size). The fractions were chosen on the basis of average characteristics (d_{50} and d_{90}) of the deposits BF<S_{+500}. These fractions could help better describing the evolution of the sediments due to the flush operation.

Overall, the plotted graphs reveal the non-uniformity of flush erosion effects for the different fractions (Fig. 4.6 a-b-c). As expected, the figure confirms the considerable erosional effect of the flush over the existing deposits. It shows, in particular, that the major part of the sediment eroded by the flush from the entire channel was made of particles finer than d_{50} (Fig. 4.6 a). Smaller contribution of sediments to erosion were associated with fractions $d_{50}<d<d_{90}$ containing fine gravels with diameters between 2 to 4.15 mm (Fig. 4.6 b-c). Conversely, an increase in the volume of sediments coarser than d_{90} occurred prevalently in the first 300 m long segment downstream of the gate (Fig. 4.6 d). This behaviour reveals the deposition of coarser sediments that were remobilized from upstream sections by the flush and re-deposited during the flow recession further downstream. As summary, it can be highlighted that the flush had a significant erosional effect on the fine and sand sediments almost over the entire sewer channel. However, the presented data cannot provide information about the ”real” eroded volume over

each section due to the occurred re-depositions of the eroded sediments originated from upstream bed. Table 4.4 shows the volume of sediment size classes BF comparing to AF.

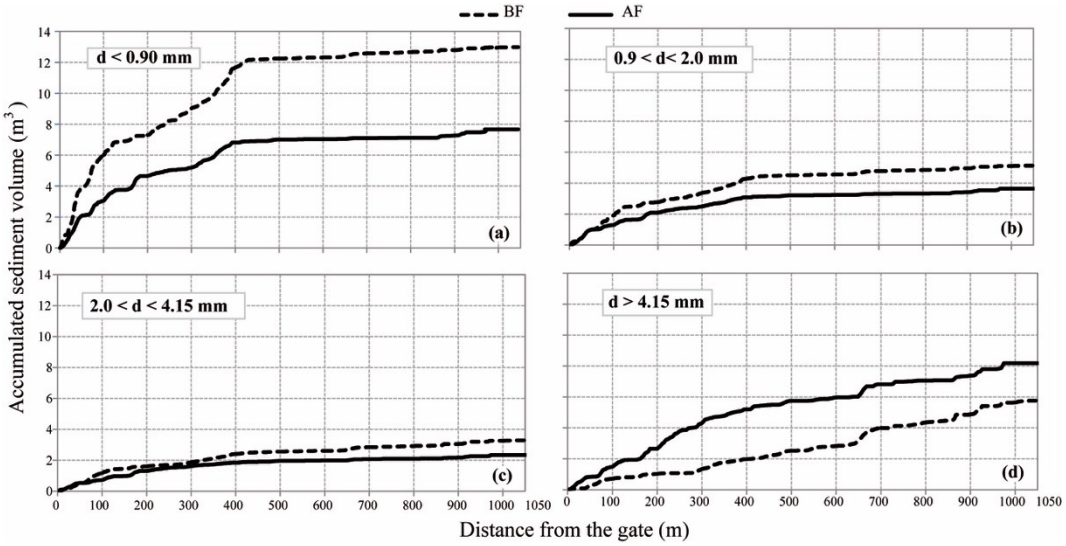

Fig. 4.6 Volumes of deposits BF comparing to the AF by size classes of four sediment fractions.

Table 4.4 Fractional volumes of sediments BF and AF.

Fraction (mm)	**BF < S_{+500}**	**BF > S_{+500}**	**AF < S_{+500}**	**AF > S_{+500}**
<0.9	15.72	0.73	9.66	0.65
0.9<d<2	5.74	0.63	4.12	0.43
2<d<4	3.23	0.73	2.54	0.38
d>4	2.97	3.28	7.20	2.43

Besides, a detailed analysis of the bed evolution in terms of the sediment composition due to the flush event was undertaken. The textural analysis consisted of evaluating selected characteristics sizes (d_5, d_{10}, d_{16}, d_{50}, d_{84}, d_{90}, d_{95}) of the bed BF and AF along the entire channel results are presented in Fig. 4.7. The grain diameter for each characteristic size BF and AF is shown in the left and right sides of the figure for the channel segments upstream and downstream of S_{+500}, respectively. For example, the figure shows that the d_{90} at S_{+70} (second to last graph in the left side of the figure) increased from 3.4 mm to about 19.4 mm after the flush. As the graphs show, composition for almost all the deposits has been subject to coarsening determined by the flush compared to their initial state. According to the graphs, coarsening in the larger size classes of sediments < S_{+500} is much more evident in particular the curves containing larger particles > d_{50}. In other words, the distribution of the grain sizes over the segment upstream of the gate has largely eroded by the flush rather than the lower segment. This can be explained by the wash-off of the finer sediments and/or with a lower probability

arrival of "new" sediments. In contrast, for the bed sediments > S_{+500}, the coarsening of the deposits occurred for the sediments with smaller sizes.

As expected, such an effect is much more evident for the large grain sizes (>d_{50}) than for the fine ones (<d_{50}). In fact, the calculated Mean Absolute Percentage Error (MAPE) of the samples BF and AF showed deviations of 34.0% and 305.9% for particles smaller and larger than d_{50}, respectively.

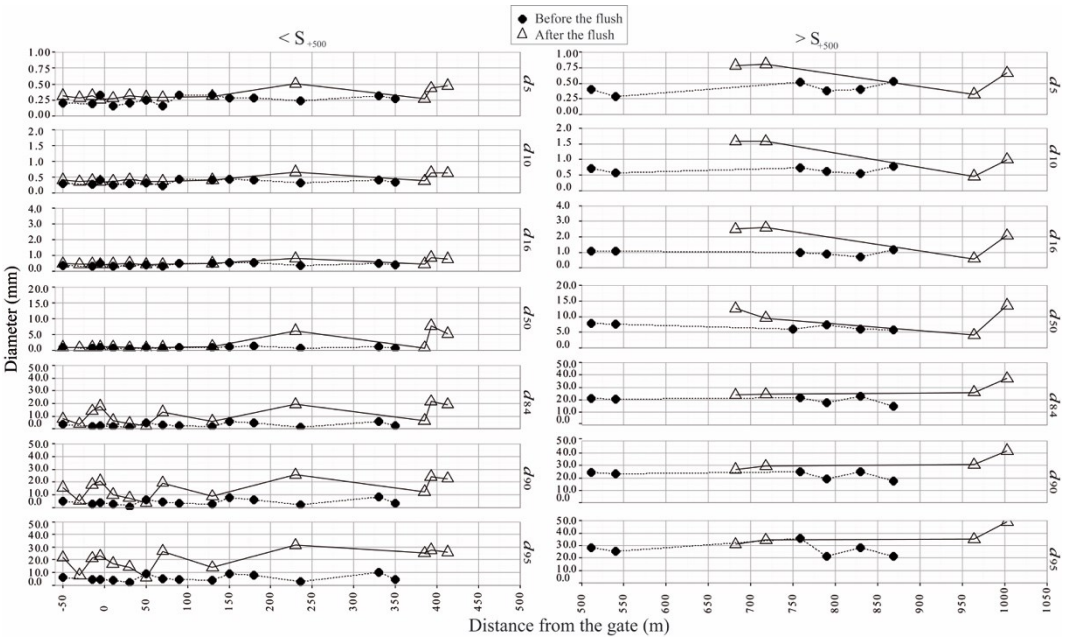

Fig. 4.7 Fractional grain-size distributions of the bed sediments AF compared to BF along the entire sewer channel.

4.2.6 Organic fraction in bed sediments

In addition to grain-size distribution, the organic content of the samples before and after the flush was also determined. The results of the laboratory analyses of the organic content of the samples are presented in Fig. 4.8. From the graph, it can be seen that the organic fraction contained in all the extracted samples did not exceed 7% in weight (average content was 2.9%) before the flush experiment. This average amount decreased down to about 2% after the flush. According to Crabtree (1989) such result would allow classifying sewer solid particles in the Collecteur des Coteaux as class A sediment type (granular sediments with weak organic content). A relatively minor organic matter content after the flush was found in the sediment samples extracted from the sections close to the gate. Based on the results presented in Fig. 4.6, such sections were also affected by the largest removal of fine sediments due to the flush; this result is in

agreement with findings by Michelbach (1995) who highlighted that the organic matter is highly related to the presence of fine sediments in the bed mixture. Interestingly, Fig. 10 also confirms that the organic matter content AF tends to decrease as the distance from the gate increases, in agreement with the observed decrease in fine sediments along the channel.

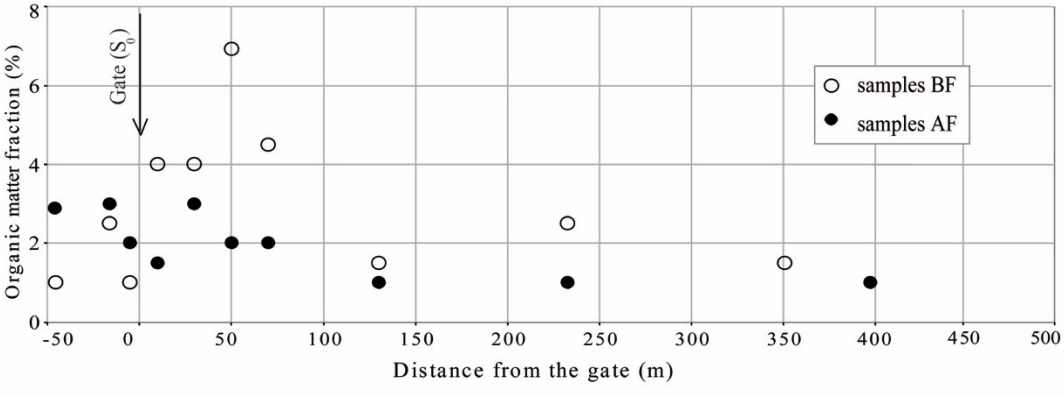

Fig. 4.8 Comparaison of the orgnaic content of the sewer sediment samples collected before and after the flush.

4.2.7 Complementary parameters

The density for three samples was measured at Paris Diderot laboratory of Geography physics. Obtained values are presented in Table 4.5. The average value of deposit densities 2338 kg/m^3 was obtained from the results of density measurement.

Table 4.5 Measured density of selected samples of deposits obtained from laboratory analysis.

Section	**Density of deposits (in kg/m^3)**
S_{-50}	2263
S_{+150}	2220
S_{+790}	2532

In addition, Table 4.6 shows the determined porosity from the laboratory test for four selected sewer samples. An average porosity of 0.41 was obtained for these samples.

Table 4.6 Dimensionless porosity of selected samples obtained at laboratory.

Sample locations	**Obtained porosity**
S_{-5}	0.425
S_{+10}	0.4
S_{+30}	0.421
S_{+50}	0.4

4.3 Performance of the experimental flushing test in *Des Coteaux* combined sewer

Beyond the effects of the geometry and operation of the used gate device, the flush release can be hydraulically assimilated to a "dam-break" process characterized by an initial sharp increase in the flow and by a relatively slow decreasing phase after the achievement of the flow peak.

The generated flow hydrograph and associated shear stresses highly depend on the water head and on the stored volume upstream of the gate at the time of the beginning of the flush release phase. The initial water level is the most crucial parameter affecting the magnitude of the shear stress generated by the flush, as it is a measure of the initial energy held by the water behind the gate. Dettmar and Staufer (2005) have shown that such a parameter mostly affects the maximum distance from the gate that could be impacted by flush erosion, thus providing insight on the potentially "cleanable" channel length. Differently, the stored volume available for the flush allows sustaining the shear stresses during time, thus having a key role on the duration of the erosional process, and consequently on the amount of sediment removed during the whole flush (Campisano *et al.* 2007). Combination of flow data presented in in Fig. 4.3 allowed calculating the average shear stress $\tau = \gamma RJ$ (γ is the water specific weight, R is the hydraulic radius, and J is the energy line slope) generated by the flush during the experiment throughout the pilot channel. The average peak shear stress achieved in proximity to the gate (at S_{+5}) was close to τ_{peak} =10.3 N/m². Dissipation processes associated with the flush propagation did not reduce significantly the shear stress, which was observed to assume values at the peak larger than 9.5 N/m² also in the downstream part of the channel. The average shear stress in the section is different from that evaluated on the sediment. The later parameter takes into account not only the value of the wall roughness but also that of the bed (sediments) represented by the d_{50}. Therefore, this allows to estimate a real shear stress which differs from the average shear stress that neglects the roughness effect.

The large stored water volume released by the gate during the flush allowed sustaining the flush with shear stress values after the flow peak always larger than 2.8 N/m² in the whole channel for more than 1 h. Based on Shields' theory (Shields 1936), such a shear stress value would be able to remobilize grains with maximum size around 4.0 mm. Notably, this is consistent with the results presented in Fig. 4.6, that show prevalent erosion and transport of fine/medium sediment sizes and stability of coarse sediments in the deposits during the flush. More in detail, Fig. 4.6 shows that more than two thirds of the total eroded sediments were smaller than the d_{50} of the segment upstream of S_{+500} BF (0.90 mm), thus confirming the high non-uniformity of sediment transport determined by the flush in the channel. This result suggests that any evaluations of the sediment transport due to the flush which would rely on the use of single sediment sizes (*e.g.,* the median sediment size) would lead to a simplistic interpretation of the

process as it would not allow taking into account the transport selectivity attitude of sediment mixtures.

Although the flush conserved erosive shear stress up to a long distance from the gate, most of the eroded sediment was remobilized from the segment between the gate location and S_{+500}. Conversely, downstream of this section the flush did not determine a significant modification of the bed, mainly due to the presence of coarser sediments forming the deposits. Furthermore, as observed during the preliminary survey, deposits close to the downstream end of the channel were also characterized by gross solids of various nature (*e.g.,* residuals of construction, pieces of asphalt, etc.) and by elements originating from sewer maintenance (*e.g.,* bolts, nuts, spikes, etc.). Much of these solids were observed to overlay granular sediments in the bed, thus potentially triggering bed armouring effects during the flush. Based on these results, sediment transport in this final segment was probably occurring mainly as wash-load without relevant exchange of sediments at the water-bed interface.

The comparison of bed profiles BF and AF presented in Fig. 4.4 shows that the flush determined sediment erosion also upstream of the flushing gate, affecting the bed up to a relatively long distance from the device. This result confirms previous findings by Ristenpart (1998) and Dettmar *et al.* (2002), that have reported erosional capacity of the up-going sunk wave generated by the flush up to tenths meters behind the gate. As a peculiarity of the considered sewer, due to the steeper invert slope of upstream stretch, the calculated shear stress behind the gate locally achieved values close to 5.5 N/m², thus potentially determining effects of re-mobilization and transport of relatively large sediments. The occurrence of such effects is supported by the results of Fig. 4.6-d that show an increase in the volume of sediments larger than d_{90} in the pilot channel AF.

Globally, erosion upstream of the gate may have had a role on the global performance of the flush. In fact, although the overall volume of sediments removed downstream of S_0 was relatively high (about 5.4 m^3), such a volume was the result of a balance between fine outgoing material (about 7.8 m^3 smaller than 4.15 mm) and more coarse incoming material (about 2.4 m^3 larger than 4.15 mm), which ended re-depositing in the channel, most likely in the first 300 m downstream of the gate. Such a hypothesis would find confirmation from Fig. 4.7 that shows sediments at sections between S_{+100} and S_{+300} to be subject to major coarsening after the flush.

Although the used equipment was one of the strength points of the experiment, unavailability of direct sediment discharge measurements during the flush was identified as one important limitation of the study. However, combined use of turbidity records and radar/sonar output, and analysis of video clips extracted by the video-cameras installed in the channel bank allowed basic interpretation of the main sediment-transport processes occurred during the flush. For example, the intermittent transport of sanitary litter observed in the video-clips at S_{+50} and S_{+100} as well as the incidental dislodgement of bed sediment packages and their en-

trainment into the flow provided potential explanation of fluctuations in the turbidity records.

A final aspect deserving discussion concerns the adopted experimental conditions for the flush. As the normal functionality of the sewer system was conserved during the period of the experiments, the normal flow (dry-weather flow and eventual flow from runoff) may have contributed to sediment erosion and transport in the channel between BF and AF sampling phases, thus leading, in principle, to overestimate the sediment removal performance of the flush. However, considering that the total period needed to develop the experiment was relatively short, contribution to sediment transport of this flow may be assumed as negligible, being eventually limited to very fine fractions only. In addition, it has to be stressed that the presence of dry weather flow at the beginning of the flush (although due to lateral inlets only) in the channel downstream of the gate may have played a role in reducing the erosive effect of the flush wave over the deposits, thus potentially leading to underestimate the flush cleaning performance. Overall, it is believed that such considerations may be valid suggestions to improve protocols for future flush monitoring tests planned by the municipality.

Chapter 5
Unsteady flow numerical modelling of sediment transport under sewer flushing

5.1 General overview

The complexity of sediment-transport dynamics in sewers is associated not only to factors related to the sediments (for example, variety in range of particle sizes, origin, response to a given flow discharge, etc.), but also to a number of interrelated processes including erosion, transport and sedimentation. Nowadays, with improvement in performance of the computers and informatics progresses, numerical simulations provide a major contribution to the analysis of sediment transport in sewer systems. However, the quality of the prediction of sediment related processes in sewer pipes through use of numerical models mainly depends on the correct calibration/validation that is on the availability of reliable experimental data (Gent *et al.* 1996; Ashley *et al.* 2000, 2004).

Models for proper evaluation of cleaning performance of flushes in sewers must have capability to describe accurately erosion, transport and deposition of sediments under highly unsteady flow conditions. To address such requirements, simulation of the flushing test carried out in Paris (described in Chapter 4), was conducted using a research-oriented numerical model developed by the urban drainage research group of the University of Catania, Italy. The model was originally setup to simulate the behaviour of flush propagation in sewer channels with fixed beds and it has been successively upgraded for the study of several physical and biochemical (cohesion) processes in sewers including sediment transport under unsteady flow conditions (Campisano and Modica 2003; Campisano *et al.* 2007a). In the recent years, the model has been integrated with new subroutines to simulate the scouring behaviour of flushes generated by various types of gate devices on sewer mobile sediment beds (Campisano *et al.* 2005a and b; Campisano *et al.* 2004, 2008). The model results have also been validated against field and laboratory experiments (Bertrand-Krajewski *et al.* 2005; Campisano *et al.* 2006; Shirazi *et al.* 2014).

The actual model allows the use of two different approaches for the analysis of sediment transport in sewers, based on the assumption of transport of uniform sediments or transport of non-uniform sediment mixtures. The conventional approach based on uniform sediment transport is simpler and may support the analysis of sewer processes involving mobile beds of sediment characterized by a relatively narrow grain-size distribution. Conversely, approaches based on sediment transport of non-uniform mixtures is expected to provide more accurate results in scenarios characterized by large spatial variation of sediment characteristics. While the use of the first approach is generally sufficient to predict the evolution of the bed profile during the flush development, the second approach is required to explore in detail the spatial evolution of the bed composition as well as to take into account a number of secondary processes occurring in sediment mixtures. A detailed description of the structure of the two modelling approaches is reported in the successive sections.

5.2 The unsteady flow model for uniform sediment transport

5.2.1 General introduction to the flushing mechanism

Sewer flushing is characterized by flow conditions similar to those of dam-break processes (Fan 2004). Thus, this high flow consists, in practice, in the development and propagation of a surge wave over the sediment bed of the sewer channel downstream of the flushing device. The generated flow is highly unsteady because the quick opening of the flushing device typically determines the full release of large amounts of water in a relatively short time (Pisano *et al.* 1998; Fan *et al.* 2001; Fan 2004).

In general, the flushing process can be summarized as follows. At time $t=0$, when the flushing device (in Fig. 5.1a) flushing gate is closed, water is stored upstream the gate (initial water level h_0). At this stage the flow discharge Q and the velocity V at the gate section are equal to *zero* (Fig. 5.1a). When the gate opens, a positive (advancing wave front moving downstream) and a negative (wave front moving upstream) water surges generate at the gate location and propagate towards two directions (Chanson 2004; Fig. 5.1b).

The effect of the two waves on the bed sediments is different depending on the hydraulic characteristics of the flush (i.ee. velocity, shear stress, etc.) as well as on the bed conditions (*i.e.,* fixed or mobile bed, dry or wet bed).

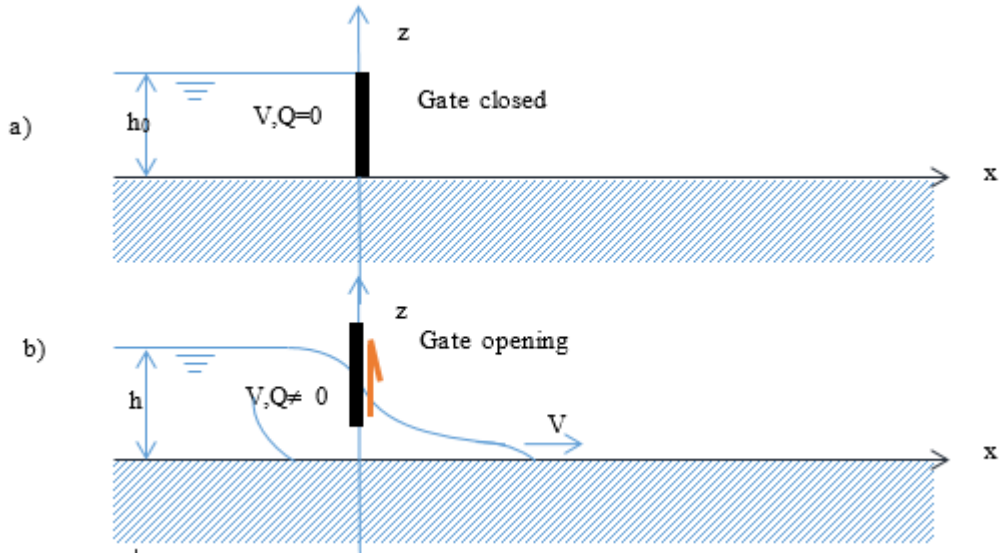

Fig. 5.1 Scheme of the flush process: a) still water upstream of the gate while closed at t =0, b) flush release after the gate opening at t >0 (Chanson 2006).

5.2.2 Governing equations for flow and sediment phases

Under the usual hypotheses of prismatic channel and neglecting lateral inflows and outflows, the 1-D De Saint Venant (DSV) equations for free-surface flows can be written in the following form:

$$\frac{\partial A}{\partial t}+\frac{\partial Q}{\partial x}=0 \qquad \text{Eq. 5.1}$$

$$\frac{\partial Q}{\partial t}+\frac{\partial}{\partial x}(V\cdot Q+\frac{F_h}{\rho})=g\cdot A\cdot(S_b-J) \qquad \text{Eq. 5.2}$$

being x [m] and t [s] the spatial and temporal independent variables, respectively; A [m^2] the cross-section of the wetted area; Q [m^3/s] and V [m/s] the flow discharge and the average flow velocity, respectively; F_h [N] the hydrostatic force over the cross-section; ρ [kg/m^3] the water density; g [m/s^2] the gravity acceleration; S_b [–] the slope of the mobile bed; J [m/m] the energy friction slope.

Additionally, the evolution of the bed of sediments can be described by the sediment mass balance equation as:

$$(1-p)\frac{\partial A_s}{\partial t}+\frac{\partial Q_s}{\partial x}+\frac{\partial(C\cdot A)}{\partial t}=q_s \qquad \text{Eq. 5.3}$$

where p [–] is the sediment porosity; A_s [m^2] the sediment cross-section area; Q_s [m^3/s] the volumetric sediment discharge, q_s [m^2/s] lateral sediment discharge per unit length (Fig. 5.2).

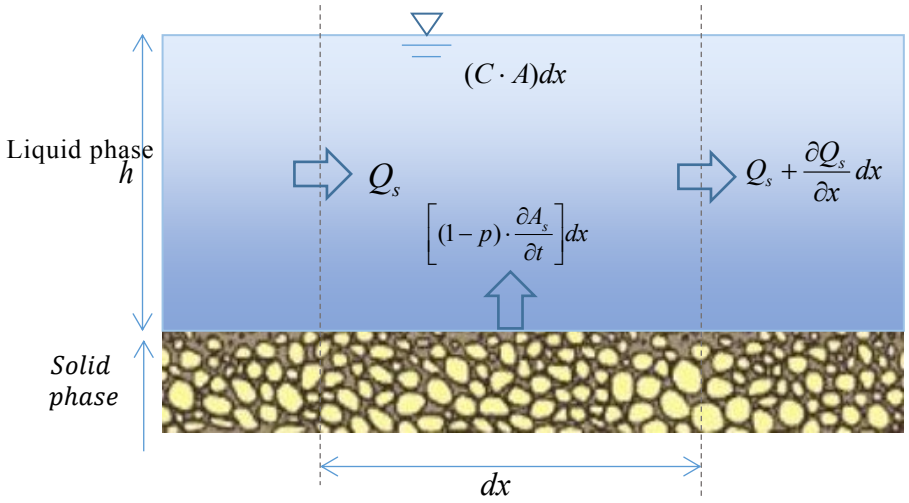

Fig. 5.2 Scheme of sediment mass balance in a given control volume.

The term $\frac{\partial(C \cdot A)}{\partial t}$ refers to the sediment concentration in the water column. In the formula, C is the average volumetric concentration of sediments in the cross section A (corresponding to water level h) as obtained from:

$$C = \frac{\int_A cc \cdot dA}{A} \qquad \text{Eq. 5.4}$$

being cc the local concentration in the cross section.

Assuming the bed-load transport to be preponderant over the suspended-load in a given flow, then it is possible to write the equation as *Exner* (1920).

$$(1-p)\frac{\partial A_s}{\partial t} + \frac{\partial Q_s}{\partial x} = q_s \qquad \text{Eq. 5.5}$$

Equation (5.5) is valid for bed with uniform sediments. The set of equations (5.1), (5.2) and (5.3) written in vectorial form is:

$$\frac{\partial U}{\partial t} + \frac{\partial F(U)}{\partial x} = D(U) \qquad \text{Eq. 5.6}$$

where U, $F(U)$ and $D(U)$ are written as follows:

$$U = \begin{bmatrix} A \\ Q \\ A_s \end{bmatrix}, \text{ dependent variable vector,} \qquad \text{Eq. 5.7}$$

$$F(U) = \begin{bmatrix} Q \\ V \cdot Q + \frac{F_h}{\rho} \\ \frac{1}{1-p} \cdot Q_s \end{bmatrix}, \text{ flux vector,} \qquad \text{Eq. 5.8}$$

$$D(U) = \begin{bmatrix} 0 \\ g \cdot A \cdot (S_b - J) \\ \frac{1}{1-p} \cdot q_s \end{bmatrix}, \text{ source term vector.} \qquad \text{Eq. 5.9}$$

The vectorial equation (5.6) allows describing the transport of sediments under unsteady flow conditions by the determining the unknown vector V of state conservative variables as a function of x and t.

In absence of lateral sediment inflow and outflow ($q_s=0$), the last term becomes:

$$D(U) = \begin{bmatrix} 0 \\ g \cdot A \cdot (S_b - J) \\ 0 \end{bmatrix} \qquad \text{Eq. 5.10}$$

To evaluate the friction slope, the Strickler equation, can be used as:

$$J = \frac{Q^2}{k_{eq}^2 \cdot A^2 \cdot R^{4/3}} \qquad \text{Eq. 5.11}$$

being R [m] and k_{eq} [$m^{1/3}/s$] the hydraulic radius and the composite roughness coefficient, respectively. Coefficient k_{eq} is typically evaluated by the Einstein equation (Einstein and Banks 1950), by assuming different roughness values on the wetted perimeter P [m]:

$$k_{eq} = \left(\frac{P}{\frac{P_w}{k_w^{3/2}} + \frac{P_b}{k_b^{3/2}}} \right)^{2/3} \qquad \text{Eq. 5.12}$$

being subscripts w and b relative to the channel walls (*e.g.,* concrete) and to the channel bed. In case of bed deposits, k_b can be evaluated as a function of the sediment characteristic size using the well-known formula by Strickler:

$$k_b = \frac{21.1}{d_{50}^{1/6}} \qquad \text{Eq. 5.13}$$

where d_{50} is the median size of sediment bed.

Further, the shear stress exerted over the sediment bed (τ_b) is evaluated as a function of the ratio between k_{eq} and k_b as:

$$\tau_0 = \rho \cdot g \cdot R \cdot J \cdot \left(\frac{k_{eq}}{k_b} \right)^{3/2} \qquad \text{Eq. 5.14}$$

5.2.3 Bed-load transport evaluation

For the evaluation of the bed-load and the suspended-load transport the models use the approach proposed by Rouse (see Chapter 2). Accordingly, the sediment particles are assumed to be transported at the bed or in suspension based on the threshold values of $R = w_s / \kappa u*$ in Table 2.2.

The solution of the system of equations (5.6) requires estimating the sediment-transport discharge Q_s [in m^3/s], which depends on the chosen sediment-transport formulas.

From more than one century, a large number of empirical relationships have been proposed by researchers to predict sediment discharge in natural/artificial channels. As already discussed in Chapter 2, many formulas have been tested with precious success in sewer systems. Several of these formulas with different range of application domains are implemented in the model. Some of the implemented formulas are summarized in Table 5.1.

Table 5.1 Example of formulas used in the model to estimate sediment-transport discharge.

Author	**Application range for d (in mm)**	**Notes**
Meyer-Peter and Müller (1948)	0.4 - 30	Coarse gravel Uniform unsteady flow
Engelund-Hansen (1967)	> 0.15	Gradually varied flow
Ackers-White (1980)	> 2.4	Coarse sediments
Van Rijn (1984)	> 0.2	Coarse sediments
Parker (1990)	> 2	Gravel particles

Generally, for the majority of the formulas, only one single representative grain size (such as d_{50}) is used to approximate sediment-transport discharge. The Meyer-Peter and Müller (1948) formula (Eq. 5.15) was used in this thesis to estimate the bed-load sediment transport associated to the flush experiment in Paris sewer system. Sediment discharge is estimated as a function of the bottom shear stress (over the bed surface), rather than the average shear stress. This empirical relationship is suggested

for ranges of sediments between sand and gravel materials. In sewer cases, this formula has been successfully applied several times to estimate the bed-load discharge (Bertrand-Krajewski *et al.* 1993; Ashley and Verbanck 1996; Lin and LeGuennec 1996). The bed-load sediment-transport discharge is calculated based on d_{50}, as a function of the grain shear stress (Shen 1971; Wu 2008).

$$\frac{q_s}{\sqrt{(s-1)\cdot g\cdot d^3}} = 8\cdot(\theta-\theta_c)^{3/2} \qquad \text{Eq. 5.15}$$

where:

- q_s is volumetric bed-load transport discharge per unit width, under equilibrium conditions;
- s is particle specific gravity ($s = \rho_s/\rho$);
- d is grain size;
- θ and θ_c are respectively non-dimensional effective bed and critical shear stresses.

For the critical shear stress (θ_c) to transport the bed sediments. Meyer-Peter and Müller (1948) suggested the value 0.047 for well-sorted sand and fine gravel.

Suspended sediment-transport evaluation

The *Velikanov* approach (1954) is implemented in the model to estimate the amount of sediments transported by the flow as suspended particles. Relationships 5.16 and 5.17 are used to calculate limit sediment concentrations into suspension as proposed by the author of the formula.

$$C_{\min} = \eta_{\min}\frac{\rho_s\rho_m}{(\rho_s-\rho)}\frac{V}{w_s}J \qquad \text{Eq. 5.16}$$

$$C_{\max} = \eta_{\max}\frac{\rho_s\rho_m}{(\rho_s-\rho)}\frac{V}{w_s}J \qquad \text{Eq. 5.17}$$

where:

$C_{\min}$ and $C_{\max}$ are limit sediment concentrations (in g/L);

$\eta_{\min}$ and $\eta_{\max}$ are efficiency coefficients (no unit);

ρ_m is the density of water-sediments mixture (in kg/m^3);

ρ_s is the density of the sediment (in kg/m^3);

w_s is the sediment settling velocity (in m/s).

According to *Velikanov*, erosion takes place if the flow real

concentration in the flow is lower than C_{min} while particle deposition occurs for concentrations higher than C_{max}. Any value between these two limits indicates that particles are in transport without erosion or deposition, in other words, the turbulence energy keeps particles in suspension (Schlütter 1999).

In these relations the choice of the threshold coefficient values (η_{min} and η_{max}) is important as parameters that impacts significantly the suspended load. Bertrand-Krajewski *et al.* (2006) report the use of Velikanov model to be of interest for the study of flushes and associated sediment transport in sewer systems.

Velikanov method has been previously applied in sewers by different authors. Zug *et al.* (1998) used it for sediment-transport analysis in sewers in both dry and wet weather conditions. Calibration of η_{min} and η_{max} was performed through experimental data from French sewers. Table 5.2 summarizes values of these coefficients as reported in literature.

Table 5.2 Velikanov coefficients found in the literature.

Author(s)	η_{min}	η_{max}
Combes (1982)	0.0005-0.002	0.002-0.007
Bujon (1988)	0.018	0.022
Zug *et al.* (1998)	0.00225	0.00275
Chebbo (1992)	0.001-0.005	0.001-0.005
Bertrand-Krajewski *et al.* (2006) Bertrand-Krajewski (2006)	2×10^{-6}	1024×10^{-6}

Furthermore, a specific module of the code allows implementing a number of flush devices with different geometry and operation in the sewer systems. Various specifications can be given to this module to describe right function of each device. All the devices are treated in the module as boundary or internal conditions within the numerical domain.

5.2.3 Numerical scheme and solution

The hyperbolic system of Eqs. 5.1 and 5.2 is discretized by means of the finite difference explicit *McCormack* scheme. The scheme is a two-step predictor – corrector with a second-order accuracy in both time and space. This scheme is suitable to predict 1D dam-break flows (*e.g.,* MacCormack 1969) because it is a "shock-capturing" scheme, *i.e.,* it is able to model shock waves caused by rapidly varied flows as well as discontinuities in the bed slope and and in the flow variables. Although the used model is not fully coupled (*i.e.*, it does not solve DVS and Exner equations simultaneously), the use of the predictor-corrector scheme enables resulting semi-coupled solution (Campisano *et al.* 2004).

In the first step of prediction, *F(U)* and *D(U)* corresponding to the flux and sources terms, respectively, are estimated based on the values of *V* vector at previous time step of *t*. Then the derivative forms of *F* in the space scale of $\partial F / \partial x$ are calculated backwards. The following equation accounts for approximating variables of the Eq. 5.7-9 in finite differences (Finite-difference method approximates the partial derivatives by divided differences on a space-time grid).

$$\frac{U_i^p - U_i^j}{\Delta t} + \frac{F_i^p - F_{i-1}^j}{\Delta x_{i-1,i}} = D_i^j \qquad \text{Eq. 5.18}$$

where *i* and *j* are representative nodes in space and in time, respectively, and Δx is the spatial step.

Therefore, this equation is applied to all the internal grid nodes of the whole domain which allows evaluating the *predicted value* of U_i^p (index *p* abbreviates predicted) of the unknown vector U_i^{j+1}.

In the second step, the scheme estimates both flux *F* and source *D* terms referring to the already predicted values of the vector U_i^p. So, the derivative terms $\partial F / \partial x$ are calculated forwards. For this aim, the following equation accounts for approximating variables of the Eq. 5.7-9 in finite differences. Therefore, this equation is applied to all the internal grid nodes of the whole domain which allows evaluating the *corrected value* of U_i^c (index *c* abbreviates corrected) of the unknown vector U_i^{j+1}:

$$\frac{U_i^c - U_i^j}{\Delta t} + \frac{F_{i+1}^p - F_i^p}{\Delta x_{i,i+1}} = D_i^p \qquad \text{Eq. 5.19}$$

The procedure ends with calculating the weighted average of estimated predicted and corrected values. To this end, all internal grid nodes of the domain are subject to the following relation (see Eq. 5.23) to obtain weighted average between the predicted and the corrected values (Creaco

2005):

$$U_i^{j+1} = \frac{U_i^p . \Delta x_{i-1,i} + U_i^c . \Delta x_{i,i+1}}{\Delta x_{i-1,i} + \Delta x_{i,i+1}} \qquad \text{Eq. 5.20}$$

If the space step is constant during the whole flow $\Delta x_{i-1,i} = \Delta x_{i,i+1}$, therefore, Eq. 5.23 can be written as:

$$U_i^{j+1} = \frac{U_i^p + U_i^c}{2} \qquad \text{Eq. 5.21}$$

A complementary third step based on Total Variation Diminishing (TVD) dissipation theory is incorporated in the solution (Garcia-Navarro *et al.* 1992; Garcia-Navarro and Saviron 1992). This solution is an efficient convective scheme to compute sharp gradient in unsteady flow with two main properties of making the solution oscillation-free by keeping the second-order accuracy both in space and time. To this aim, this additional step was applied to the mean velocity U_i^{j+1} obtained after the explained steps of McCormack method.

5.2.4 Domain discretization

The domain was split in time and space. Suitable time (Δt) and space (Δx) steps were chosen allowing to better reproduce the flush as a rapidly varying flow and the associated sediment transport. Moreover, the computer capacity and time consumption for simulation were also taken into account in the spatial mesh choice. The used numerical scheme is explicit, thus requires to satisfy the stability conditions. The Courant – Friedrichs – Lewy (CFL) condition was used. This means assuming values of the Courant number, $C_r < 1$ to obtain the stability of the solution (Bhallamudi and Chaudhry 1991). In particular, Courant number was fixed equal to 0.8 for the successive simulations thus enabling calculation of adequate time step:

$$\Delta t = C_r \frac{\Delta x}{V + c} \qquad \text{Eq. 5.22}$$

where, V is the mean flow velocity and c is the celerity of the disturbance. The celerity is obtained from $c = \sqrt{g \cdot \frac{A}{B}}$ for irregular cross-sections (A and B being as wetted area and free surface width, respectively).

The space-time integrated scheme written in meshes $\Delta x \cdot \Delta t$ in finite difference grid for solving the domain is shown in Fig. 5.3. This scheme enables the forward or backward difference scheme in each time space.

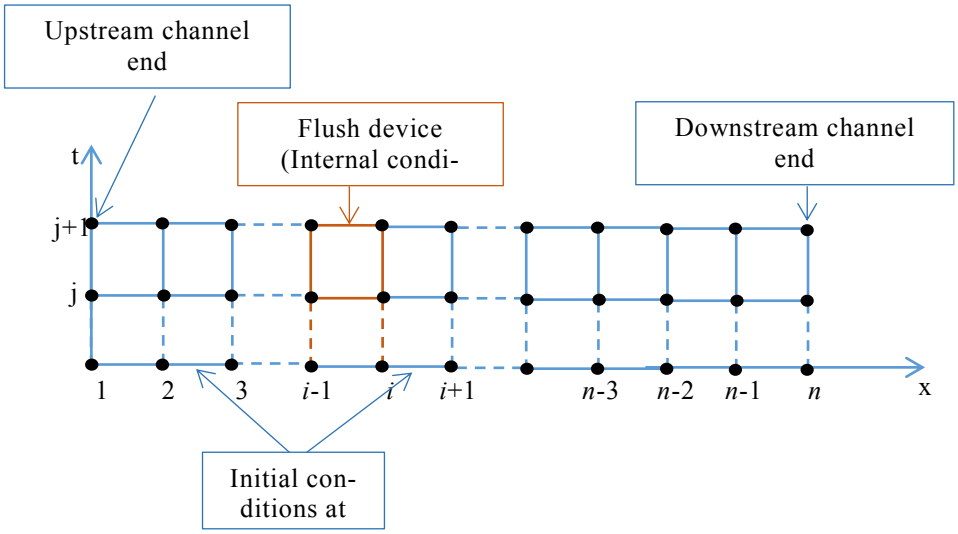

Fig. 5.3 Discretization scheme of domain in terms of time and space.

5.2.5 Initial and boundary conditions

The boundary conditions provide the information about boundary limits of the domain. They determine the flow and the sediment properties at the inlet and outlet of the channel (Wu 2008). Modelling the unsteady flow determined during flushing, requires prescribing flowing conditions at the upstream (inlet) and downstream (outlet) ends of the domain. The application of the McCormack numerical scheme to solve the DSV-Exner equation system requires to know hydrodynamic data of the U vector (*i.e., A(t)* and *Q(t)* at both boundaries of the numerical domain. In particular, concerning the flow variables, the method of characteristics is implemented to determine the values of unknown variables which are not prescribed at the boundaries (Garcia-Navarro and Saviron 1992). In case of supercritical flow, in particular, two conditions are requested at the upstream boundary such as the functions: *Q(t)* and *A(t)* for entering hydrograph. At the downstream boundary, one can use the positive and negative characteristic lines along which the 1D DSV equations turn from partial differential equations into ordinary differential equations. Conversely, in case of subcritical flow at the upstream boundary one can prescribe the function *Q(t)* correspond to the negative characteristic line. At the downstream boundary, a boundary condition such as a function *Q(t)* can be prescribed together with using the positive characteristic line. As for sediment continuity equation can be used at the boundary where the physical conditions have been prescribed.

The model allows to prescribe specific boundary conditions at the upstream and downstream ends of the domain. It allows also adopting specific conditions allow defining correctly the hydraulic behaviour of various flushing devices inside the domain as internal conditions. In particular, the numerical domain is solved through separation into sub-

domains by only internal conditions. Fig. 5.4 illustrates a general scheme of application of boundary and internal conditions that is possible to impose for the flush modelling.

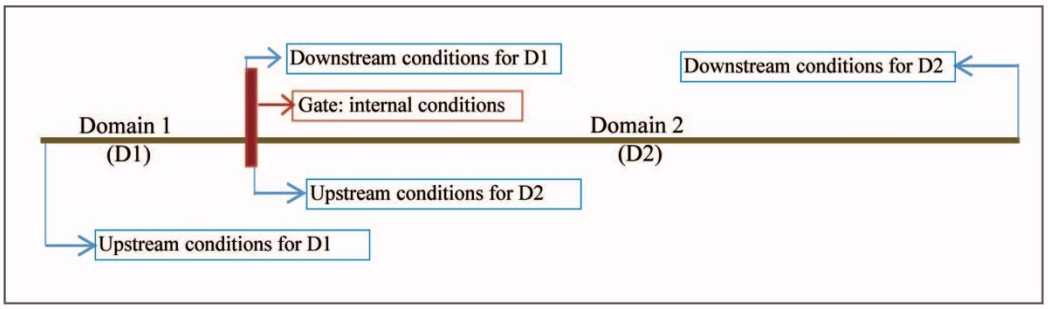

Fig. 5.4 General scheme of the boundary conditions for domains upstream and downstream of the gate (D1, D2 are domains upstream and downstream of the gate, respectively).

5.3 The unsteady flow model for non-uniform sediment transport

A novel aspect of the present modelling analysis is to take into account the non-uniformity of sediments for the analysis of the flush impact. The use of models for non-uniform sediments allows predicting the bed evolution not only in terms of bed heights but also in terms of modification of the composition of the deposits (Armanini 1992; Di Silvio 1992). Collected data from experimental flushing test (in Chapter 3) were then used also to validate the non-uniform sediment-transport model.

5.3.1 Governing equations for flow and sediment phases

Compared to the described model for uniform sediments, the used model for transport of non-uniform sediments is more complex. A two-layer approach is used to schematize the sediment bed (Fig. 5.5), with :

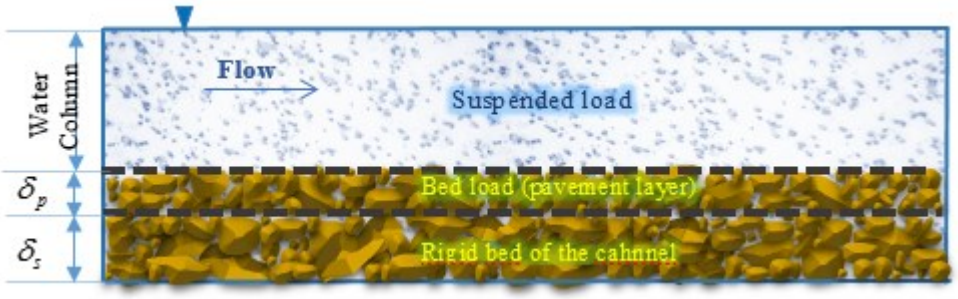

Fig. 5.5 Simple scheme of bed and suspended load in an open flow used in the non-uniform model.

- pavement layer (as active layer) having thickness δ_p that contains sediment particles that are liable to frequent vertical movements (entrainment to and settlement from the upper transport layers).
- sub-pavement layer, having thickness δ_s, that contains particles liable to occasional vertical movements to and from the upper transport layers.

As compared to other models (*e.g.,* Di Silvio, 1992) that have been originally developed for mobile river beds, the used model does not include the third storage layer under the sub-pavement where particles are assumed to be undisturbed (unless degradation takes place). Instead, being developed for artificial channels, the used model assumes that the sub-pavement overlays the rigid bed of the channel (concrete); therefore, elevation of $\delta_p + \delta_s$ represents sewer deposits as well as the mobile bed level for sewer flows. Based on this schematization of the system, the following equations are used for the mass balance of the pavement layer:

$$(1-p)\cdot\frac{\partial(A_s^p\cdot\beta_k^p)}{\partial t}+\frac{\partial(Q_s)_k}{\partial x}=(1-p)\cdot\beta_k^*\cdot\frac{\partial(A_s^p-A_s)}{\partial t}+(q_s)_k \qquad \text{Eq. 5.23}$$

in which: β_k^p is the percent (concentration) of sediments of size class *k* in the pavement layer, A_s^p is the sediment area of the pavement (equal to $\delta_p\cdot B_s$ in case of rectangular channel cross section with B_s as the channel width); $(q_s)_k$ is lateral input of sediment (per unit length), *i.e.,* the transport capacity of the class *k* of the sediment. $(Q_s)_k$ is the total sediment discharge (as sum of bed and suspended-load transport capacity) of the *k* size class of the sediment in the pavement and A_s is the area of the sediment deposits.

The term $(A_s^p\cdot\beta_k^p)=(W_{mix}^p)_k$ is called "mixing volume of the pavement" and represents the volume of the sediments of class *k* that is present in the pavement (per unit channel length).

The term $(1-p)\cdot\beta_k^*\cdot\frac{\partial(A_s^p-A_s)}{\partial t}$ clearly represents the temporal variation of the sediment area of the pavement for the *k*-class.

Similarly, the "mixing volume in the sub-pavement" $(W_{mix}^s)_k=(A_s^s\beta_k^s)$ is defined for the sediments belonging to the *k*-class in the sub-pavement layer. In particular, based on the mass balance equation for the sub-pavement:

$$\frac{\partial(W_{mix}^s)_k}{\partial t}=-\beta_k^*\cdot\frac{\partial(A_s^p-A_s)}{\partial t} \qquad \text{Eq. 5.24}$$

The concentration of β_k^s belonging to each class-*k* in the sub-pavement is then calculated based on the following relationship where *M* is the number of grain sizes that constitute the mixture:

$$\beta_k^s=\frac{(W_{mix}^s)_k}{\sum_{k=1}^{M}\left[(W_{mix}^s)_k\right]} \qquad \text{Eq. 5.25}$$

It should be stressed that the value of β_k^* is process-dependent. In fact, $\beta_k^*=\beta_k^s$ if erosion/degradation occurs while $\beta_k^*=\beta_k^p$ in the case of deposition/aggradation in the channel.

It should be noticed that, it is assumed that the interactions between sediment particles are neglected and sediment population is supposed to be low concentrated. Thus, each grain size's transport behaves separately as uniform sediment. Therefore, each moving class size of sediments within the sediment mixture will be assumed to have its own sediment-transport discharge as in the uniform sediment-transport approach (Wu 2008). The total sediment-transport discharge (Q_s in the Exner equation) is thereby provided by the sum of discharges $(Q_s)_k$ for all the *J* classes.

Differential equations (5.26) and (5.27) for pavement and sub-pavement mass balance are solved together with the DSV-Exner equations and enable the possibility to take into account deposition and erosion processes for each class of sediment grain-size distribution. The used approach allows also including a number of important processes associated to the mobility of non-uniform sediments mixtures, *i.e.,* hiding/exposure, differential erosion, armoring, etc. (Rahuel *et al.* 1989; Holly and Karim, 1986; Holly and Rahuel, 1990).

Function for hiding/exposure

Hiding function takes into account the explained sheltering effect being as an important phenomenon in natural flows (Einstein 1950; Egiazaroff 1965; Andrews and Parker, 1987). In fact, bed material sorting accounts for the hiding and exposure phenomena (Rahuel *et al.* 1989). This factor indicates the increase or reduction of a specific size class in the sediment mixture discharge (Campisano *et al.* 2007b).

Hiding /exposure factor (ξ_k) was implemented in the model from the relationship provided by Ashida and Michiue (1972).

$$\xi_k = \left(\frac{\log_{10}(19)}{\log_{10}(19 \cdot \frac{d_k}{\bar{d}})} \right)^2 \qquad \text{Eq. 5.26}$$

where, $\bar{d}$ is generally the mean diameter (d_{50}) of the mixture (m), and d_k is the diameter of k^{th} fraction of grain-size distribution (in m).

Another relationship for the hiding factor is implemented into the model which is used in the current thesis (see Eq. 5.27). In this formula the exponential value of n is an empirical parameter for the transport condition of the given particle; n=1 denotes the incipient motion condition while n<1 indicates the sediment-transport condition.

$$\xi_k = \left(\frac{\bar{d}}{d_k} \right)^n \qquad \text{Eq. 5.27}$$

Different values for n are suggested in the literature. Andrews (1983) by studying the mobility of sediment mixture, proposed a value of 0.872 to calculate the critical shear stress. For the same study goal, Parker and Klingenman (1982) used n=0.982. In any case, the n value must be smaller than 1. In the current thesis the value of n=0.982 is applied to the simulations.

Function for bed surface armoring process

Being one of the most typical phenomena encountered in gravel beds, the bed armoring process is a vertical sorting of the surface bed. This phenomenon consists of hiding or "trapping" fine particles in substrate below by the coarse ones. Such phenomenon is taken into account by hiding effect because fine sediments are hidden by the large-diameter particles at the bed surface that are more exposed to the flow. Armored bed is achieved when the equilibrium condition for bed sediments is obtained due to the vertical sorting mechanism. Many researchers (Armanini, 1995; Hirano, 1971; Karim and Holly, 1986; Little and Mayer, 1976; Parker and Andrews, 1985; Sanford 2008) have extensively investigated this topic. In the context of this research this function was not used.

5.3.2 Scheme, initial and boundary conditions in non-uniform model

Initial conditions

The model allows:

1) bed sediment heights from BF
2) grain-size distributions at the different sections with linearization between the sampling sections.

Boundary conditions

Upstream allows introducing a sediment discharge curve on time with specific grain-size distribution.

Solution scheme

The same scheme as for uniform sediment-transport model was applied for the non-uniform model to solve the system equations. An additional procedure was implemented into the numerical scheme (predictor-corrector) to take into account the transport of class of sediment sizes between pavement and sub-pavement layers.

In particular, the following equations were implemented in the numerical solution using predictor-corrector scheme. For pavement layer corrector and predictors are as written in Eq. 5.28 and 5.29, respectively.

$$(1-p)\cdot\frac{(W^{p}_{mix_i})_{1k}-(W^{J}_{mix_i})_{1k}}{\Delta t}+\frac{(Q^{J}_{s_i})_k-(Q^{J}_{s_{i-1}})_k}{\Delta x}=(1-p)\cdot(\beta^{J*}_{i})_k\cdot\frac{\Delta(A^{p}_{si}-A^{J}_{si})}{\partial t}+(q^{J}_{si})_k \quad \text{Eq. 5.28}$$

$$(1-p)\cdot\frac{(W^{p}_{mix_i})_{k}-(W^{J}_{mix_i})_{k}}{\Delta t}+\frac{(Q^{J}_{s_i})_k-(Q^{J}_{s_i})_k}{\Delta x}=(1-p)\cdot(\beta^{J*}_{i})_k\cdot\frac{\Delta(A^{p}_{si}-A^{J}_{si})}{\partial t}+(q^{J}_{si})_k \quad \text{Eq. 5.29}$$

Also for the sub-pavement the same relationships are:

$$\frac{(W^{s}_{mix_i})_k - (W^{s,J}_{mix_i})_k}{\Delta t} = -(\beta^{*J}_i)_k \cdot \frac{\Delta(A^p_{si} - A^J_{si})}{\Delta t} \qquad \text{Eq. 5.30}$$

$$\frac{(W^{s_1 c}_{mix_i})_k - (W^{s,J}_{mix_i})_k}{\Delta t} = -(\beta^{*J}_i)_k \cdot \frac{\Delta(A^p_{si} - A^J_{si})}{\Delta t} \qquad \text{Eq. 5.31}$$

Chapter 6
Model application to the flush experiment Paris sewer

6.1 Data preparation for simulation by both uniform and non-uniform sediment-transport models

Numerical models described in the previous chapter were applied to the experiment carried out in the sewer trunk of Paris Municipality. The collected experimental data were therefore, prepared as input to the model. Both models take into account various input files containing data such as hydro- and sediment-graphs entering the sewer channel, geometry data of the sewer channel as well as other parameters concerning the sediment characteristics. The following sections are aimed to present data preparation procedure for both models.

6.1.1 Modelling the geometry of the sewer channel

The cross-section of the channel was provided as input both models. A unique cross-section was prescribed through a detailed elevation width-cross-sectional area curve. Also, along the longitudinal axis of the channel, elevation of the bed invert was specified on every $\Delta x = 1\text{m}$ based on the data provided during the experiment campaign. The used Δx was considered to be sufficiently small as compared to the total channel length (more than 1 km) for appropriate description of the flush propagation and impact on sediment transport. Use of such Δx determined the channel discretization into a numerical domain of 1101 numerical sections.

6.1.2 Basic input data for the uniform sediment-transport model

The following parameters (Table 6.1) summarize basic input values provided to the model for simulations.

Table 6.1 Summary of the input parameters defined into the uniform sediment-transport model.

Number	Parameter	Given value
(1)	Grain size (uniform) (in mm)	2.176
(2)	Sediment porosity (-)	0.41
(3)	Sediment specific weight (in kg/m^3)	2317
(4)	Flow density (kg/m^3)	1000
(5)	Strickler coefficient of channel walls (in m$^{1/3}$/s)	50
(6)	Minimum Velikanov efficiency coef. (-)	$\eta_{\min} = 0.00125$
(7)	*Courant* number (-)	0.8
(8)	Spatial step (s)	1 m
(9)	Flush duration (in s)	18,000 (5 h)

In particular:

(1) A unique grain size was obtained for the whole sewer channel for the simulation with the model for uniform sediment, which was calculated as average $d_{50_{av}}$ for all the channel (*i.e.,* based on the grain-size distribution curves sampled along the channel). This grain size was determined from the equation below:

$$d_{50_{av}} = \frac{\sum_{i=1}^{1101}(d_{50_i} \cdot h_{s_i} \cdot \Delta x)}{\sum h_{s_i} \cdot \Delta x} \qquad \text{Eq. 6.1}$$

being $d_{50_{av}}$ the median diameter for each section and h_{si} is the sediment height at each section.

(2) An average porosity of 0.41 was calculated for the four samples analysed in laboratory.
(3) The specific weight of the sediments measured from the laboratory analysis was based on the weighted average of all the measured values along the longitudinal sewer channel.
(4) The Strickler coefficient for the walls of the channel was (according to the literature) determined as 50 [in m$^{1/3}$/s] based on the bottom texture

coupled water level-flow measurements under (quasi-)uniform flow conditions in the sewer channel.

(5) $\eta_{\min}$ was set for the condition in which sediments are going into suspension (erosional threshold) (see Section 5.2.2). The value reported in Table 6.1 is the average value proposed by different authors (see Chapter 5). Since direct observation of the flush (through the installed cameras) as well as the analysis of the experimental results (see Chapter 4) showed suspension of sediments with negligible re-deposition during the flush, only C_{min} was used for the simulations. In other words, this would mean assuming that bed particles from the entire channel are remobilized by the flush and then put into suspension are flushed out from the channel as wash load.

(6) Courant Number (C_r) was defined as 0.8 for the stability of the scheme. The same value was used for previous studies in sewer such as in Campisano *et al.* (2004).

(7) The time step was calculated based on the McCormack scheme using the following relationship.

$$C_r = \frac{\Delta x}{\Delta t} \times c \qquad \text{Eq. 6.2}$$

being c as flow wave celerity (in m/s).

(8) The model was run with a computing time of 18000 s (5 h) that was shown as sufficient to describe the whole flush process and its impact on the bed deposits.

Additionally, the previous information, the heights of the initial sediment deposits was provided as input to the model for each section of the numerical domain (*i.e.,* 1101 values of sediment heights throughout the channel) based on the data collected by the experimental campaign BF.

6.1.3 Basic input data for the non-uniform sediment-transport model

The non-uniform sediment-transport model required further information mainly concerning the initial deposit bed before the flush (*i.e.,* the bed composition and relative grain-size distribution curves). In particular, the grain-size distribution for the different channel sections were discretized into twenty classes of grain size with variable ranges from 0.075 to 50 mm as model input. The percentage of particles for each size class is constituted the matrix of the initial concentration β_k of the different *k*-lasses in the initial pavement and sub-pavement layers of the bed. Since information on grain-size distribution was available only at 20 locations (see Chapter 4 and Fig. 6.1), spatial linearization of grain-size distribution was used to estimate the initial bed composition for all the channel sections. The percent of twenty classes of size are presented in Appendix C.

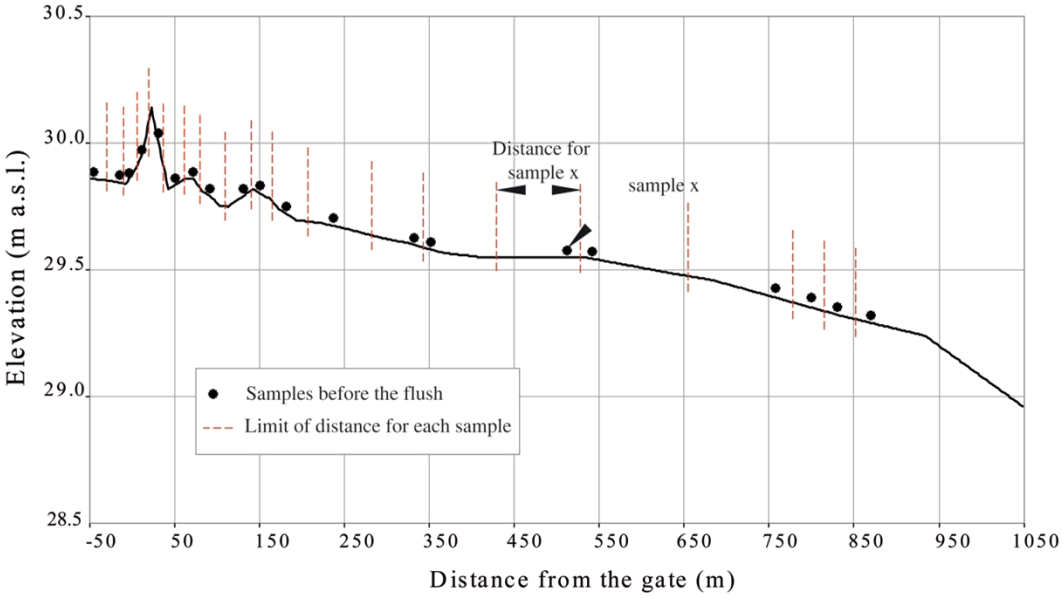

Fig. 6.1 Attributed distance of samples collected before the flush along the longitudinal studied sewer channel.

Moreover, by default the thickness for the pavement layer (δ_p) was defined as $3\times d_{90}$ of the bed deposits at each section. However, this was not respected if the thickness of the real bed was smaller or higher. In other words, if δ_p is smaller than $3\times d_{90}$, so the whole thickness of the bed deposits were given to the corresponding section. In this case no sub-pavement was exist. Otherwise, when δ_p is larger than $3\times d_{90}$, so the thickness of the sub-pavement is equal to the reste of the bed height.

6.1.4 Initial, internal and boundary conditions for uniform and non-uniform sediment-transport approaches

Initial conditions for the flow

Before gate opening for flush releasing, at $t = 0$, while the 'reservoir' behind the gate was filled to the maximum level, the following settings for flow parameters were applied for the two models:

- Initial water levels in the upstream reach of the gate (upstream domain) were assumed under stationary conditions (Q=0). Consistently, with the maximum water level in store of 2.15 m immediately behind the flushing gate;
- Similarly, water levels in the downstream domain were assumed under stationary conditions, consistently to water level measurements recorded by all the water level probes before the flush release (average value of 0.5 m).

Initial conditions for the sediments

For the uniform sediment-transport model, the initial condition for the sediments was described in terms of height over the fixed bed, on every 1m along the sewer channel, as regarded from the real experiment.

The same bed heights were provided as input for the non-uniform sediment-transport model for each mesh node. Additionally, the real composition of the non-uniform bed mixture of the entire channel was provided to the model as the initial bed sediment BF as described in the previous sections.

Boundary and internal conditions for the flow at the upstream and downstream channel ends

Presence of the flushing device in the sewer channel was numerically described as an internal condition. Therefore, prescription of the numerical condition was different before and after the gate opening at the beginning of the flush release. The outflow relationship was determined based on the experimental test. The outflow function was implemented in the code. From recorded data, the gate took about 56 s to be completely open, so, after 56 s the gate does not exist any more from the numerical point of view.

Boundary conditions were imposed at the upstream end of the

channel. In particular, the inflow hydrograph *Q(t)*, which was recorded during the experimental campaign was provided as input file to the model. The method of characteristics was used through determination of the negative characteristics line to determine the corresponding unsteady flow value of the upstream water level *h(t)*.

Up to the complete opening of the gate, the channel was numerically described by two sub-domains: upstream (S_{-50}, S_0) and downstream (S_{-50}, S_0) of the gate. Later, when the gate opening phase was ended (so that the gate was physically embedded in the sewer bottom), the domain was considered as one, thus eliminates any internal condition due to the gate. Internal condition at the gate upstream section (S_0) was the gate outflow relationship coupled with the positive characteristic line for determining the value of the water level. Similarly, the internal condition at the gate downstream section (S_{+1}) was obtained through prescription of *Q(t)* relationship as well as use of the negative characteristic line. Fig. 6.2 schematizes the above description of the boundary condition for both during the gate opening (Fig. 6.2 a) and after the gate opening (Fig. 6.2 b).

As the downstream end of the channel is considered (S_{+1050}), the critical flow curve Q(h) was prescribed (provided the presence of the free outfall conditions). Similarly to the upstream section end, the method of characteristics was used to determine the value of the corresponding water level.

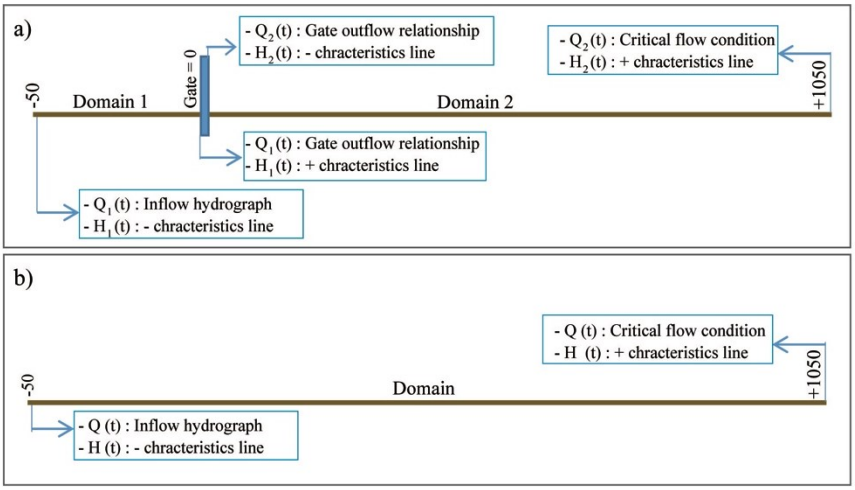

Fig. 6.2 Simple scheme representing the flow boundary conditions for the entire channel when a) the gate is in opening operation (first 56 s); b) when the gate 'numerically elimi-nated' after 56. s.

Boundary and internal conditions for the sediments

As for the flow, the sediment conditions were imposed also for the sediments at the boundaries. At upstream end of the domain (S_{-50}) the sediment discharge $Q_s(t)$ was prescribed as calculated with the sediment-transport formulas based on local time varying flow conditions determined by the entering flow hydrograph $Q(t)$. The Exner mass continuity equation is then used to determine the value of the sediment height $h_s(t)$ at the downstream channel end (S_{+1050}). The same approach is used to calculate the values of Q_s and h_s.

As coupled to the flow, no additional conditions are required at the gate sections for the sediments. During the gate opening phase, as well as, later, during the release phase, the domain for sediment transport is automatically determined by local flow variables of $Q(t)$ and $h(t)$ at the gate site. This is done without need of superimposition of internal conditions for the sediments.

6.2 Results from the simulations with the uniform sediment-transport model

Simulations with the uniform sediment-transport model were performed that allowed to provide results concerning both flow and sediment parameters. Hereafter, the analysis of the results will be presented.

6.2.1 Results of the hydraulics of the flush

Hydraulic variables (*i.e.,* water level and flow discharge) at the monitoring sections (S_{-50}, S_{-5}, S_{+5}, S_{+50}, S_{+100}) were compared to the values obtained experimentally to evaluate the model capacity to reproduce the hydraulics of the flush. Graphs in Fig. 6.3 and Fig. 6.4 show the comparison between experimental and modelled water levels and flow discharges for all the five measuring sections. In these graphs, the x-axis shows the variable of time. According to the graphs, it can be seen that globally the uniform sediment-transport model provides relatively good results hydraulically reproducing the flush propagation in the channel. In particular, the water level is shown to increase abruptly for all sections downstream of the gate device (form about 0.5 m to about 1.5 m) in the instants after the gate opening. Oppositely, the negative (entering) wave propagating upstream the gate provides water levels at section S_{-50} and S_{-5} to drop down from 2.15 m to about 1.5 m. The differences between simulated and measured water levels at the five monitoring sections of the channel are shown for the first 1.5 h of the flush simulation. For example, Table 6.2 presents the calculated standard deviation from the mean for the flow discharge obtained from the model compared to the experimental data over 1 h from the beginning of the flush. A good match of observed and simulated values is also observed for flow discrepancies of the five sections including time and magnitude of the flush peak value. Unfortunately, missing data did not allow visualizing how the model reproduced the flow time series at the downstream sections: S_{+50} and S_{+100}.

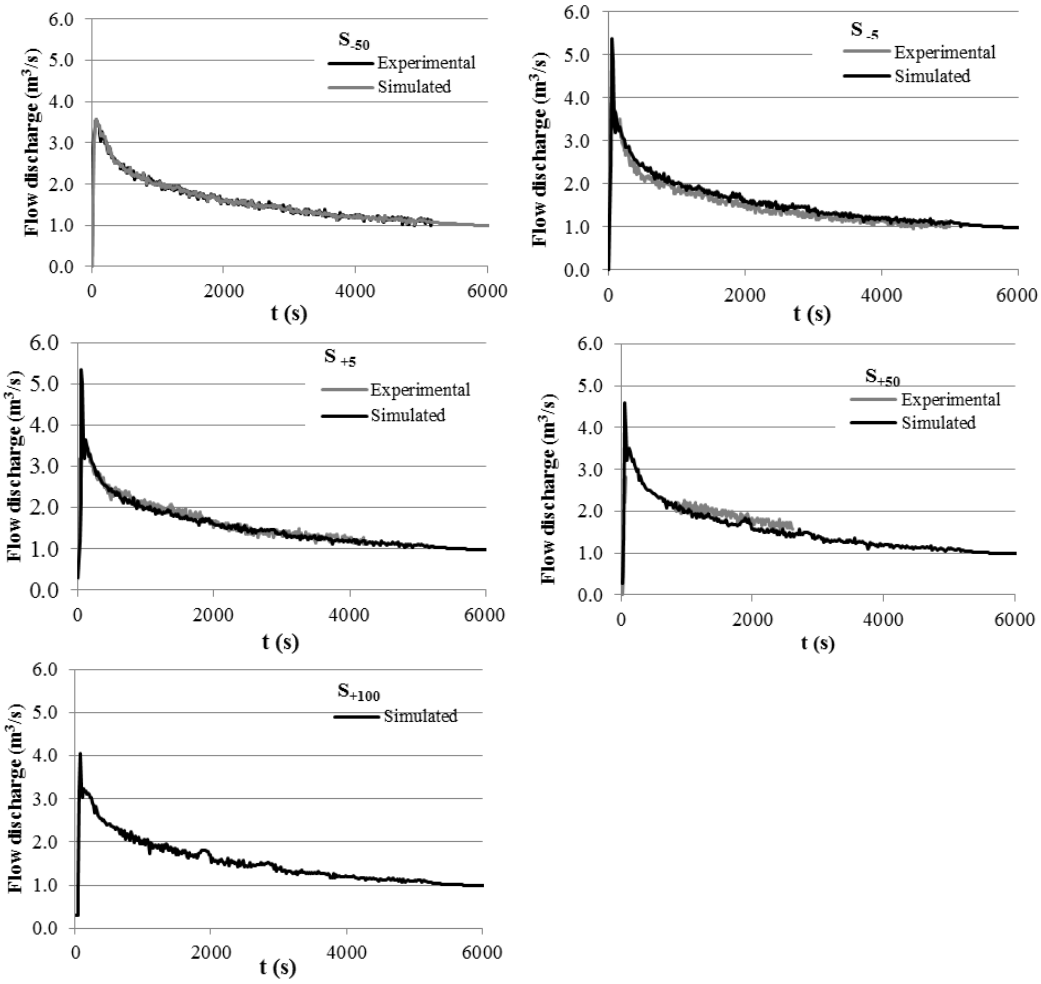

Fig. 6.3 Comparison of the measured and simulated flow discharge for all five measuring sections using the uniform sediment-transport approach.

Table 6.2 Standard deviation from the mean for the measured flow discharges compared to the experimental data for the first 1 h.

Measuring sections	**S_{-50}**	**S_{-5}**	**S_{+5}**	**S_{+50}**	**S_{+100}**
Experimental	0.523	0.578	0.564	-	-
Modelled	0.532	0.571	0.553	-	-

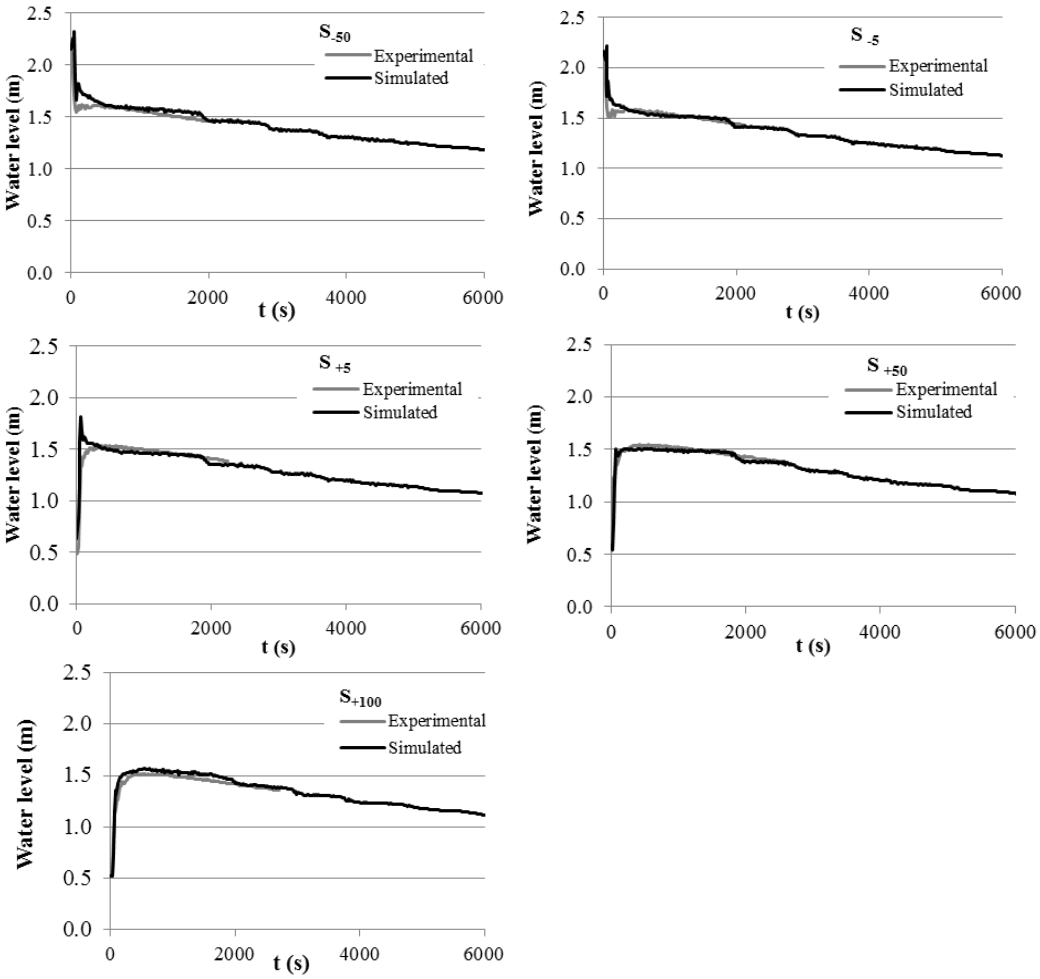

Fig. 6.4 Comparison of the measured and simulated water levels for all five measuring sections using the uniform sediment-transport approach.

Bottom shear stress due to the flush

In addition to water level and flow discharge, Fig. 6.5 shows the bed shear stress evaluated in five channel cross-sections. The figure shows the evolution of the shear stress for the first 30 min from the beginning of the flush for both upstream (S_{-30}) and downstream (S_{+10}, S_{+180}, S_{+810}) of the gate. As it was expected, the peak shear stress is obtained at the beginning of the flush. The peak of about 14.5 N/m² at S_{+10} is in agreement with experimental results (Shahsavari *et al.* 2017). The peak is evidently delayed for the downstream sections due to the flush propagation. The shear stress is then observed to decrease on time. Spatially, the flush had a considerable effect throughout the entire channel. Based on the plotted curves, in fact, the shear stresses remained high enough (>5 N/m²) to allow bed erosion in the downstream segment of the channel (see S_{+180} and S_{+810}). Erosional effects of the flush in the upstream segment occurred instead only during the first

minutes of the flush. The difference in the long-term value of the shear stress may be principally imputed to the increase by the channel invert slope between upstream and downstream segments. Moreover, the figure shows a significant effect of the negative waves behind the gate with peak values in the order of 9 N/m² through S_{-30}. Thus, the numerical results confirm the erosional effects of the flushing surge after the gate opening.

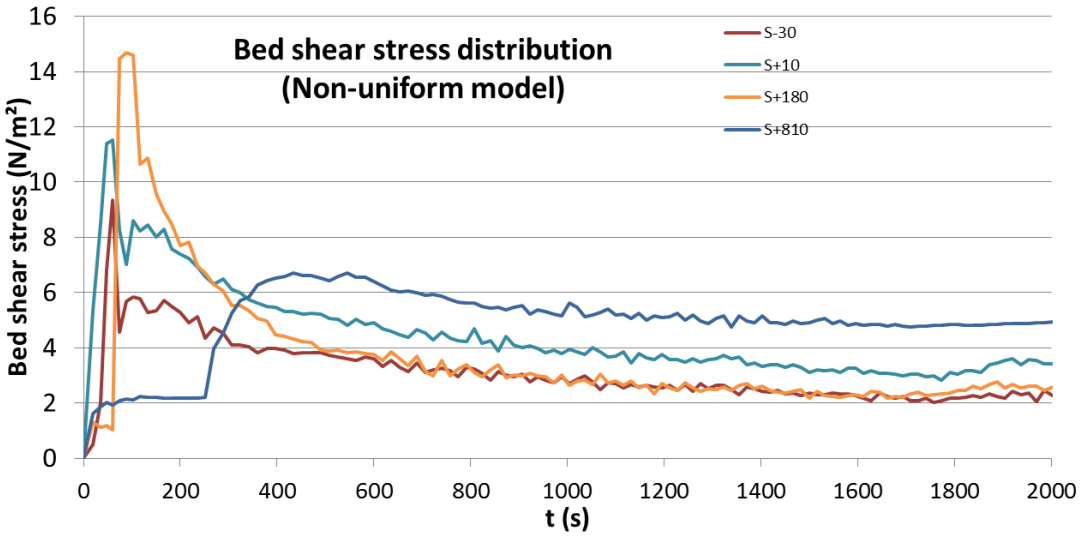

Fig. 6.5 Propagation of the bed shear stress upstream and downstream of the gate along in sections S_{-30}, S_{+10}, S_{+180} et S_{+810} for the first half an hour (uniform sediment-transport model).

6.2.2 Results concerning the sediment-bed evolution

Previous section has shown relatively good capacity of the model in reproducing the hydraulics of the flush propagation in the channel. In addition, the model allowed describing in a relatively successful way the sediment-transport processes associated to the flush.

Sediment-transport discharge due to the flush

The simulations carried out using the uniform sediment-transport model led to obtain the sediment-transport discharge during the flush flow. The results of the simulation conducted with parameter values summarized in Table 6.1 showed that the considered sediment size was transported as bed load only because of the high value of the rouse number corresponding to the generated shear stresses. Then the total sediment transported by the flush was evaluated through the Meyer-Peter and Müller (1948) formula. Fig. 6.6 illustrates the simulated bed-load transport at three sections of the sewer channel downstream of the gate (S_{+200}, S_{+500}, S_{+1000}). Interestingly, the flush provided erosional effects that covered the whole channel downstream the gate.

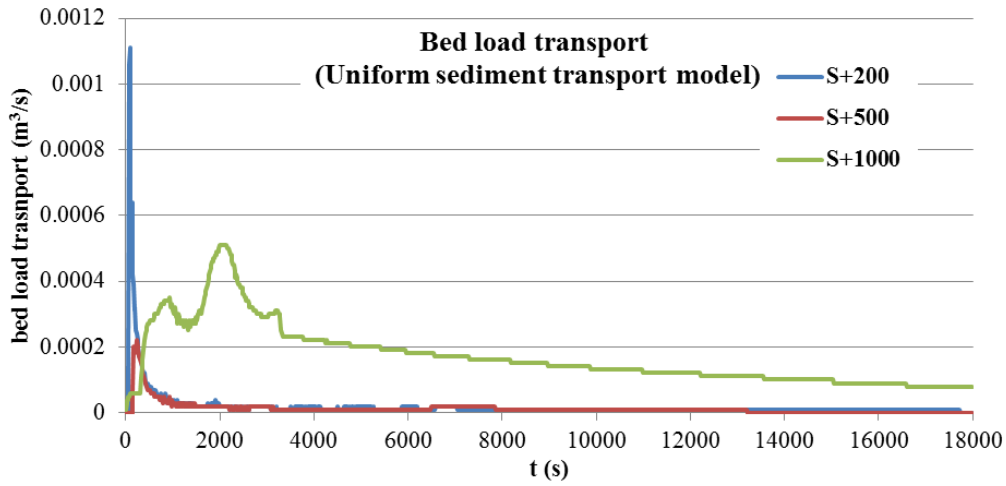

Fig. 6.6 Bed-load sediment-transport discharge from three sections through the channel downstream the gate.

Moreover, Fig. 6.7 shows the simulated bed heights (average value of the experimental and simulated being 29 and 30 cm, respectively) at the end of the flush (AF) against the experimental data. Globally, the model allowed to describe the bed modifications due to the flush, although peaks and sections of simulated sediments accumulation were not in good agreement with observed values. Differences highlight the model inability to correctly reproduce the flush bed profile after the flush. The maximum and

average values of the measured sediment heights are 26 and 3 cm, respectively, while the model reproduced a smaller value of the maximum (20 cm). However, model results and experimental data showed almost the same averaged height of the deposits. Example of the sections over which the model was not able to reproduce is remarked with hatched polyline on the Fig. 6.7. For example, at nearby end of the channel, no accumulation of sediment was reproduced conversely to the observed data form the experimental campaign. Also, mismatches can be observed for the peaks close to the gate.

The fitting degree between experimental and numerical results is evaluated by calculating three indices presented in Table 6.3. The Root Mean Squared error (RMSE) of the sediment profiles obtained considering is equal to 0.045 m. According to the graphics and mismatching between observed and modelled data, this indicator value of error, corresponds to less-accurate but acceptable results.

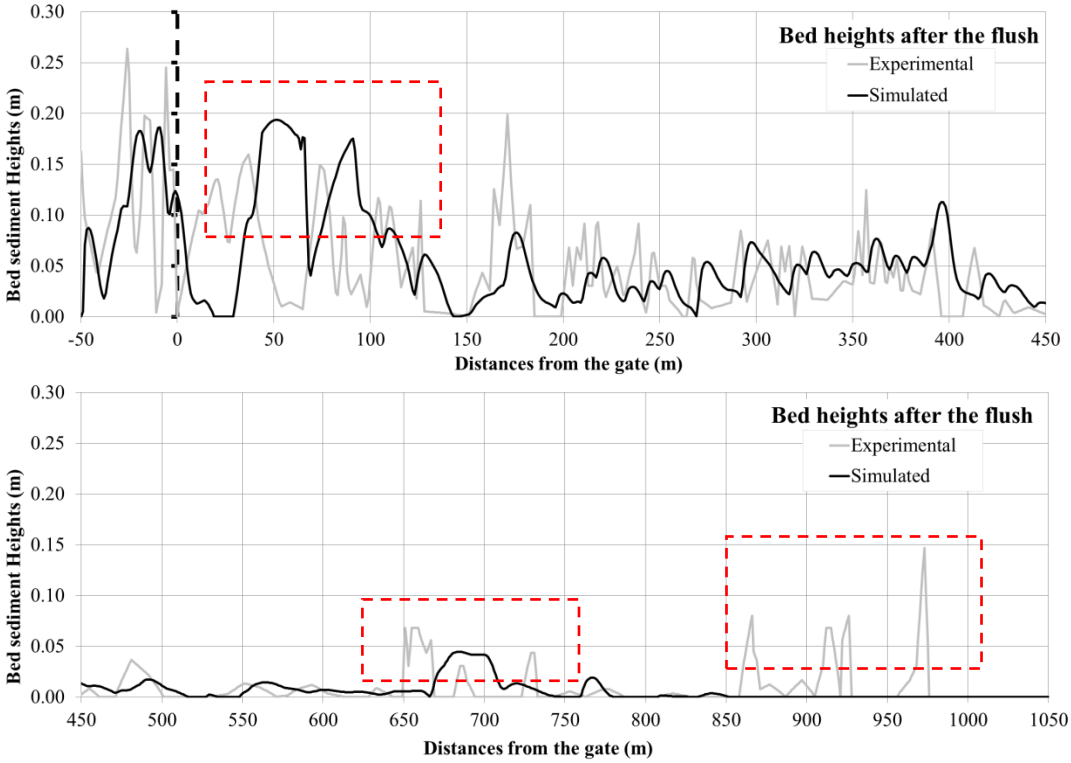

Fig. 6.7 Comparison of the simulated and experimental bed heights after the flush event using the uniform sediment-transport approach.

Table 6.3. Statistical indices to evaluate the agreement between simulated results and measured bed heights between S_0 and S_{+1050} using the uniform sediment-transport model.

Coefficient	Root Mean Square Error (RMSE)	MAE
value	0.045	0.026

The volumetric estimation of the deposits by the model (results schematized in Fig. 6.8), showed that 3.69 m^3 (against 5.4 m^3) of the bed sediments were flushed out from the channel trunk downstream of the gate (S_0 to S_{+1050}). However, it was considered that the results of deposits profile at the end of the flush includes a balanced between the sediment flushed out (at S_{+1050}) and the sediments entering from upstream of the gate (at S_0). In fact, the flush eroded about 0.83 m^3 sediment upstream of the gate transporting such volume through the channel downstream of the gate. Based on model simulations, all the sediment flushed out from the channel was transported as bed load. In agreement with Shields (1936), in fact, the uniform sediments grain size considered for the simulation (2.176 mm) could not be transported as suspended load with the developed shear stresses. Evidently, this clearly shows that the model for uniform sediment transport may provide a limited capacity to fully describe all the processes occurred during the flush test (*e.g.,* flow selectivity or correspondent transport of different sediment size and bed or suspended load).

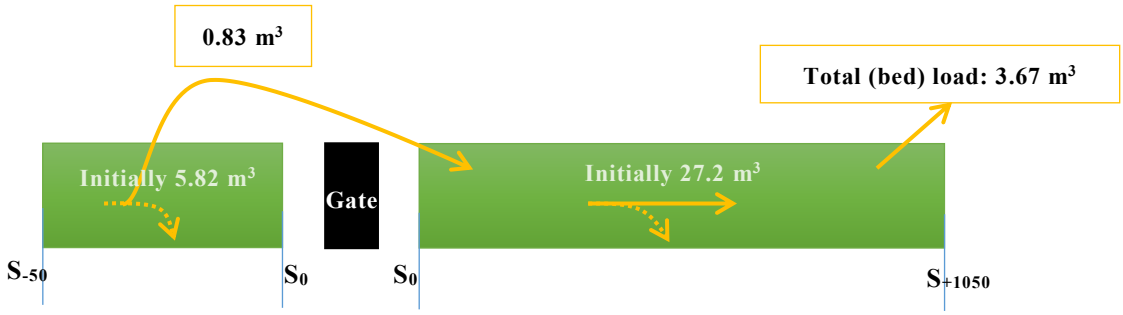

Fig. 6.8 Summary of the numerical results of uniform sediment-transport model in terms of the transported volume of sediments.

Consequently, the above results obtained from the uniform sediment-transport model have showed relatively acceptable hydraulic performance of the model. However, in terms of the sediment related parameters, the uniform model did not provide accurate-enough results for a detailed investigation on sediment transport processes.

The following sections will present the application of the non-uniform sediment-transport model to the experimental data using more sophisticated model that is able to take into account a variety of sediment sizes found in the sewer bed deposits. It is expected to achieve more improved and realistic results as the non-uniformity of sewer sediments is one of the main properties of such environment.

6.3 Results from the simulation with the non-uniform sediment-transport model

6.3.1 Model consistency test

Preliminary to the simulation analysis with the model for sediment transport of mixtures, tests were carried out to verify the consistency of the model with the model for uniform sediment transport. In particular, initial simulations were carried out with the two models using the same input data, as well as by "forcing" the developed model for sediment mixtures to simulate cores characterized by uniform characteristics of the bed sediment. This test included, for example, running the model for sediment mixtures with initial bed conditions characterized by grain distribution curves with a single size if the particles.

As an example of these test, the results of the simulation run using the same parameters of Table 6.1 (*i.e.*, all the mixtures were assumed to be made of uniform sand with d=2.176 mm) are shown in Fig. 6.9. The simulation provided almost identical results in terms of flow parameters (water levels, flow discharge, shear stress), as well as in terms of final bed configuration as compared to Fig. 6.7.

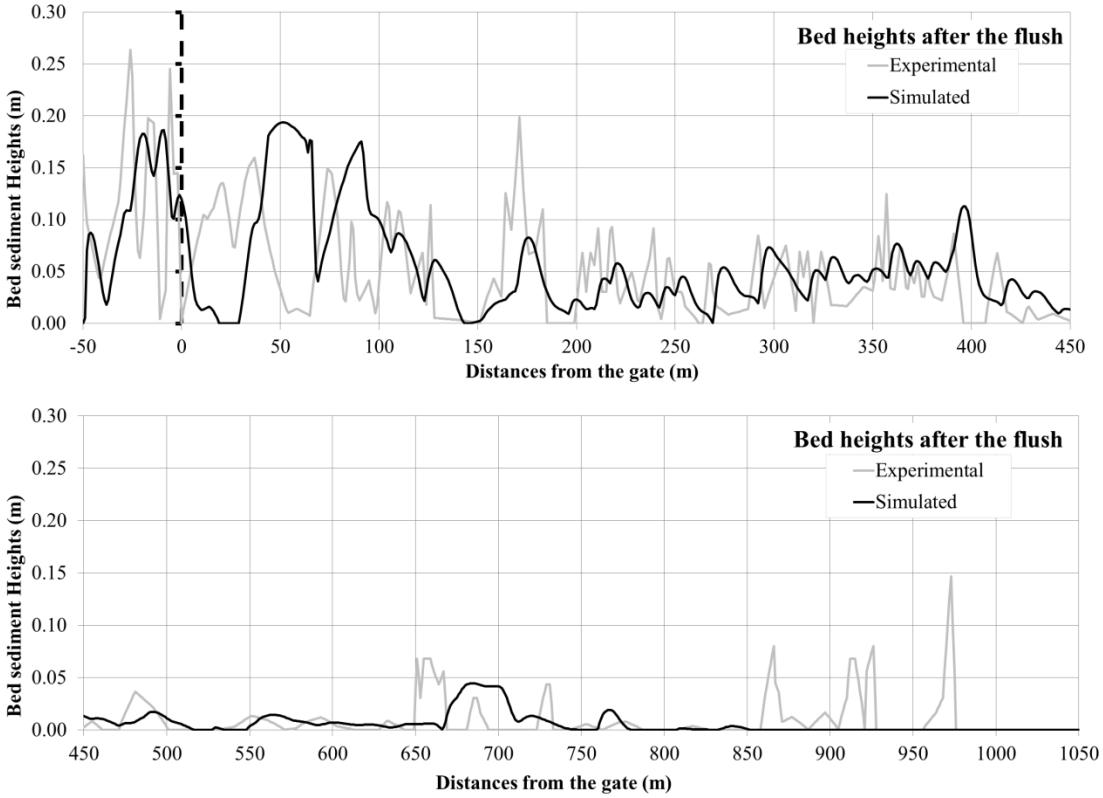

Fig. 6.9 Comparison of the simulated and experimental bed heights after the flush event using non-uniform sediment-transport model with uniform sediment condition.

Sediment heights were basically reproduced by the two models at the same way. Also, the model has remarkably shown that the same sediment volumes were flushed out from the sewer channel (3.67 m^3).

Similar tests conducted under other conditions allowed to obtain a consistency proof of the two models, thus enabling appropriate comparison of the relative results.

6.3.2 Hydraulics of the flush

The non-uniform sediment transport model needs a longer calculating time (more than 24 hours) than for the uniform-approached model (5 hours). Simulated and experimental values of the hydraulic variables of the flush (*i.e.,* water head and flow discharge) in all the measuring sections are compared in Fig. 6.10 and Fig. 6.11. Globally the model has reproduced better curves comparing to the uniform sediment-transport model. In particular, the comparison of the simulated values with the experiments at initial stage of the flush including the peak discharge of the flushing is shows an improved model flushing. According to the simulation results, a maximum instantaneous flow discharge of 4.2 and 4.0 m^3/s were reproduced against 4.1 and 3.9 m^3/s for S_{-5} and S_{+5}, respectively. The slight amelioration of the results by this model is the results of a better description of the bed composition and then of the bottom roughness that contributes to the friction slope and in terms of the flow parameters. The graphs show a good reproduction of the hydraulic parameters (in particular at the peak flow discharge) for all the measuring sections. The same as uniform sediment-transport model, the abrupt chute the water level and increasing of flow discharge is visible due to the wave propagation at the initial stage. Table 6.2 presents the calculated standard deviation from the mean for the flow discharge obtained from the model compared to the experimental data over 1 h from the beginning of the flush. The table confirms the amelioration and perfect agreement of the results using non-uniform sediment-transport model rather than using the uniform sediment-transport model.

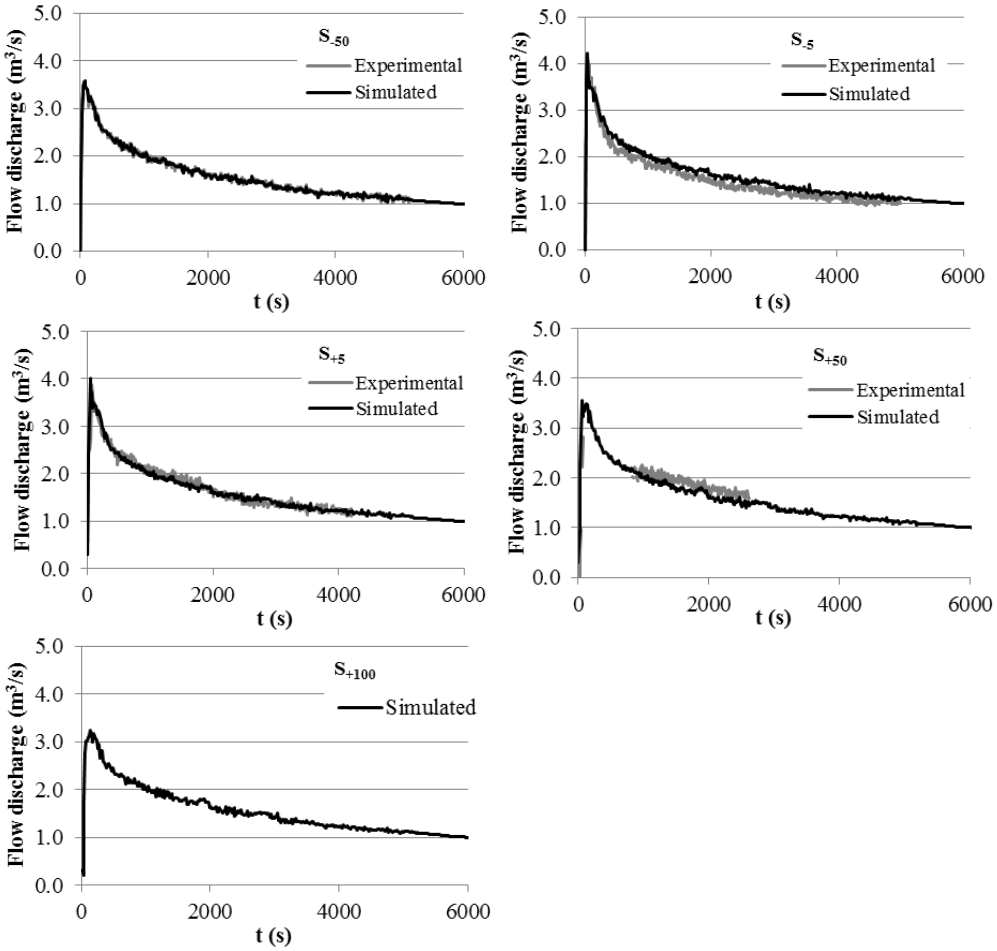

Fig. 6.10 Comparison of the measured and simulated flow discharges for all five measuring sections using the non-uniform sediment-transport approach.

Table 6.4 Standard deviation from the mean for the measured flow discharges compared to the experimental data for the first 1 h.

Measuring sections	**S_{-50}**	**S_{-5}**	**S_{+5}**	**S_{+50}**	**S_{+100}**
Experimental	0.522	0.578	0.564	-	-
Modelled	0.541	0.576	0.567	-	-

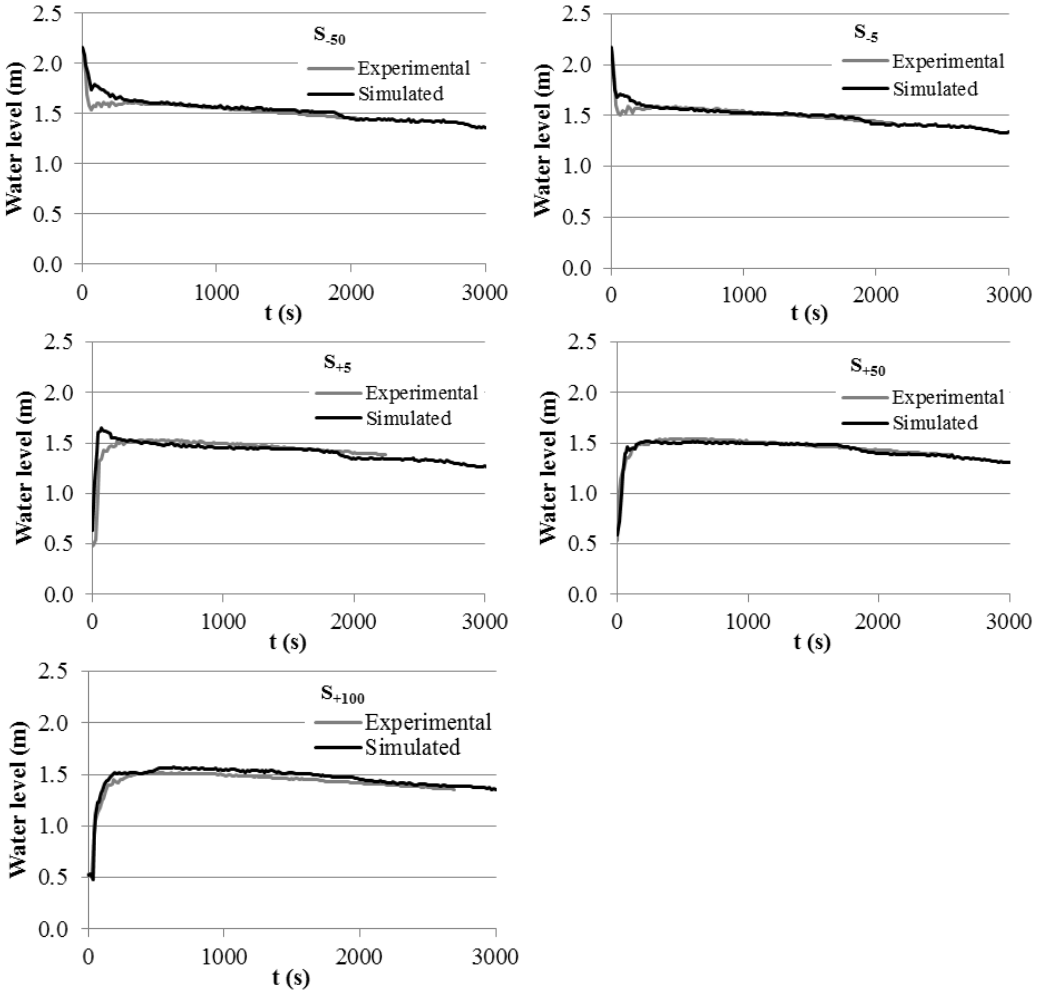

Fig. 6.11 Comparison of the measured and simulated water levels for all five measuring sections using the non-uniform sediment-transport approach.

Bottom shear stress due to the flush

Bottom shear stress through the channel was calculated as output of the non-uniform sediment-transport model. Results are presented for four selected cross-sections and illustrated in Fig. 6.12 during about the first 30 min. According to the shear stresses, almost the same trends as found for the uniform sediment-transport model can be seen for the evolution of the shear stresses on time. A remarkable difference can be observed for the maximum values provided by the results. Comparing the results from the non-uniform model and the estimated shear stresses by the uniform sediment-transport model, it can be concluded that the uniform sediment-transport model overestimates the values of shear stress values at the initial stage of the flushing event. In particular this overestimation was observable at the sections near the gate (both upstream and downstream). For example, the maximum shear stress obtained using the non-uniform sediment-transport

model for the closest section downstream of the gate (at S_{+10}) was estimated to be around 10 N/m² against almost 11.5 N/m² from the uniform sediment-transport model. The value from the non-uniform is considered to be much close to the experimental one. As already explained above, the non-uniform model takes into account the bed sediment roughness represented by the d_{50} to estimate the bed shear stress. As this characteristic diameter is different for each section, thus the shear stress is more reliable. In the contrast, in the uniform model, the d_{50} is the same everywhere, thus the shear stress is overestimated. This would confirm the results by Staufer *et al.* (2007) who concluded that 1D uniform sediment-transport model overestimates the bed shear stress generated by flushing.

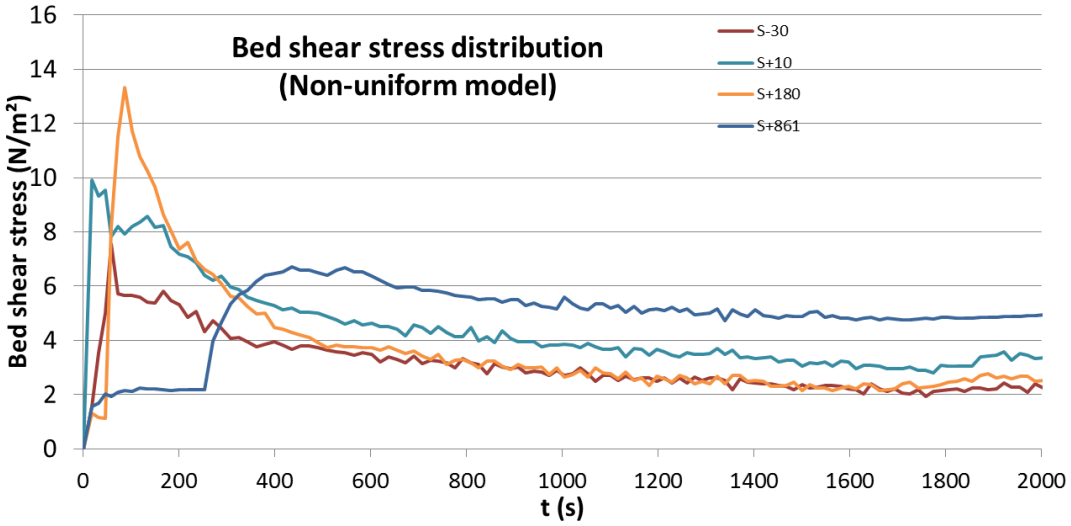

Fig. 6.12 Propagation of the bed shear stress upstream and downstream of the gate along in sections S_{-30}, S_{+10}, S_{+180}, S_{+810}, S_{+970} for the first half an hour (non-uniform sediment-transport model).

6.3.3 Results of the sediment-transport processes

The main results of the non-uniform sediment-transport model have concerned the deposited bed in terms of bed heights and composition under the flushing effect. It was aimed to consider the evolution of these two elements longitudinally through the entire sewer channel due to the flush. In the next sections these parameters will be presented.

Sediment-transport discharge due to the flush

Transport of particles as bed load as well as suspended load was obtained with the simulation. According to the simulation results sediments were flushed with both transport modalities. According to the results, much of the suspension occurred immediately with a sudden and high peak of the

beginning of the flush. The bed load is then predominant for the rest of the sediments. The main part of the suspension occurred during almost the first 7 min after the beginning of the flush. Interestingly, this process was also observed from the videos recorded from the "cunette camera", with the suspension being the predominant mode of transport before the peak arrival, then switching into bed-load mode, after the peak. However, very small amounts of sediment are transported during the flow recession as suspended load. In contrast, according to the same graph, bed-load mode of transport took place along the whole flushing time with a decreasing trend after the peak.

In particular, the bed-load discharge was extracted from various sections downstream of the channel (S_{+50}, S_{+680}, S_{+970}, S_{+1050}) to show the bed-load transport discharge and its evolution along the sewer channel. Fig. 6.13 presents the bed-load discharge of the mentioned sections. The figure shows that a high and at the same time sudden value of the bed load discharge took place at the closest section to the gate with almost 0.016 m^3/s. This shows a quick transport of the bed sediments as bed load due to the flush head energy with a short effect. Interestingly, the value of the bed load discharge in downstream segment of the channel peak increases toward downstream end of the channel that may be explained by the effect of the sleep bed slope together with the effect of the flushing waves. Moreover, the decreasing phase of the bed load discharge is slow demonstrating continuously transporting the sediments from upstream segment.

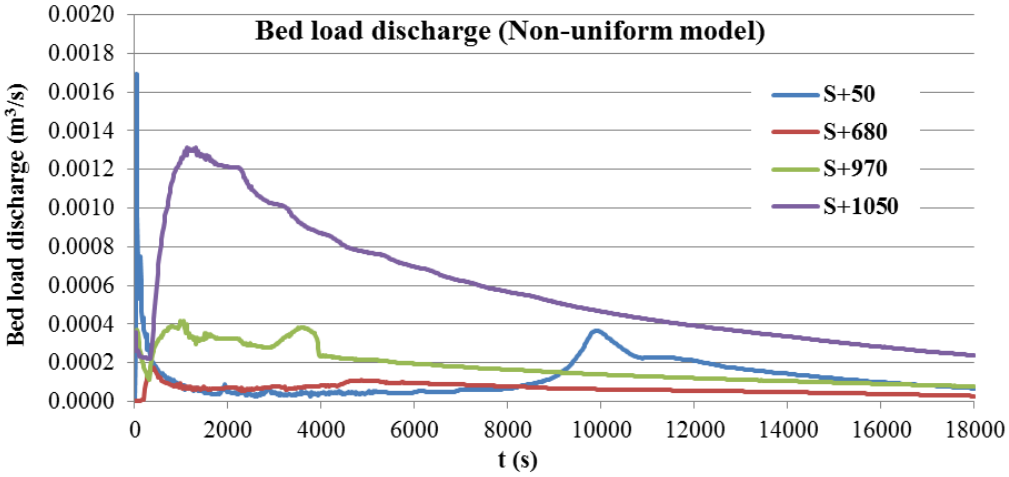

Fig. 6.13 Bed-load sediment-transport discharge from four sections through the channel downstream the gate.

Results of the sediment heights after the flush event

Results of the simulations related to the longitudinal topography of the bed along the sewer channel are presented in Fig. 6.14. The graphics illustrate good performance of the non-uniform sediment-transport model. In

particular, the model has properly reproduced the peaks of the bed heights with a relatively good match. On the figure, various sections are indicated by dashed polylines are those improved by the developed model that were not (well-) drawn by the uniform sediment-transport model. Thus, results indicates well-reproduction of deposit peaks through quasi the whole channel. Also, data from simulation shows a good agreement of the results against the experimental obtained measured from the flushing campaign. According to the data, maximum and average of the modelled sediment heights over the entire studied channel are 24.5 and 3.0 cm, respectively, against 26 and 2.9 cm obtained experimentally.

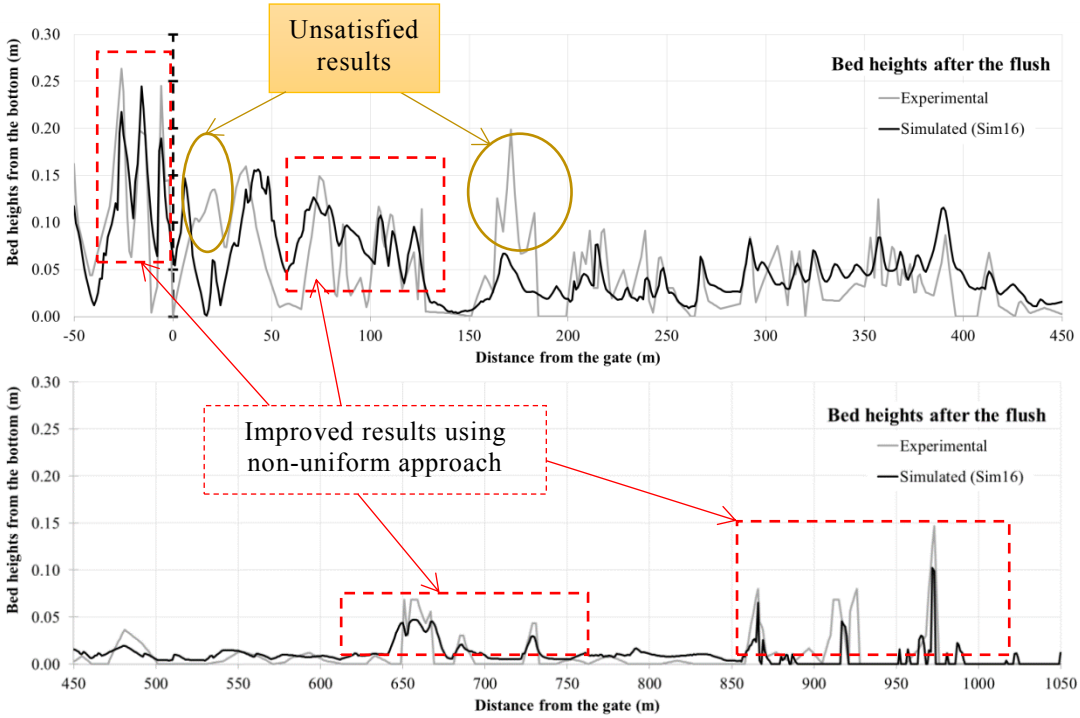

Fig. 6.14 Comparison of the measured and simulated bed heights along the studied sewer channel using the non-uniform sediment-transport approach.

From the Table 6.5, the Root Mean Squared error (RMSE) value for the sediment heights is equal to 0.028 while the uniform sediment-transport model has provided the same value in the order of 0.045. Therefore, the results the developed model showed clearly its ability to describe the impacts of the flushing flow on the bed sediments thus fitting better the experimental with numerical bed heights after the flushing operation.

Table 6.5. Statistical indices to evaluate the agreement between simulated results and measured bed heights of the studied channel using the non-uniform sediment-transport model.

Coefficient	Root Mean Square Error (RMSE)	MAE
value	0.028	0.018

However, the figure shows some sections for example those indicated by circles where the model was reproduced unsatisfied results. Such mismatch between the results can be explained by the accumulated rags as presented in section 3.2.2 (and see Fig. 6.15) that was observed during the experiments that are not considered as typical sediments. Thus, the model was not able to consider such deposits that are different from particle-type sediments.

Fig. 6.15 Example of the accumulated rags in the studied channel.

Results of sediment grain-size distribution (composition)

During the flush operation deposits over these reaches were eroded and based on the flow conditions were redeposited over downstream or flushed out from the sewer channel. Other important result of the non-uniform sediment-transport model is the estimation of eroded and transported volumes of the initial bed deposits from the channel downstream of the gate (being initially 27.2 m^3). The simulation results in terms of transported sediment volume are schematized in Fig. 6.16. A variety of sediment-transport processes are shown to occur over the downstream reach of gate. Other effect of the flush is through the channel section upstream of the gate. Therefore, according to the results of the simulation, a total volume of 4.49 m^3 was flushed out from the downstream sewer channel (between S_0 and S_{+1050}) against 5.4 m^3 measured volume that provides a reliability of 83%.

The same values regarding to the sediments eliminated from the entire channel (S_{-50} to S_{+1050}) shows almost an accuracy of 91% comparing to the experimental data (5.09 against 5.61 m^3). Thus, the model has shown a deposited volume of 22.74 m^3 against 21.82 m^3 obtained experimentally (0.92 m^3 higher). Results have also shown additional information about the volume of sediments transported as bed or suspended load thanks to the Velikanov method (*i.e.,* minimum efficiency coefficient). This module was allowed to estimate the volume of suspended load transported by the flush and thus estimate the bed load separately. It should be reminded that the suspended load comprises only the particles that go into suspension and "disappear" (no re-deposition occurs) without any interaction with deposited bed. In this regard, as indicated on the Fig. 6.16, almost half (48%) of the estimated total flushed volume from the entire channel (2.40 from 5.06 m^3) were transported as bed load that contains variable sediment class of sizes.

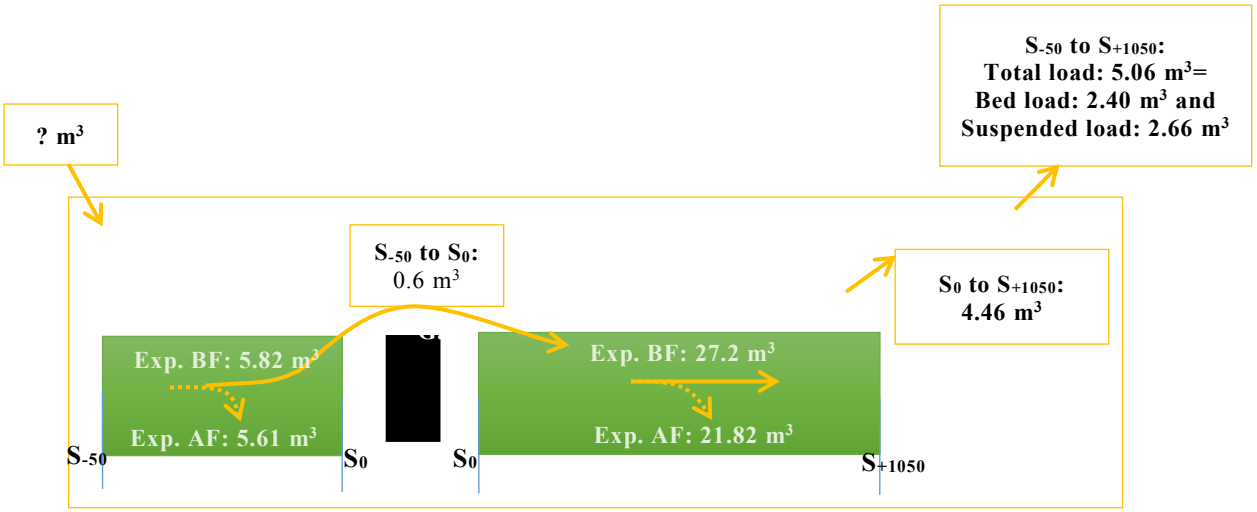

Fig. 6.16 Schematic summary of the experimental and numerical results from non-uniform sediment-transport model in terms of the transported volume of sediments.

Results from the simulations showed that a volume of 0.6 m^3 was eroded from the upstream part of the gate that is greater than the measurement from the experimental campaign. The difference of the eroded volume from upstream of the gate (S_{-50} to S_0) between measured and modelled values can be partially explained by the probable entrance of only fine particles to the studied sewer channel. Probably, this was occurred during the storage or evacuation phases. Unfortunately, no information exists about the amount of sediments entered to the studied channel from upstream of S_{-50}.

Simulation results allow evaluating other valuable information concerning the compositions of sediment in terms of the modification of the

fractional size of classes. This explains in details the evolution of the bed particles due to the flush. The results of the simulations were used to predict the final composition of the bed after the flush throughout the entire channel on every $\Delta x = 1m$. The results showing the evolution of specific characteristic grain sizes (*i.e.,* d_{16}, d_{50} and d_{90}) are presented in the graphs of Fig. 6.17. In this graph the numerical results for all the sampled locations taken before and after the flush (in total 28 points taken with the experimental values along the sewer channel from before and/or after the flush) are compared. Overall, simulated results show similar trend to the experimental values. In particular, a good fit was obtained for d_{16} and d_{50}. More discrepancies can be observed for the larger fractional size (*i.e.,* d_{90}). This might rise from the in-sewer sampling conditions that may have minor accuracy of the samples in particular from the downstream segments of the channel (>500 m). In particular, the downstream section (*e.g.,* S_{+1003}) shows a considerable difference as compared to the experimental value, which may be explained by experimental errors at the downstream segment of the channel. In particular downstream near the end of the channel, the number of samples taken and relative sampling intervals may not be enough to explain correctly the composition. As another reason, the small accuracy in results can be also explained by the influence of the downstream boundary conditions imposed at the downstream channel end.

Moreover, simulation of a real flushing phenomenon cannot be expected to have a long accuracy in sediment data. In fact, due to the complexity of sewers as well as presence of variable singularities along the sewer channel, sewer sediment transport cannot follow its normal process. Further, in these graphs, corresponding bed heights along the sewer channel are also added to the results. Over some sections mainly along the downstream segment (>500 m) bed height are small where the size distributions range up to gravel-type particles (This is the channel section where the sediment seemed to be as pavement form that was not took into account in the model). This could be a reason of the poor agreement between experimental and numerical results over the concerned sections.

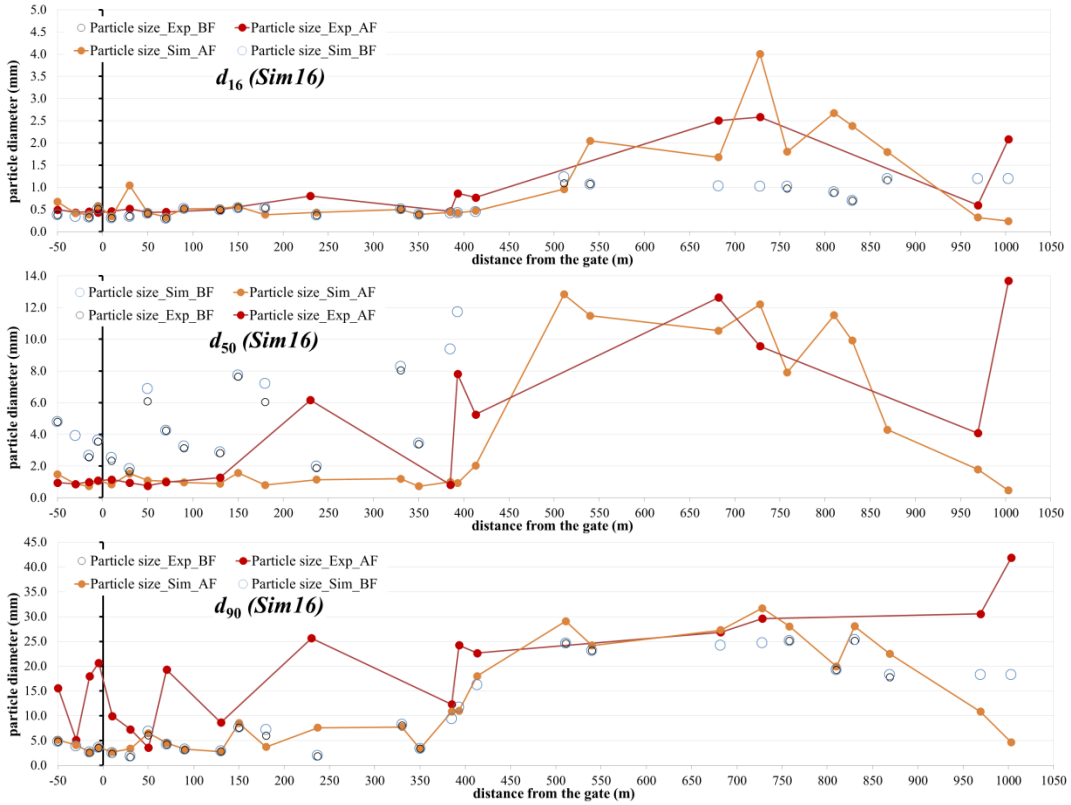

Fig. 6.17 Comparison of the measured and simulated the characteristic grain sizes (d_{16}, d_{50} and d_{90}) BF and AF along the studied sewer channel using the non-uniform sediment-transport approach obtained from the basic simulation set up (Sim16).

Described trend of evolution for sediment sizes is confirmed by three statistical parameters of the results as presented in Table 6.6. The table indicates that the average magnitude of the errors in terms of RMSE and MAE indicate a good fit in particular for d_{16}, d_{50} between experimental and modelled results mainly at the upstream segment of the channel.

Table 6.6 Statistical evaluation factors calculated for three sediment sizes (d_{16}, d_{50} and d_{90}) simulated by the non-uniform sediment-transport model compared to the experimental values for all the sampled sections (Sim16).

Characteristic size	RMSE	MAE
d_{16}	0.641	0.395
d_{50}	4.030	2.240
d_{90}	13.870	10.320

Such results are valuable when it is aimed to study the detailed impact of the flushing over sediments and analyse the sediment transport processes during the flushing flow.

6.4 Sensitivity analysis of the model parameters

Values of much of the parameters used for the described simulations are known from the experiments. However, values for some other parameters have been fixed based on the literature results. A sensitivity analysis of the model is then required for these parameters in order to evaluate potential range of validation of the results. Firstly, a number of simulations were carried out to evaluate the response of the model to different values of the efficiency coefficient $\eta_{\min}$ in Eq. 5.16 for suspended solid estimation. Secondly, the response of the model to modifications of different values of the bed pavement thickness was evaluated as this parameter affects the sediment transport in the channel. Moreover, the sensitivity of the model results was tested with reference to the introduction of a formula to model the sediment hiding processes. Each sensitivity analysis was carried out with reference to basic case simulated in section 6.3.

Model sensitivity to coefficient $\eta_{\min}$

Parameter $\eta_{\min}$ constitutes a critical erosion coefficient to consider the particles eroded during the flush that leave the bed-load zone and go into suspension. The basic simulation (called hereafter Sim16, discussed in Section 6.3) was carried out using $\eta_{\min}$ equal to 0.00125 being this the average value of the experimental campaign which was identified by Combes (1982) for the sewer systems. For the sensitivity analysis of the model to this parameter further simulations were carried out using the minimum (0.0005, simulation called hereafter Sim24) and the maximum (0.002, simulation called hereafter Sim24) values of the range suggested by the author. Both values are comprised inside the rage of this parameter recommended by other authors (*e.g.,* Combes 1982; Zug *et al.* 1998).

All the results (hydraulic and sediment-transport performance) of the two simulations are presented in Appendix D. As expected, $\eta_{\min}$ did not affect significantly the hydraulics of the flush and almost the same hydraulic results as Sim16 were obtained in all measuring sections along the entire sewer channel. The results obtained from Sim24 provide also bed heights AF through the sewer channel. Major modifications determined by the different values of this parameter include differences in the bed heights. In particular, modifications are considered as increasing of the heights in the upstream segment (with predominant finer sediment bed) and a decreasing of heights in the downstream segment (with coarser-type sediment bed). According to the graphs, remarkable changes can be seen over first 100 m downstream the gate comparing to Sim16. Based on the simulation, results show mean and maximum values of 3.1 and 24.6 cm, respectively for the modelled bed heights AF against 2.9 and 26.4 cm of experimental values. Comparison between simulations 16 and 24 is shown in Table 6.7 in terms of RMSE and MAE. Based on the table slightly higher value of error was obtained with

$\eta_{min} = 0.005$. Despite this, the differences between two model simulations in terms of bed heights AF were relatively small.

Table 6.7. Statistical indices to evaluate the agreement between simulated results and measured bed heights of the studied channel using the non-uniform sediment-transport model obtained from Sim24.

Coefficient	Root Mean Square Error (RMSE)	MAE
Sim16	0.028	0.018
Sim24	0.029	0.019

Values of the sediment volume flushed out of the channel was also compared (Table 6.8). Based on the table results, difference between the two models was small with reduction of about 5% in total sediment transported out of the channel. As expected much of the reduction can be imputed to the reduced suspended sediment transport. Interesting negligible differences were observed upstream of the gate (S_{-50} – S_0), thus revealing a very limit sensitivity of the model to η_{min}.

Table 6.8. Comparison of the quantitative results of the sensitivity analyses obtained from Sim24.

Flushed volume (in m^3)	Experimental	Sim16	Sim24	Evolution from Sim16 to Sim24
From S_{-50} to S_{1050}	5.61	5.06	4.81	-4.9%
From S_{-50} to S_0	0.21	0.6	0.60	-0.8%
From S_0 to S_{+1050}	5.4	4.46	4.22	-5.5%

Relatively, small differences of d_{50} in the bed composition AF as comped to Sim16 (Appendix A). Table 6.9 shows RMSE and MAE values as compared to experimental values for the two simulations.

Table 6.9 Statistical evaluation factors calculated for three sediment sizes (d_{16}, d_{50} and d_{90}) simulated by the non-uniform sediment-transport model (Sim24) compared to the experimental values for all the sampled sections.

Characteristic size	RMSE		MAE	
	Sim16	Sim24	Sim16	Sim24
d_{16}	0.641	0.624	0.395	0.389
d_{50}	4.030	3.577	2.240	2.156
d_{90}	13.870	14.427	10.320	10.667

Similarly, a synthesis of results of the simulation using $\eta_{min} = 0.002$ is shown in Table 6.10. Although relatively small, as expected, an increase of (15%) the volume transported as suspended bed was obtained as compared to

Sim16.

Table 6.10. Comparison of the quantitative results of the sensitivity analyses obtained from Sim32.

Flushed volume (m^3)	**Experimental**	**Sim16** $\eta_{min} = 0.00125$	**Sim24** $\eta_{min} = 0.0005$	**Sim32** $\eta_{min} = 0.002$	**Evolution Sim32 comparing to Sim16**
From S_{-50} to S_{1050}	5.61	5.06	4.81	5.09	+0.5%
From S_{-50} to S_0	0.21	0.60	0.60	0.60	-1.2%
From S_0 to S_{+1050}	5.4	4.46	4.22	4.49	+0.8%

Concerning the bed height, the results from Sim32 show the same values of the statistics as Sim24 and Sim16 (Table 6.11). In addition, for the test of completeness, Table 6.12 reports the detailed results concerning the bed composition AF and the comparison between Sim16, Sim24 and Sim32.

Table 6.11. Statistical indices to evaluate the agreement between simulated results and measured bed heights of the studied channel using the non-uniform sediment-transport model obtained from Sim32.

Coefficient	**Root Mean Square Error (RMSE)**	**MAE**
Sim16	0.028	0.018
Sim24	0.029	0.019
Sim32	0.029	0.019

Table 6.12 Statistical evaluation factors calculated for three sediment sizes (d_{16}, d_{50} and d_{90}) simulated by the non-uniform sediment-transport model using η_{min} equal to 0.00125, 0.005 and 0.002 (in Sim16, Sim24 and Sim32, respectively) compared to the experimental values for all the sampled sections.

Characteristic size	**RMSE**			**MAE**		
	Sim16	**Sim24**	**Sim32**	**Sim16**	**Sim24**	**Sim32**
d_{16}	0.641	0.624	0.564	0.395	0.389	0.336
d_{50}	4.030	3.577	4.027	2.240	2.156	2.132
d_{90}	13.87	14.427	14.117	10.32	10.667	10.393

Globally, variation of η_{min} in the whole range of values had a

relatively minor effect on the results, thus revealing a limited sensitivity of the model for non-uniform sediment transport to this parameter. These results could find same confirmation from the previous numerical sensitivity analysis carried out by Bertrand-Krajewski *et al.* (2006) who used a simple uniform sediment-transport model for a long-term sediment-transport monitoring.

Model sensitivity to the pavement thickness (Sim31)

The effect of choosing different values of the thickness of the pavement layer (δ_p) on the transport of sediments by the model was examined. To this end, the thickness of the pavement layer (from $3\times d_{90}$ in Sim16) was reduced to $1\times d_{90}$. Although this value is not recommended in the literature for the types of sediments present in the channel, the sensitivity of the results in terms of erosional pattern was explored. Indeed, reducing the thickness of the pavement layer means reducing the source of the available sediments for eroding and transport. Table 6.13 shows the comparison of the basic simulation (Sim16) with Sim31 and also the experimental data. The last column indicates the evolution of the results comparing to the results of the basic simulation. As expected, the lower value of δ_p determines a significant reduction of the volume of sediments flushed out from the channel (about minus 27%). Moreover, such reduction is more evident in the upstream part of the channel where the values of sediment bed heights are larger.

Table 6.13. Comparison of the quantitative results of the sensitivity analyses obtained from Sim31.

Flushed volume (m^3)	**Experimental**	**Sim16**	**Sim31**	**Evolution Sim31 comparing to Sim16**
From S_{-50} to S_{1050}	5.61	5.06	3.67	-27.6%
From S_{-50} to S_0	0.21	0.60	0.24	-59.8%
From S_0 to S_{+1050}	5.4	4.46	3.42	-23.2%

Further, results of Sim31 concerning the bed heights are statistically evaluated and summarized in Table 6.14 with the corresponding results of Sim16 to enable a comparison. Based on the simulated data from Sim31, maximum and mean value of 28.04 and 3.2 cm, respectively, were obtained. These values show a considerable increase comparing to the basic model.

Table 6.14. Statistical indices to evaluate the agreement between simulated results and measured bed heights using the non-uniform sediment-transport model obtained from Sim31.

Coefficient	Root Mean Square Error (RMSE)	MAE
Sim16	0.028	0.018
Sim31	0.028	0.018

In addition to the previous results, details of the fractional sediment transport presented in Table 6.15 for Sim31, show that the transport of fine sediments increased while the larger particles was not available to be transported as in Sim16. Such behaviour might be a reflect of the model with a poor ability to accurately predict the phenomenon mainly for the transport of coarser particles (*i.e.*, d_{90}). This can explain the decrease of the total volume of the bed flushed out by the flow.

Table 6.15 Statistical evaluation factors calculated for three sediment sizes (d_{16}, d_{50} and d_{90}) simulated by the non-uniform sediment-transport model (Sim31) compared to the experimental values for all the sampled sections.

Characteristic size	RMSE			
	Sim16	Sim31	Sim16	Sim31
d_{16}	0.64	1.47	0.50	0.23
d_{50}	4.03	2.90	0.32	0.60
d_{90}	13.87	13.22	0.19	0.25

From the above simulation, it can be concluded that significant modification of parameter has an important impact on the results of the model for non-uniform sediment transport. The selection of proper values of this parameter according to the results from the literature and to the sediment size in the channels is of parameter importance. This would confirm the need of experimental data concerning sediment characteristics for the correct model setup.

Model sensitivity to the effect of the hiding (Sim29)

The aim of this simulation was to consider the effect of hiding/exposure amongst the bed particles. This effect is a natural phenomenon existing in non-uniform bed materials. Integrating this effect into the model could modify the behaviour of the sediment transport during the entrainment of the particles. In fact, this empirical coefficient is a correcting function to adjust the threshold prediction of the different grain sizes (Sutherland 1922, adapted from Ashley *et al.* 2004; Wu 2008). Numerically, hiding effect handles the influence of the size classes on each other during while sediment transport or entrainments. Application of this

effect into the basic has shown relatively significant modifications in particular in terms of eroded sediment volume (Table 6.16). A total volume of 3.44 m^3 was estimated as the volume of the sediments flushed out from the sewer channel downstream of the gate against 5.4 obtained experimentally (almost 63.7 m^3 was reproduced). Application of the hiding factor had different effect on the flushed volumes of bed load and suspended load downstream of the gate by increasing (20.5%) and decreasing (12.8%), respectively comparing to Sim16. Therefore, the major transport of sediment by the flush occurs as bed load though the entire sewer channel.

Table 6.16. Comparison of the quantitative results of the sensitivity analyses obtained from Sim29.

Flushed volumes (m^3)	**Experimental**	**Sim16**	**Sim29**	**Evolution Sim29 comparing to Sim16**
From S_{-50} to S_{1050}	5.61	5.06	5.22	+3.0%
From S_{-50} to S_0	0.21	0.60	1.10	+82.6%
From S_0 to S_{+1050}	5.4	4.46	4.11	-7.8%

The graphics representing the simulated bed heights by Sim29 are illustrated in Appendix D, showing that the correction factor of hiding phenomenon had a considerable effect on the transport of the particles and thus the bed heights through the entire sewer channel. By comparing the graphs between results of Sim16 and Sim29 Table 6.17, it can be observed that the peaks of have subjected to changes in over almost a long length of the sewer channel. Some sections were found to have a smoother or sharper peak of the bed heights; in other sections the accumulated sediment was eroded faster. The observations can be supported by Garcia (2008) indicating that the use of hiding correcting factor can increase or decrease the transported volume of a particular class of size in a bed mixture.

Table 6.17. Statistical indices to evaluate the agreement between simulated results and measured bed heights using the non-uniform sediment-transport model obtained from Sim29.

Coefficient	**Root Mean Square Error (RMSE)**	**MAE**
Sim16	0.028	0.018
Sim29	0.041	0.024

The fractional sizes within the bed composition AF obtained from Sim29 are illustrated in graphs in Appendix D. Further, statistical errors are presented in Table 6.18. According to the table, finer fraction has subjected to small degradation (higher value of error indexes) of the particles whereas two other sizes (d_{50} and d_{90}) have shown a better agreement with the experimental data.

Table 6.18 Statistical evaluation factors calculated for three sediment sizes (d_{16}, d_{50} and d_{90}) simulated by the non-uniform sediment-transport model (Sim31) compared to the experimental values for all the sampled sections.

Characteristic size	RMSE		MAE	
	Sim16	Sim29	Sim16	Sim29
d_{16}	0.641	0.653	0.395	0.403
d_{50}	4.030	3.116	2.240	2.110
d_{90}	13.870	12.025	10.320	10.107

Globally, it can be concluded that implementing hiding effect among non-uniform sediment particles did not improve the total and fractional modelled sediment-transport volumes. Indeed, hiding behaviour of the coarse sediment to make expose fine particle to the flow can be negligible for the current studied case.

It is worth to highlight that the higher thickness of the pavement layer (and therefore the availability of sediment size classes) plays a role in determining more evident hiding effect by supplying the materials for the remobilisation process. Therefore, these two mechanisms can be complementary elements to study in the future to improve the results.

Chapter 7
Conclusions and future perspectives

7.1 Summary and general conclusions

Cleaning sewer channel is a primordial task to avoid negative consequences of deposited sediments in sewers. Among cleaning techniques to tackle sedimentation problems, practice of flushing (manual or automatic) method has been developed since many years in Parisian combined sewer system. The municipalities around the world are more and more trying to reduce the manual application of flushing in large-size sewers mainly because of the significant costs of management. Manual cleaning of sewers is difficult, time-consuming and very harmful for the health of sewer operators who are involved in cleaning procedures every year or month. Thus, a main reason of this study is to contribute to the reduction of their intervention inside sewers during cleaning performance. In this regard, automatic cleaning devices have become an ideal, economic and efficient option to overcome solid accumulation in sewers in large-size sewer channels. This is the reason why from many decades, the possibility to generate big and efficient flushes in such sewers has incited sewer managers/device designers/researchers to explore flushing performance at both laboratory or field scales. On the one hand, laboratory experiments allowed evaluating various parameters such as volume and cleaned distance along the downstream flushing line under indoor controlled experimental conditions. On the other hand, the simplified conditions of the laboratory experiments are sometimes limited in terms of transferability to the field. To this end, it is worth to study flushing operation in real sewers to reduce the existing gap of knowledge in understanding the dynamics of sediments associated to the flushes. Indeed, flushes cause altering the deposited bed in terms of bed physical properties as well as bed composition. Such impacts still require experimental efforts. The complex behaviour of highly-variable sewer solids needs to be better described.

In the context of the current work, as a summary, three main objectives was achieved:

A field measurement campaign was undertaken allowed to obtain a series of data with a relatively high degree of accuracy. The data analysis has led to obtain an analytic understanding of the processes associated to the flushing operation in sewers.

A model was adopted to the studied case that was able to simulate the observed flushing flow. Moreover, a novel approach was developed based on the same numerical code for modelling non-uniform sediment transports during the flushing. Both model were able to describe the flushing impacts on the sediments with different level of accuracy in prediction. The second model has provided further detailed description and information on the evolution of the sediments.

Both model were compared by analysing the advantages and

disadvantages as a tool for management of the sediments in sewers.

Firstly, using a downstream gate, a flush experiment was performed in a large size sewer (man-entry trunk) of the Parisian combined sewer network was carried out. The full-scale flush was experimentally and numerically investigated in order to describe the potential sediment removal efficiency of the used gate. The experimental study allowed evaluating several parameters within three time-periods: before the flush, during the flush and after the flush. During the flushing operation many parameters were monitored at specific monitoring sections through the entire sewer channel to record variables related to hydraulic as well as turbidity. Such observation allowed characterizing the flush event in terms of wave propagations and distributed shear stresses in time and in space. Besides, both before and after the flush, identical sediment measuring, sampling and analysing procedures were realized along the entire sewer channel. Data were acquired using novel techniques and high-quality measuring apparatus that were relatively adapted to the flushing in sewer conditions. Because the main focus of this research was on the sediment dynamics, various examinations of deposits were carried out. For example, implemented cameras inside sewer were used to visualize directly movements of the bed sediments. Moreover, a sonar/radar technique was applied, which allowed sampling the bed deposits (3D topographic estimation) before and after the flush with reasonable intervals along the whole sewer channel. Globally, various aspects of deposited bed before and after the flush were provided that permitted various qualitative and quantitative analyses of sediments. Results from the field experiment showed that such gate was able to provide a significant erosional effect which remobilized sediments through the whole channel.

Results from the **experimental** investigation include:

- complexity of the sewer conditions made difficult measuring parameters and observing processes related to the sediment transport. Measuring instruments were installed for few hours, thus they were protected against corrosion.
- due to various sources of inaccuracy, full-scale measurement of flow and sediment parameters present uncertainties. However, field data for modelling sediment-transport processes were considered as important parameter compared to laboratory data.
- importance of non-uniformity of sewer sediments as mixtures to estimate the sediment-transport capacity of the flush was highlighted. Even more, the non-uniformity of the mixtures is unique to each location and is varying in time and in space along the sewer channels.

Thus, realistic description of sediment transport requires considering the heterogeneity of sewer sediments dynamics.

- the importance of flush characteristics (*i.e.,* flushing volume and water level) regarding to the erosional impacts on the bed sediment was confirmed to be factors of 'sustainable' wave propagation.

Another objective of the thesis was to investigate the hydrodynamics and associated sediment transport of the in-sewer mobile bed sediments during the flush. Two models developed by the urban drainage research group of the University of Catania were used for this scope: *(i)* a simple model for uniform sediment transport being as the most common used approach; and *(ii)* a more complex model for non-uniform sediment transport of mixtures. Flow and sediment boundary as well as internal conditions were imposed to the models. In particular, the latter model was developed and used for the first time for application to the flush experiment in Paris. Overall, both models have described hydraulics of the flushing with a good level of performance as was observed during the experiment. However, a very slight amelioration was provided using the non-uniform model principally at the initial stage of the flushing (flow peak) where the flow is highly unsteady.

Main results of the simulations are:

From uniform sediment-transport model:

- fairly good hydraulic description of the variables comparing to the experimental data;
- poor results of the bed heights for almost the entire sewer channel;
- poor results of the volume of the flushed-out sediment because the sediment-transport discharge can be easily underestimated or overestimated;
- overestimation of the average shear stress;
- apart from the bed heights, no more information about different aspects of the bed sediment can be provided.

From non-uniform sediment-transport model:

- excellent hydraulic description of the variables comparing to the experimental data;
- very good description of the bed evolution because of the correct estimation of the shear stresses;

- very good evaluation of the of the transported sediment volumes;
- ability of the model to provide different aspects of the bed sediments e.g. erosional/depositional behaviour;
- And additional useful information about the evolution of the bed composition by class sizes.

Additionally, time consumption of the non-uniform model could be less suitable for practical applications depending on the study objectives. Uniform models can be sufficient enough when only a rough estimation of the shear stresses or furthermore the study of bed heights evolution due to the flush are required. Conversely, the need of detailed information about the fractional sediment dynamics and the composition of the bed requires the use of the model for non-uniform sediment transport. Thus, the choice of model to simulate sediment transport relates to many elements *e.g.,* economic (time/expertise/cost of the software development), time, required level of accuracy.

Besides, a sensitivity analysis was conducted for the non-uniform sediment transport model. To this end, the input parameters of which the values are based on the literature were subjected to this analysis: 1) threshold of erosion (η_{min}) in the Veliknaov module; 2) the pavement thickness of the bed layer (δp). In addition, the *hiding* effect of the sediments was activated to observe the impacts on results. This analysis has showed that:

- Changing the value of the erosional threshold of the Velikanov does not modify the results in a significant way.
- Reducing the pavement's thickness of the bed layer has considerable effect as this layer is responsible for sediment availability to be eroded by the flush.
- Hiding effect does not have considerable effect on the results.

7.2 Future works and perspective

Different areas for future research can be stated regarding to the limitations and eventual possibilities to develop the actual work that were outside of this PhD dissertation time.

Numerical analysis could be carried out to identify flush design patterns as well as flushing operation scheduling for optimal sewer cleaning and sediment management (*e.g*., number of flushes per year,

type of flush device, and hydraulic parameters of the flush for effective cleaning of sewers. Since the used models were observed to successfully describe the conditions and the impacts of the flush experiment in Paris. Such data can help sewer managers to schedule efficient flushes as basic and preventive mean that can allow overcoming the sedimentation in channels.

Further investigations to process the obtained videos images from the cunette cameras are required to contribute to estimate the bed-load discharge transported over the bed during the flush.

Apart from being heterogeneous in terms of sizes, sewer sediments are also wide in range in terms of densities. Measuring density of each sample together with the grain-size distribution within the non-uniform sediment-transport model could improve the results. Such information can provide appropriate description of the sediment transport in time and space.

Moreover, the possibility to incorporate the effect of organic matter (obtained from the field samples) by inducing cohesion for critical shear stress evaluation in both models could be another interesting aspect to develop.

As a suggestion for future flush experiments in sewers, is important to undertake more precision to limit the number missing data. This would require a prelaminar study of the sewer and sediment conditions. In addition, as such experiences cost too much to the municipalities, many standard precisions should be headed *e.g.,* installation of turbidimeters and further experimental investigation related to this parameter. Also, external factors such as climate conditions (*i.e.,* rainfall) need to be taken into account in order to observe only the influence of the flushing on the deposited bed.

And finally, the comparison between results from the 1D non-uniform sediment transport model with a 3D model could be valuable to conduct.

References

Ab Ghani, A., Salem, A. M., Abdullah, R., Yahaya, A. S. and Zakaria, N. A. (1999). Incipient Motion of Sediment Particles Loose Deposited Beds in a Rigid Rectangular Channel, in In Proc. the Eighth International Conference on Urban Storm Drainage.

Ab Ghani, A., Azamathulla H Md. (2010). Gene-expression programming for sediment transport in sewer pipe systems. Journal of Pipeline Systems Engineering and Practice (August): 102-106. doi:10.1061/(ASCE)PS.1949-1204.0000076.

Ab Ghani, A., Bong, C. H. J. and Lau, T. L. (2013). Sediment Flushing using Tipping Flush Gate in an Open Storm Concrete Drain–A Case Study in Nibong Tebal, Penang, Malaysia, in IAHR World Congress, p. 7.

Ab. Ghani, A., Sadegh Safari, M. J. and Mohammandi, M. (2018). Experimental studies of self-cleansing drainage system design: a review, Journal of Pipeline Systems Engineering and Practice, (March).

Abbott M (1966). An introduction to the method of characteristics. Elsevier, New York.

Ackers, J. C, Butler, D. and MAY, R. W. P. (1996), Design of Sewers to control Sediment Problems. CIRIA project report 141. ISBN 086017 443 3. 181 pp. ACKERS,

Ahrens, J.P. (2000). A fall-velocity equation. J. Waterw. Port Coast. Ocean Eng. 126(2), 99–102.

Ahyerre, M. and Chebbo, G., (2002). Identification of in-sewer sources of organic solids contributing to combined sewer overflows. Environmental technology 23 (9): 1063-73.

Ahyerre, M. (1999) Bilan and mécanismes de migration de la pollution organique en réseau d'assainissement unitaire. PhD thesis, University Paris 6.

Ahyerre M., Chebbo G. and Saad M. (2000) Sources and erosion of organic solids in a combined sewer. Urban Water N°2, 305–315.

Ahyerre, M., Chebbo, G., and Saad, M., 2001. Nature and dynamics of water sediment interface in combined sewers. Journal ofenvironmental engineering, 127 (3), 233–239.

Aiguier, E., Chebbo G., Bertrand-Krajewski J.L., Hedges P., and Tyack N., 1996. Methods for determining the settling velocity profiles of solids in storm sewage. In Water Science and Technology, 33:117-125.

Ashley R.M., Coghlan B.P., Jefferies E. (1989). The quality of sewage flows and sediment in Dundee. Wat. Sci. Tech. 24 (6), 39-46.

Ashley, R., Bertrand-Krajewski, J. L., Hvitved-Jacobsen, T. (2005). Sewer solids - 20 years of investigation. Water Science and Technology 52 (3): 73 84.

Ashley, R. M., Wotherspoon, D. J. J., Goodison, M. J., McGregor, I. and Coghlan, B. P. (1992). The deposition and erosion of sediments in sewers, Water Science and Technology, 26(5‐6), p. 1283‐1293.

Ashley, R.M., Wotherspoon, D.J.J., Coghlan, B.P. and McGregor, I. (1992). The Erosion and Movement of Sediments and Associated Pollutants in Combined Sewers. Water Science and Technology 25 (8): 101-114.

Ashley, R.M., Arthur, S., Coghlan, B.P., McGregor, I. (1994). Fluid sediment in combined sewers. Water Science and Technology 29 (1-2): 113-123.

Ashley, R.M., Verbanck, M.A. (1996). Mechanics of sewer sediment erosion and transport. Journal of Hydraulic Research 34: 753-770.

Ashley, R., Nalluri, C., Tait, S., Arthur, S. (1999). Sediment Transport in Sewers - a Step Towards the Design of Sewers To Control Sediment Problems. Proceedings of the ICE - Water Maritime and Energy 136: 9-19.

Ashley, R. M., Hvitvedjacobsen, T., Bertrand-Krajewski, J. L. (1999). Sewer Process Modelling, Water Science and Technology. Elsevier, 39(9), p. 9-22.

Ashley, R., Nalluri, C., Tait, S. and Arthur, S. (1999). Sediment Transport in Sewers - a Step Towards the Design of Sewers To Control Sediment Problems. Proceedings of the ICE - Water Maritime and Energy, 136, p. 9-19.

Ashley, R.M., A. Fraser, R. Burrows and J. Blanksby. (2000). The management of sediment in combined sewers. Urban Water.

Ashley, R.M., Bertrand-Krajewski, J.L., Hvitved-Jacobsen, T., Verbanck, M. (2004). Solids in Sewers - Characteristics, Effects and Control of Sewer Solids and Associated Pollutants. Scientific and technical report. IWA, London, 360p.

Ashley, R., J. L. Bertrand-Krajewski and T. Hvitved-Jacobsen. (2005). Sewer solids - 20 years of investigation. Water Science and Technology 52 (3): 73-84.

Artières O. (1987). Les dépôts en réseau d'assainissement unitaire. Thèse de doctorat, Université Louis Pasteur de Strasbourg, ENITRTS, 214 p.

Arthur, S., Ashley, R.M. (1998). The influence of near bed solids transport on first foul flush in combined sewers. Water Science and Technology 37 (1). International Association on Water Quality: 131-138. Doi:10.1016/S0273-1223(97)00762-2.

Arthur, S., Ashley, R.M., Tait, S.J., Nalluri, C. (1999). Sediment transport in sewers - a step towards the design of sewers to control sediment problems. Proceedings of the ICE, 9-19.

Alzabadi, H. (2010). Evaluation de l'Exposition des Egoutiers aux G?enotoxiques. Ph.D Thesis. Université de Nancy, 286 p.

American Public Works association (1969). Water pollution aspects of urban runoff. Water pollution control research series. Federal Water Quality administration report WP-20-15, January.

Asano, T., Burton, F. L., Leverenz, H. L., Tsuchihashi, R. and Tchobanoglous, G. (2007) Water Reuse Issues, Technologies, and Applications.

Aflak, A., Gendreau, N. and Pascal, O. (2007). Gestion préventive de l'ensablement des collecteurs visitables d'assainissement and optimisation des interventions de curage, Novatech, p. 1325-1332.

Andrews, E. D., (1983). Entrainment of gravel from naturally sorted riverbed material, Geol. Soc. Am. Bull., 94, 1225–1231.

Andrews, E. D. and G. Parker, (1987). Formation of a coarse surface layer as the response to gravel mobility. Sediment Transport in Gravel-bed Rivers, C. R. Thorne, J. C. Bathurst, and R. D. Hey, Eds., John Wiley and Sons, 269-325.

APUR (Atelier Parisien d'Urbanisme), 2016. Les réseaux commerciaux poursuivre leur développement à Paris. Note N° 108. 8P.

Armanini, A. and Di Silvio G. (1988). A one-dimensional model for the transport of a sediment mixture in non-equilibrium conditions. Journal of Hydraulic Research 26 (3): 275-292.

Armanini, A., Di Silvio, G. (1991). Fluvial Hydraulics of Mountain Regions. In , sous la dir. de S M Bhallamudi, G.M. Friedman, H.J Neugebauer, and A. Seilacher, 465. s.l.: LNEARTH.

Armanini, A., (1992). Variation of Bed and Sediment Load Mean Diameters due to Erosion and Deposition Processes. Dynamic of Gravel-bed Rivers. Wiley, New York, pp. 351–359.

Armanini, A. (1995). Non-uniform sediment transport: Dynamics of the active layer. Journal of Hydraulic Research, 33(5), 611–622.

Armanini, A. (2018). Principles of River Hydraulics: 217.

Balayn, P. (1996). Modélisation du transfert de sédiments lors d'un lâcher d'eau en réseau d'assainissement – approche numérique, Université Louis Pasteur, Strasbourg.

Balayn, P., Paquier, A. and Lapuszek, M. (2003). 1-D sediment transport model : presentation of mixtures and calibration, in XXX IAHR Congress, p. 557-564.

Barco, Janet, Sergio Papiri and Michael K. Stenstrom. 2008. First flush in a combined sewer system. Chemosphere 71 (5) : 827-833.

Barré de Saint-Venant, A.J.C. (1871a). Théorie du Mouvement Non Permanent des Eaux, avec Application aux Crues de Rivières and à l'Introduction des Marées dans leur Lit. (Comptes Rendus des séances de l'Académie des Sciences: Paris, France) Séance 17 July 1871, 73, 147–154 (in French).

Barré de Saint-Venant, A.J.C. (1871b) Théorie du Mouvement Non Permanent des Eaux, avec Application aux Crues de Rivières and à l'Introduction des Marées dans leur Lit. (Comptes Rendus des séances de l'Académie des Sciences: Paris, France) 73(4), 237–240 (in French).

Bertrand-Krajewski, J. L., Briat, P. and Scrivener, O. (1993). Sewer sediment production and transport modelling: A literature review, Research, Journal of Hydraulic, 31(1993), p. 26.

Bertrand-Krajewski, J. L. (2002). Sewer Sediment Management: Some Historical Aspects of Egg-Shape Sewers and Flushing Tanks. Proc of the 3rd International Conference on Sewer Processes and Networks, Paris, France. 15-17 April 2002.

Bertrand-Krajewski, J. L., Bardin, J. P., Gibello, C. and Laplace, D. (2003). Hydraulics of a sewer flushing gate, Water Science and Technology, 47(4), p. 129-136.

Bertrand-Krajewski, J L, J P Bardin, M Mourad and Y Béranger. (2003). Accounting for sensor calibration, data validation, measurement and sampling uncertainties in monitoring urban drainage systems. Water Science and Technology 47 (2): 95-102.

Bertrand-Krajewski, J L. (2004). TSS concentration in sewers estimated from turbidity measurements by means of linear regression accounting for uncertainties in both variables. Water science and technology 50 (11): 81-8.

Bertrand-Krajewski, J.L., A. Campisano, E. Creaco and C. Modica. (2004). Experimental study and modelling of the hydraulic behaviour of a Hydrass flushing gate. Novatech: 557-564.

Bertrand-Krajewski, J. L., Almeida, M., Matos, J. and Abdul-Talib, S. (2005). Sewer Networks and Processes within Urban Water Systems, Water Intelligence Online, 4.

Bertrand-Krajewski, J.L., A. Campisano, E. Creaco and C. Modica. (2005). Experimental analysis of the hydrass flushing gate and field validation of flush propagation modelling. Water science and technology 51 (2): 129-37.

Bertrand-Krajewski, J. L., Bardin, J. P., Gibello, C. (2006). Long term monitoring of sewer sediment accumulation and flushing experiments in a man-entry sewer. Water Science and Technology 54 (6-7): 109-117.

Bertrand-Krajewski, J. L. (2006). Modelling of Sewer Solids Production and Transport. Transport. Laboratoire Hydrologie Urbaine_INSA Lyon.

Bertrand-Krajewski, J. L., Bardin, J.P., Gibello, C. (2006). Mesure and modélisation de l'accumulation des sédiments dans un collecteur d'assainissement unitaire Mesure and modélisation de l'accumulation des sédiments dans un collecteur d'assainissement unitaire. Revue Européenne de Génie Civil.

Bertrand-Krajewski, J. L. (2008) Flushing urban sewers until the beginning of the 20th century, sbe.hw.ac.uk, p. 1-10.

Bertrand-Krajewski, J. L., and C. Gibello. (2008). A new technique to measure cross-section and longitudinal sediment profiles in sewers. 11th international Conference on Urban Drainage: 1-9.

Bertrand-Krajewski, J. L., Bardin J. P., Gibello, C. (2011). Mesure and modélisation de l'accumulation des sédiments dans un collecteur d'assainissement unitaire. Revue Européenne de Génie Civil. 10(3). p 339-359.

Billi, P, R D Hey, C R Thorne and P Tacconi. 1992. Dynamics of gravel-bed rivers: 688p.

Bhallamudi S.M. and Chaudhry M.H. (1991). Numerical modeling of aggradation and degradation in alluvial channels. Journal of Hydraulic Engineering, ASCE, Vol. 117, No. 9, pp. 1145-1164, 1991.

Bonakdari, H., Larrarte, F. (2006). Experimental and numerical investigation on self-cleansing and shear stress in sewers, Proceedings, 2nd International Conference on Sewer Operation and Maintenance (SOM 06), October 26–28 2006, Vienna, Austria.

Bonnefille, R. 1963. Essais de synthèse des lois de début d'entraînement des sédiments sous l'action dun courant en régime continu. Bulletin Centre de Recherhce Chatou 5, 67–72.

Bong, C. H. J., Lau, T. L. and Ab Ghani, A. (2013). Hydraulics characteristics of tipping sediment flushing gate, Water Science and Technology, 68(11), p. 2397-2406.

Bong, C. H. J., Lau, T. L. and Ab. Ghani, A. (2016). Potential of tipping flush gate for sedimentation management in open stormwater sewer, Urban Water Journal, 13(5), p. 486-498.

Bong, C. H. J., Lau, T. Z. E. L. and Ab. Ghani, A. (2017). Duration of Hydraulic Flushing and Its Effect on Sediment Bed Movement, in Proceedings of the 37th IAHR World Congress. Kuala Lumpur, Malaysia, 13-18 august.

Bujon, G. (1988). Prevision des debits and des flux polluants transites par les reseaux d'egouts par temps de pluie, Le modele FLUPOL. La HouilleBlanche. I, 11·23.

Brownlie, W. (1981), Compilation of alluvial channel data: laboratory and field. Tech. Rep. KH-R-43B, California Institute of Technology, Pasadena, California, USA.

Butler, D., May, R. and Ackers, J. (2003) Self-Cleansing Sewer Design Based on Sediment Transport Principles, Journal of Hydraulic Engineering, 129(4), p. 276-282.

Berlamont, J., Ockenden, M., Toorman, E., Winterwerp, J. (1993). The characterisation of cohesive sediment properties. Coastal Engineering 21 (1-3): 105-128. doi:10.1016/0378-3839(93)90047-C.

Berndtsson, J. C. (2013). Storm water quality of first flush urban runoff in relation to different traffic characteristics. *Urban Water Journal* (January 2015): 1-13.

Perrusquía, G., Lyngfelt, S. and Sjöberg, A. (1987) Flow capacity of sewers with a sediment bed. 4th International Conference on Urban Storm Drainage, Lausanne, Switzerland, 331–336. Ed Yen B C. pub.Secretariat of the XXII Congress IAHR Laboratoire d'hydraulique Ecole Polytechnique Federale Lausanne, Switzerland.

Beyer, G. (1989). Contribution à l'étude de l'érosion des dépôts en réseau d'assainissement unitaire. PhD Thesis, University Louis Pasteur, Strasbourg, November, 136 pp.

Brombach, H., Michelbach, S., Wöhrle, C. (1992). Sedimentations- und Remobilisierungsvorgange im Abwasserkanal, Schlubericht des Teilprojektes 3 im BMFT-Verbundprojekt NIEDERSCHLAG, Eigenverlag Umwelt- und Fluid-Technik GmbH, Bad Mergentheim.

Butler, D. and Davies, J. W. (2011) *Urban Drainage*. 3rd Editio. Spon Press. Campisano, A., Creaco, E., and Modica, C. (2005a). Discussion of 'Gate and vacuum flushing of sewer sediment: Laboratory testing'. J. Hydraul. Eng., 131(12), 1145–1146.

Campisano, A., Creaco, E., Modica, C. (2004). Experimental and numerical analysis of the scouring effects of flushing waves on sediment deposits, Journal of Hydrology, 299(3), p. 324‐334.

Campisano, A., Creaco, E., Modica, C. (2005). A dimensionless approach for determining the scouring performances of flushing waves in sewer channels. In 10th International Conference on Urban Drainage. Denmark 21-26 August.

Campisano, A., Creaco, E., and Modica, C. (2005b). Experimental analysis of the Hydrass flushing gate and laboratory validation of flush propagation modelling. Proc., 10th Int. Conf. on Urban Drain age, Institute of Environment and Resources, Technical Univ. of Denmark, Copenhagen, Denmark.

Campisano, A., Creaco, E., Modica, C. (2006). Experimental analysis of the hydrass flushing gate and laboratory validation of flush propagation modelling, Water Science and Technology, 54(6-7), p. 101-108.

Campisano A., Creaco E., Modica C., and Reitano S. (2006a). Simulazione numerica dei processi di aggradation mediante modelli monogranulari e plurigranulari. Convegno di Idraulica e Costruzioni Idrauliche - IDRA2006.

Campisano, A., E. Creaco, C. Modica and S. Reitano. (2006b). Flushing experiments with cohesive sediments. In International Conference on Sewer Operation and Maintenance, 27 34. Viena, Austria, pp27-34.

Campisano, A., Creaco, E., Modica, C. (2007). Dimensionless Approach for the Design of Flushing Gates in Sewer Channels. Journal of Hydraulic Engineering 133 (8): 964‐972.

Campisano, A., Creaco, E., Modica, C., Reitano, S. (2007b). Sensitivity analysis of the formulas for predicting hiding processes in simulating bed aggradation. Communications to SIMAI Congress ISSN: 1827-9015, vol.2.

Campisano, A., Creaco, E., Modica, C. (2008). Laboratory investigation on the effects of flushes on cohesive sediment beds. Urban Water Journal 5 (1): 3‐14.

Campisano, A. and C. Modica. 2003. Flow velocities and shear stresses during flushing operations in sewer collectors. Water science and technology 47 (4): 123‐8.

Campisano, A., E. Creaco and C. Modica. (2013). Numerical modelling of sediment bed aggradation in open rectangular drainage channels. Urban Water Journal 10 (6): 365-376.

CIRIA (1986) Sediment movement in combined sewerage and storm-water drainage systems. Phase 1. Project report. CIRIA research project, No. 366.

Coghlan, Brian P., Ashley, R. M., Smith, G. (1996). Empirical equations for solids transport in combined sewers. Water Science and Technology 33 (9): 77-84.

Chanson, H. (2004). Hydraulics of Open Channel Flow: An Introduction, 2nd Edition, Butterworth-Heinemann, ISBN 0-750-65978-5.

Chebbo, G., Musquere. P., Milisic, V. and Bachoc, A. (1990). Characterization of Solids Transferred into Sewer Trunks During Wet Weather. Waf. Sci. Tech., 22(10/11),231-238.

Chebbo, G. (1992). Solides des rejets urbains par temps de pluie - Caractérisation and traitabilité. Thèse de doctorat de l'ENPC, Paris, 1992, 410 p.

Chebbo, G., Bachoc, A., Laplace, D. and Le Guennec, B. (1995). The transfer of solids in combined sewer networks. Water Science and Technology 31 (7): 95-105.

Chebbo, G., D. Laplace, A. Bachoc, Y. Sanchez and B. Le Guennec. (1996). Technical solutions envisaged in managing solids in combined sewer networks. Water Science and Technology 33 (9): 237-244.

Chebbo, G., Ashley, R.M. and Gromaire, M.C. (2002). The nature and pollutant role of solids at the watersediment interface in combined sewer networks. Water Sci. Tech., 47(4), 1–10.

Perrusquía, G. and Nalluri, C. (1995). Modelling of bedload transport in pipe channels. Proc. Int. Conf. on the Transport and Sedimentation of Solid Particles, Prague.

Chanson, H. (1999). The Hydraulics of Open Channel Flow - Basic principles, sediment motion, hydraulic modelling, design of hydraulic structures. Elsevier Butterworth-Heinemann, 2nd Edition. 634p.

Chanson, H. 2006. Analytical solutions of laminar and turbulent dam break wave. River Flow (1955): 465‑474.

Combes. V. (1982). Etude de modèles mathématiques de transporte mauriau solides en réseau d'assainissement, DBA de mecan ique INP de Toulouse, France.

Celestini, R, G Silvagni, M Spizzirri and F Volpi. 2007. Sediment transport in sewers. In WIT Transactions on Ecology and the Environment, 103:273-282.

Clegg, S. Forster, C. F. and Crabtree, R. W. (1992), Sewer sediment characteristics and their variation with time. Environmental Technology, Vol. 13, pp 561-569.

Clegg, S., Forster, C.F. and Crabtree, R.W. (1992) Sewer sediment characteristics and their variation with time. Environmental Technology, 13, 561–569.

Clegg, S., C. F. Forster and R. W. Crabtree. 1992. Sewer sediment characteristics and their variation with time. Environmental Technology 13 (6): 561-569.

Crabtree, R. W. and Forster, C. F., 1989. Preparation Protocols for the Analysis of Combined Sewer Sediment Samples. WRc ER354E, Water Research Centre, Swindon.

Crabtree, R.W. (1989) Sediment in sewers. Journal of the Institution of Water and Environmental Management, 3(6), 569–578.

Crabtree, R. W., 1988. A Classification of Combined Sewer Sediment Types and Characteristics. WRc ER 324E, Water Research Centre, Swindon, 54p.

Creaco, E. and Bertrand-Krajewski, J. L. (2007) Modelling the flushing of sediments in a combined sewer, p. 1293-1300.

Creaco E. (2005). Devices for the removal of solids from sewer channels: Experimental investigations and numerical models. PhD Thesis, Department of Civil and Environmental Engineering, University of Catania, Catania, Italy. December 2005.

Creaco. E., Bertrand-Krajewski, J. K. (2009) Numerical simulation of flushing effect on sewer sediments and comparison of four sediment transport formulas. Journal of Hydraulic Research 47:2, pages 195-202.

Davis, R. A. et Dalrymple, R. W. (2010) « Principles of tidal sedimentology », Principles of Tidal Sedimentology, p. 1-621.

Dessoy S., (1987). Contribution à l'étude du comportement des matières en suspension dans un tronçon de collecteur d'eaux usées. Travail de fin d'études d'ingénieur Civil chimiste, Université Libre de Bruxelles, Faculté des Sciences Appliquées, Service de Traitement des Eaux and Pollution, 109 p.

De Feo, G., G. Antoniou, H. Fardin, F. El-Gohary, X. Zheng, Ieva Reklaityte, D. Butler, S. Yannopoulos and Andreas Angelakis. 2014. The Historical Development of Sewers Worldwide. Sustainability 6 (6): 3936-3974.

De Sutter, R. 2000. Erosie and transport van cohesieve sedimentmen- gels in niet-permanent regime Erosion and transport of cohesive sedi- ment mixtures in unsteady flow. PhD thesis, Univ. of Ghent, Ghent, Belgium.

Du Sutter and al. 2003 : it can be considered that the inorganic particles are transported in bed load mode.

De Sutter, R., Rushforth, P. J., Tait, S. J., Huygens, M., Verhoeven, R. and Saul, A. J. (2001). The erosion of cohesive mixed deposits: implications for sewer fow quality modelling, Urban Water Journal, 2(2000), p. 285-294.

De Sutter, R., P. Rushforth, S.J. Tait, M. Huygens, R. Verhoeven and S. Adrian. 2003. Validation of Existing Bed Load Transport Formulas Using In-Sewer Sediment. Journal of Hydraulic Engineering 129 (4): 325-333.

Dettmar, J. 2005 «Beitrag zur Verbesserung der Reinigung von Abwasserkanälen», (Contribution to the improvement of the cleaning of wastewater sewers), PhD dissertation. In German, 237p.

Dettmar, J., Rietsch, B. and Lorenz, U. (2002) Performance and Operation of Flushing Devices - Results of a Field and Laboratory Study, Proceeding, p. 1-10.

Dettmar, J. (2007) A new planning procedure for sewer flushing, Novatech, p. 1301-1308.

Dettmar, J. and Staufer, P. (2005a) Modelling of flushing waves for optimising cleaning operations, in Water Science and Technology. Dresden, p. 233‑240.

Dettmar, J. and Staufer, P. (2005b) Behavior of the activated storage-volume of flushing waves on cleaning performance, in 10th International Conference on Urban Drainage. Copenhagen/Denmark, p. 8.

Di Silvio, G., 1992. in: Billi and al. (Ed.), Modelling sediment transport under different hydrological and morphological circumstances. Dynamic of Gravel-bed Rivers. Wiley, New York, pp. 363–371.

Dressler, R. (1954) Comparison of theories and experiments for the hydraulic dam-break wave. Proceedings of the International Association of Scientific Hydrology Assemblée Générale, Rome, Italy, 3(88), 319–328.

Ebtehaj, I., Bonakdari, H., Sharifi, A. (2014). Design criteria for sediment transport in sewers based on self-cleansing concept. Journal of Zhejiang University SCIENCE A 15 (11): 914-924. Ebtehaj, I. and Bonakdari, H. (2016) Bed Load Sediment Transport in Sewers at Limit of Deposition, Scientia Iranica, 23(3), p. 1‐32.

Einstein, H. A., 1950. The bedload function for sediment transport in open channel flows. Tech. Bull. No. 1026, U.S. Dept. of Agriculture, Soil Conservation Service, Washington, D.C.

Einstein, H.A. and Chien, N. (1953). Can the rate of wash load be predicted from the bed-load function. Transactions, American Geophysical Union 34.

Einstein, H.A. and R.B. Banks. 1950. Fluid resistance of composite roughness. Earth & space science news 31 (34): 603‐610.

El Kadi Abderrezzak, K. and Paquier, A. (2007) Numerical modeling of flushing waves in sewer channels, Novatech, session 6., p. 1285‐1292.

El Kadi Abderrezzak, Kamal and Andre Paquier. 2009. One-dimensional numerical modeling of sediment transport and bed deformation in open channels. Water Resources Research 45 (5).

Egiazaroff, I. V. (1965). Calculation of nonuniform sediment concentra- tions. J. Hydraul. Div., Am. Soc. Civ. Eng., 91(4), 225–247.

Exner, F. (1920). Zur physik der dünen. Akad. Wiss. Wien Math. Naturwiss. Klasse, 129(2a):929–952.

Exner, F. (1925). Über die wechselwirkung zwischen wasser und geschiebe in flüssen. Akad. Wiss. Wien Math. Naturwiss. Klasse, 134(2a):165–204.

EPA (1999) Collection Systems O & M Fact Sheet Sewer Cleaning and Inspection, Techniques.

Fan, Chi-Yuan. 2004. Sewer Sediment and Control. A management practices reference guide (EPA/600/R-04/059). 72p.

Fan, C. Y., Field, R. and Lai, F. (2003) Sewer-sediment control: overview of an environmental protection agency wet-weather flow research program, Journal of Hydraulic Engineering, 129(4), p. 253-259.

Fan, Chi-Yuan, Richard Field, William C. Pisano, James Barsanti, James J. Joyce and Harvey Sorenson. 2001. Sewer and Tank Flushing for Sediment, Corrosion, and Pollution Control. Journal of Water Resources Planning and Management 127 (3): 194-201.

Faram, M. G. and R. Harwood. 2003. A method for the numerical assessment of sediment interceptors. Water Science and Technology 47 (4): 167-174.

Fraccarollo, L., & Capart, H., 2002. Riemann wave description of erosional dam-break flows. Journal of Fluid Mechanics, 461, 183-228.

Field, R., Heaney, J P. and Pitt, R. (2000) Innovative Urban Wet-Weather Flow Management Systems. Technomic Pub. Lancaster Pa. ISBN 1-56676-914-0.

Exner, F. M. (1931), Zur Dynamik der Bewegungsformen auf der Erdoberfla¨che (in German), Ergeb. Kosmisch. Phys., 1, 374 – 445.

García-Navarro, P., F. Alcrudo and J. M. Savirón. 1992. 1-D Open-Channel Flow Simulation Using TVD-McCormack Scheme. Journal of Hydraulic Engineering 118 (10): 1359.

García-Navarro P. and Savirón J.M. (1992). McCormack's method for the numerical simulation of one- dimensional discontinuous unsteady open channel flow. Journal of Hydraulic Research, 30(1), 95-104.

Garcìa, M.H., 2008. Sedimentation engineering: processes, measurements, modeling, and practice. ASCE Manuals Rep. Eng.1132. Practice No. 110.

Gaume, E., J.-P. Villeneuve, and M. Desbordes (1998). Uncertainty assessment and analysis of the calibrated parameter values of an urban storm water qualitymodel. Journal of Hydrology 210, 38(50).

Gent, R., B. Crabtree and R.M. Ashley. 1996. A review of model development based on sewer sediments research in the UK. Water Science and Technology 33 (9): 1-7.

Gessler, J. (1971) Aggradation and Degradation. Ins.H.W. Shen (Editor) River Mechanics Vol. 1, Ch. 8, Publisher H.W. Shen, Fort Collins, Colorado.

Goormans, T., Engelen, D., Bouteligier, R., Willems, P. and Berlamont, J. (2009). Design of self-cleansing sanitary sewer systems with the use of flushing devices, Water Science and Technology, 60(4), p. 901-908.

Gromaire, M.C., Garnaud, S., Saad, M., and Chebbo, G., (2001). Contribution of different sources to the pollution of wet weather flows in combined sewers. Water research, 35 (2), 521–533.

Gromaire, M.-C., (1998) La pollution des eaux pluviales urbaines en réseau d'assainissement unitaire, caractéristiques and origines. PhD thesis, ENPC, Paris, France, 503pp. + appendices.

Graf, W.H., Song, T. (1995). Sediment transport in unsteady flow. Proc., XXVI Congr., Int. Assoc. Hydr. Res., Vol. 1, London, GB.

Graf, W.H., 1971. "Hydraulics of Sediment Transport" Mc Graw-Hill Book Company.

Graf, W.H., and Song, T., 1995, Bed-shear stress in non-uniform and unsteady open-channel flows: Journal of Hydraulic research, v. 33, p. 699-704.

Grasso, M., Guidice, O., Campisano, A., Shahsavari, G., Battiato, S., Modica, C. (2017). Testing Computer Vision techniques for bedload sediment transport evaluation in sewers. ICUD conference, Prague (The Czech Republic) - 10-15 September.

Gujer, W. and Krejci, V. (1987) Urban storm drainage and receiving waters ecology. Proceedings of 4th International Conference on Urban Storm Drainage, Lausanne, Switzerland.

Guo, Q., C. Y. Fan, R. Raghaven and R. Field. 2004. Gate and Vacuum Flushing of Sewer Sediment: Laboratory Testing. Journal of Hydraulic Engineering 130 (5): 463–466.

Hallermeier, R.J., Terminal settling velocity of commonly occurring sand grains. Sedimentology 28(6), 859–865 (1981).

Hannouche A. 2012 Analyse du transport solide en réseau d'assainissement unitaire par temps de pluie : exploitation de données acquises par les observatoires français en hydrologie urbaine (Analysis of solid transport in combined sewer network during wet weather: exploitation of data acquired by the French observatories in urban hydrology), PhD Thesis, Universite Paris-Est, France, 485p.

Hirano, M., 1971. River-bed degradation with armoring, in Proceedings of the Japan Society of Civil Engineers, vol. 1971 (Japan Society of Civil Engineers, pp. 55–65.

Holly, F. M., Jr., and Karim, M. F. (1986). "Simulation of Missouri River bed degradation." J. Hydr. Engrg., ASCE, 112(6), 497-517.

Holly, F. M. and J.-L. Rahuel. 1990. New numerical/physical framework for mobile-bed modelling: Part 1: Numerical and physical principles. Journal of Hydraulic Research 28 (4): 401-416.

Hsu, H.C., A. Torres-Freyermuth, T.J. Hsu, H;H. Hwung and P.C. Kuo. 2014. On dam-break wave propagation and its implication to sediment erosion. Journal of Hydraulic Research 52 (2): 205‑218.

Hrissanthou, V. and S. Hartmann. 1998. Measurements of critical shear stress in sewers. Water Research 32 (7): 2035-2040.

IAU (Institut d'Aménagement and d'Urbanisme) de la région île-de-France, 2012. Fiche des arrondissements. 2012. FICHE DES ARRONDISSEMENTS.

Ingénierie, PROLOG, ARTELIA and Sepia. 2013. Etude de vannes à effacement rapide sur le réseau SAP-Phases I and II, étape 1. Paris, France, p.

Jefferies, C.J. and Ashley, R.M. (1994) The behaviour of gross solids in sewer systems. Journal of the European Water Pollution Control Association, 4(5), 11–17.

Joannis, C. & Aumond, M. 2005 Turbidity monitoring in sewage, 10th International Conference on Urban Drainage proceedings on CD, Copenhagen, Denmark, 21–26 August.

Johanson, Kerry. 2015. The Influence of Cohesion on Segregation Mechanisms. Water Science and Technology 25 (May): 2015.

Joannis, C., A. Hannouche and G. Chebbo. 2015. An assessment of the respective contributions of flow-rate and concentration variations to mass discharge variations at the outlets of two combined catchments during rain events. Urban Water Journal 12 (8): 653-659.

Kim, W. J., S. Managaki, H. Furumai and F. Nakajima. 2010. Washoff behavior of in-sewer deposit in combined sewer system through artificial flushing experiment. Water Science and Technology 61 (11): 2835-2842.

Kleijwegt, R.A. (1992) On Circular Transport in Circular Sewers with Non-Cohesive Deposits. Ph.D. thesis, Delft University of Technology, The Netherlands.

Krejci, V., Dauber, L., Novak, B. and Gujer, W. (1987) Contribution of different sources to pollutant loads in combined sewers. Proc. 4th Int. Conf. Urban Storm Drainage, Lausanne, 34–39. Edited by B.C. Yen, pub. Secretariat of XXII Congress IAHR Laboratoire d'hydraulique, Ecole Polytechnique Fédérale Lausanne, Switzerland.

Lacour, C. 2009 Apport de la mesure en continu pour la gestion de la qualité des effluents de temps de pluie en réseau d'assainissement (Contribution of continuous turbidity measurements to the management of effluent quality in sewer systems during wet weather). PhD Thesis, Universite Paris-Est, France, 309p.

Laplace, D., C. Oms, M. Ahyerre, G. Chebbo, J. Lemasson and L. Felouzis. (2003). Removal of the organic surface layer in combined sewer sediment using a flushing gate. Water Science and Technology 47 (4): 19-26.

Laplace, D., Robbe, D., Valentian, F. (1988). Protocole de prélèvement de dépôt dans les collecteurs d'assainissement. Rapport n° 397 lMFTlESL.

Laursen, E.M. (1956). The Hydraulics of a Storm-Drain System for Sediment-Transport Flow. Bulletin No. 5, Iowa Highway Research Board, USA.

Lau, Y L and I G Droppo.(2000). Influence of antecedent conditions on critical shear stress of bed sediments. Water Research 34 (2): 663-667.

Lazarova, V. and Bahri, A. (2005) Water reuse for irrigation: Agriculture, landscapes, and turf grass.

Lepot, M., Jean Baptiste Aubin and Jean Luc Bertrand-Krajewski. 2013. Accuracy of different sensors for the estimation of pollutant concentrations (total suspended solids, total and dissolved chemical oxygen demand) in wastewater and stormwater. Water Science and Technology 68 (2): 462-471.

Lepot, M., Pouzol, T., Borruel, X. A., Suner, D., Lyon, U. De, Lyon, I. and Villeurbanne, F.- (2014). Monitoring Sediments in Sewer With Sonar Technology : From Laboratory Experiments to In Situ Tests, in 13th ICUD - International Conference on Urban Drainage. Kuching, Sarawak, Malaysia, p. 7-12.

Lepot, M., Pouzol, T., Aldea Borruel, X., Suner, D. and Bertrand-Krajewski, J.-L. (2016) Measurement of sewer sediments with acoustic technology: from laboratory to field experiments, Urban Water Journal, p. 1-9.

Lorenzen, A, E Ristenpart and W Pfuhl. 1996. Flush cleaning of sewers. Water Science and Technology 33 (9). International Association on Water Quality: 221-228.

Lorenzen, A., Willms, M. and Dinkelacker A., 1992. The Göttingen boat. Wat. Sci. Tech., 25(8), 57-62.

Little, W. C., Mayer, P. G. (1976). Stability of channel beds by armoring. J.of the Hydr.Div. 102 (HY11): 1647‑1661.

Lin, Q.,Wu W. (2013). A one-dimensional model of mixed cohesive and non-cohesive sediment transport in open channels. Journal of Hydraulic Research 51 (5): 506-517.

Mark, O., Appelgren, C. and Larsen, T. (1995) Principles and approaches for numerical modelling of sediment transport in sewers, Water Science and Technology. International Association on Water Quality, 31(7), p. 107-115.

Marion, A. 1992. Dynamic armoring: an experimental procedure for the calibration of a multi-layer sediment-transport model. In 23° Convegno di Idraulica e Construzioni Idrauliche, 413‑424. Firenze: 31 Agosto-4 settembre.

May, R.P.W., Martin, P. and Price, N.J. (1998) Low-Cost Options for Prevention of Flooding from Sewers. CIRIA Report C506.

McCormack R.W., 1969. The effect of viscosity in hypervelocity impact cratering. AIAA Paper, 1969, 75-1.

Meyer-Peter, R., Muller, R., 1948. Formulas for bedload transport. Proceedings 2nd Meeting International Association of Hydraulic Research, Stockholm, pp. 39 – 64.

Momplot, A., Lipeme Kouyi, G., Bertrand-Krajewski, J. L., Mignot, E. and Riviere, N. (2013). Modélisation tridimensionnelle des écoulements multiphasiques en régime instationnaire au droit d'ouvrages spéciaux présents en réseau d'assainissement : performances des modèles and analyse de sensibilité, La Houille Blanche, 4, p. 16-24.

Mouri, Goro and Taikan Oki. 2010. Modelling sewer sediment deposition, erosion, and transport processes to predict acute influent and reduce combined sewer overflows and CO2 emissions. Water Science and Technology 62 (10): 2346-2356.

Morin, A., Flochel, J. M. and Schaffner, J. (2008). Un dispositif de chasses préventives pour le nettoyage de siphons and de collecteurs, Eau, l'INDUSTRIE, les Nuisances.

Nalluri, C., Alvarez, E., (1990). The influence of cohesion on sediment behaviour in pipes and channels. University of Newcastel Upon Tyne. SERC, Final paper.

Novak, P. and C. Nalluri. (1984). Incipient motion of sediment particles over fixed beds. Journal of Hydraulic Research 22(3): 181-197.

Neill, C.R. (1968). A re-examination of the beginning of movement for coarse granular bed materials. Report INT 68, Hydraulics Research Station, Wallingford, England.

Nguyen, L.S., Schaeli, B., Sage D., Kayal, S., Jeanbourquin, D., Barry D.A. and Rossi, L.. (2009). Vision-based system for the control and measurement of wastewater flow rate in sewer systems. Water Science and Technology 60: 2281-2289.

Ota, J.J., Nalluri, C., Perrusquía, G. (1999). Graded sediment. transport—the influence of particle size on sediment. transport over deposited loose beds in sewers. Proc., 8th International Conference on Urban Storm Drainage. Pp. 626-634.

Papanicolaou, A. N., Elhakeem, M., Krallis, G., Prakash, S., and Edinger, J. (2008), Sediment transport modeling review - current and future developments, J. Hydraul. Eng., 134, 1–14.

Parker, G. 2008, Transport of gravel and sediment mixtures. In Sedimentation Engineering Processes, Measurements, Modelling and Practice, edited by M. Garcia, Chap. 3, ASCE.

Parker, G., Klingeman P.C., McLean D.G. (1982). Bedload and size distribution in paved gravel-bed streams, Journal of Hydraulics Division, ASCE, Vol. 108 (HY4), pp. 544-571.

Parker, G. and E.D Andrews. (1985). Sorting of bedload sediments by flow in meander bends. Water Resources Research 21: 1361‐1373.

Park, I., Kim, H., Chae, S. K., Ha, S. (2010). Probability mass first flush evaluation for combined sewer discharges, Journal of Environmental Sciences. The Research Centre for Eco-Environmental Sciences, Chinese Academy of Sciences, 22(6), p. 915-922.

Perrusquía, G., and Nalluri, C. (1995) Modelling of bedload transport in pipe channels. Proc. Int. Conf. on the Transport and Sedimentation of Solid Particles, Prague.

Perrusquía, G., Petersen, O and Larsen, T. (1995). Influence of sewer sediments on flow friction and shear stress distribution. Water Science and Technology 31 (7): 117-126.

Pisano, W.C. and Queiroz, C. (1977) Procedures for Estimating Dry Weather Deposition in Sewerage Systems. US EPA Report EPA-600/2-77-1, 20 July.

Pisano, W.C., J Barsanti and J Joyce. 1998. Sewer and Tank Sediment Flushing, Case Studies. (December): 113.

Pisano, W. C., 1979. Dry-Weather Deposition and Flushing for Combined Sewer Overflow Pollution Control. US EPA-60012-79-133.

Pisano, W. C., G. L. Aronson, C. S. Queiroz, F. C. Blanc and J. C. O. Shaughnessy. 1979. Dry-weather deposition and flushing for combined sewer. EPA publication, 362p.

Piro, P., Carbone, M. and Tomei, G. (2011). Assessing settleability of dry and wet weather flows in an urban area serviced by combined sewers, Water, Air, and Soil Pollution, 214(1-4), p. 107-117.

Qin, Y.Y. (1980). Incipient motion of nonuniform sediment', J. Sediment Res., No. 1 (in Chinese).

Rahuel J. L. (1988). Modélisation de l'évolution du lit des rivières alluvionnaires à granulométrie étendue, Thèse Doel. Spécialité Mécanique, Inst. Nat. Polytec. de Grenoble.

Rahuel, J. L. and P. J. Belleudy. (1989). La simulation numérique des phénomènes de tri granulométrique. La Houille Blanche 3/4: 268‑272.

Rahuel, J. L., F. M. Holly, J. P. Chollet, P. J. Belleudy and G. Yang. 1989. Modeling of Riverbed Evolution for Bedload Sediment Mixtures. Journal of Hydraulic Engineering 115 (11): 1521‑1542.

Raudkivi, A.J. (1990) Loose boundary hydraulics. Pergamon Press, Oxford, UK.

Reichstetter, M. & Chanson, H. (2013) Negative Surges in Open Channels: Physical and Numerical Modeling, Journal of Hydraulic Engineering, 139(3), p. 341-346.

Reitano, S. 2004. Elaborazione e validazione di un modello numerico per lo studio del transporto di sedimenti a granulometria non uniforme. Università di Catania.

Reitano, S. 2008. Temporal evolution of the check dam filling process. Experimental investigations and numerical models. Università di Catania.

Regueiro-Picallo, M., Anta, J., Suárez, J., Puertas, J., Jácome, A. and Naves, J. (2018) Characterization of sediments during transport of solids in circular sewer pipes, Water Science and Technology.

Ristenpart, E. 1995. Sediment properties and their changes in a sewer. Water Science and Technology 31 (7). International Association on Water Quality: 77-83.

Ristenpart, E., 1993. Behaviour and pollution of sewer sediments.

Ristenpart, E., R. Gitzel and M. Uhl. 1992. Examination of Sediment Samplers. Water Science and Technology 25 (8): 63-69.

Ristenpart, E., R.M. Ashley and M. Uhl. 1995. Organic near-bed fluid and particulate transport in combined sewers. Water Science and Technology 31 (7). International Association on Water Quality: 61-68. doi:10.1016/0273-1223(95)00323-F.

Ristenpart, E. (1995a) Feststoffe in der Mischwasserkanalisation Vorkommen, Bewegung und Verschmutzungpotential, PhD thesis, University of Hannover, Germany.

Robinson, G.W. 1922. Note on the mechanical analysis of humus soils. J. Agric. Sci. 12:287.

Rocher, V., S. Azimi, R. Moilleron and G. Chebbo. 2004. Hydrocarbons and heavy metals in the different sewer deposits in the “Le Marais” catchment (Paris, France): stocks, distributions and origins. The Science of the total environment 323 (1-3): 107-22.

Ruiloba, L. C., Valentin, M. G., Russo, B., Choi, G. et Jang, D. (2018) « Toward Sustainable Management: 2D Modelling of a Self-Cleaning System to Improve Geometry in Front of the Flushing Gate », Sustainability, 10(3), p. 745.

Rushforth, P., S. J. Tait and A. Saul. 2003. Modeling the Erosion of Mixtures of Organic and Granular In-Sewer Sediments. Journal of Hydraulic Engineering 129 (4): 308–315. doi:10.1061/(ASCE)0733-9429(2003)129:4(308).

Rushforth, P., S. J. Tait and A. Saul. 2003a. Modeling the Erosion of Mixtures of Organic and Granular In-Sewer Sediments. Journal of Hydraulic Engineering 129 (4): 308–315. doi:10.1061/(ASCE)0733-9429(2003)129:4(308).

Rushforth, J., Tait, S. J. and Saul, A. J. (2003b) Full-Scale Test Facility Sewer-Sediment Mobility, The Journal, 17(1), p. 40-44.

Sanford, Lawrence P. 2008. Modeling a dynamically varying mixed sediment bed with erosion, deposition, bioturbation, consolidation, and armoring. Computers and Geosciences 34 (10): 1263–1283. doi:10.1016/j.cageo.2008.02.011Meyer-Peter, E., Müller, R., 1948. Formulas for bed load transport. Proceedings of Third Meeting of IAHR, Stockholm, pp. 39–64.

Sakrabani, R., J. Vollertsen, R.M. Ashley and T. Hvitved-Jacobsen. 2009. Biodegradability of organic matter associated with sewer sediments during first flush. Science of the Total Environment 407 (8). Elsevier B.V.: 2989-2995. Doi:10.1016/j.scitotenv.2009.01.008.

Sanchez, Y. (1987). Curage des ouvrages visitables des réseaux d'assainissement – Synthèse des principales méthodes appliquées en France. TSM, 2, 91–97.

Schaffner, J. (2008). Numerical investigations on the function of flush waves in a reservoir sewer, Fachbereich Bauingenieurwesen und Geodäsie, 265p.

Schaffner, J. and Steinhardt, J. (2009). Numerical investigations of sewer flushing sunk waves - Analysis of hydraulic boundary conditions and cleaning effectiveness, in, p. 8.

Schaffner, J. and Steinhardt, J. (2011). Numerical investigations on the cleaning efficiency of artificial created surge waves in sewer siphons, (September), p. 11–16.

Schaffner, J. and Steinhardt, J. (2011). Numerical Investigations on the Effect of Sewer Cleaning Flush Waves under the Influence of Downstream Water Levels, in Journal of Water management modeling, p. 57-80.

Schaffner, J. (2016). Sewer and tank flushing – Influence of flushing volume vs . storage height – Comparison of 3-d and 1-d modelling results, in Sewer Processes & Network, p. 100–110.

Schlütter, F. (1999). A conceptual model for sediment transport in combined sewer systems, Water Science and Technology. Elsevier, 39(9), p. 39-46. doi: 10.1016/S0273-1223(99)00214-0.

Schlütter, F. (1999). Numerical Modelling of Sediment Transport in Combined Sewer Systems. The Hydraulics and Coastal Engineering Group, Dept. of Civil Engineering, Aalborg University. Series Paper, No. 19

Schlütter, F., Kjeld S.J. (1998). Sediment transport under dry weather conditions in a small sewer system. Water Science and Technology 37 (1): 155-162. Doi:10.1016/S0273-1223(97)00765-8.

Schütze, M., Butler, D., Davives, J.W., Jefferies, C., (2000). Modelling aesthetic pollution in sewer systems. 1st ICUD.

Schütze, Manfred, Roni Penn, Eran Friedler, Malka Gorfine and Jens Alex. (2014). Simulation of Gross Solids Generation and Transport in a Separate Sewer System in Israel. (September): 7-12.

Schellart, Alma N. A., Simon J. Tait, Richard M. Ashley, C. Howes and M. McLoughlin. 2007. Development of a Guideline for Sewer Operation and Maintenance in Austria. Water Practice & Technology 2 (1).

Schellart, A., S.J. Tait, R.M. Ashley, C. Howes and M. Mcloughlin. (2007). Developing appropriate sediment management strategies for combined sewers. Water Science and Technology 2 (1). doi:0.2166/WPT.2007026.

Seco, Irene, Alma Schellart, Manuel Gómez-Valentín and Simon Tait. (2018). Prediction of Organic Combined Sewer Sediment Release and Transport. Journal of Hydraulic Engineering 144 (3): 4018003. Doi:10.1061/(ASCE)HY.1943-7900.0001422.

Seco, I, M Gómez Valentín, A Schellart and S. J. Tait. (2014). Erosion resistance and behaviour of highly organic in-sewer sediment. Water Science and Technology 69 (3): 672-679.

Sequeiros, O. E., Niño, Y. and Garcia, M. H. (2006). Erosion of Sediment Beds by Turbulent Wall Jets in Combined-Sewer-Overflow Reservoirs, in Summit on Environmental Modelling and Software, p. 1-6.

Shahsavari G., Arnaud-Fassetta G., Campisano A. (2017). A field experiment to evaluate the cleaning performance of sewer flushing on non-uniform sediment deposits. Water Research, 118, 59-69.

She, K., Trim, L., Pope, D. (2005). Fall velocities of natural sediment particles: A simple mathematical presentation of the fall velocity law. Journal of Hydraulic Research, 43 (2), 189–195.

Shen, H.W. (Ed.), (1991). Movable Bed Physical Models. Kluwer Academic, Boston.

Shields A.F. (1936). Application of similarity principles and turbulence research to bed-load movement, vol 26. Mitteilungen der Preussischen Versuchsanstalt f€ur Wasserbau und Schiffbau, Berlin, Germany, pp 5–24

Shirazi, R. H. S. M. (2013). Application of Flushing Devices in sewer systems. Katholieke Universiteit Leuven, 227p.

Shirazi, R. H. S. M., A. Campisano, C. Modica and P. Willems. (2014). Modelling the erosive effects of sewer flushing using different sediment transport formulae. Water science and technology 69 (6): 1198‑204. doi:10.2166/wst.810.

Skipworth, P. J., Tait, S. J. and Saul, A. J. (1999) Erosion of Sediment Beds in Sewers: Model Development, Journal of Environmental Engineering, 125(6), p. 566-573. doi: 10.1061/(ASCE)0733-9372(1999)125:6(566).

Sikora, B. (1989) Vanne cyclique autocurante à décantation. French Patent No. 2643971.

Stokes, G. C., 1851, “On the Effect of the Internal Friction of Fluids on the Motion of Pendulums,” Trans. Cambridge Philos. Soc., 9, pp. 8–106.

Song, T., and W. Graf (1995). "Bedload Transport in Unsteady Open-channel Flow," in Rapport Annuel, Laboratoire de Recherches Hydrauliques, Ecole Polytechnique Federal, Lausanne, Switzerland.

Spence, K. J., Digman, C., Balmforth, D., Houldsworth, J., Saul, A. and Meadowcroft, J. (2016) Gross solids from combined sewers in dry weather and storms, elucidating production, storage and social factors, Urban Water Journal, 13(8), p. 773-789. doi: 10.1080/1573062X.2015.1025081.

Spence, Kevin John, Christopher Digman, David Balmforth, James Houldsworth, Adrian Saul and James Meadowcroft. 2016. Gross solids from combined sewers in dry weather and storms, elucidating production, storage and social factors. Urban Water Journal 13 (8): 773-789. doi:10.1080/1573062X.2015.1025081.

Staufer, P., Dettmar, J. and Pinnekamp, J. (2007). Impact of the Level of Approximation on Modeling Flushing Waves, Water Practice and Technology, 2(2). doi: 10.2166/wpt.2007.036.

Staufer, P., Dettmar, J. and Pinnekamp, J. (2008) Upstream processes within a flushing wave, in 11th International Conference on Urban Drainage. Edinburgh, Scotland, UK, p. 10.

Staufer, P. and J. Pinnekamp. 2008. In situ measurements of shear stresses of a flushing wave in a circular sewer using ultrasound. Water Science and Technology 57 (9): 1363-1368. doi:10.2166/wst.2008.300.

Sutherland, A. J., 1992. Hiding functions to predict self-armoring. Proc., Int. Association of Hydraulic, Research Int. Grain Sorting Seminar, M. Jaeggi and R. Hunziker, eds., Mitteilungen der Versuchsanstalt fu¨r Wasserbau, Hydrologie und Glaziologie No. 117, ETH, Zurich. Switzerland.

Tanaka, H. (1988). Bed Load transport of sediment with non-uniform grain size due to wave motion. Costal Engineering in Japan 31 (2): 265‑276.

Tait, S. J., Chebbo, G., Skipworth, P. J., Ahyerre, M. and Saul, A. J. (2003a) Modeling In-Sewer Deposit Erosion to Predict Sewer Flow Quality, Journal of Hydraulic Engineering, 129(4), p. 316-324. doi: 10.1061/(ASCE)0733-9429(2003)129:4(316).

Tait, S.J., R.M. Ashley, R. Verhoeven, F. Clemens, R. Sakrabani, A. Schellart, R. Veldkamp and L. Aanen. (2003b). The characteristics of an in-sewer erosion event-observations from environmentally controlled annular flume. In Towards a balanced methodology in european hydraulic research, 22-23.

Tait, S.J., J.R. Peter and A.J. Saul. (1998). A laboratory study of the erosion and transport of cohesive-like sediment mixtures in sewers. Water Science and Technology 37 (1). International Association on Water Quality: 163-170. doi:10.1016/S0273-1223(97)00766-X.

Tait, S. J., A. Marion and G. Camuffo. (2003a). Effect of environmental conditions on the erosional resistance of cohesive sediment deposits in sewers. Water Science and Technology: 27-34.

Thornton, R.C. and Saul, A.J. (1986) Some quality characteristics of combined sewer overflows. The Public Health Engineer, 14(3), 35–38.

Todeschini, S., Ciaponi, C. and Papiri, S. (2008). Experimental and numerical analysis of erosion and sediment transport of flushing waves, 11th International Conference on Urban Drainage, 4(3), p. 1-10.

Todeschini, S., Ciaponi, C. and Papiri, S. (2010). Laboratory Experiments and Numerical Modelling of the Scouring Effects of Flushing Waves on Sediment Beds, Engineering Applications of Computational Fluid Mechanics, 4(3), p. 365-373. doi: 10.1080/19942060.2010.11015324._

Tranckner, J., S. Hoeft, M. Wachsmuth, A. Kimmersdorfer and M. Rinas. (2017). Sewer flashing in weir controlled channel combined sewers_from feasibility study to full scale tests. In 14th International conference on Urban drainage, 403-406. Prague, Czech Republic.

Tränckner, J., G. Bönisch, V. R. Gebhard, G. Dirckx and P. Krebs. 2008. Model-based assessment of sediment sources in sewers. Urban Water Journal 5 (February 2014): 277-286.

Vanoni, V.A., 2006. In: Sedimentation engineering: American Society of Civil En- gineers. Manuals and Reports on Engineering Practice, no. 54, 745p.

Van Rijn, L.C., Sediment transport, part I: bedload transport. J. Hydraul. Eng. 110(10), 1431–1456 (1984a).

Van Rijn, L.C., (1984b). Sediment transport, part II: suspended load transport. J. Hydraul. Eng. 110(11), 1613–1641.

Van Rijn L. C. (1993). Principles of sediment transport in rivers, estuaries and coastal seas, Aqua Publications, Oldemarkt, The Netherlands.

Verbanck, M. A. (1990). Sewer Sediment and its Relation with the Quality Characteristics of Combined Sewer Flows. Water Science and Technology 22 (10): 247-257.

Verbanck, M. A., Ashley, R. M., Bachoc A. (1994). International workshop on origin, occurrence and behaviour of sediments in sewer systems: Summary of conclusions. Water Research 28 (1): 187-194.

Verbanck, M.A. (1995) Capturing and releasing settleable solids: the significance of dense undercurrents in combined sewer flows. Wat. Sci. Tech., 31(7), 85–93.

Verbanck, M. A. (1996). Assessment of sediment behaviour in a cunette-shaped sewer section. Water Science and Technology 33 (9). International Association on Water Quality: 49-59.

Verbanck, M.A. (2001). Computing near-bed solids transport in sewers and similar sediment-carrying open-channel flows. Urban Water Journal 2 (2000): 277-284.

Velikanov M.A., (1954). Principle of the gravitational theory of the movement of sediments", Academy of Sciences Bulletin, Geophysical Series, Moscow, USSR, n° 4, p. 349-359 (in Russian).

Vollertsen, Jes and Thorkild Hvitved-Jacobsen. (2000). Resuspension and oxygen uptake of sediments in combined sewers. Urban Water 2 (1): 21-27.

Wan Mohtar, W. H. M., Afan, H., El-Shafie, A., Bong, C. H. J. and Ab. Ghani, A. (2018). Influence of bed deposit in the prediction of incipient sediment motion in sewers using artificial neural networks, Urban Water Journal, p. 1-7.

Walski, T., Falco, J., McAloon, M. and Whitman, B. (2011) Transport of large solids in unsteady flow in sewers, Urban Water Journal, 8(February 2014), p. 179-187. doi: 10.1080/1573062X.2011.581298.

Wilcock, Peter R, M Asce and Joanna C Crowe. (2003). Surface-based Transport Model for Mixed-Size Sediment. Journal of Hydraulic Engineering 129 (2): 120-128.

Williams, K. J. J., Tait, S. J. and Ashley, R. M. (2009) In-sewer sedimentation associated with active flow control, Water Science and Technology, 60(1), p. 55-63. doi: 10.2166/wst.2009.286.

Wotherspoon, D.J.J. (1994). The movement of cohesive sediment in a large combined sewer. PhD thesis, Dundee Institute of Technology, UK.

Wotherspoon, D.J.J. and R.M. Ashley. (1992). Rheological Measurement of the Yield Strength of Combined Sewer Sediment Deposits. Water Science and Technology 25 (8): 165-169.

Woo, H. S., Julien, P.Y., Richardson, E. V. (1988). Suspension of large concentration of sands. J.Hydraul. Eng. ASCE, 114(8): p888-898.

Wu, W. (2008). Computational River Dynamics. MS, USA: Taylor & Francis/Balkema, 509p. doi:10.4324/978020393848, London.

Wu, J and He, C. (2010). Experimental and modeling investigation of sewage solids sedimentation based on particle size distribution and fractal dimension. Environmental Engineering 7 (1): 37-46. doi:10.1007/BF03326115.

Yan, H. (2013). Expérimentations and modélisations tridimensionnelles de l'hydrodynamique, du transport particulaire, de la décantation and de la remise en suspension en régime transitoire dans un bassin de retenue d'eaux pluviales urbaines. INSA de Lyon, 238p.

Yang C. T., Randle T. J., Daraio J. and Al. 2006. Erosion and Sedimentation Manual. U.S. Department of the Interior Bureau of Reclamation. . doi:10.1300/J155v07n03_01.

Zanke, U.C.E. (2003), On the influence of turbulence on the initiation of sediment motion, International J. of Sediment Research 18(1), 1-15.

Zhang, Shiyan and Jennifer G. Duan. 2011. 1D finite volume model of unsteady flow over mobile bed. Journal of Hydrology 405 (1-2): 57-68. doi:10.1016/j.jhydrol.2011.05.010.

Zhou, Y. and Li, T. (2010) Optimized operation plan for sewer sediment control, Journal of Zhejiang University SCIENCE A, 11(5), p. 335-341. doi: 10.1631/jzus.A0900082.

Zug, M., D. Bellefleur, L. Phan and O. Scrivener. 1998. Sediment transport model in sewer networks - A new utilisation of the Velikanov model. Water Science and Technology 37 (1). International Association on Water Quality: 187‑196. doi:10.1016/S0273-1223(97)00769-5.

Appendixes

Appendix A

Turbidity paper presented in SPN8 in Rotterdam (Netherlands) -2016

SPN8

8 th International Conference on Sewer Processes and Networks
August 31 –September 2, 2016, Rotterdam, The Netherlands

Preliminary analysis of turbidity measurements during a flushing operation in combined sewer channel

Gashin Shahsavari[1], Gilles Arnaud-Fassetta[1], Roberto Bertilotti[2], Hossein Bonakdari[3], Isa Ebtehaj[3], Hamid Moeeni[3], Carlo Modica[4], Alberto Campisano[4]

[1]Department of Geography, University of Paris Diderot, Rue Albert Einstein - 75013 Paris, France (Email: *gashin.shahsavari@univ-paris-diderot.fr, gilles.arnaud-fassetta@univ-paris-diderot.fr*)
[2]PROLOG Ingénierie, 3-5 Rue de Metz -75010 Paris, France, (E-mail: *bertilotti@prolog-ingenierie.fr*)
[3]Department of Civil Engineering, Razi University, Kermanshah, Iran (Email: *bonakdari@yahoo.com, isa.ebtehaj@gmail.com, h.moeeni68@gmail.com*)
[4]Department of Civil Engineering and Architecture, University of Catania, Viale A. doria, 6, 95125 Catania, Italy, (E-mail: *cmodica@dica.unict.it, acampisa@dica.unict.it*)

Abstract
Flow turbidity at different elevations was continuously monitored in five cross-sections of a real combined-sewer channel stretch during a flush experiment. The preliminary analysis of the collected turbidity data in terms of quality and spatial variability of the time series is presented in this paper. Also, an Autoregressive Moving Average (ARMA) model was setup to evaluate potential prediction of turbidity values showing a good estimation performance with relatively small errors.

Keywords
ARMA model, combined sewer, flush, turbidity monitoring.

INTRODUCTION

Sewer flushing is recognized as an economically and operationally efficient technique to limit the sediment accumulation in combined sewers and then to restore the full flow capacity of channels (Ashley et al., 2005). Since more than two decades, the use of this technique has been studied to evaluate the sediment-removal efficiency associated to different types of flushing devices. However, sediment transport during the flush in sewer channels is not yet well understood due to the complexity of sewer conditions as well as the lack of observations. Researches mainly conducted under laboratory controlled conditions have allowed characterizing the flow and sediment parameters playing a major role during the flush (Dettmar et al., 2002; Campisano et al., 2004; Creaco and Bertrand-Krajewski, 2009). Field experiments pointed out the occurrence of both bedload and suspended load transport depending on established flow conditions (Shahsavari et al., 2016).

Turbidity has been recognized to be an indicator of suspended (total) sediment transported by the flow in natural and artificial channels (Christensen et al., 2001; Hannouche et al., 2011). Recently, the use of turbidity sensors is considered to be effective for the continuous monitoring of in-sewer turbidity dynamics during dry weather as well as wet weather conditions (Bertrand-Krajewski, 2004; Métadier and Bertrand-Krajewski, 2011). Many challenges are rising from this technology, basically concerning methods to convert turbidity readings into sediment transport measurements or relationships between turbidity and flow (Bertrand-Krajewski et al., 2007; Lepot et al., 2013).

The Paris Municipality (Ville de Paris) has elaborated a plan for investigating the scouring performance of flushing operation in a large-size channel of the combined sewer network of the city. In this regard, a field flush experiment in a pilot channel was carried out for a full monitoring flow and turbidity during the flush.

This paper presents the preliminary results of the analysis of the turbidity time series collected during the experiment. First the analysis addressed to the data consistency. Secondly, the potentiality of using an Autoregressive Moving Average (ARMA) model to predict turbidity was analysed for one of the available turbidity time series.

METHODOLOGY

Field experimental setup and data storage

Field experiments were conducted in a large size trunk characterized by a compound cross-section with lateral banks in the sewer subnetwork of combined sewer network of Paris 11th arrondissement. The pilot channel is 1.1 km long (signed hereafter by S_{-50} and S_{+1050} with reference to the gate location at S_0) and it is prone to sedimentation. The average slope of the trunk is 0.8‰ and some longitudinal irregularities are present along the channel. The channel cross-section and longitudinal profile are illustrated in Figure 1a. The channel was equipped with a flushing gate that allows in-line storage of dry-weather flow in the upstream portion. For the experiment, the flush is produced followed by a sudden opening of the gate and release of the stored water through the channel.

The channel stretch was equipped by flow devices and automated turbidity sensors in five cross-sections (called hereafter, S_{-50}, S_{-5}, S_{+5}, S_{+50} and S_{+100} ; see Figure 1b). Figure 1c shows the position of these devices in the cross-section. At each measuring section a flow meter, an ultrasound sensor and three turbidity sensors were installed. Turbidity was measured in nephelometric turbidity unit (NTU) in 10s time intervals. Technical properties of the monitoring devices such as sampling range, accuracy, and measuring interval are outlined in table 1.

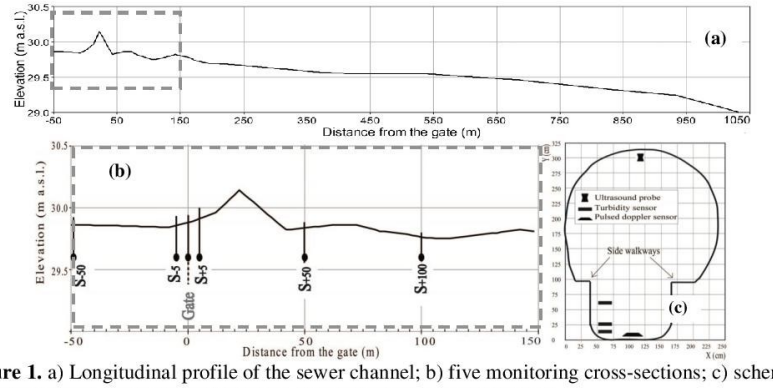

Figure 1. a) Longitudinal profile of the sewer channel; b) five monitoring cross-sections; c) scheme of measuring devices and their position in the transversal cross-section.

Table 1. Summary of flow and turbidity instruments used for the flush experiment.

Devices	Sampling range	Accuracy at full scale	Measuring technique	Acquisition frequency (Hz)
Pulsed doppler sensor	±5 m/s	±1% of readings	beam-pulsed doppler	0.1
Turbidity sensor	0-4000 NTU	±5% of readings	Nephelometric (θ=90°)	0.1
Ultrasound sensor	0-3 m	4 mm	acoustic imaging	0.067

Three elevations were chosen for turbidity sensors installation (15, 25 and 65 cm from the bed, called hereafter T15, T25 and T65) at each of the five monitoring sections (15 turbidity sensors in total) in order to observe the turbidity vertical pattern during the flush. Turbidity sensors were calibrated off-line before the flush experiment using Formazin solution between 0-2000 NTU. During the flush test, real-time data acquisition was obtained using a portable PC. Flow data time series were provided by all the flow sensors with the exception of sections S_{+100} as well as of S_{+50} during the peak period. Turbidity time series were obtained from all the sensors except for two (T15-S_{+5} and T25-S_{+50}).

Turbidity data analyzing

The dataset was firstly "cleaned" by eliminating records showing values out of the detection range of sensor. The noisiest time series correspond to the sensors close to the bed (T15) where the sediment fouling and bed load transport during the flush were mainly were more developed.
The analysis of turbidity values from all sensors was carried out to assess the quality of the measurements. To this purpose, the distribution of data obtained from each sensor was separately checked using Normal, Lognormal, Exponential and Weibull functions to verify the best fitting distribution. Then, the best fitting distribution was identified to compare distribution parameters among all the turbidity sensors installed at the same elevations to evaluate the consistency of recorded data.
Furthermore, in order to show the application of the validated turbidity values (in NTU) the analyses developed by plotting these turbidity values against the corresponding flow discharge (in m^3/s) in 10s time scale. This method could help to describe the overall impact of the flush on the turbidity during the fast rising and falling limbs of the flow showing by hysteresis loop of the both time series (discharge vs turbidity) which could support the investigation of flow turbidity variations.

Autoregressive model

Turbidity time series were used to test application of Autoregressive Moving Average model (ARMA) in order to obtain the relationship between turbidity values at different times. The used ARMA model is based on following equation:

$$(1-\varphi_1 B-\varphi_2 B^2-\ldots-\varphi_p B^p)x_t=(1-\theta_1 B-\theta_2 B^2-\ldots-\theta_q B^q)\varepsilon_t \qquad (1)$$

where x_t is the observed value of turbidity, ε_t is the stochastic or noise term, B is a differential operator as $B(x_t)=x_{t-1}$, p and q are order of autoregressive and moving average (respectively) and φ and θ are the parameters of autoregressive parameters and moving average orders (respectively).
Among the 469 turbidity records, 329 values are used to model calibration and the rest of data (140 data) were considered for the validation. The number of autoregressive order was taken between zero and ten and allowed combining 121 different models.
To evaluate the performance of the proposed model Mean Absolute Percentage Error (*MAPE*), Root Mean Square Error (*RMSE*) and Scatter Index (*SI*) were used as indicated in Eq. 2 to 4.

$$RMSE=\sqrt{\left(\frac{1}{n}\right)\sum_{i=1}^{n}(x_i-y_i)^2} \qquad \text{(NTU)} \qquad (2)$$

$$MAPE=\left(\frac{100}{n}\right)\sum_{i=1}^{n}\left(\frac{|x_i-y_i|}{x_i}\right) \qquad (\%) \qquad (3)$$

$$SI = \frac{RMSE}{\bar{x}} \quad (-) \quad (4)$$

where y_i and x_i are the modelled and observed values, respectively, and $\bar{x}$ is the mean of observed values.

RESULTS

Turbidity data analyzing

Preliminary fitting distribution check was applied for all T15 sensors and revealed that time series were Weibull distributed (Eq. 5), which was then confirmed by an analytical Chi-square test (with significant level of ≤ 0.05). The two maximum likelihood parameters of fitted Weibull distribution (a and b as scale and shape, respectively) are presented in Table 2.

$$f(x|a,b) = \frac{b}{a}\left(\frac{x}{a}\right)^{b-1} e^{-(x/a)^b} \quad (5)$$

Table 2. The Weibull distribution parameters obtained for all T15 time series.

parameters	S_{-50}	S_{-5}	S_{+50}	S_{+100}
a (scale)	1683.8	4247.1	4806.0	2959.0
b (shape)	3.21	1.54	1.94	1.01

The probability distribution of turbidity time series for all T15 is illustrated in Figure 2 for the sections S_{-50}, S_{-5}, S_{+50}, S_{+100}. The figures clearly show good fitness of turbidity time series distribution to records for all the T15 sensors, which is indicating the data consistency among the sensors positioned at the same elevation. In other words, the sensors from the same position behaved in the same way to observe the turbidity variation during the flush and this is indicating the consistency of the recorded data.

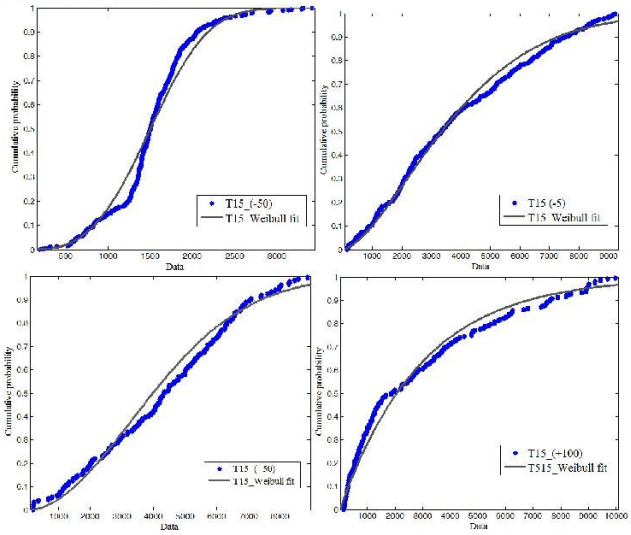

Figure 2. Cumulative probability plot and fitted Weibull distribution for the sections S_{-50}, S_{-5}, S_{+50}, S_{+100}.

The spatial variation of the turbidity records during the flush for all sensors was evaluated. Table 3 presents the main statistics of turbidity data.
On one hand, the vertical comparison of mean values confirms that the higher values of turbidity in the water column were observed close to the bed with values decreasing going from the bed to the water surface. Also, the more the sensor is far from the bed (T15), the more it provided dispersed values. On the other hand, a decrease of the average turbidity throughout the channel reveals the effect of the flush. Sensors located close to the gate exhibit high values of the turbidity with a general decreasing trend toward downstream. The same decreasing trend was observed for all three vertical positions except for T65. In fact, the T65 sensor in the last measuring cross-section has strangely recorded a very high peak after about 45 minutes after the flush releasing which was lasting for a few minutes. This was perhaps due to a temporary covering of the sensor by sanitary paper.

Table 3. Statistical description of all turbidity time series in NTU included mean and standard deviation (Values exceeding the detection range are excluded).

	Sensors	Mean (NTU)	SD (NTU)	CV (-)
T65	S_{-50}	35.4	26.9	0.8
	S_{-5}	335.5	355.2	1.1
	S_{+5}	132.8	16.4	0.1
	S_{+50}	40.1	66.8	1.7
	S_{+100}	428.1	989.7	2.3
T25	S_{-50}	219.6	75.1	0.3
	S_{-5}	460.3	283.6	0.6
	S_{+5}	2666.6	1469.5	0.6
	S_{+50}	---	---	---
	S_{+100}	1819.4	1890.3	1.0
T15	S_{-50}	1515.3	497.0	0.3
	S_{-5}	3836.0	2447.0	0.6
	S_{+5}	---	---	---
	S_{+50}	4301.4	2210.8	0.5
	S_{+100}	3105.3	2775.4	0.9

In addition, as an example, the flow and turbidity data from S-5 were chosen to investigate the relationship of the two time series. Linear regression between discharge and NTUs showed a weak relationship with a coefficient of determination R2 of 0.01. The fluctuations of turbidity time series were reduced by applying the linear filtering over 1-min time scale. The figure 3 shows the NTU values and corresponded flow discharge in m3/s. Interestingly, the figure shows a hysteretic behaviour with the rising and falling limbs of the flush hydrograph for flow discharge-turbidity relations similarly to what has been observed in river streams (Lawler et al., 2006; Lloyd et al., 2015; Mukundan et al., 2013). This anticlockwise hysteresis indicates the last-flush process with time-lagged arrival of turbidity peak after the flow peak characterizing the chronological contribution of turbidity sources to the flow. Also, the form of the hysteresis is indicating the rate of the transport of turbidity sources. The result would be a material for future work to analyse the response of the turbidity to the flush flow by evaluating the pattern of the hysteresis for other sensors.

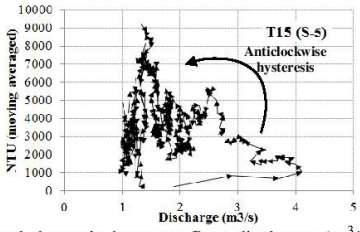

Figure 3. Example of temporal dynamic between flow discharge (m^3/s) and associated turbidity (NTU) in S_{-5}.

Model results

The results of ARMA model provided the following equation:

$$x_t = 0.9994x_{t-1} - 0.5184\varepsilon_{t-1} - 0.2635\varepsilon_{t-2} \quad (6)$$

Figure 4a shows the results of the calibration of the model. Globally, the observed values show the peaks larger than the modelled values. The model validation graph (figure 4b) shows also the same trend reducing the amount of maximum and minimum values in fluctuations. Overall, the ARMA model shows good performance in estimating turbidity so that the difference between predicted and observe value are relatively small. The *RMSE*, *MAPE* and *SI* for proposed model are equal to 174.3 NTU, 8.33 % and 0.107 (-) for validation. Therefore, the use of ARMA model (Eq. 6) in prediction of turbidity leads to reliable results.

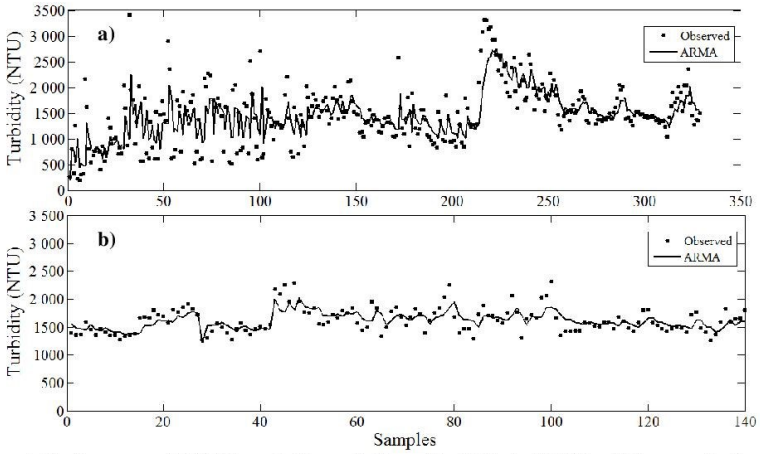

Figure 4. Performance of ARMA model in prediction of turbidity in NTU for T15 sensor in S_{-50}, a) for the calibration, and b) for the validation.

CONCLUSION

The turbidity fluctuations during a flush event were preliminary continuously monitored in three different elevations in five cross-sections of a real combined-sewer channel stretch. The preliminary results of the analysis of the collected turbidity time series were investigated in terms of data quality and spatial variability was presented. The relationship between these data and corresponding flow discharge was evaluated and was showing a characteristic hysteretic behaviour. Also, an Autoregressive Moving Average (ARMA) model was setup to evaluate potential prediction of turbidity values showing a good estimation performance with RMSE, MAPE and SI equal to 174.3 NTU, 8.33 % and 0.107 (-), respectively.

Further work is needed to investigate the quality of the time series recorded from other sensors in different elevations of each section and their relationship with the flow discharge in order to confirm the results.

ACKNOWLEDGEMENT

This project has been financially supported by the PROLOG Ingénierie consulting company as well as the Paris Municipality-major structure services of sewer network of *Ville de Paris*. A special thank is given to Jean-François Ferrandez and Fabien Riou.

REFERENCES

Ashley, R.M., Bertrand-Krajewski, J.L., Hvitved-Jacobsen T. and Verbanck M. (2005). Solids in sewers - Characteristics, effects and control of sewer solids and associated pollutants, Scientific and technical report, IWA, London, 360p.

Bertrand-Krajewski, J.L. (2004). TSS concentration in sewers estimated from turbidity measurements by means of linear regression accounting for uncertainties in both variables, *Wat. Sci. Tech*., 50 (11): 81‑8.

Bertrand-Krajewski, J.L. Barraud, S., Lipeme Kouyi, G., Torres, A. and Lepot, M. (2007). On-line monitoring of particulate pollutant loads in urban sewer systems: stakes, methods, example of application. In Transports solides et gestion des sédiments en milieux naturels et urbains, 5‑16.

Campisano, A., Creaco, E. and Modica, C. (2004). Experimental and numerical analysis of the scouring effects of flushing waves on sediment deposits. In *Journal of Hydrology*, 299 (3): 324‑334.

Christensen, V.G., Jian, X. and Ziegler, A.C. (2001). Continuous turbidity monitoring and regression analysis to estimate total suspended solids and fecal coliform bacteria loads in real time, In 7th Fedral Interagency Sedimentation Conference, March 25-29: III-49-III-101.

Creaco, E., Bertrand-Krajewski, J.L. (2009). Numerical simulation of flushing effect on sewer sediments and comparison of four sediment transport formulas. In *Journal of Hydraulic Research* 47 (2): 195‑202.

Dettmar, J., Rietsch., B. and Lorenz, U. (2002). Performance and Operation of Flushing Devices - Results of a Field and Laboratory Study. In 9th International Conference on Urban Drainage, Proceeding: 1‑10.

Hannouche, A., Chebbo, G., Rubann G., Tassin, B., Lemaire, B.J. and Jonnais, C. (2011). Relationship between tubidity abd total suspended solids concentration within a combined sewer system. *Wat. Sci. Tech*., 64(12), 2445-52.

Lawler, D. M., G. E. Petts, I. D L Foster et S. Harper. 2006. « Turbidity dynamics during spring storm events in an urban headwater river system: The Upper Tame, West Midlands, UK. » Science of the Total Environment 360 (1-3): 109‑126.

Lepot, M., Aubin, J.B. and Bertrand-Krajewski, J.L. (2013). Accuracy of different sensors for the estimation of pollutant concentrations (total suspended solids, total and dissolved chemical oxygen demand) in wastewater and stormwater, *Wat. Sci. Tech*., 68 (2): 462‑471.

Lloyd, C.E.M., Freer, J.E., Johnes, P.J. and Collins, A.L. (2015). Technical Note: Testing an improved index for analysing storm nutrient hysteresis, *Hydrology and Earth System Sciences Discussions* 12 (8): 7875‑7892.

Mukundan, R., D. C. Pierson, E. M. Schneiderman, D. M. O'Donnell, S. M. Pradhanang, M. S. Zion et A. H. Matonse. 2013. « Factors affecting storm event turbidity in a New York City water supply stream. » Catena 107: 80‑88.

Shahsavari, G., Arnaud-Fassetta, G. and Campisano, A. (2016). Non-uniform mobile sediment bed evolution under flushing operation in a real compound sewer channel. Submitted on May 5th to *Water Research Journal*.

Appendix B

Image analysis paper presented in ICUD2017-Prague (Czech Republic)-Sep2017

ICUD-0304 Testing Computer Vision techniques for bedload sediment transport evaluation in sewers

M. Grasso[1], O. Giudice[2], A. Gullotta[1], G. Shahsavari[3], S. Battiato[2], C. Modica[1], A. Campisano[1]

1 *University of Catania, Department of Civil Engineering and Architecture, Catania, Italy*
2 *University of Catania, Department of Mathematics and Computer Science, Catania, Italy*
3 *Paris Diderot University, Paris, France*

Summary

The potential of Computer Vision techniques to support estimation of bedload transport in sewers is investigated. A specific methodology combining the use of algorithms for sediment detection and tracking with advanced image filtering procedures was setup in order to identify the sediment particles contributing to the bedload transport. The methodology was preliminary applied to a large combined sewer channel of Paris City for which videos capturing sediment transport processes during a flush experiment are available.

Keywords

sewer sediment transport, computer vision, image processing, field experiments, sewer flushing

Introduction

Sediment transport in sewer systems has been the subject of several studies in the past two decades (see for instance Ashley et al., 2004). Although large efforts have been devoted to understand the behaviour of in-sewer sediments, many aspects concerning the dynamics of sediment transport processes in sewer channels still remain unclear. One of the reasons of the existing gap of knowledge is associated to the difficulty to run field experiments for monitoring the transport of sediments in real sewers.

Recently, the use of Computer Vision (CV) techniques has gained the attention of researchers as a non-intrusive method to evaluate sediment transport in open channels. Algorithms to detect spherical particles and track their trajectories in the flow have been successfully developed by various researchers (e.g. Böhm et al, 2006; Radice et al., 2006). However, the available results have been obtained under laboratory-controlled experimental conditions only, i.e. steady flow conditions, uniform sediments, optimal light conditions, etc. Conversely, applicability of CV methods for sediment transport evaluation in real sewers has not been tested, yet.

The objective of this paper is to investigate the potential of CV techniques to support bedload transport estimation in sewer channels. A specific methodology combining particle detection and tracking techniques with advanced image filtering algorithms was developed to identify bed particles contributing to bedload transport.

The methodology was developed based on the video data recorded during field experiments in a large combined sewer channel of Paris City. The experiments were carried out within the framework of a larger research project aiming at analysing the performance of flushing in sewers (Shasavari et al., 2016).

Methods and Materials

Videos were recorded by a GoPro camera placed in a plexiglass box and encased in the sewer channel side wall. The videos (1920x1080 pixels, 24fps) show the hydraulic and sediment-related

processes including sediment transport during a 3.5 hour long flush experiment. Videos were firstly pre-processed to improve the quality of the images, and eliminate distortions. A control window (ROI – Region Of Interest) (350×80 pixels) was selected for each frame in proximity of the water-bed interface with the aim to focus on bedload transport (see Fig. 1), thus including particles that may move only by rolling, sliding, and by saltation.

Two sets of 24 frames (one second video each) were selected in which each particle was manually labelled in order to be used as training samples for a CV-based supervised machine learning algorithm.

Firstly, algorithms for particle detection were developed. Two classes of sediment particles were identified based on their appearance in each frame. In particular, sediments moving faster than the exposure time of the camera appear as "stripes", while others showed a "core" shape. A single-layered Convolutional Neural Network was trained to find the optimal image filters needed to achieve the best classification results with a shape-based detection algorithm for the detection of particle geometry on the plan on the image (Battiato et al., 2016). Overall, 24 frames were used for the calibration of the algorithms, while the remaining 24 frames were used for the validation. Secondly, particle tracking analysis was carried out to evaluate velocities of the detected particles. Dense Optical Flow (DOF)-based tracking algorithms (Tao et al., 2012) following the particles on time through subsequent frames were used for core particles. Instead, velocities of "stripes" particles were calculated based on the analysis of the path left by the particle in each frame. Finally, area and velocity of particles subject to motion were automatically evaluated by the algorithm for comparison with the values obtained manually for the 24 frames of the validation sample. Sediment transport in the ROI control window was finally evaluated based on the sum of the products of area and horizontal velocity for each detected sediment particle.

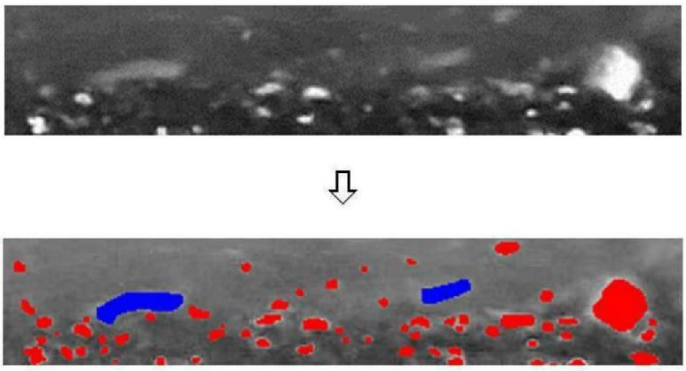

Fig.1. *Example of application of the particle detection procedure within the ROI of the frame.*

Results and Discussion

The results of the application of the used CV techniques for particle detection are summarized in Fig. 2. The figure shows the number of particles labelled manually and detected by the used machine learning algorithm. Globally, average 95% of the sediment particles were correctly detected by the algorithm for each frame.

The particle tracking algorithm was able to automatically attribute a velocity vector to about 80% of the detected particles. Conversely, the remaining 20% particles were not identified by the tracking

procedure. Reasons of this relatively low performance were: i) some particles went out of the ROI without the possibility to identify them in the subsequent frames; ii) some particles were "covered" by other sediments; and iii) turbidity locally impeded particle vision.

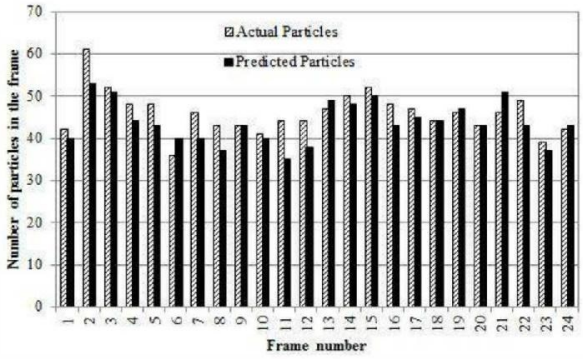

Fig. 2. *Comparison between number of particles detected manually and by CV algorithms. Calibration procedure.*

Conclusions

Globally, the obtained results are to be considered as preliminary. However, the used CV techniques showed promising results with relatively high accuracy also under non-optimal experimental conditions in sewer systems.

References

Ashley, R., Bertrand-Krajewski, JL., Hvitved-Jacobsen, T., & Verbank, M. 2004 Solids in sewers. Characteristics, effects and control of sewer solids and associated pollutants. 14, IWA Publishing.

Battiato, S., Farinella, G. M., Giudice, O., & Puglisi, G. 2016 Aligning shapes for symbol classification and retrieval. Multimedia Tools and Applications, 75(10), 5513-5531.

Böhm, T., Frey, P., Ducottet, C., Ancey, C., Jodeau, M., & Reboud, JL. 2006 2D motion of a set of particles in a free surface flow with image processing. Expe in fluids, 41(1), 1-11.

Radice, A., Malavasi, S., Ballio, F. 2006 Solid transport measurements through image processing. J Expe fluids.

Shahsavari, G., Arnaud-Fassetta, G., Bertilotti, R., Campisano, A. & Riou, F. 2015 Bed evolution under one-episode flushing in a trunk sewer in Paris, France. Journal of Civil and Environmental Engineering, 9 (7), 759-768.

Appendix C

Concentration percentages imposed in the sediment initial condition.

D (in mm) Distance	0.075	0.1	0.2	0.3	0.4	0.5	0.6	0.7	0.85	1	2	3	4	5	10	15	20	25	40	50
-50	0.01	0.01	0.03	0.05	0.07	0.08	0.07	0.06	0.08	0.04	0.18	0.12	0.06	0.06	0.09	0.00	0.00	0.00	0.00	0.00
-15	0.01	0.01	0.04	0.08	0.11	0.11	0.10	0.09	0.12	0.07	0.13	0.05	0.02	0.03	0.02	0.00	0.00	0.00	0.00	0.00
-5	0.01	0.00	0.01	0.03	0.05	0.06	0.07	0.08	0.13	0.08	0.23	0.11	0.06	0.05	0.03	0.00	0.00	0.00	0.00	0.00
10	0.02	0.01	0.05	0.08	0.09	0.09	0.09	0.10	0.16	0.01	0.17	0.05	0.02	0.02	0.03	0.00	0.00	0.00	0.00	0.00
30	0.01	0.01	0.03	0.06	0.11	0.13	0.13	0.11	0.15	0.08	0.10	0.05	0.02	0.00	0.00	0.00	0.00	0.00	0.00	0.00
50	0.01	0.00	0.02	0.05	0.07	0.07	0.07	0.07	0.09	0.06	0.13	0.09	0.06	0.06	0.11	0.03	0.00	0.00	0.00	0.00
70	0.02	0.01	0.05	0.08	0.09	0.08	0.07	0.06	0.07	0.04	0.15	0.11	0.06	0.07	0.05	0.00	0.00	0.00	0.00	0.00
90	0.01	0.00	0.01	0.02	0.04	0.06	0.08	0.09	0.14	0.09	0.23	0.11	0.05	0.04	0.02	0.00	0.00	0.00	0.00	0.00
130	0.01	0.00	0.01	0.02	0.05	0.07	0.09	0.09	0.14	0.13	0.21	0.09	0.05	0.02	0.01	0.00	0.00	0.00	0.00	0.00
150	0.01	0.00	0.02	0.03	0.04	0.05	0.06	0.07	0.12	0.07	0.20	0.10	0.05	0.03	0.16	0.00	0.00	0.00	0.00	0.00
180	0.01	0.01	0.02	0.02	0.04	0.05	0.05	0.06	0.10	0.07	0.19	0.11	0.06	0.06	0.16	0.00	0.00	0.00	0.00	0.00
230	0.01	0.01	0.02	0.06	0.10	0.11	0.11	0.11	0.16	0.10	0.13	0.05	0.02	0.01	0.01	0.00	0.00	0.00	0.00	0.00
330	0.01	0.00	0.01	0.02	0.05	0.06	0.07	0.07	0.11	0.06	0.13	0.08	0.05	0.07	0.14	0.05	0.00	0.00	0.00	0.00
350	0.01	0.00	0.01	0.05	0.10	0.11	0.10	0.10	0.13	0.07	0.13	0.06	0.04	0.05	0.03	0.00	0.00	0.00	0.00	0.00
510	0.00	0.00	0.02	0.01	0.01	0.02	0.02	0.02	0.02	0.03	0.08	0.06	0.05	0.06	0.18	0.14	0.10	0.09	0.09	0.00
540	0.01	0.00	0.02	0.02	0.02	0.02	0.02	0.02	0.02	0.01	0.08	0.06	0.04	0.05	0.19	0.17	0.07	0.12	0.05	0.00
750	0.00	0.00	0.00	0.01	0.01	0.02	0.02	0.03	0.04	0.03	0.10	0.08	0.05	0.05	0.18	0.11	0.07	0.09	0.07	0.03
810	0.00	0.00	0.01	0.01	0.02	0.02	0.02	0.02	0.04	0.02	0.08	0.06	0.04	0.05	0.19	0.15	0.19	0.07	0.00	0.00
830	0.01	0.00	0.01	0.01	0.03	0.03	0.04	0.04	0.06	0.04	0.09	0.05	0.03	0.04	0.13	0.09	0.08	0.13	0.10	0.00
870	0.00	0.00	0.01	0.01	0.01	0.01	0.02	0.02	0.04	0.02	0.10	0.10	0.06	0.06	0.24	0.14	0.09	0.07	0.00	0.00

Appendix D

U Graphical results of the sensitivity analysis of the model input parameters are presented hereafter. For each simulation case the hydraulic variables (i.e., Flow discharge and Water head) followed by the sediment-related results (i.e., bed heights and fractional size classes of deposits) are illustrated. On the graphs it can be observed that numerical results are compared with the experimental measured data.

1) **Sim24**: Effect of the minimum Velikanov efficiency coefficient.

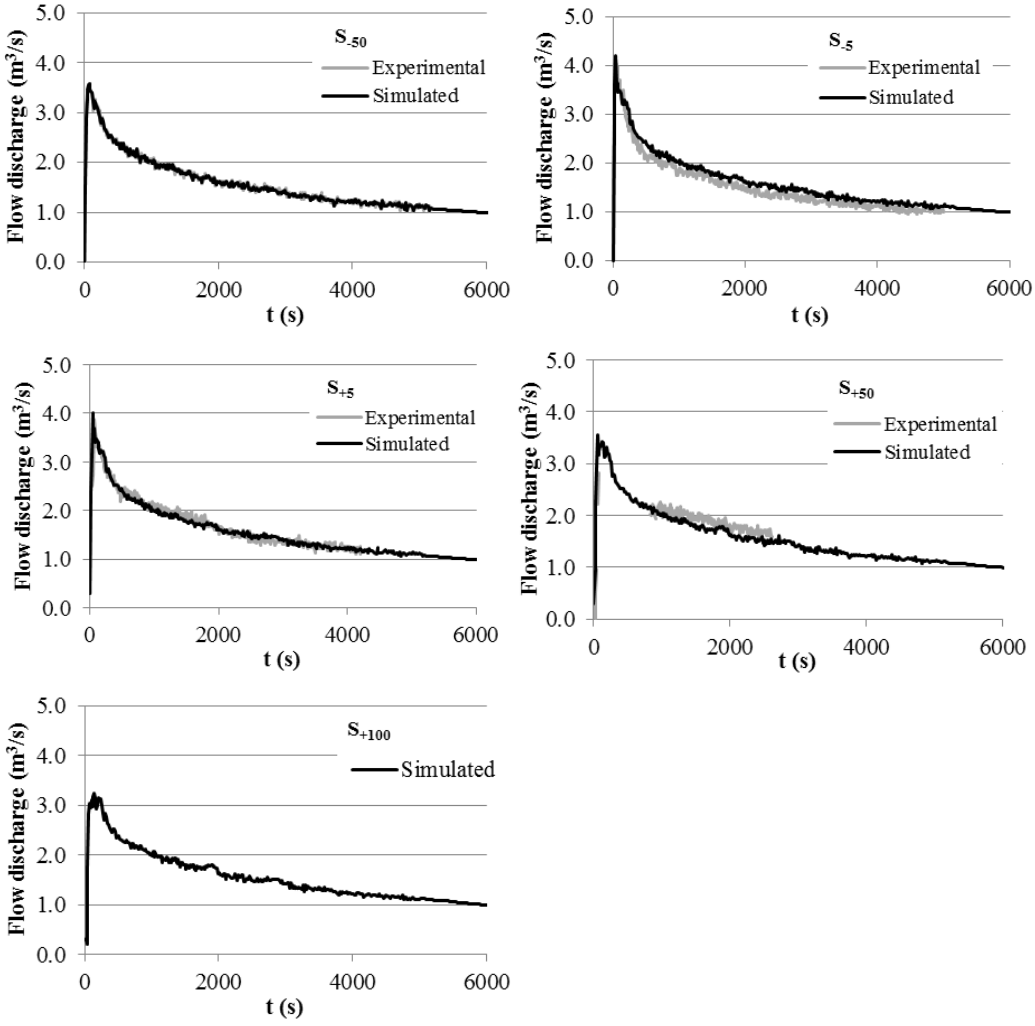

Comparison of the measured and simulated flow discharges for all five measuring sections using the non-uniform sediment transport approach obtained from Sim24.

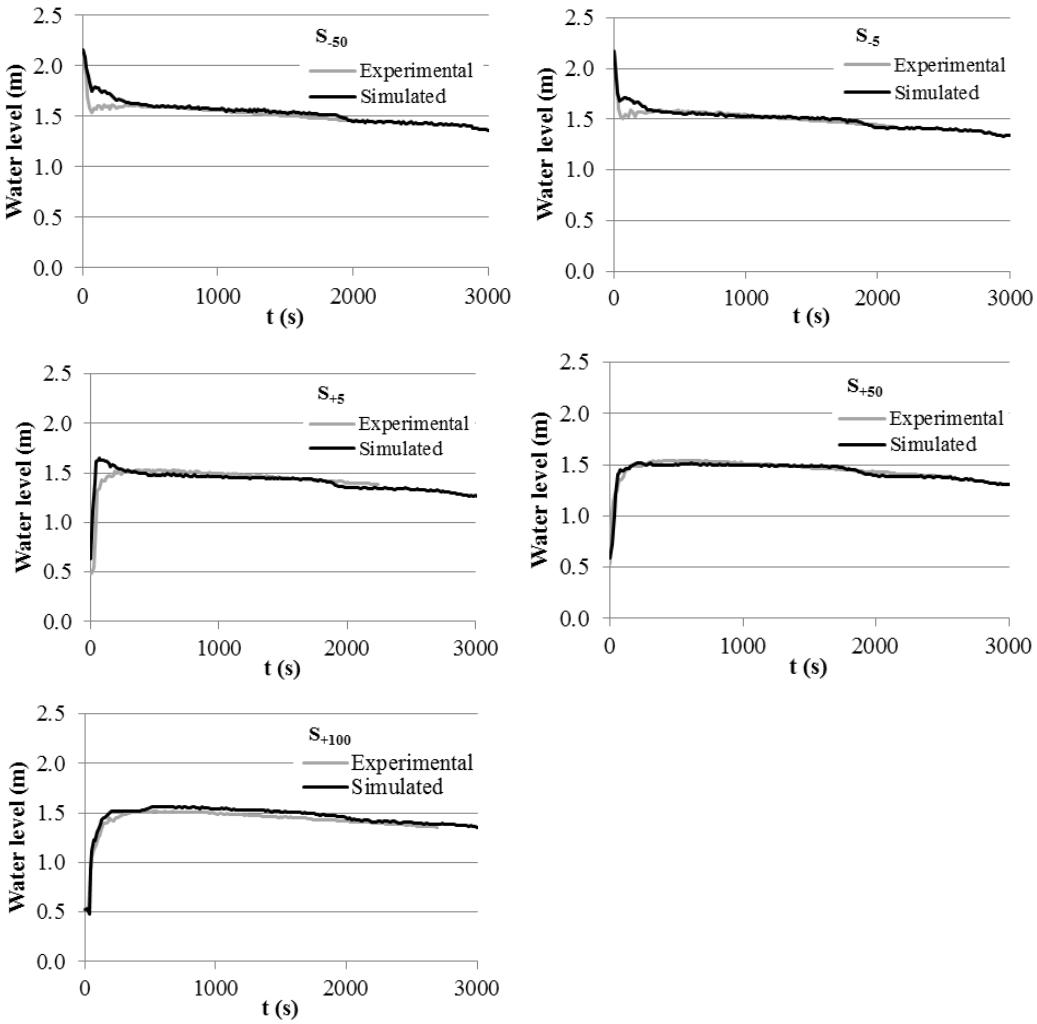

Comparison of the measured and simulated water levels for all five measuring sections using the non-uniform sediment transport approach obtained from Sim24.

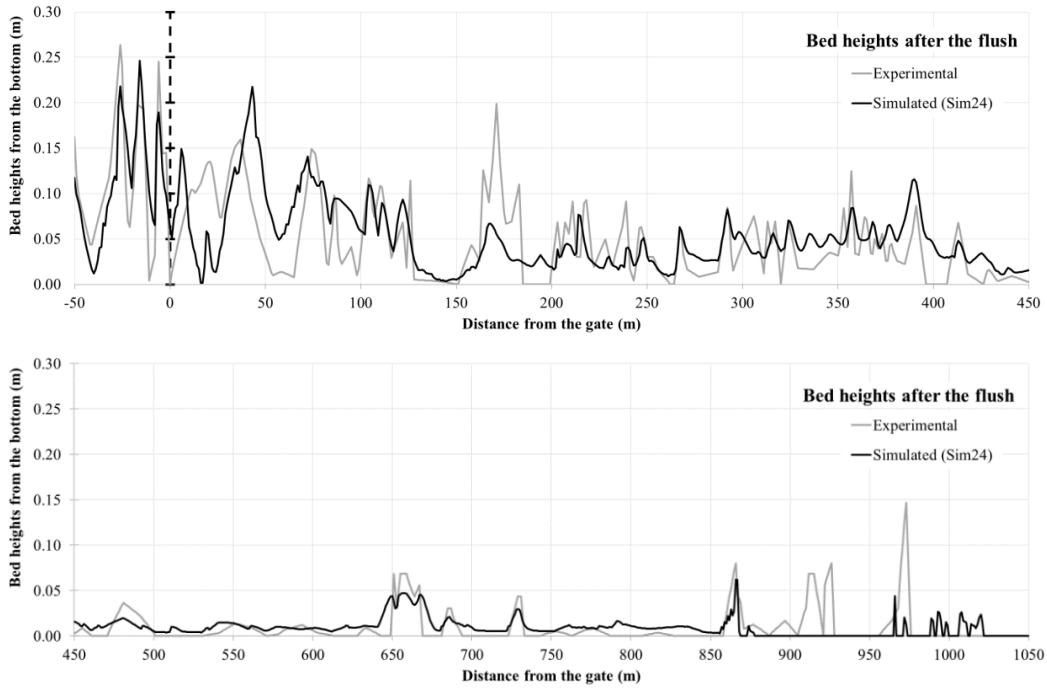

Comparison of the measured and simulated bed heights along the studied sewer channel using the non-uniform sediment transport approach obtained from Sim24.

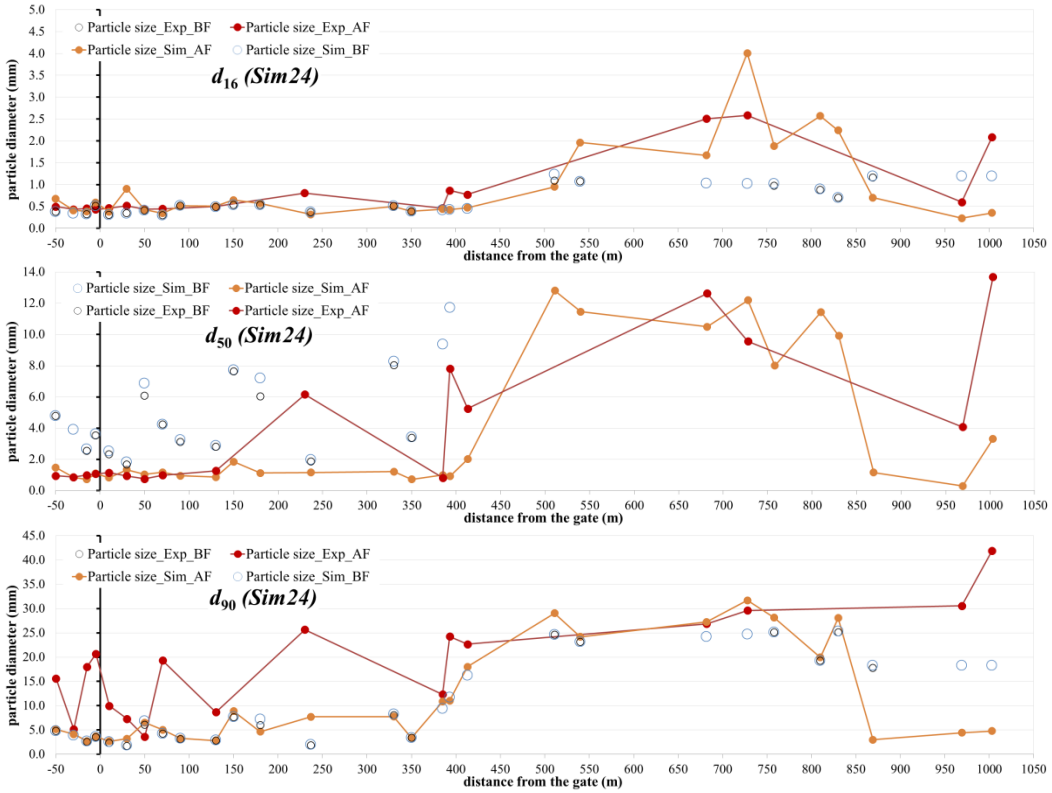

Comparison of the measured and simulated the characteristic grain sizes (d_{16}, d_{50} and d_{90}) BF and AF along the studied sewer channel using the non-uniform sediment transport approach obtained from Sim24.

2) **Sim32**: Effect of the maximum Velikanov efficiency coefficient.

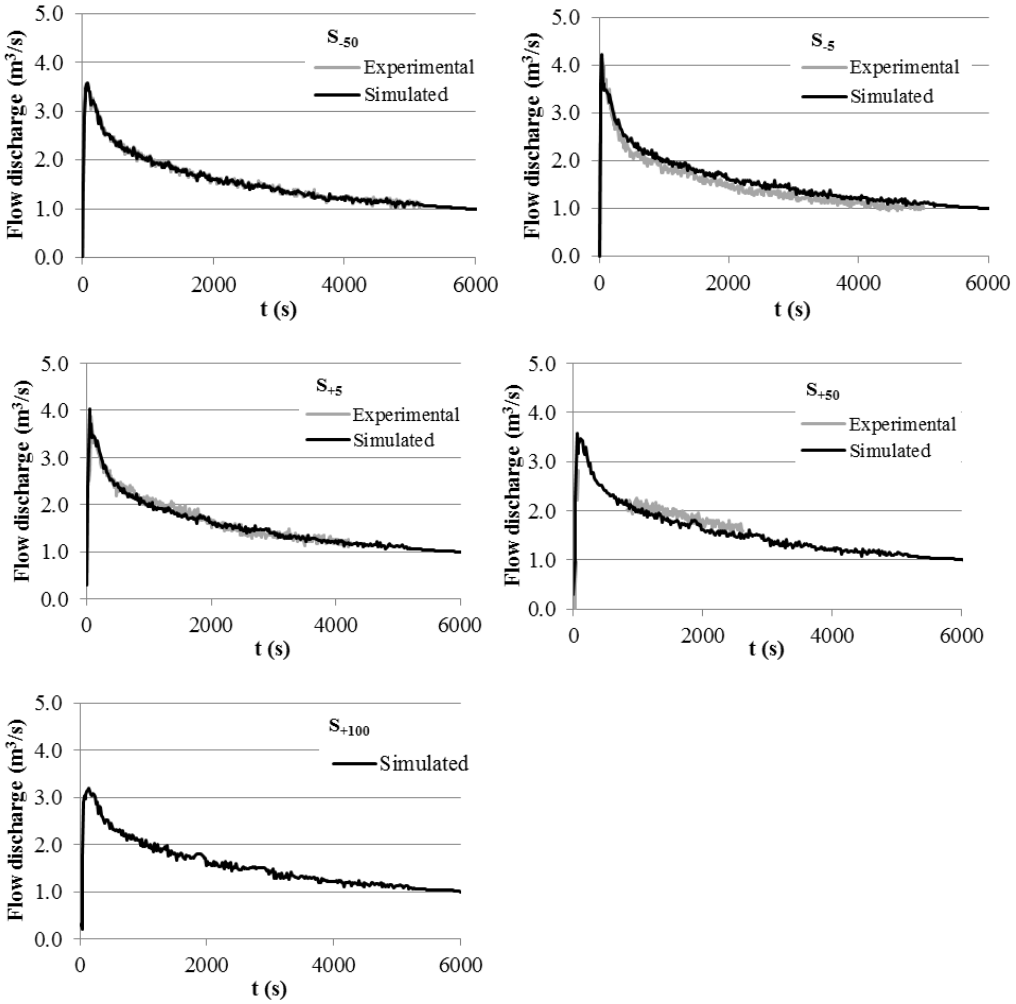

Comparison of the measured and simulated flow discharges for all five measuring sections using the non-uniform sediment transport approach obtained from Sim32.

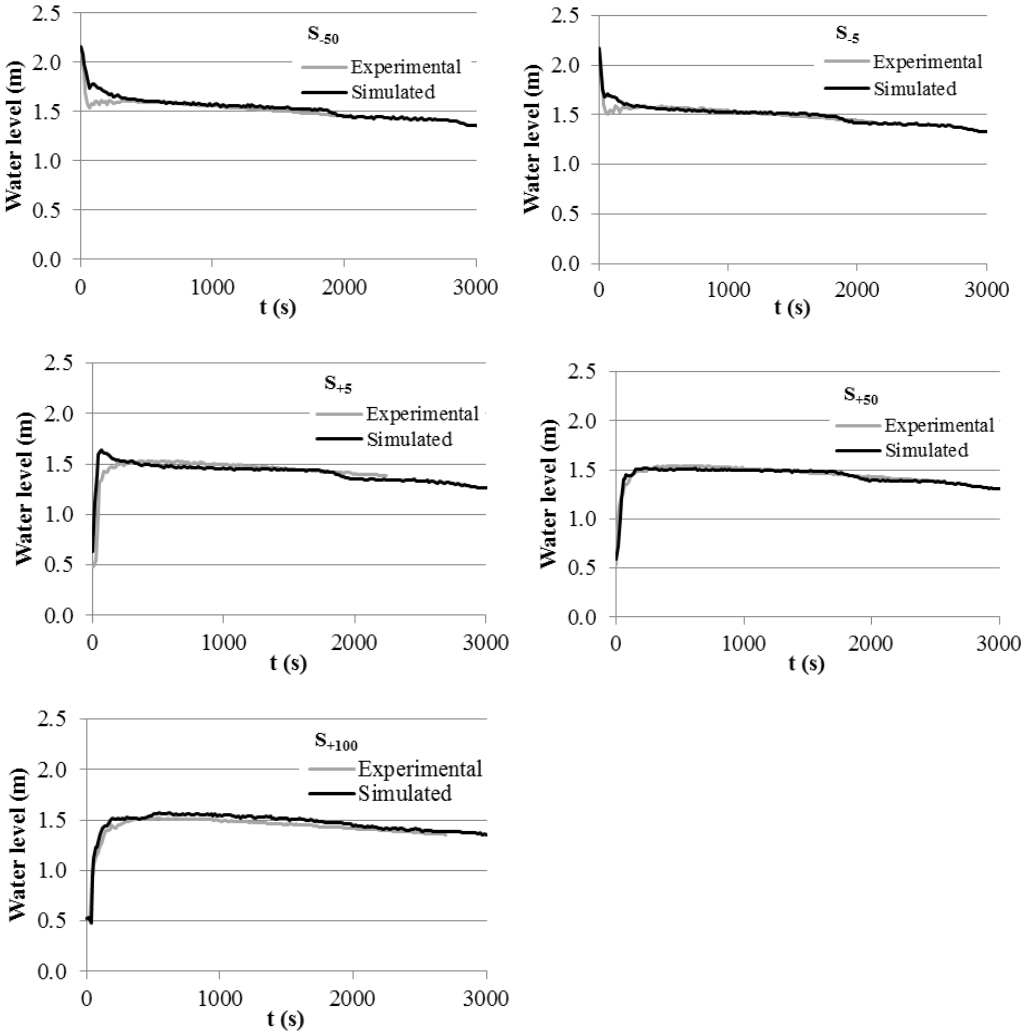

Comparison of the measured and simulated water levels for all five measuring sections using the non-uniform sediment transport approach obtained from Sim32.

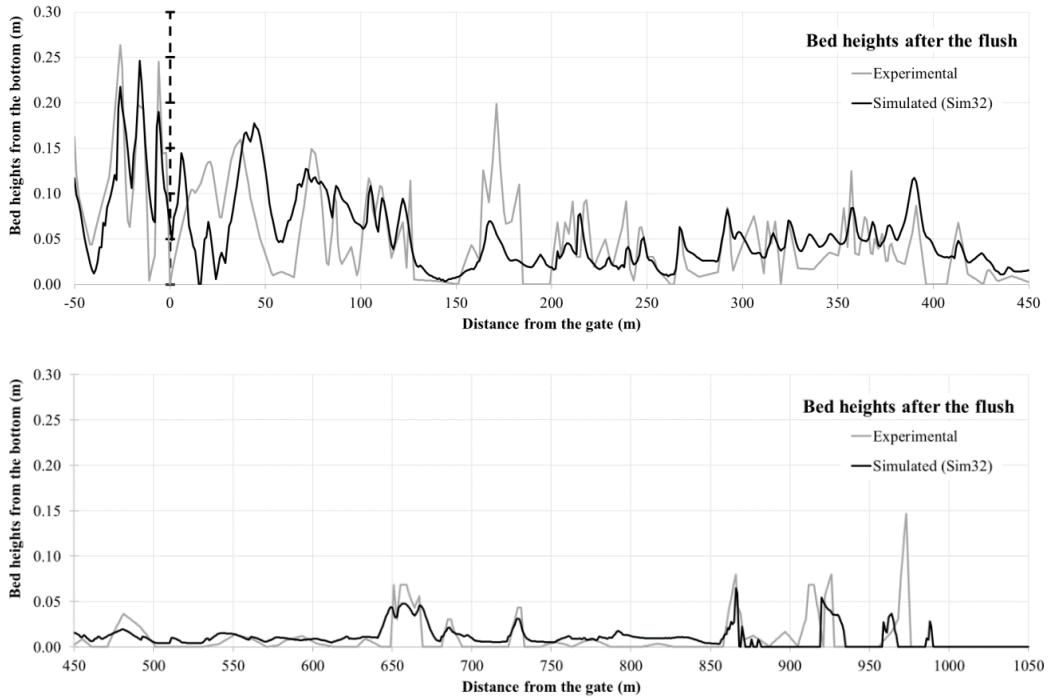

Comparison of the measured and simulated bed heights along the studied sewer channel using the non-uniform sediment transport approach obtained from Sim32.

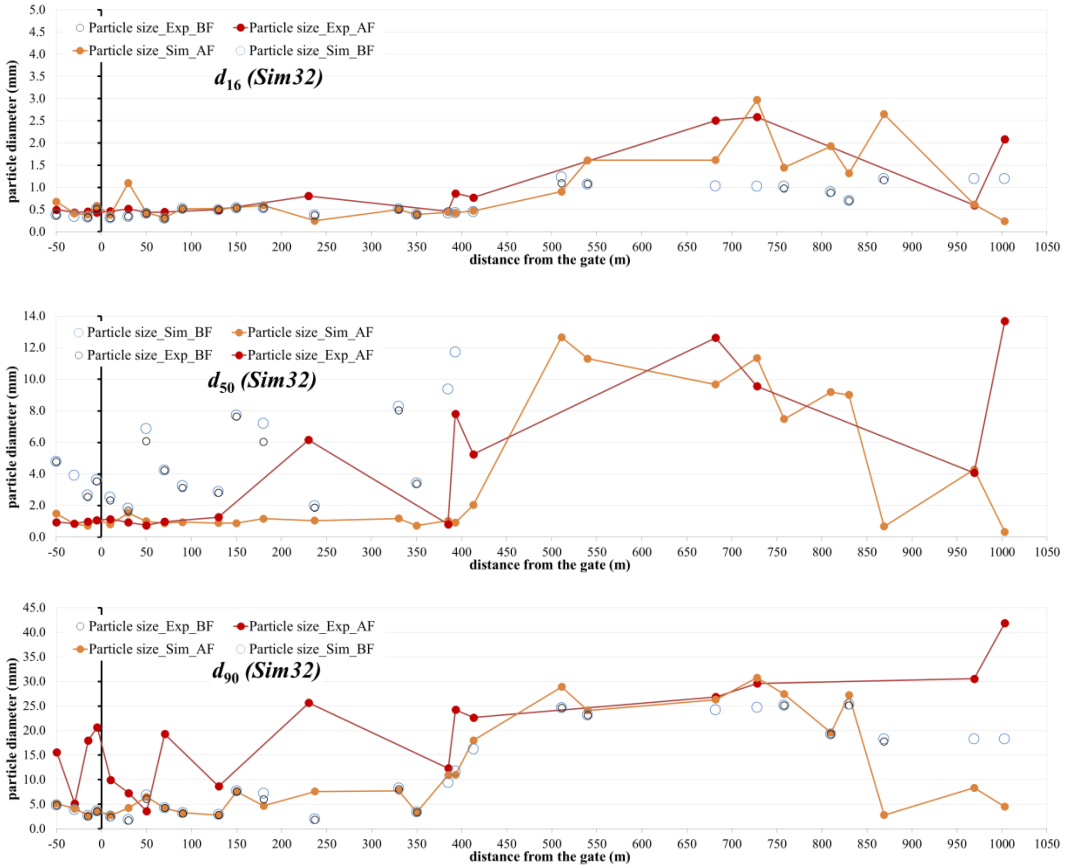

Comparison of the measured and simulated the characteristic grain sizes (d_{16}, d_{50} and d_{90}) BF and AF along the studied sewer channel using the non-uniform sediment transport approach obtained from Sim32.

3) **Sim31**: Effect of the pavement (mixing) layer's thickness.

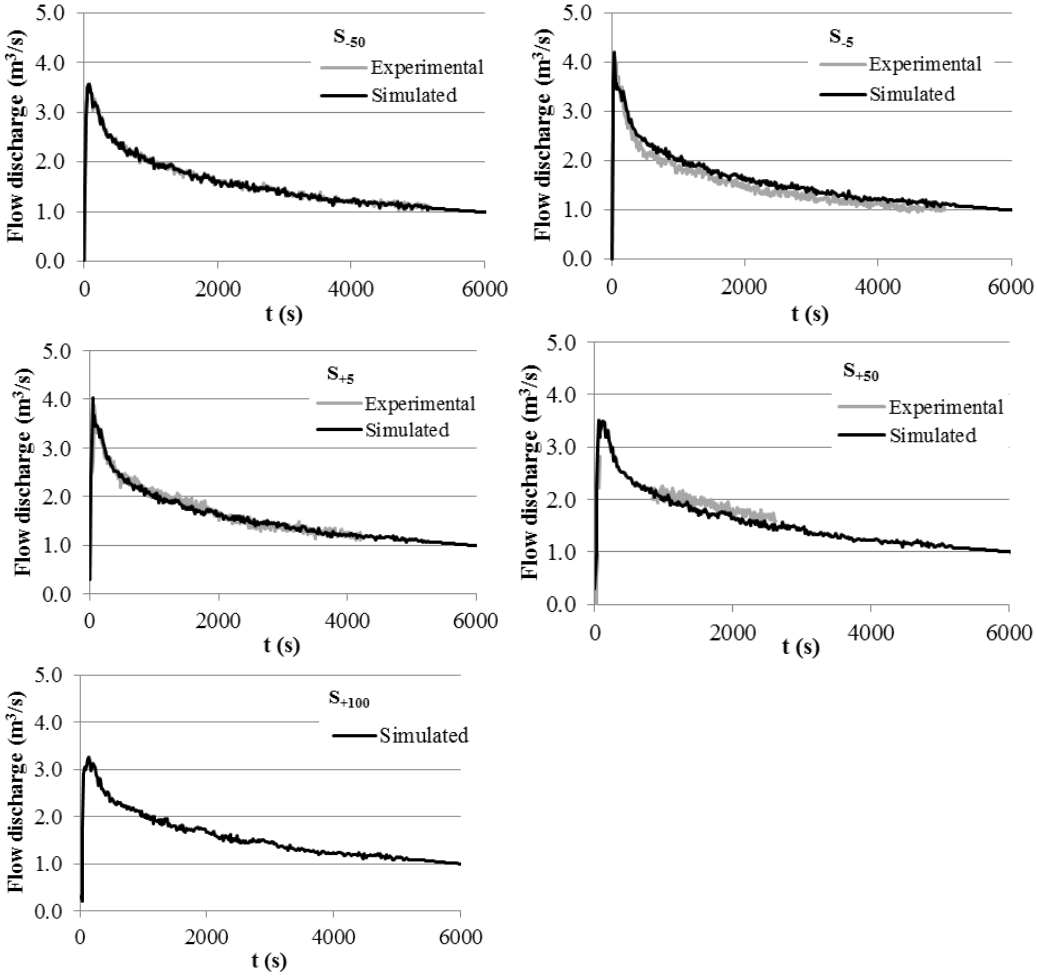

Comparison of the measured and simulated flow discharges for all five measuring sections using the non-uniform sediment transport approach obtained from Sim31.

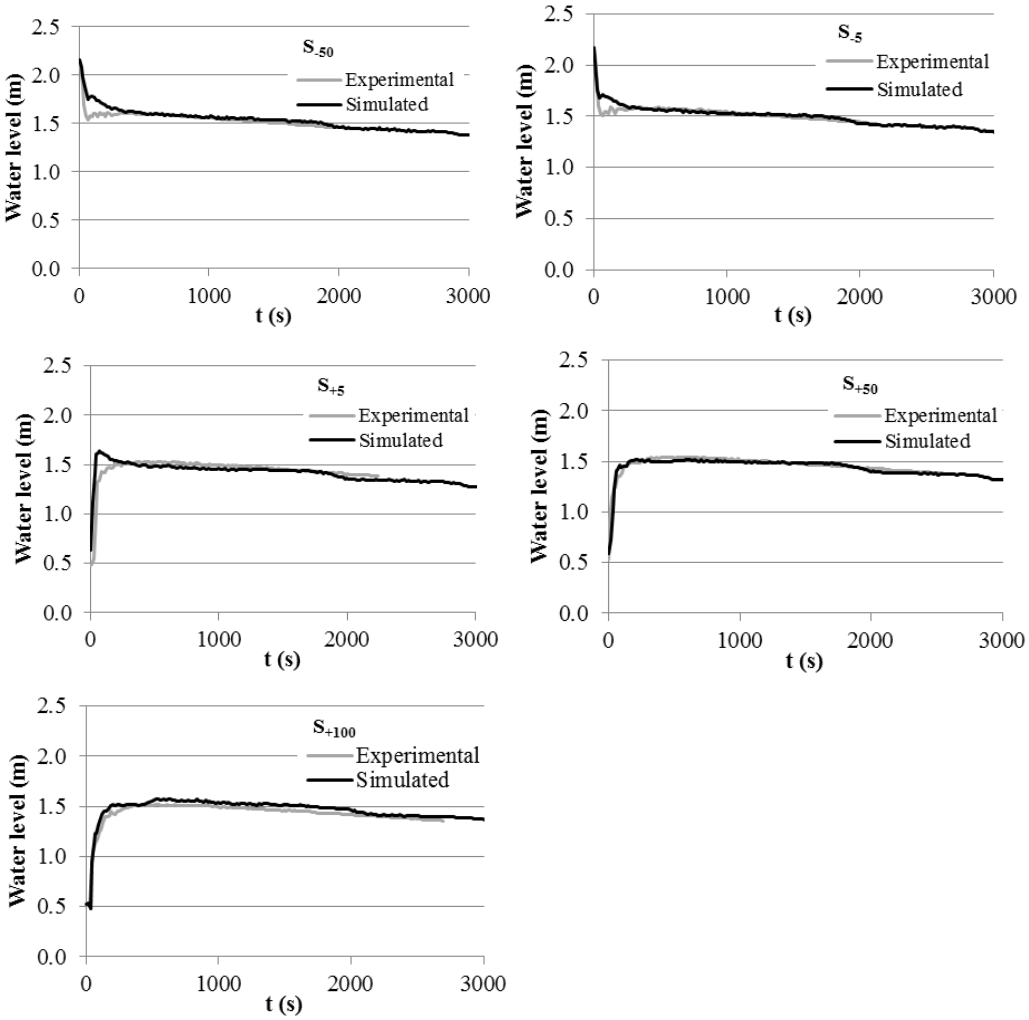

Comparison of the measured and simulated water levels for all five measuring sections using the non-uniform sediment transport approach obtained from Sim31.

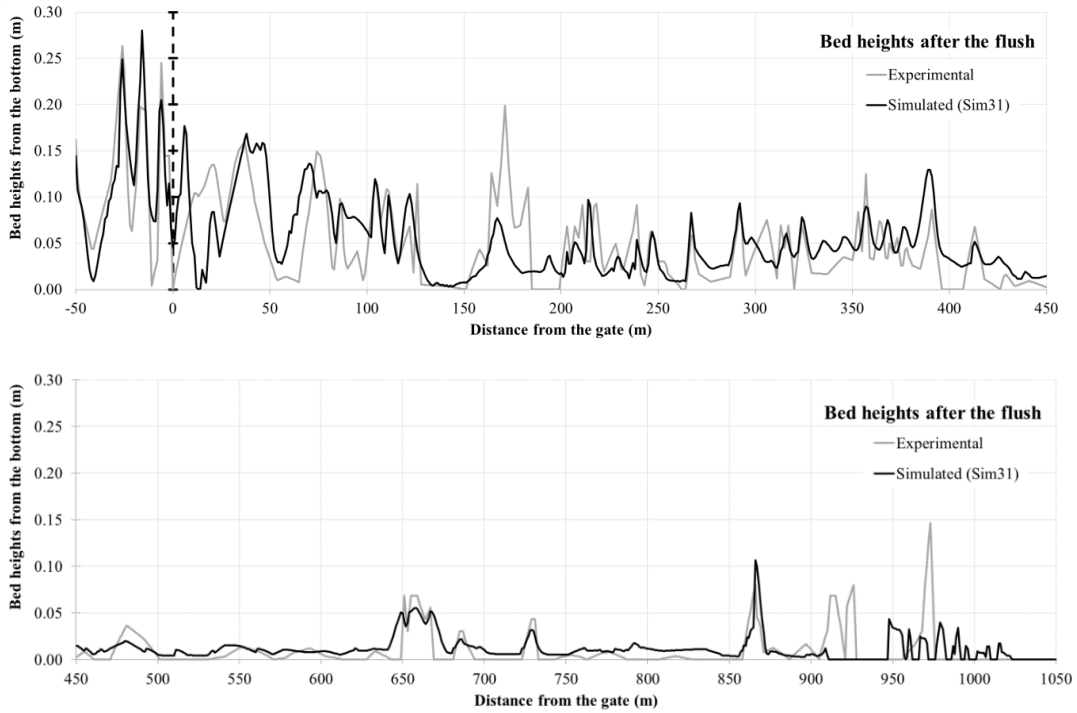

Comparison of the measured and simulated bed heights along the studied sewer channel using the non-uniform sediment transport approach obtained from Sim31.

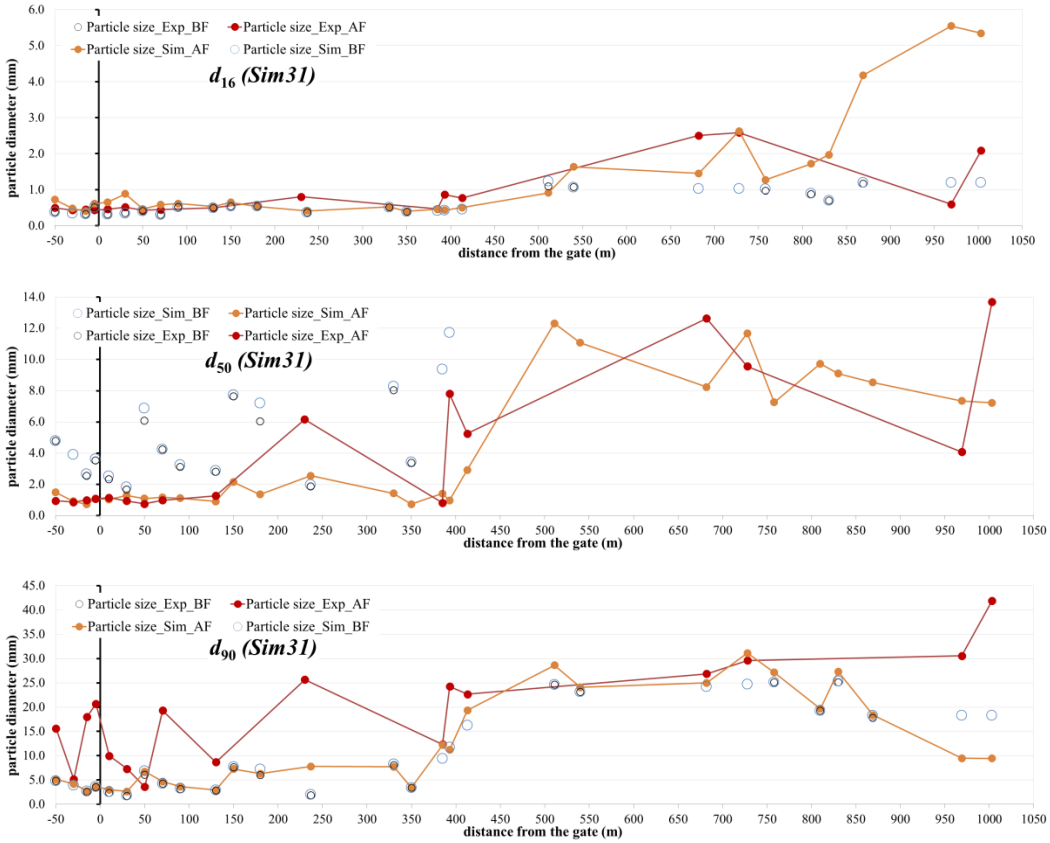

Comparison of the measured and simulated the characteristic grain sizes (d_{16}, d_{50} and d_{90}) BF and AF along the studied sewer channel using the non-uniform sediment transport approach obtained from Sim31.

4) **Sim29**: Effect of hiding among the bed sediments.

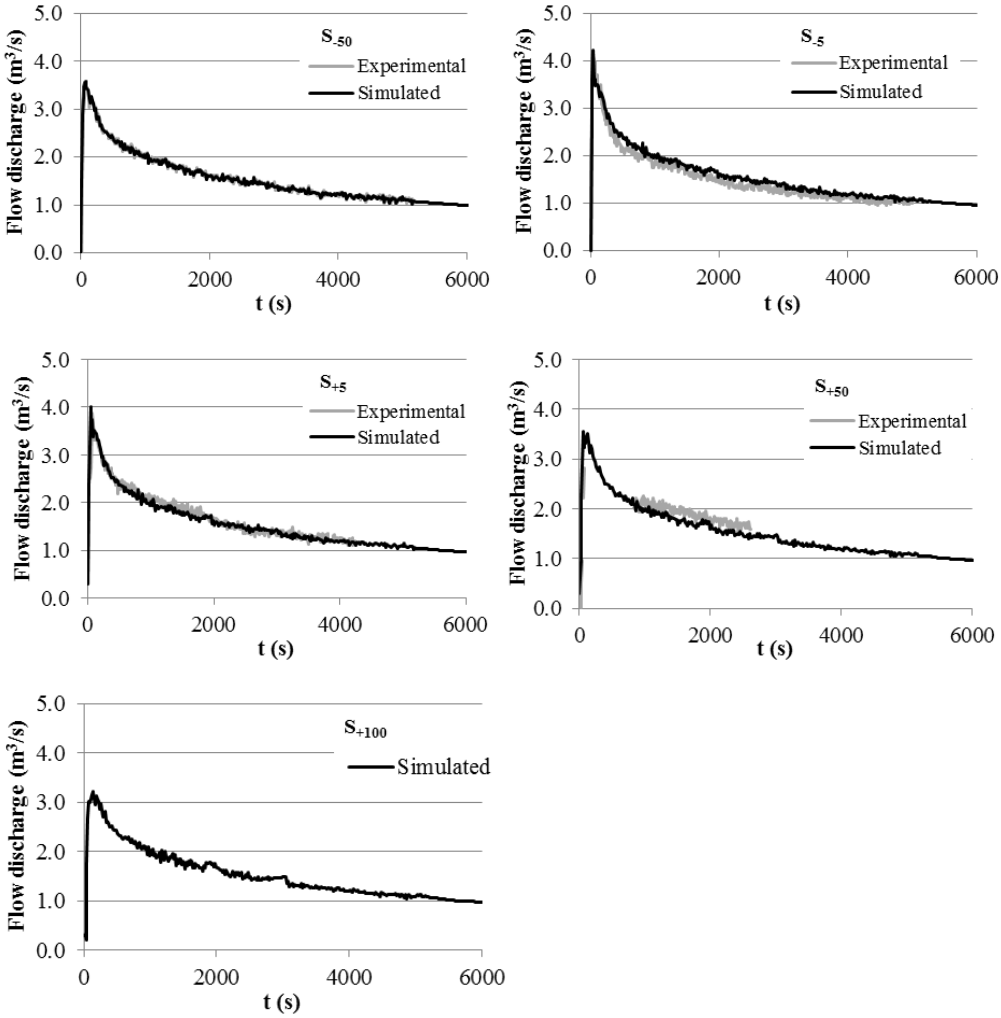

Comparison of the measured and simulated flow discharges for all five measuring sections using the non-uniform sediment transport approach obtained from Sim29.

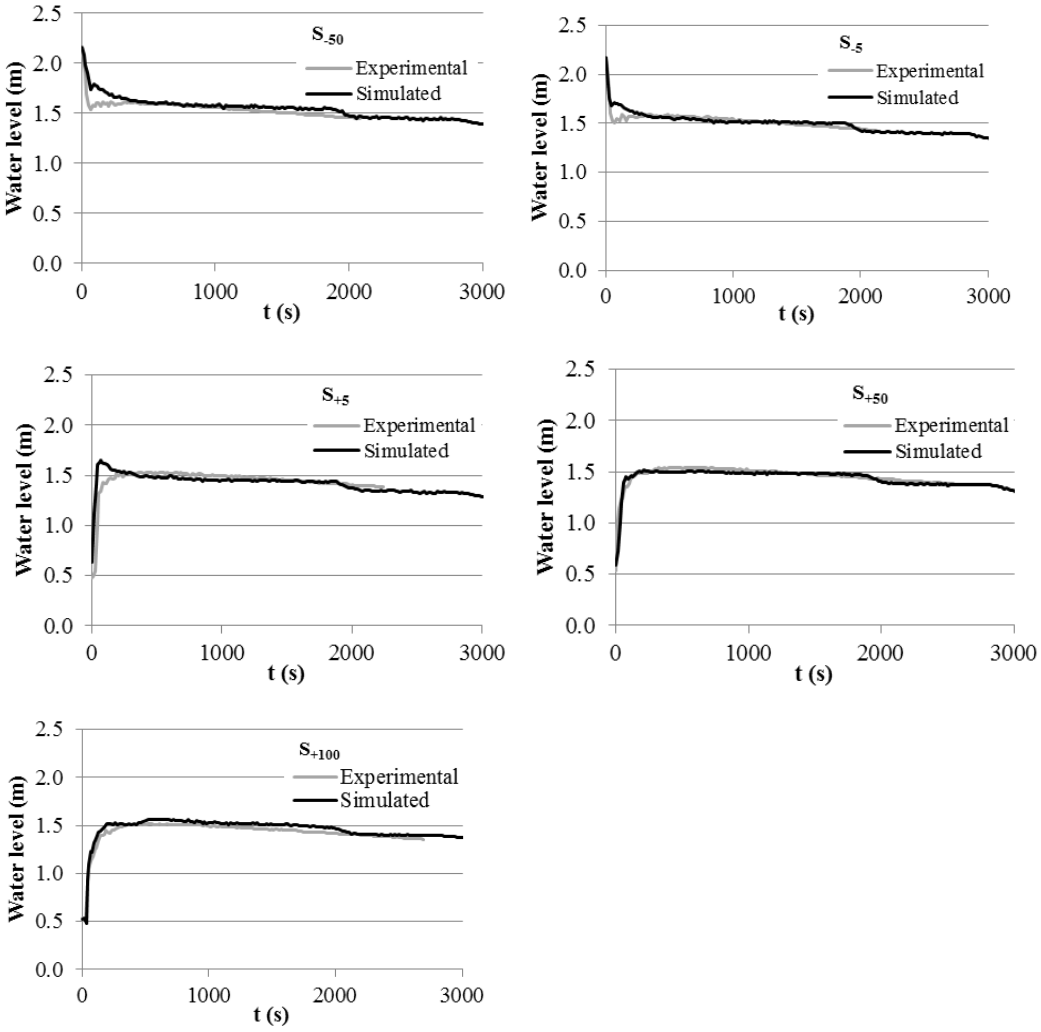

Comparison of the measured and simulated water levels for all five measuring sections using the non-uniform sediment transport approach obtained from Sim29.

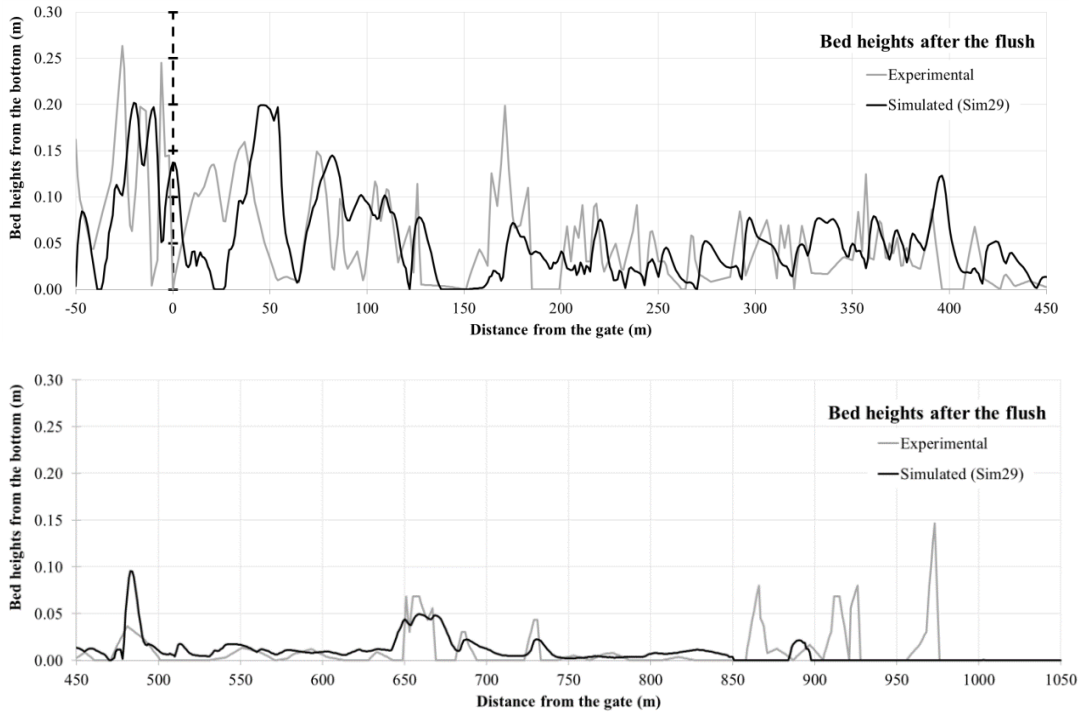

Comparison of the measured and simulated bed heights along the studied sewer channel using the non-uniform sediment transport approach obtained from Sim29.

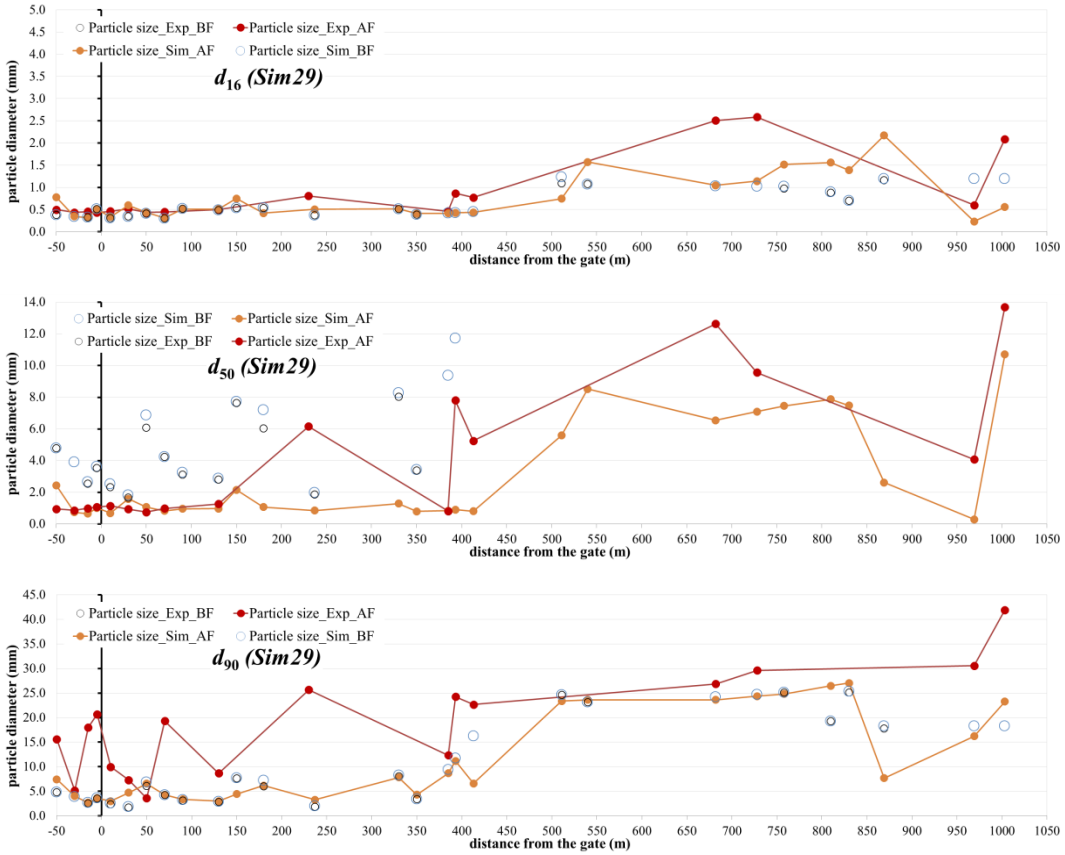

Comparison of the measured and simulated the characteristic grain sizes (d_{16}, d_{50} and d_{90}) BF and AF along the studied sewer channel using the non-uniform sediment transport approach obtained from Sim29.

Expérimentations et Modélisations de la Chasse Hydraulique dans les Réseaux d'Assainissement Unitaires – Cas d'étude d'un Collecteur Parisien

Experimental and Numerical investigation of Flushing in Combined sewer Networks –Case study of a Parisian Trunk Sewer

Par

Mme Gashin Shahsavari